



University
of Glasgow

Gingell-Littlejohn, Marc (2014) Cellular senescence and renal transplantation. MD thesis.

<http://theses.gla.ac.uk/4986/>

Copyright and moral rights for this thesis are retained by the author

A copy can be downloaded for personal non-commercial research or study, without prior permission or charge

This thesis cannot be reproduced or quoted extensively from without first obtaining permission in writing from the Author

The content must not be changed in any way or sold commercially in any format or medium without the formal permission of the Author

When referring to this work, full bibliographic details including the author, title, awarding institution and date of the thesis must be given.

Cellular Senescence and Renal Transplantation

Marc Gingell-Littlejohn

MD (Malta), MRCSEd, USMLE

Submitted in fulfilment of the requirements for the Degree of Doctor of Medicine

Department of Surgery
College of Medical, Veterinary and Life Sciences
Institute of Cancer Sciences
University of Glasgow

February 2014

Table of Contents

Chapter 1

BIOMARKERS OF AGEING, RENAL ALLOGRAFT FUNCTION AND TRANSPLANTATION	12
1.1 Introduction.....	12
1.1.1 ESRF and Donor Organ Shortfall	12
1.1.2 Renal Replacement Therapy	14
1.1.3 Extended Criteria Donation	15
1.1.4 Serum Creatinine	16
1.1.5 Estimated Glomerular Filtration Rate (eGFR).....	17
1.1.6 Urinary Protein Creatinine Ratio	18
1.1.7 White Cell Count	18
1.1.8 Human Leukocyte Antigen System	19
1.1.9 Cellular Senescence	20
1.1.10 Cellular Senescence and Age Related Diseases.....	24
1.1.11 Senescence and the Kidney.....	27
1.1.12 Biomarkers of Ageing.....	28
1.1.13 Telomeres.....	28
1.1.14 The Structure and Function of Telomeres	29
1.1.15 The “End Replication Problem”	31
1.1.16 Senescence and STASIS	36
1.1.17 Cyclin Dependant Kinase 2A - CDKN2A.....	38
1.1.18 CDKN2A functions in vitro and in vivo.....	38
1.1.19 CDKN2A, Tumour Suppression and the Senescent Phenotype	40
1.1.20 Telomeres, p16, p21 and senescence	41
1.1.21 Epigenetic regulation of renal function and Model testing.....	42
1.2 Hypothesis.....	44
1.3 Aims.....	44

1.4 Materials and Methods.....	45
1.4.1 RNA extraction using TRIzol [®] technique.....	45
1.4.2 DNA extraction.....	45
1.4.3 Spectrophotometry.....	46
1.4.4 Gel Electrophoresis.....	46
1.4.5 DNase Treatment.....	46
1.4.6 cDNA Synthesis.....	47
1.4.7 Taqman RT-PCR.....	47
1.4.8 Telomere Assay Protocol.....	51
1.4.9 Statistics.....	56
1.4.10 Ethics.....	56
1.5 Renal Database.....	56
1.6 Study Population.....	57
1.7 Results.....	57
1.7.1 Demographics, Biological Age and Donor Chronological Age.....	57
1.7.2 BoA and Correlation with Renal Function Post-Transplant.....	59
1.7.3 Biological Age and Serum Creatinine.....	63
1.7.4 Biological Age and UPCR.....	63
1.7.5 ECD Kidneys and DCA vs Renal Function.....	64
1.7.6 ECD Kidneys and DCA vs Post-operative WCC.....	66
1.7.7 CDKN2A, Delayed Graft Function and Rejection.....	68
1.7.8 Univariate Regression Analysis.....	69
1.7.9 Multivariate Regression Analysis.....	73
1.8 Discussion.....	75
1.8.1 CDKN2A – most robust BoA in modern era.....	75
1.8.2 CDKN2A, SASP and rejection.....	77
1.8.3 CDKN2A based pre-transplant scoring system.....	77
1.9 Conclusion.....	79

Chapter 2

PHENOTYPIC CHARACTERISATION OF THE AS/AGU MUTANT RAT	80
2.1 Introduction.....	80
2.1.1 AS/AGU PKC γ mutation.....	80
2.1.2 Physiological calculation of renal blood flow and GFR.....	81
2.1.3 Inulin clearance and the measurement of true GFR.....	82
2.1.4 Serum Creatinine Clearance and estimated GFR (eGFR).....	83
2.2 Hypothesis.....	84
2.3 Aims.....	85
2.4 Methods.....	85
2.4.1 Animal Groups and Housing.....	85
2.4.2 Preparation of FITC-Inulin Solution.....	85
2.4.3 Experimental Design and Surgical Technique.....	86
2.4.4 GFR Analytical Technique.....	90
2.4.5 GFR and IR Injury Studies - Initial Testing Phase.....	93
2.4.6 Biochemical Serum and Urine Analysis.....	95
2.4.7 Immunohistochemical analysis for bio-age in rat kidney.....	96
2.4.8 TUNEL assay protocol.....	96
2.4.9 SA-Beta-Gal Staining on Tissue Sections.....	98
2.4.10 IHC using MOUSE p16 Antibody F-12.....	100
2.4.11 IHC using MOUSE p21 Antibody C-19.....	101
2.5 Results.....	102
2.5.1 GFR Validation.....	102
2.5.2 Parallel Strain Analysis.....	105
2.5.3 Biochemical Analysis.....	106
2.5.4 Subgroup Analysis – Sex Differences.....	109
2.5.5 Ischaemia Reperfusion Injury Studies.....	109
2.5.6 Global Urine Analysis.....	109

2.5.7 Individual Strain Urine Analysis	111
2.5.8 Immunohistochemistry	111
2.6 Discussion	115
2.6.1 GFR and Renal Function	115
2.6.2 The possible role of Protein Kinase C in explaining differences in GFR..	116
2.6.3 Urea Transport	118
2.6.4 Mammalian Urea Transporters	120
2.6.5 IR Studies - Urine Biochemistry	123
2.6.6 IR Studies - Urine Urea and Specific Gravity	124
2.6.7 IR Studies - Immunohistochemistry	125
2.7 Conclusion	134

Chapter 3

ISCHAEMIA REPERFUSION INJURY AND ANTI-ISCHAEMIC COMPOUNDS – AN EXPERIMENTAL ANIMAL MODEL

3.1 Introduction.....	136
3.1.1 mTOR inhibitors and AZ-6.....	137
3.2 Hypothesis.....	140
3.3 Aims.....	140
3.4 Methods.....	140
3.4.1 Animal Groups and Housing	140
3.4.2 Experimental Design and Surgical Technique.....	141
3.5 Results.....	145
3.5.1 Biochemical Analysis	145
3.5.2 Bioage Genetic Expression and Immunohistochemical Staining	152
3.5.3 Gene Expression Analysis Assays.....	152
3.6 Discussion.....	156
3.6.1 Biochemical response to AZ-6.....	156

3.6.2 mTOR Inhibitors and Renal Function.....	157
3.6.3 CDKN1A and CDKN2A	158
3.6.4 Telomere Length and CDKN2A synchrony	160
3.6.5 Model Testing, Biological Ageing and Novel Clinical Entities	161
3.7 Conclusion	162
General Summary	163
Acknowledgements.....	164
References.....	165
List of Publications	195

LIST OF FIGURES

- Figure 1.1 Diagram depicting primary causes and consequences of cellular senescence
- Figure 1.2 Mammalian telomere structure and microscopic appearance
- Figure 1.3 The “End Replication Problem”
- Figure 1.4 Telomeres, Hayflick limit and Crisis
- Figure 1.5 Critical telomere shortening and p53
- Figure 1.6 Pathways controlled by the CDKN2A locus
- Figure 1.7 Real time Taqman PCR reaction
- Figure 1.8 Scatter plots showing the correlation between biomarkers of ageing and donor chronological age
- Figure 1.9 Scatter plots showing the relationship between telomere length and renal function, as measured by MDRD 4 eGFR
- Figure 1.10 Scatterplots showing the relationship between CDKN2A and renal function, as measured by MDRD 4 eGFR
- Figure 1.11 The relationship between WCC at 2 years and DCA
- Figure 1.12 Boxplot depicting a significantly lower WCC in ECD kidneys at 2 years
- Figure 2.1 Depiction of surgical setup
- Figure 2.2 Images of surgical technique
- Figure 2.3 Dependence of FITC Inulin fluorescence on pH
- Figure 2.4 Schematic representation of operative methods
- Figure 2.5 Graphical representation of plasma FITC Inulin concentration through a typical experiment
- Figure 2.6 Scatterplot showing the expected increase in GFR with weight for both AS and mutant strains
- Figure 2.7 Total GFR difference between control and mutant strain
- Figure 2.8 Corrected GFR difference between control and mutant strain
- Figure 2.9 Mammalian urea transporters
- Figure 2.10 Biological processes implicated in IR Injury
- Figure 2.11 Outcomes of the p16 and p21 cellular pathways
- Figure 2.12 Immunohistochemical staining for senescence markers
- Figure 3.1 A model of mTOR signalling cascade and its function
- Figure 3.2 Clustered Bar Graph with 95% CI error bars
- Figure 3.3 Changes in corrected creatinine compared to Group I
- Figure 3.4 Weight recordings for experimental groups I-V
- Figure 3.5 Compound treatment effects on CDKN2A transcriptional expression in two human primary cell types, HDF and HREpi
- Figure 3.6 Expression levels for CDKN1A in rat kidney ischemia model with or without AZ-6 treatment
- Figure 3.7a Nuclear histoscores for p16 protein in rat kidney tissue sections
- Figure 3.7b Nuclear histoscores for p21 proteins in rat kidney tissue sections

LIST OF TABLES

Table 1.1	Mastermix preparation
Table 1.2	Plate layout of both telomere and 36B4 plates
Table 1.3	Roche Lightcycler® Telomere Running Conditions
Table 1.4	Roche Lightcycler® 36B4 Running Conditions
Table 1.5	Demographics
Table 1.6	DCD and ECD correlations with renal function and glomerular damage
Table 1.7	Correlation between DCA and ECD kidneys with WCC at 6 months, 1 year and 2 years
Table 1.8	Association between DGF and rejection episodes with renal function up to 5 years
Table 1.9	Univariate linear regression analysis at 6 months
Table 1.10	Univariate linear regression analysis at 1 year
Table 1.11	Multivariate model outcome for eGFR at 6 months
Table 1.12	Multivariate model outcome for eGFR at 1 year.
Table 1.13	A donor risk classification based on ECD and CDKN2A
Table 2.1	Rodent GFR experimental documentation
Table 2.2	Demographics of rodent population for GFR studies
Table 2.3	Demographics of rodent population for biochemical studies
Table 2.4	Reagents used in SA-Beta-Gal Staining
Table 2.5	Final SA-Beta-Gal solutions at pH4 and pH6
Table 2.6	Results of GFR analysis
Table 2.7	GFR comparison between strains
Table 2.8	Mean GFR between female and male strains
Table 2.9	Biochemical differences between AS and AS/AGU rats
Table 2.10	Urine Biochemical changes in response to IR injury
Table 2.11	IR Injury Urine Biochemical data
Table 2.12	TUNEL IHC – Control vs IR Injured Kidneys
Table 2.13	SA β GAL IHC Results – Control vs IR Injured Kidneys
Table 2.14	p16 IHC Results – Control vs IR Injured Kidneys
Table 2.15	p21 IHC Results – Control vs IR Injured Kidneys
Table 3.1	The five separate groups used in the animal model
Table 3.2	Details of the group demographics, weight, individual creatinine values and adjusted creatinine/100gr body weight
Table 3.3	Creatinine values at Day 3
Table 3.4	Creatinine values at Day 6
Table 3.5	Creatinine values at Day 10
Table 3.6	Clustered Bar Graph with 95% CI error bars
Table 3.7	Changes in corrected creatinine compared to Group I
Table 3.8	Changes in corrected creatinine compared to Group II

LIST OF ABBREVIATIONS

AKI	Acute Kidney Injury
ATN	Acute Tubular Necrosis
ARF	Alternate Reading Frame / Acute Renal Failure
AS/AGU	Albino Swiss/Albino Glasgow University
ANOVA	Analysis of Variance
AZ	Astra Zeneca
APKD	Adult Polycystic Kidney Disease
BMI	Body Mass Index
BoA	Biomarker of Ageing
cAMP	cyclic Adenosine Monophosphate
CDKN2A	Cyclin Dependant Kinase 2A
CIT	Cold Ischaemic Time
CC	Correlation Coefficient
CKD	Chronic Kidney Disease
CNI	Calcineurin Inhibitor
CVD	Cerebro Vascular Disease
DBD	Donation After Brain Death
DCA	Donor Chronological Age
DCD	Donation after Cardiac Death
DDR	DNA Damage Response
DEPC	Diethylpyrocarbonate
DGF	Delayed Graft Function
DNA	Deoxyribonucleic acid
ECD	Extended Criteria Donor
ESRF	End Stage Renal Failure
FAM	6-carboxy-fluorescein
FITC	Flourescein Isothiocyanate Inulin
GFR	Glomerular Filtration Rate
GN	Glomerulonephritis
HDF	Human Diploid Fibroblast
HLA	Human Leukocyte Antigen
HPRT	Hypoxanthine Phosphoribosyltransferase
HIF	Hypoxia Inducable Factor
IHC	Immunohistochemistry
IL	Interleukin
IMCD	Inner Medullary Collecting Ducts
IRI	Ischaemia Reperfusion Injury
Kda	Kilodalton
OPTN	Organ Procurement and Transplantation Network
MDRD	Modification of Diet in Renal Disease
MHC	Major Histocompatibility Complex
MMP	Matrix Metalloprotein
M.O.M	Mouse on Mouse
miRNA	micro Ribonucleicacid

mTOR	Mammalian Target of Rapamycin
NCE	Novel Clinical Entity
NICE	National Institute for Health and Clinical Excellence
NKF	National Kidney Foundation
NO	Nitric Oxide
PBL	Peripheral Blood Leukocyte
PBS	Phosphate Buffered Saline
PCR	Polymerase Chain Reaction
PHD	Prolylhydroxylase
PKC	Protein Kinase C
PNF	Primary Non Function
PTEN	Phosphatase and Tensin Homologue
RB	Retinoblastoma
SA β Gal	Senescence Associated Beta Galactosidase
SASP	Senescence Associated Secretory Phenotype
SG	Specific Gravity
STASIS	Stress or Aberrant Signaling Induced Senescence
TAMRA	6-carboxy-tetramethyl-rhodamine
TCR	T Cell Receptor
TL	Telomere Length
TLR	Toll-like Receptor
TUNEL	Terminal deoxynucleotidyl transferase dUTP nick end labeling
UNOS	United Network for Organ Sharing
UPCR	Urinary Protein Creatinine Ratio
UT	Urea Transporter
VEGF	Vascular endothelial growth factor
WCC	White Cell Count
WBC	White Blood Cell

To my wife Elaine for her unconditional support throughout the years of research and writing of this thesis. To my family and my children Nick and Andy who brought smiles and joy during those difficult moments. Lastly, to Nicky BC (1982-2009) whose courage and strength during his battle with leukaemia continues to motivate me as a person and a devoted surgeon.

I declare that, except where explicit reference is made to the contribution of others, that this dissertation is the result of my own work and has not been submitted for any other degree at the University of Glasgow or any other institution.

Signature:

Printed name: Marc Gingell-Littlejohn

Chapter 1

BIOMARKERS OF AGEING, RENAL ALLOGRAFT FUNCTION AND TRANSPLANTATION

1.1 Introduction

1.1.1 ESRF and Donor Organ Shortfall

Renal transplantation is the optimum treatment for kidney failure, but is limited by donor shortage. A large proportion of end stage renal failure (ESRF) patients must therefore receive alternative renal replacement therapies in the form of peritoneal, or haemodialysis. This treatment results in increasing morbidity, particularly affecting the cardiovascular system, a severely reduced lifespan and poorer quality of life. Older and marginal donors are increasingly used to meet this shortfall in kidney supply even though elevated numbers of senescent cells within chronologically older organs may negatively influence transplant outcome (1-4). In essence, such organs will have more 'miles on the clock' and thus not work as well, or last as long. Even though such organs may function adequately in the short term, the presence of substantial physiological senescence will make them more susceptible to the effects of transplant-related stresses (5;6). As a consequence, the biological age of the organ, rather than just its chronological age, may have a major impact on organ function post transplant. This is also pertinent to delayed graft function (DGF).

This short term outcome, defined as failure of serum creatinine to fall by half within seven days of transplant, or need for dialysis within seven days of the transplant except dialysis performed for fluid overload or elevated serum potassium levels (7) affects around 40% of deceased donor kidney transplants in the UK and is a strong independent risk factor for long term deleterious outcomes. Its multifactorial causes remain poorly identified, but are thought to be related to cellular damage induced by multiple redox reactions during cold storage, reperfusion, drug toxicity and other related factors.

In the early decades of renal transplantation, strict donor criteria were used for deceased and live donors, such that virtually all kidneys came from relatively young people with

excellent health who died suddenly due to an isolated event, such as trauma or brain haemorrhage. As the treatment became established, increasing numbers of patients were listed for transplantation, creating a shortfall of young and previously healthy donors, putting the transplant community under considerable strain. In order to address this, an expanded donor pool began to be utilised comprising kidneys from older patients, many with pronounced cardiovascular problems.

These so-called extended criteria donors (ECD) were needed in order to match the increasing need for organs and address the extremely high rates of death among patients waiting for a kidney transplant: more than 40% of those waiting will die within 5 years, a prognosis worse than for many cancers. As time has passed, we have therefore moved into an era where the “extended criteria donor” has become the standard donor, with younger and healthier deceased donors increasingly rare. Although such organs incur elevated risks of DGF and ultimately have unfavorable long term outcomes compared with younger donor kidneys, average results remain far superior to alternative treatment modalities, such as haemodialysis. Some grafts however perform poorly – or never function adequately, a clinical condition termed primary non-function (PNF). The reasons for this phenomenon are unclear but seem likely to relate to the inability of older kidneys to tolerate and recover from the multiple injurious processes associated with transplantation. Poor function however, is difficult to predict as many older organs perform adequately despite advanced chronological age (8;9).

DGF is itself a form of acute renal failure resulting in post-transplantation oliguria, increased allograft immunogenicity, increased risk of acute rejection episodes, and decreased long term survival (10). Most deceased donors (up to 50%) and some live donors (up to 5%) manifest some degree of DGF. Improvements in the management of donors and recipients as well as other therapeutic modalities have done little to modify the rates of this clinical state, however it has recently been shown that machine cold perfusion does have a positive effect on Donation after Cardiac Death (DCD) kidneys (11). The effects of reducing the cold ischaemic time are well known and universally practised (12). An inherent problem when studying DGF and its interpretation in clinical trials is ambiguity regarding its definition. Early renal function post transplantation ranges from total anuria or non oliguric acute tubular necrosis (ATN), to slow recovery of function, to rapid and immediate function (10). The definition for DGF in this thesis is “Failure of serum creatinine to fall by 50% in the first 7 days post transplantation or need for dialysis

during the first 7 days post transplantation except haemodialysis for volume overload or hyperkalaemia”

Dependent upon the numbers of senescent cells present in the organ, tissue integrity may be impaired and the capacity to withstand stress reduced. Furthermore, senescence-associated upregulation of pro-inflammatory cytokine gene expression may lead to chronic persistent inflammation. As a consequence, the biological age of the organ, rather than just its chronological age, may have major impact on organ function post transplant. This would imply that the expression of genes involved in cellular processes regulating biological ageing, should provide suitable reporters for investigating such a hypothesis.

In fact, robust and reproducible studies have shown that gene expression of senescence markers of a donor organ (bioage), can predict renal function in vivo, irrespective of classical parameters currently in use, particularly donor chronological age and other comorbidities such as impaired pre-retrieval serum creatinine(13;14).

Life expectancy can vary considerably between neighboring communities and reliance on donor age alone, as the strongest predictor of function may prove increasingly costly and misleading.

1.1.2 Renal Replacement Therapy

Haemodialysis is a method for removing waste products from the body for patients in end stage renal failure. It is one of three forms of renal replacement therapy together with peritoneal dialysis and kidney transplantation. Kidney transplantation is highly cost-effective and is the treatment of choice for many patients with ESRF. There are over 37,800 patients with end-stage renal failure in the UK. Nearly 21,000 are on dialysis, whilst the remainder have a transplant. Of those on dialysis, 76% are on haemodialysis and 24% on peritoneal dialysis. The indicative cost of maintaining a patient with end-stage renal failure on renal replacement therapy (dialysis) is £35,000 per patient per year for a patient on hospital haemodialysis. Kidney transplantation leads to an overall cost benefit of £25,800 per annum. (NHS Blood and Transplant Data – October 2009). It can be seen therefore that besides transplantation offering improved quality of life and an enhanced lifespan to patients in ESRF, there is an overwhelming economic advantage to governmental health budgets.

1.1.3 Extended Criteria Donation

The clinical characteristics that differentiate marginal renal allografts are derived from the social and medical history of the donor (age, history of hypertension or diabetes, the risk of transmitting infectious disease and/or malignancy), the cause of donor death (trauma vs. cerebrovascular accident), the mechanism of donor death (brain death or DBD vs. cardiac death or DCD), the anatomy of the allograft (vessel abnormalities), the morphology on biopsy (glomerulosclerosis, interstitial nephritis and/or fibrosis), and the functional profile (serum creatinine or calculated glomerular filtration rate) prior to transplantation (15;16).

Kidneys transplanted from older donors are considered to be from the expanded pool because these allografts have a higher rate of delayed graft function, more acute rejection episodes, and decreased long-term graft function. Several factors, including prolonged cold ischemia time (CIT), increased immunogenicity, impaired ability to repair tissue and impaired function with decreased nephrons mass may contribute to this (17). But recently, Ojo et al. have demonstrated that the recipients of expanded kidneys receive the benefit of extra life-years when compared to wait-listed dialysis patients (18). Still, placement of these organs is often difficult and delayed, and some centres continue to prefer not to utilize them (19).

Three additional significant donor medical risk factors were identified by the Organ Procurement and Transplantation Network (OPTN): history of hypertension, cerebrovascular accident as a cause of death, and final pre-procurement creatinine $> 133\mu\text{mol/L}$. Donor kidneys were characterized according to combinations of these four parameters, and a relative risk of graft loss was determined for each donor profile. The ECD kidney was precisely defined as any kidney whose relative risk of graft failure exceeded 1.7 when compared to a reference group of ideal donor kidneys i.e those from donors of chronological age 10–39 years, who were without hypertension, who did not die of a cerebrovascular accident, and whose terminal pre-donation creatinine level was $< 133\mu\text{mol/L}$. Using this definition based on the relative risk of graft loss, all donors over age 60 and donors aged 50–59 with at least two of the three medical criteria are identified as ECD (20).

Therefore according to OPTN and United Network for Organ Sharing (UNOS), an Expanded Criteria Donor (ECD) is one which is (21):

- a. 60 years or over

- b. 50-59 years with at least 2 of the following three medical criteria
 - i. Cerebro-Vascular Accident as the cause of death
 - ii. History of hypertension
 - iii. Pre retrieval creatinine more than $133\mu\text{mol/L}$

Classically, donor chronological age has been used as one of the most important predictors of post transplant performance irrespective of concurrent donor or recipient factors. Donor chronological age has therefore been the “Gold Standard” marker for post transplant function since the birth of renal transplantation in the 1950s. It is well known that increasing chronological age is related to poorer performance, however chronologically older kidneys may actually have excellent function for extended periods of time. This is because the kidneys chronological age does not always reflect the extent of cellular damage and hence it’s biological age. Older kidneys may have very few “miles on the biological clock” and perform better. This principle also applies to kidneys from young donors with significant co-morbidities such as hypertension, diabetes, smoking history and death by cerebro-vascular incident. Kidneys from such donors could be allocated to an older population of recipients or possibly rejected for transplantation, should the biological age prove to be significantly raised and hence the importance of a modern scoring system incorporating BoAs.

1.1.4 Serum Creatinine

Creatinine is a breakdown product of creatine phosphate in muscle. Depending on the individuals muscle mass, the rate of production of serum creatinine is approximately constant and falls within a specific range of values ($\sim 80\text{-}120\ \mu\text{mol/L}$). In general, patients with a larger Body Mass Index (BMI) have a higher baseline creatinine value. Men who in general have more muscle mass than women, also have higher serum concentrations. Creatinine is chiefly filtered out of the blood by the kidneys, specifically in the glomerulus and the proximal tubules. There is very little tubular reabsorption and therefore if the filtration system of the kidney is impaired, the level of creatinine in the blood rises. This is used as the cheapest and most effective way of determining an individuals kidney function. The concentration of creatinine in the plasma varies in parallel to that of urea. Urea serves an important role in the metabolism of nitrogen containing compounds by animals and is the main nitrogen-containing substance in the urine of mammals. Further expansion on serum urea and its physiology is not within the scope of this thesis. It is important to

mention however that blood urea concentration and serum creatinine will not be raised above the normal range until 50-75% of total kidney function is lost. Hence, the more accurate Glomerular Filtration Rate or its approximation of the creatinine clearance is measured whenever renal disease is suspected.

1.1.5 Estimated Glomerular Filtration Rate (eGFR)

The Glomerular Filtration Rate (GFR) is traditionally considered the best overall index of renal function in health and disease. Because GFR is difficult to measure in clinical practice, most clinicians estimate the GFR from the serum creatinine concentration, the eGFR. However, the accuracy of this estimate is limited because the serum creatinine concentration is affected by factors other than creatinine filtration (22;23). To compensate for these limitations, several formulas have been developed to estimate GFR and Creatinine Clearance from serum creatinine concentration, age, sex, and body size (24-31). True GFR values are obtained by the inulin method, but this is time consuming and invasive and so not suitable for routine clinical practise. (Reference is made to Chapter 2 of this thesis for methodology of GFR determination)

A GFR of $<60 \text{ mL/min/1.73m}^2$ represents loss of $\geq 50\%$ of kidney function in adults, resulting in an increased rate of Chronic Kidney Disease (CKD) complications (32). A decreased GFR is associated with numerous complications, including hypertension, anaemia, malnutrition, bone disease, neuropathy, and decreased quality of life. All can be prevented or ameliorated by earlier treatment of CKD. Cardiovascular events are more common in patients with CKD (33-36) and CKD appears to be a risk factor for Cerebro-Vascular Disease (CVD). CVD in patients with CKD is treatable and potentially preventable.

In 2000, Levey et al. (37) published the MDRD 4 equation, which uses age, sex, ethnicity, and serum creatinine to predict the GFR:

$$GFR = 186(Cr^{-1.154} \times age^{-0.203}) \times (1.212 \text{ if black}) \times (0.742 \text{ if female})$$

In 2002, the National Kidney Foundation (NKF) revised its practice guidelines for CKD and now recommends the use of a four-variable modification of diet in renal disease

(MDRD 4 equation) or the Cockcroft–Gault equation for creatinine clearance (CL_{cr}) to estimate the glomerular filtration rate and better detect early-onset CKD (32;38).

1.1.6 Urinary Protein Creatinine Ratio

Proteinuria may be a sign of renal damage. Since serum proteins are readily reabsorbed from urine, the presence of excess protein indicates either an insufficiency of absorption, or impaired filtration through the glomerulus. Although the eGFR is considered to be the best overall index of renal function, it is relatively insensitive at detecting early renal disease and does not correlate well with tubular dysfunction (39). The urine protein/creatinine ratio (UPCR) detects total urinary protein due to glomerular and/or tubular pathology (the urine albumin/creatinine ratio detects protein leakage from the glomerulus and has a greater sensitivity than UPCR for low levels of proteinuria). The UPCR is recommended by NICE as a method for quantification and monitoring of proteinuria. Significant proteinuria is usually referred to as a level more than or equivalent to 50mg/mmol (NICE CKD Guidelines 2008)

1.1.7 White Cell Count

The number of white blood cells (WBC) in the blood is often an indicator of disease. There are normally between 4×10^9 and 11×10^{10} white blood cells in a litre of blood, and ranging from 7 and 21 microns in diameter, they make up approximately 1% of blood in a healthy adult. An increase in the number of WBCs or leukocytes over the upper limits is termed leukocytosis, and a decrease below the lower limit is termed leukopenia.

Some medications can have an impact on the number and function of white blood cells. Drugs which can cause leukopenia include immunosuppressive agents used in transplantation such as sirolimus, mycophenolate mofetil, tacrolimus, and cyclosporine. Renal transplant recipients are frequently monitored to assess for changes in total white cell count (WCC). A higher than normal WCC may indicate underlying inflammation or infection. A low WCC may also indicate infection but may also be a sign of over-immunosuppression necessitating a reduction in dose. The drug Mycophenolate Mofetil (an antimetabolite) is frequently implicated with leukopenia and subsequent neutropenia. Patients experiencing acute allograft rejection need potent immunosuppressive agents such as targeted monoclonal antibodies resulting in an increased risk of leukopenia.

1.1.8 Human Leukocyte Antigen System

The human leukocyte antigen (HLA) system, the major histocompatibility complex (MHC) in humans, is controlled by genes located on chromosome 6. It encodes cell surface molecules specialized to present antigenic peptides to the T-cell receptor (TCR) on T cells. MHC molecules that present antigen (Ag) are divided into 2 main classes.

Class I MHC molecules are present on the surface of all nucleated cells and platelets. These polypeptides consist of a heavy chain bound to a β_2 -microglobulin molecule. The heavy chain consists of 2 peptide-binding domains, an Ig-like domain, and a transmembrane region with a cytoplasmic tail. The heavy chain of the class I molecule is encoded by genes at HLA-A, HLA-B, and HLA-C loci. Lymphocytes that express CD8 molecules react with class I MHC molecules. These lymphocytes often have a cytotoxic function, requiring them to be capable of recognizing any infected cell. All nucleated cells express class I MHC molecules and can thus act as antigen-presenting cells for CD8 T cells (CD8 binds to the nonpolymorphic part of the class I heavy chain). Some class I MHC genes encode non classical MHC molecules, such as HLA-G (which may play a role in protecting the fetus from the maternal immune response) and HLA-E (which presents peptides to certain receptors on natural killer cells).

Class II MHC molecules are usually present only on professional Ag-presenting cells (B cells, macrophages, dendritic cells, Langerhans' cells), thymic epithelium, and activated (but not resting) T cells; most nucleated cells can be induced to express class II MHC molecules by interferon (IFN)- γ . Class II MHC molecules consist of 2 polypeptide (α and β) chains; each chain has a peptide-binding domain, an Ig-like domain, and a transmembrane region with a cytoplasmic tail. Both polypeptide chains are encoded by genes in the HLA-DP, -DQ, or -DR region of chromosome 6. Lymphocytes reactive to class II molecules express CD4 and are often helper T cells. With respect to MHC compatibility, a renal transplant match is currently based primarily on HLA locuses A, B and DR, however, ABO incompatibility is no longer a barrier to transplantation (40). The recognised role of CDKN2A in determining renal function post transplant (13;14) paves the way for accurate determination of biological age of the graft prior to implantation and enhanced donor-recipient matching criteria.

1.1.9 Cellular Senescence

Cellular senescence was originally described more than 40 years ago as a process that limited the proliferation of somatic human cells in culture (41). In this seminal paper from Hayflick and Moorhead (1961), it was suggested that normal somatic cells could only escape from senescence by assuming a cancer like phenotype. In addition, it was also suggested that cessation of cell growth in culture, may reflect senescence or ageing *in vivo*. Recent data have confirmed these previous observations - cellular senescence induces cell cycle arrest and is important for tumour suppression, the ageing process itself and beyond simple cellular growth arrest – the emergence of complex senescent phenotypes, as detailed below.

Cellular senescence refers to the essentially irreversible growth arrest that occurs when cells that can divide encounter significant stressor stimuli. With the possible exception of embryonic stem cells (42) most division-competent cells, including some tumour cells, can undergo senescence when appropriately stimulated (43;44). Causes of senescence are multifactorial. It is widely established that the limited growth of human cells in culture is due in part to telomere attrition. Telomeric DNA is lost with each S phase because DNA polymerases are unidirectional and cannot prime a new DNA strand, resulting in loss of DNA near the end of a chromosome – “the end replication problem”; additionally, most cells do not express telomerase, the specialized enzyme that can restore telomeric DNA sequences *de novo* (45;46). Eroded telomeres also generate a persistent DNA damage response (DDR), which initiates and maintains the senescence growth arrest (47-50).

Many cells senesce when they experience strong mitogenic signals, such as those delivered by certain oncogenes (51-54) or when damage to the structure of DNA is detected, particularly DNA double strand breaks (55-57). Thus, many senesce-inducing stimuli cause a certain degree of genomic damage. Senescent cells are not quiescent or terminally differentiated cells, although the distinction is not always straightforward. Senescent cells in fact, display several phenotypes, which, in aggregate, define the senescent state. In addition, the expression of CDKN2A is characteristic of most cells in this state and other cells with neoplastic transformation.

The content of this thesis attempts to elucidate such hallmarks of senescence and relates them primarily to organ function following kidney transplantation.

Salient features of senescent cells are generally (but not limited) to the following:

- Late senescence growth arrest is essentially permanent and cannot be reversed by known physiological stimuli. Senescence is reversible if the state is early senescence (58;59).
- Senescent cells increase in size, sometimes enlarging more than twofold relative to the size of non-senescent counterparts (60).
- Senescent cells express Senescence Associated Beta Galactosidase (61), which partly reflects the increase in lysosomal mass (62).
- Most senescent cells express CDKN2A, which is not commonly expressed by quiescent or terminally differentiated cells (53;63-66).
- There is generally increased telomere attrition in relation to the senescence state.
- In some cells, CDKN2A, by activating the pRB tumour suppressor, causes formation of senescence-associated heterochromatin foci (SAHF), which silence critical pro-proliferative genes (67).
- Senescent cells with persistent DDR signalling secrete growth factors, proteases, cytokines, and other factors that have potent autocrine and paracrine activities (68-71). This is known as the senescence-associated secretory phenotype (SASP).

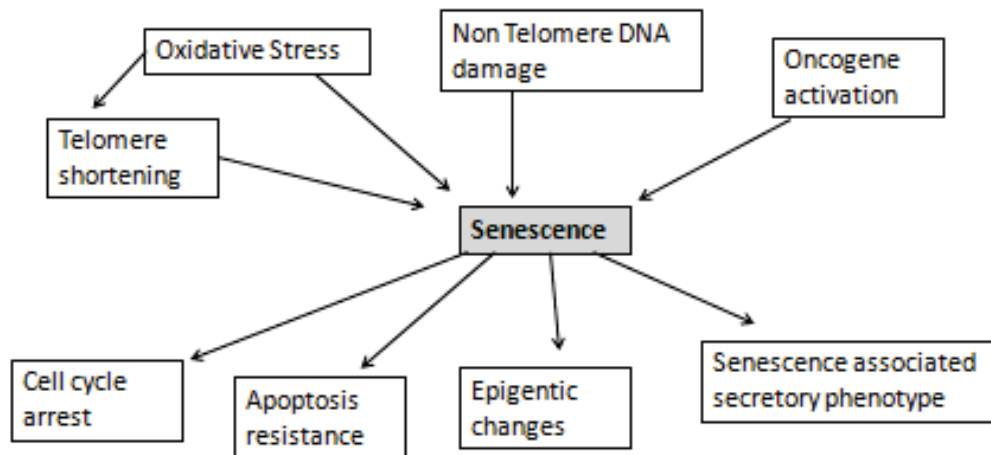


Figure 1.1 Diagram depicting primary causes and consequences of cellular senescence

It has become increasingly clear that cellular senescence is a crucial anticancer mechanism that prevents the growth of cells at risk for neoplastic transformation. The stimuli that elicit a senescence response all have the potential to initiate or promote carcinogenesis. Moreover, to form a lethal tumour, cancer cells must acquire a greatly expanded growth potential and ability to proliferate while expressing activated oncogene (72) traits that are suppressed by the senescence program.

Further to the above, cellular senescence depends critically on two powerful tumour suppressor pathways: *the p53 and pRB/p16INK4a pathways* (43;48;52;70-80). Both pathways integrate multiple aspects of cellular physiology to determine and orchestrate cell fate. In humans and mice, most, if not all, cancers (43;48;52;73-83) harbour mutations in one or both of these pathways. Moreover, defects in either pathway compromise cellular ability to undergo senescence, and greatly increase organismal susceptibility to cancer.

Dismantling the senescence response by inactivating p53 causes a striking acceleration in the development of malignant tumours (75). In addition, some tumour cells retain the ability to senesce (44), and do so in vivo in response to chemotherapy for example (70;82) or, in some tissues, after reactivation of p53 (84;85). In these cases, the senescence response is associated with tumour regression. It is interesting to note that the regressing tumour elicits an inflammatory response that stimulates the innate immune system, which in turn eliminates the senescent cells.

Although still debatable, studies argue that cellular senescence restrains cancer by imposing a block to the proliferation of damaged/stressed cells (86). It is surprising, then, to see that senescent cells also can promote cancer progression. Even though senescence per se is closely associated with cancer, it is not within the scope of this thesis to focus on the cancer phenotypic pathway; instead an increased emphasis of senescence in relation to ageing and organ function will be reviewed in more detail. Albeit, because all pathways are very closely related, a brief mention on senescence and tumour progression will ensue precisely because the idea of senescence causing tumourigenesis seems paradoxical and a very brief explanation is thus merited.

Firstly, it is important to remember that cancer is primarily an age-related disease (87;88). Age is the largest single risk factor for developing a malignant tumour, and cancer incidence rises approximately exponentially after about age 50 in humans. In these respects, cancer is very similar to the degenerative diseases of ageing. How the senescence response actually promotes cancer in later life is still debatable. Senescent cells increase with age in a variety of mammalian tissues (61;89-93). It is not known whether this rise is caused by increased generation, decreased elimination, or both. Whatever the genesis, the age-related increase in senescent cells occurs in mitotically competent tissues, which, of course, are those that give rise to cancer.

Second, the senescent associated secretory phenotype (SASP) can affect the behaviour of neighbouring cells. Strikingly, many SASP factors are known to stimulate phenotypes associated with aggressive cancer cells (70;94). Senescent cells also secrete high levels of interleukin 6 (IL-6) and interleukin 8 (IL-8), which can stimulate premalignant and weakly malignant epithelial cells to invade a basement membrane (69).

It has also been shown through the work of several groups that senescent cells can stimulate tumourigenesis in vivo. Senescent, but not non-senescent, fibroblasts stimulate

pre-malignant epithelial cells, which do not ordinarily form tumours, to form malignant cancers when the two cell types are co-injected into mice (95). Further, co-injection of senescent, but not non-senescent, cells with fully malignant cancer cells markedly accelerates the rate of tumour formation in mice (70;95-98). Thus, at least in mouse xenografts, senescent cells have been shown to promote malignant progression of precancerous, as well as established cancer cells, *in vivo*.

In summary therefore, senescent cells arrest growth owing to cell intrinsic mechanisms, imposed by the p53 and pRB/p16INK4a tumour suppressor pathways, and cell non-intrinsic mechanisms, imposed by some of the proteins that comprise the SASP. The growth arrest is the main feature by which cellular senescence suppresses malignant tumourigenesis but can contribute to the depletion of proliferative (stem/progenitor) cell pools. Additionally, components of the SASP can promote tumour progression, facilitate wound healing, and, possibly, contribute to ageing.

1.1.10 Cellular Senescence and Age Related Diseases

In most age-related diseases, normal cellular/tissue functions fail and thus, most age-related pathologies are degenerative in nature. Cancer in contrast requires the cell to assume a completely new phenotype and can hardly be considered a degenerative process. There is increasing evidence that cellular senescence contributes to ageing and age-related diseases other than cancer.

Among the more compelling evidence that senescent cells can drive degenerative ageing pathologies are the phenotypes of transgenic mice with hyperactive p53. Two landmark papers described mouse models with induced, chronically elevated p53 activity (99;100). These mice were exceptionally cancer-free (as expected) since p53 is a critical tumour suppressor. What was surprising was their shortened life span and premature ageing. Notably, cells from these mice underwent rapid senescence in culture (99). Moreover, tissues from these mice rapidly accumulated senescent cells, and, in lymphoid tissue, the p53 response shifted from primarily apoptotic to primarily senescent *in vivo* (101). Thus, there was a strong correlation between excessive cellular senescence and premature ageing phenotypes.

In all these (and other) models of both accelerated and normal ageing, it is important to note that the crucial roles for the p53 and/or pRB/p16INK4a pathways are not singular. There is mounting evidence that these pathways interact and modulate each other (102-105).

Although these mouse models and other findings indicate a strong association between ageing phenotypes, certain pathologies and cellular senescence, other processes undoubtedly also contribute to ageing and age-related disease. One such process is cell death. In addition, some cells in ageing organisms simply lose functionality, which certainly also contributes to ageing phenotypes. Neurons, for example, lose the ability to form synapses, despite cell bodies remaining viable, which is an important component of many neurodegenerative pathologies (106). Likewise, cardiomyocytes lose synchronicity of gene expression, which almost certainly affects heart function (107).

So how is it that senescent cells promote age related pathologies? and in particular relevance to renal transplantation, how is it that senescence contributes to impaired renal function several months or years after implantation?

There are currently three theories that may explain this phenomenon:

Firstly, as suggested by Liu et al. (98), cellular senescence can deplete tissues of stem or progenitor cells. This depletion will compromise tissue repair, regeneration, and normal turnover, leading to functional decrements (108). Secondly, the factors that senescent cells secrete affect vital processes, such as cell growth and migration, tissue architecture, blood vessel formation and differentiation, so are tightly regulated. The inappropriate presence of these factors can disrupt tissue structure and function. Thirdly, the SASP includes several potent inflammatory cytokines (109). Low-level, chronic, “sterile” inflammation is a hallmark of ageing that initiates or promotes most, if not all, major age-related diseases (110;111). Chronic inflammation can destroy cells and tissues because some immune cells produce strong oxidants. Also, immune cells secrete factors that further alter and remodel the tissue environment, which can cause cell/tissue dysfunction and impair stem cell niches. As will be shown in the results section to this thesis, increased donor chronological age and extended criteria kidneys are associated with lower white cell counts at six, twelve and twenty four months post transplant. The reason behind this most probably attributed to increasing doses of immunosuppression administered to counteract clinical or subclinical

rejection episodes, as a result of transplanted organs with increased background inflammatory oxidative damage.

Concrete evidence that senescence drives the ageing process remains contentious however. Studies have shown that organisms in which cells fail to undergo senescence do not live longer; rather, they die prematurely of cancer (81). Several other studies are ongoing to elucidate cause and effect in this particular field (112).

Surprisingly, it has recently been shown that the senescence response may have a role in tissue repair. The SASP is associated with the secretion of growth factors and proteases that participate in wound healing, attractants for immune cells that kill pathogens, and proteins that mobilize stem or progenitor cells. Thus, the SASP may serve to communicate cellular damage/dysfunction to the surrounding tissue and stimulate repair, if needed (113;114). It could be that this new senescence associated function in tissue repair is suggesting that the growth arrest was selected during evolution to suppress tumourigenesis, and possibly excessive cell proliferation or matrix deposition during wound repair.

In summary therefore, cellular senescence seems to be a part of four complex processes (tumour suppression, tumour promotion, ageing, and tissue repair), some of which have apparently opposing effects. Upon experiencing a potentially oncogenic insult, cells assess the stress and must “decide” whether to attempt repair and recovery, or undergo senescence. After an interval or “decision period”, the length of which is imprecisely known, the senescence growth arrest becomes essentially permanent, effectively suppressing the ability of the stressed cell to form a malignant tumour.

One early manifestation of the senescent phenotype is the expression of cell surface-bound IL-1 α (115). This cytokine acts in a juxtacrine manner to bind the cell surface-bound IL-1 receptor, which initiates a signalling cascade that activates transcription factors (NF- κ B, C/EBP β). The transcription factors subsequently stimulate the expression of many secreted (SASP) proteins, (68;71;109) including increasing the expression of IL-1 α and inducing expression of the inflammatory cytokines IL-6 and IL-8. These positive cytokine feedback loops intensify the SASP until it reaches levels found in senescent cells. SASP components such as IL-6, IL-8, and Matrix Metalloproteinases (MMPs) can promote tissue repair, but also cancer progression. Some SASP proteins, in conjunction with cell surface ligands and adhesion molecules expressed by senescent cells, eventually attract immune cells that kill and clear senescent cells. A late manifestation of the senescent phenotype is the expression

of microRNAs (mir-146a and mir-146b), which tune down the expression IL-6, IL-8, and possibly other SASP proteins. MicroRNAs (miRNA) are non-coding, single-stranded RNA molecules that are involved in the regulation of a variety of biological processes, including embryogenesis, differentiation, and senescence. The CDKN2 locus is complex, comprising a series of developmentally and epigenetically regulated transcript isoforms. We have demonstrated that transcriptional regulation of CDKN2 isoforms by certain miRNAs are able to predict the functional status of renal allografts up to six months post transplant. We have also demonstrated an association with rejection episodes and have proved an association between certain miRNA levels and increasing cold ischaemic time (CIT) (McGuinness et al, Sci Trans Med. In submission). The data from this research indicates that miRNA profiling has clear potential to be used for pre transplant assessment of post transplant allograft function.

The reason for which certain miRNAs tune down the expression of senescence associated interleukins is not really understood but is primarily believed to prevent the SASP from generating a persistent acute inflammatory response (116). Despite this dampening effect, the SASP can nonetheless continue to generate low level chronic inflammation.

The accumulation of senescent cells that either escape or outpace immune clearance and express a SASP at chronic low levels is hypothesized to drive ageing phenotypes. Thus, senescent cells, over time, develop a phenotype that becomes increasingly complex, with both beneficial (tumour suppression and tissue repair) and deleterious (tumour promotion and ageing) effects on the health of the organism.

1.1.11 Senescence and the Kidney

Ageing is associated with renal structural changes and functional decline. The age-related loss of renal parenchyma approximates 10% per decade of increasing age (117). This loss is accompanied by a decrease in renal plasma flow (118-121) and tubular dysfunction (122). The average age related loss in glomerular filtration rate (GFR) is reported as 0.40–1.02 ml/min per year (123-125) and has been attributed to a reduced number of functioning glomeruli and an increased number of sclerotic glomeruli (126).

The kidney is one of the organs that ages fastest, and expression of senescence markers have been shown to correlate best with renal ageing and function (13;14). Classically, organs from older donors show poorer function post transplant and have a decreased

lifespan. Although this holds true in most cases, there are times when such organs perform excellently and last beyond their life expectancy. The theory put forward from the results of this thesis indicate that such variation in organ function could be attributed to the difference in biological age. In fact, the data shows that CDKN2A is the single, strongest biomarker of ageing (BoA) for renal function up to 1 year post operative.

Although the assay used in this thesis targeted specifically the CDKN2A transcript of the CDKN2 locus, a recognized limitation of a typical CDKN2A assay is the inability to discriminate between the two CDKN2 locus transcripts corresponding to the cognate proteins for p16INK4A and p14ARF. Both transcripts share a common functionality in cell cycle G1 control (105;127) and therefore studies determining the contribution p14ARF to transplant outcome and function will be of great interest.

1.1.12 Biomarkers of Ageing

A valid biomarker of ageing must demonstrate variation of sufficient magnitude in short-term longitudinal or in cross-sectional studies to be of predictive value within a population or cohort with regard to physiological capacity at a later chronological age. Indeed, it was Baker and Sprott who coined the most accurate definition for a true biomarker of ageing (BoA) (125)

“A biological parameter of an organism that either alone or in some multivariate composite will, in the absence of disease, better predict functional capacity at some later age than will chronological age”

To date very few biomarkers of ageing have been tested (128), namely Senescence Associated β Galactosidase (SA- β -GAL), advanced glycation end products, lipofuscin etc. However, only 2 have been conclusively validated in the literature: Cyclin Dependant Kinase 2A (CDKN2A) and telomere length (13;14).

1.1.13 Telomeres

Traditionally, bio-ageing has been assessed through a measurement of telomere length. Telomeres are nucleo-protein complexes with a DNA component consisting of a simple repeat sequence (TTAGGG)_n and are approximately 8-11 kilo base pairs long, decreasing

by approximately 30% throughout the human lifespan (129). They are found at the end of each chromosome and shorten in normal dividing cells because of the “end replication problem”. The primary role of telomeres is to provide stability and protection of chromosomes (130). The proteins maintaining the structure of the telomere, also function in sensing, signalling and repair of DNA damage as will be discussed below.

1.1.14 The Structure and Function of Telomeres

Besides the (TTAGGG)_n repeat sequence, telomeres possess an obligate single-stranded 3 end overhang, measuring a few hundred nucleotides (131). The single-stranded overhang can fold back on the double-stranded telomere to form what is called the t-loop (132). Double-stranded telomere sequences are bound directly by two sequence-specific DNA binding proteins TRF1 (telomeric repeat binding factor 1) and TRF2 (telomeric repeat binding factor 2), which in turn interact with a larger number of proteins.

TRF2 is critical for telomere end protection and can facilitate formation of the t-loop conformation. Disruption of TRF2 leads to loss of the protective capped structure, resulting in a change of conformation in the 3 end overhang and loss of chromosome ends (133;134). TRF1 can serve to modulate telomere length, but it also serves to facilitate DNA replication through the telomere repeats, which act as fragile DNA sites (135;136). TRF1 and TRF2 each interact with a common factor - TIN2 (TRF1- interacting nuclear factor) (8), which form part of a six-member complex, termed shelterin, that also includes POT1 (protection of telomeres protein 1) and TPP1 (tripeptidyl peptidase I) (137).

TRF2-interacting protein as its name suggests, is a TRF2 interacting factor which is recruited to telomeres through its interaction with TRF2 and where it may act to aid in repression of non-homologous end joining (138;139). TIN2 itself also interacts with the subcomplex of shelterin that binds the single-stranded overhang - TPP1 and POT1, two oligonucleotide/ oligosaccharide binding (OB)-fold containing proteins (140-142).

POT1 directly binds the single-stranded telomere sequences and interacts directly with TPP1. POT1 and TPP1 serve a role in protecting the single-stranded portion of the telomere because loss of POT1 impairs telomere capping (143-146). In addition, POT1 and TPP1 can control telomerase action at telomeres. Overexpression of POT1 leads to telomere shortening by inhibiting telomerase action at the telomere (147). In contrast, POT1 and TPP1 in vitro serve as potent enhancers of telomerase (148;149), thus this

single-stranded telomere complex serves an important role in regulating telomerase at the telomere.

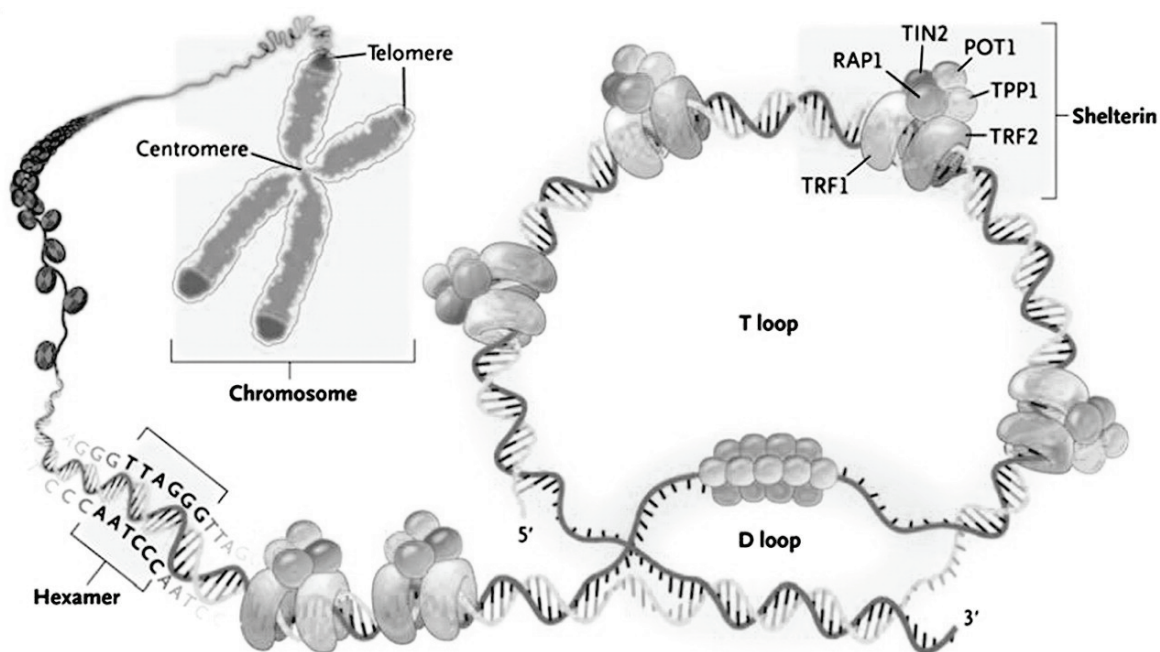


Figure 1.2 Mammalian telomere structure and microscopic appearance

A simplified diagram of telomere structure and subcellular location. Telomeres are located at the ends of linear chromosomes; in humans, they are composed of hundreds to thousands of tandem DNA repeat sequences: hexameric TTAGGG in the leading strand and CCCTAA in the lagging strand. Additional protective proteins are also associated with telomeric DNA and are collectively called shelterin (TRF1, TRF2, TIN2, POT1, TPP1). The 3' end of the telomeric leading strand terminates as a single-stranded overhang, which folds back and invades the double-stranded telomeric helix. (Figure adapted from: Calado RT, Young NS. Telomere diseases. *N Engl J Med.* 2009;361:2353–2365)

1.1.15 The “End Replication Problem”

The so-called "end-replication" problem applies primarily to somatic cells and is a direct consequence of DNA polymerase's biochemical properties (Figure 1.3). DNA polymerase requires short RNA primers to initiate replication, and it then extends the primers in a 5'-to-3'-direction. Thus, as the replication fork moves along the chromosome, one of the two daughter strands is synthesized continuously. The other daughter strand, known as the lagging strand, is synthesized discontinuously in short fragments known as Okazaki fragments, each of which has its own RNA primer. The RNA primers are subsequently degraded, and the gaps between the Okazaki fragments are then filled in by the DNA repair machinery. A problem arises at the end of the chromosome, however, because the DNA repair machinery is unable to repair the gap left by the terminal RNA primer. Consequently, the new DNA molecule is shorter than the parent DNA molecule by at least the length of one RNA primer.

The ends of telomeres in germline and immortal cell populations are replicated by the enzyme telomerase, a specialised ribonucleoprotein. Here, it functions to maintain a constant telomere length. In human cells, shortening of telomeres is fundamental to replicative senescence and is considered to be an anti-neoplastic mechanism (150). Indeed, unrestrained telomere attrition can expose chromosome ends, trigger cell cycle checkpoints and lead to a senescent state (151) (M1 in Figure 1.4). Cells that are driven to continue dividing by abnormal stimuli develop massive genomic instability or crisis (M2 in Figure 1.4). Germline cells and immortal cell populations like most cancer cell lines possess mechanisms (telomerase activation or an alternative mechanism) to preserve their telomere length indefinitely despite cell division, thus protecting their genome (152).

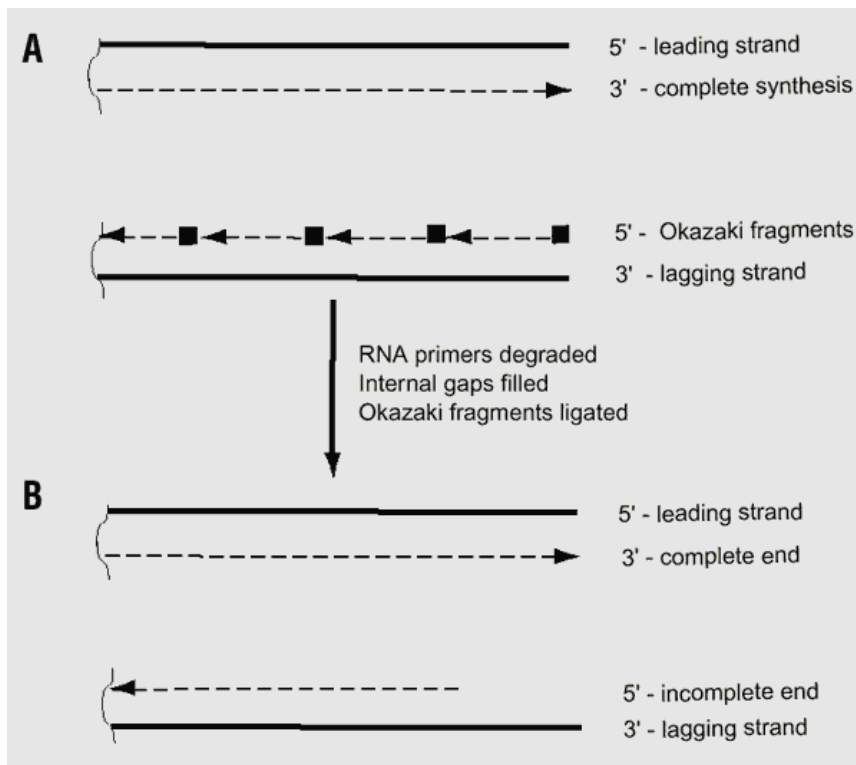


Figure 1.3 The “End Replication Problem”

The 3'–5' leading strand (above) is copied continuously to the end of the DNA molecule using DNA polymerase; the 5'–3' lagging parental strand (below) is copied in discontinuous Okazaki fragments initiated by labile RNA fragments (black boxes). The RNA primers are degraded, the internal gaps are filled, and the Okazaki fragments ligated. The terminal gap is not filled, leaving an unreplicated terminal region varying between the size of the RNA primer and the Okazaki fragment. The function of telomerase is to fill the terminal gap in the telomere. If telomerase is not present, as is generally true for human cells *in vitro*, the 5' end of the progeny strand is shortened every time the cell divides and DNA is replicated, eventually resulting in cessation of division.

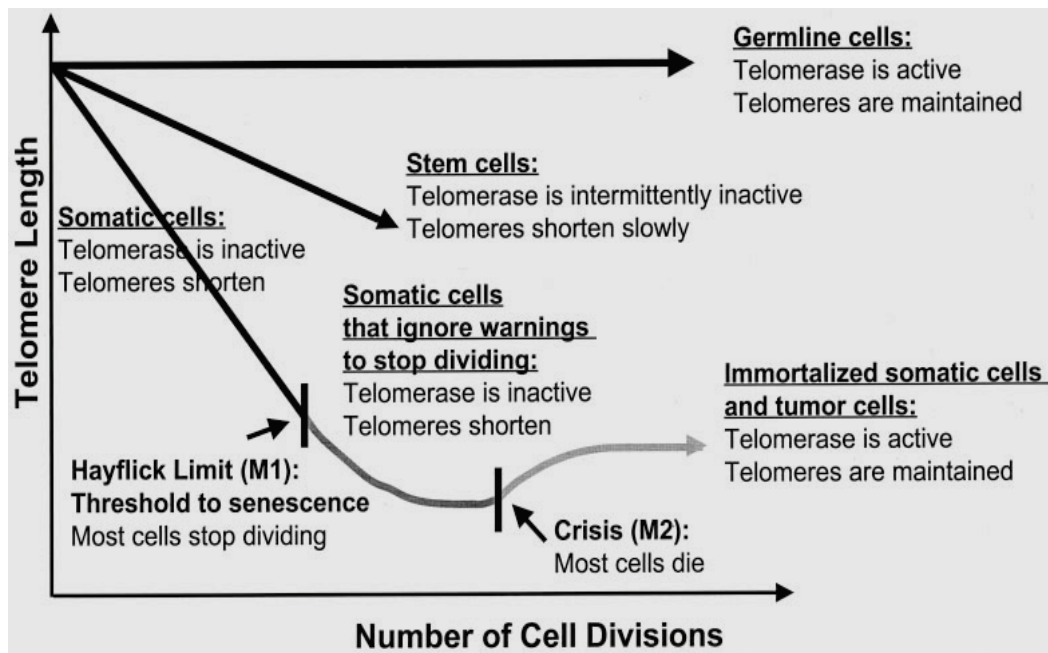


Figure 1.4 Telomeres, Hayflick limit and Crisis

Telomerase is active in germline cells, maintaining long stable telomeres, but is repressed in most normal somatic cells, resulting in telomere loss in dividing cells. At M1, the Hayflick limit, there is a presumed critical telomere loss in one or perhaps a few chromosomes signalling irreversible cell cycle arrest. This corresponds to the phenotype of replicative senescence. Transformation events may allow somatic cells to bypass M1 without activating telomerase. When chromosomes become critically short on a large number of telomeres, cells are genomically unstable and enter crisis (M2). Rare clones that activate telomerase escape M2, stabilize their genome, and acquire indefinite growth capacity. (Figure adapted from: Melk and Halloran – Cell Senescence and its implications for nephrology, J Am Soc Nephrol 12: 386, 2001)

The term cellular senescence was coined by Hayflick and Moorhead who described the phenomenon that human diploid fibroblasts have a limited proliferative capacity in culture (41). After 50–70 generations, human fibroblasts show a permanent and irreversible growth arrest change in cell morphology. Subsequently, it was shown that replicative senescence occurs as soon as telomeres become critically shortened (46). Bodnar et al showed how telomerase, an enzyme that maintains telomere length, is able to rescue fibroblasts from replicative senescence (45). As the majority of human cells do not express telomerase, their ability to divide is therefore limited to a certain threshold (Hayflick number). If telomeres become critically short, they have the potential to unfold from their presumed closed structure, this may precipitate chromosomal fusions. The cell may detect this uncapping as DNA damage and then either stop growing (entering senescence), or begin programmed self-destruction (apoptosis). Alternatively, the cell may enter a state of immortality, depending on the cell's genetic background/p53 status (153) (Figure 1.5).

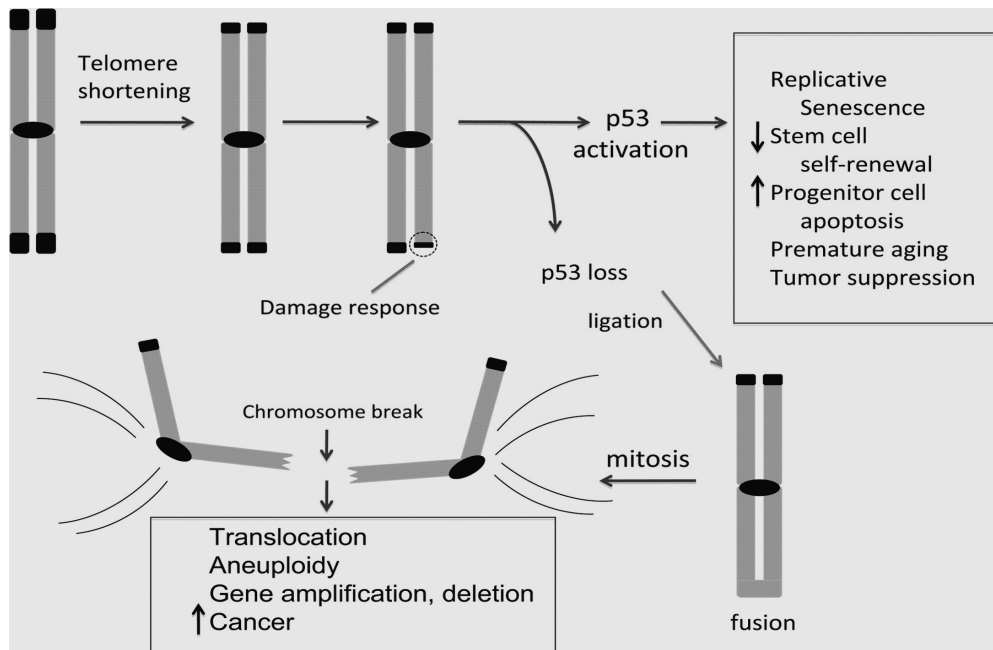


Figure 1.5 Critical telomere shortening and p53

Telomere shortening activates p53 and drives formation of epithelial cancers through gene amplification and deletion. Telomeres shorten progressively with cell division due to the end-replication problem in cells with no telomerase. Critical telomere shortening compromises the telomere cap and results in a DNA damage response that activates the p53 tumour suppressor protein. This activation of p53 induces replicative senescence in cultured human fibroblasts, impairs stem cell self renewal, induces apoptosis in tissue progenitor cells, causes premature ageing and strongly suppresses tumour formation. If p53 is mutated or deleted, these responses to telomere dysfunction are mitigated and chromosomal fusions are tolerated. Chromosome breakage subsequently occurs predisposing to translocations, deletions and amplifications with resultant carcinogenesis. (Adapted from: Artandi and DePinho – Telomeres and telomerase in cancer, *Carcinogenesis* Vol.31 no.1 pg 10, 2010)

Paradoxically therefore, an age-related decline in telomere length may promote genetic instability and increase the risk of malignancy (154). This is associated with an increase in oxidative damage accruing in biologically ageing tissues. Organs deteriorate as more and more of their cells die off or enter cellular senescence. A wide range of different diseases exhibit accelerated telomere attrition including psychological, cardiovascular, neurodegenerative, renal, osteo- and hepatic diseases (1;4;155-160). With respect to patients in end stage renal failure (ESRF), Carrero and colleagues, first showed that shortened telomere length is associated with higher levels of DNA damage (8-OH-dG) and increased mortality in haemodialysis patients (161). These findings were independent of age and gender which may be considered strong confounders for telomere length in humans (162). Such data proves invaluable as a means of progression to studies in enhancing the quantity of kidneys available for transplantation. Interestingly, the latter study also confirmed observations by Nawrot et al that females show less age related telomere attrition. They hypothesize that oestrogen may directly or indirectly exert protective effects on telomere length due to its anti inflammatory and anti oxidant properties (155;163;164).

Replicative senescence and critical telomere attrition result in the activation of a number of cyclin dependent kinase inhibitors. Typically, p21 expression is elevated following acute oxidant insult followed by elevation of CDKN2A (p16INK4a) expression, necessary for the maintenance of the senescent state (165).

1.1.16 Senescence and STASIS

In addition to progressive telomere shortening (leading to replicative senescence as detailed above), telomere dysfunction can be initiated by a change of state (uncapping) that leads to a rapid induction of growth arrest. This is also termed senescence (44;54;61;166-179). As depicted above, when the telomeric DNA structure or sequence is altered, or telomere proteins are depleted or mutated, cells undergo chromosome end-associations and fusions leading to growth arrest or death. This growth arrest is similar to telomere based replicative senescence in most, but not all, regards. For example, in both types of growth arrest a) cells cannot divide even if stimulated by mitogens b) cells remain metabolically active and c) cells show characteristic changes in morphology.

It has been shown that growth inhibitory genes can be activated in cell culture and in vivo due to a variety of environmental stresses in a process called “Stress or Aberrant Signaling Induced Senescence” - STASIS (also called premature senescence, culture shock and stress-induced senescence) (44;53;168;178;179). While cells undergoing replicative senescence can be immortalized by expression of hTERT (telomerase reverse transcriptase – a catalytic subunit of the enzyme telomerase) to maintain telomere homeostasis, this does not occur in cells undergoing growth arrest due to STASIS (167;169;171-173). This has led many authors to follow a simple definition for replicative senescence to be: ‘Growth arrest under adequate culture conditions if telomeres are rate-limiting for continued cell proliferation and hTERT can directly immortalize the cells.’ It is important to make this distinction as the triggering agents are different (short telomeres versus a stress or damage-induced signaling pathway that may or may not involve telomeres i.e telomere dependant or telomere independent).

STASIS may be an evolutionarily conserved mechanism that helps guard cells against oncogenic insults. It would be advantageous to prevent normal and pre-cancerous cells from proliferating if placed in an inappropriate environment (e.g. not receiving the proper mitogens or other signals from their neighbors), or following stresses likely to induce multiple mutations (44). Treatment of most types of tumour cells with conventional anticancer therapies activates DNA damage-signaling pathways and can induce a rapid onset of STASIS. Another example of the induction of STASIS apart from oncogenic stimuli or cancer treatment is the cellular response to oxidative damage (44;179). Of particular importance is the fact that in these instances, the expression of hTERT does not result in the bypass of STASIS, thus demonstrating that this type of growth arrest does not involve counting cell replications (e.g. telomere-based replicative senescence) (53;54;61;166-179).

In both replicative senescence and STASIS, the initiating event can be triggered by similar mechanisms including recognition by cellular sensors of DNA double-strand breaks leading to the activation of cell-cycle checkpoint responses and recruitment of DNA repair foci. There is much research underway trying to elicit the diverse signaling pathways that cause cells, in some contexts, to undergo replicative senescence and in other contexts to initiate STASIS or apoptotic signaling programs.

1.1.17 Cyclin Dependant Kinase 2A - CDKN2A

CDKN2A plays an important role in regulating the cell cycle, and mutations in this gene increase the risk of developing a variety of cancers. Increased expression of CDKN2A at the cellular level, is a robust marker of the senescent state and has also been shown to reduce the proliferation of stem cells (180). The amount of CDKN2A increases dramatically as tissue ages in both humans and rodents (181-185) and could potentially be used as a test that measures how fast the body's tissues have aged at a cellular level. This would be of enormous significance to the transplant community in particular, by allowing for enhanced screening methods in the selection of kidneys from chronologically older and marginal donors.

1.1.18 CDKN2A functions in vitro and in vivo

Senescence is a tumour suppressor mechanism, and many cancers contain cells that have escaped from senescence to become immortalized. Immortalization is associated with loss of normal function of the tumour suppressor locus, CDKN2A. Two proteins, CDKN2A (p16INK4A) and CDKN2A isoform 4 (p14ARF in humans; p19ARF in rodents), are encoded by this locus (186).

CDKN2A is a specific inhibitor of cyclin dependent kinase 4 (cdk4) and cyclin dependent kinase 6 (cdk6), which participate in the cyclin D-dependent phosphorylation of the retinoblastoma susceptibility gene product, Rb (187). Hypophosphorylated pRB acts with E2F proteins to repress transcription of genes necessary for the G₁-S phase transition. Hyperphosphorylation of Rb inactivates its growth-suppressive properties, allowing cells to enter S phase.

P14ARF is an alternate reading frame (ARF) product of the CDKN2A locus. Therefore, both CDKN2A and p14ARF are involved in cell cycle regulation. p14ARF inhibits murine double minute (mdm2), thus promoting p53, which promotes p21 activation, which then binds and inactivates certain cyclin-CDK complexes, which would otherwise promote transcription of genes that would carry the cell through the G₁/S checkpoint of the cell cycle. Loss of p14ARF by a homozygous mutation in the CDKN2A gene will lead to

elevated levels of mdm2 and, therefore, loss of p53 function and eventual loss of cell cycle control. Mdm2 is therefore an important negative regulator of the p53 tumour suppressor (188).

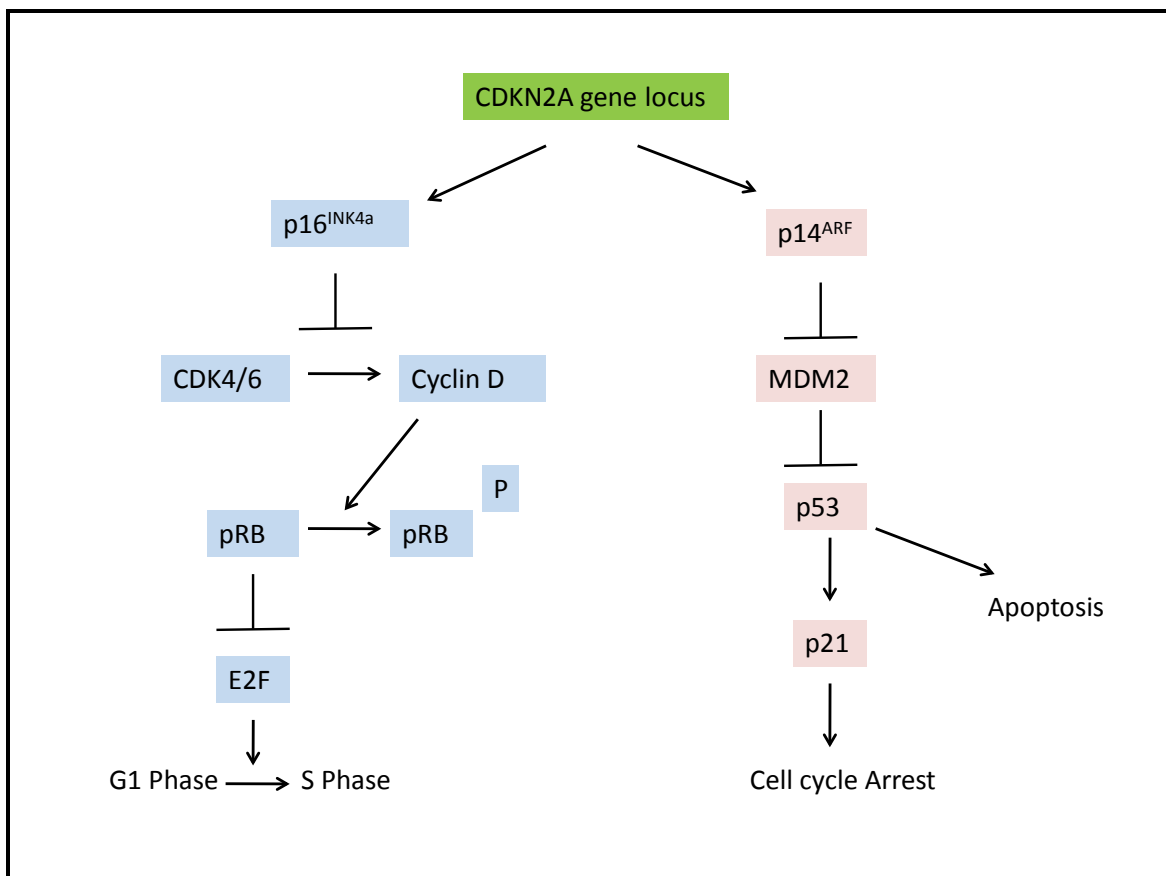


Figure 1.6 Pathways controlled by the CDKN2A locus

The CDKN2A gene locus encodes two proteins p16INK4a and p14ARF in humans. In the p16 pathway, high levels of p16 inhibit the conversion of Cyclin Dependent Kinases 4 & 6. This enables product of Retinoblastoma (pRB) to remain hypophosphorylated and therefore interacts with E2F to inhibit cell cycle progression. Conversely, low levels of p16 would allow activation of Cyclin D which hyperphosphorylates pRB and allows E2F to promote cell cycle progression. In the p14 pathway, high levels of p14 would inhibit MDM2. Low levels of MDM2 would allow for uninhibited and therefore greater levels of p53 leading to apoptosis directly and activation of p21 pathway leading to cell cycle arrest.

1.1.19 CDKN2A, Tumour Suppression and the Senescent Phenotype

Several lines of evidence indicate that CDKN2A is a tumour suppressor. Firstly, its gene maps to 9p21, a chromosomal locus rearranged in many human cancers (189). Secondly, CDKN2A is commonly deleted, mutated, or hypermethylated and transcriptionally silenced in tumours that retain wild-type Rb, and ectopic expression of CDKN2A in these cells at high levels results in G1 arrest (190-195). Furthermore, CDKN2A-deficient mice are susceptible to several types of malignancies (196), and germ line mutations of CDKN2A in humans are associated with familial syndromes involving malignant melanoma and pancreatic cancer (197-200).

The precise mechanism by which CDKN2A exerts its tumour suppressive effects is less clear. One straightforward suggestion is that inactivation of CDKN2A is required for malignant cells to enter S phase efficiently. However, many normal cells express CDKN2A throughout G1 and are able to proliferate, suggesting that other mechanisms of tumour suppression must be operating. An alternative mechanism involves the link between CDKN2A expression and cellular senescence (63;65;196;201). As fibroblasts or epithelial cells age, CDKN2A levels increase dramatically, and it has been proposed that loss of CDKN2A expression is required for cells to escape senescence during their progression to malignancy. Another possibility is that CDKN2A plays a role in the maintenance of genome integrity (202). Frequently, following DNA damage, normal cells arrest their proliferation at cell cycle checkpoints, the most prominent of which occur at the G1-S and G2-M boundaries. Arrest allows time for repair prior to continued cell cycle progression. One G1 arrest checkpoint is controlled by p53 (203;204). In response to DNA damage, p53 levels increase by a post-transcriptional mechanism, resulting in the transcriptional activation of p21, a universal inhibitor of cyclin-dependent kinases, which can mediate G1 arrest (205-207). Inactivation of p53 is the most common genetic event in human cancer, suggesting that loss of a DNA damage induced G1 checkpoint is an essential step in tumour progression. This allows damaged DNA to be replicated, which leads to the accumulation of additional mutations and the eventual emergence of a malignant clone.

1.1.20 Telomeres, p16, p21 and senescence

Many senescence inducing stimuli cause genomic damage or epigenomic disruption. Besides increased expression of CDKN2A (p16INK4a), the limited growth of human cells in culture is due in part to telomere erosion. Also, many cells senesce when they experience strong mitogenic signals, such as those delivered by certain oncogenes or highly expressed pro-proliferative genes (51-54).

Senescence is not a static condition. Stein et al (1999), postulated different age related patterns of accumulation of CDKN2A and p21 in Human Diploid Fibroblasts (HDFs). Because p21 and CDKN2A have very different age-related patterns of accumulation in HDFs, they proposed that replicative senescence in HDFs comprises two events: an increase in p21 that is driven by the “mitotic clock” and an upregulation of CDKN2A as part of a program of differentiation that is turned on in senescent cells.

Firstly, the progressive age-dependent accumulation of p21 suggests that it occurs as a consequence of replication related processes such as telomere shortening (46), DNA demethylation (208), and the effects of DNA damage (209;210). It results in inactivation of all G1 cyclin-Cdks, such that pRb fails to be phosphorylated, E2F transcription factors are not released, late-G1 genes necessary for DNA synthesis are not expressed, and the cells become irreversibly arrested in G1 phase.

Secondly, they hypothesized that at senescence a program of differentiation is initiated that involves the accumulation of CDKN2A, as well as changes in the morphology, size, and functional attributes of the cells (61;63;65;211-215). The concomitant decline of p21 from its peak in early senescence could occur owing to decay of the replication-related signals that drove its increase as the cells were ageing, or p21 might be down regulated as a necessary part of the putative differentiation program. Consequently, in late senescent cells Cdk inactivation and the cell cycle arrest are maintained through the combined effect of CDKN2A and p21. A further explanation of this is found in Chapter 2 of this thesis.

The kidney itself is potentially, an ideal marker for the measurement of human senescence. Most studies would agree that there is an age dependant decline in renal function (GFR). In fact, GFR descent usually begins around 30 to 40 years of age and appears in both males

and females. This finding has also been reproduced in the animal model presented in chapter 2 of this thesis. In humans, the average rate of decline in GFR averages about 0.8mL/min/1.73m² after age 30. There have also been suggestions that the decline in GFR accelerates after age 65 to 70 (216;217). Longitudinal studies by Lindeman et al and Rowe et al have shown that a decline in glomerular filtration rate is part of ageing and can be considered as one of the many biological manifestations of senescence rather than a result of the disease processes that commonly accompany senescence e.g atherosclerosis and congestive heart failure (218;219). It thus may be fitting to apply the Baker and Sprott criterion to the use of kidney tissue as an indicator of organ specific and possibly even total body senescence.

Although the change in telomere length (TL) with chronological age is undeniable, the use of TL as a marker of ageing has recently been questioned. Several authors have recently reviewed the literature with respect to the utilisation of telomere length as a biomarker of ageing. They conclude that whilst there is clear evidence that telomeres are involved in ageing and diseases of premature ageing, the data supporting TL as a biomarker of ageing is inconclusive (128;220;221). There are a number of potential reasons highlighted by this review including; the high degree of inter-individual variability at similar chronological ages and the lack of definitive association between telomere length and functional capacity. Indeed in order to fully conform to Baker and Sprott's definition of a BoA, telomere length must predict lifespan better than chronological age. Studies investigating this specific issue are again inconclusive. Issues with methodology are also potentially confounding as certain studies use southern blot analysis to determine TL whereas the others use q-PCR. This further highlights the importance of future standardisation of research protocols to prevent potential issues with interpretation of results.

CDKN2A on the other hand has been validated as both a robust biomarker of ageing and shows significant relation to renal function in the post transplant phase when assessed prior to implantation (13;14) as demonstrated below.

1.1.21 Epigenetic regulation of renal function and Model testing

Assessment of organ bioage therefore, together with the testing of models for bioage effects and epigenetic regulation could be of vital significance to optimize patient selection and counseling prior to transplantation. The most well studied epigenetic regulatory

mechanisms include covalent chemical modification of DNA (methylation), chromatin (covalent histone post-transcriptional modifications) and non-coding RNAs (miRNAs). These mechanisms are ultimately related to the regulation of gene expression and chromatin structure. Epigenetics is the study of phenotypic changes that occur in a cell independent of changes to the underlying genome (222). It refers to functionally relevant modifications to the genome that do not involve a change in the nucleotide sequence. Genetic programmes for development, differentiation, and response to stress at a cellular or organ level can be altered by epigenetic modifications. Indeed, as a parallel project, Shiels lab has shown the importance of epigenetic regulation on the performance of kidney transplants post-operatively with promising results (McGuinness et al, *Sci Trans Med*. In submission). Renal function is complex and multifactorial and the most clinically relevant consequences of dysfunction are subtle and systemic. Agents tested in vitro and effective in cytoprotection were evaluated in in-vivo studies (Chapter 3) for their effects on preserving renal function in the context of renal ischaemia reperfusion injury. The rodent model is the most reproducible and appropriate one in which to study these systems and is widely used in the published literature. The validity of this model is confirmed by the fact that a variety of drug agents established in clinical transplantation have been developed in this way. As discussed in further detail in Chapter 2, the AS/AGU rat was chosen as an ideal target to study the effects of premature ageing on ischaemia reperfusion injury on the kidney thereby mimicking a similar scenario to ECD kidneys undergoing transplant related stress. The thesis provides sound evidence that TL is not an ideal biomarker in determining post transplant renal function when compared to CDKN2A. This finding was carried forward to a comprehensive in vivo animal model to test the protective effects of novel clinical entities (NCE) with respect to IR injury in the kidney. NCEs were vigorously validated in vitro prior to their application in vivo and such experiments also serve as a platform to engage in further studies involving NCEs and renal allograft transplantation in rodents (Whalen et al in prep).

1.2 Hypothesis

- i.** Biological, as opposed to chronological age - the previous gold standard for predicting post transplant allograft function, is a better predictive and prognostic marker for allograft function.
- ii.** Use of a validated Biomarker of Ageing (CDKN2A) offers superior predictive and prognostic power for determination for post transplant allograft function.
- iii.** Telomere length known as the “Gold standard” Biomarker of Ageing is not as robust as CDKN2A in predicting renal function

1.3 Aims

- i.** Is telomere length a validated Baker and Sprott Biomarker of ageing?
- ii.** Is CDKN2A superior to TL and donor chronological age in predicting post transplant renal function?
- iii.** Can we use CDKN2A and/or TL in a multivariate model to better predict post transplant renal function? How do they cross-compare?
- iv.** In the evaluation of deceased kidneys, is a pre-transplant scoring system incorporating biomarkers of ageing a realistic target for the future?

1.4 Materials and Methods

1.4.1 RNA extraction using TRIzol[®] technique

The following method is a slightly modified version of the manufacturer's protocol. Time zero pre-implantation kidney biopsies are stored in RNA Later[®] (Invitrogen) and refrigerated at 4°C.

50-100mg of kidney tissue is homogenised in 1ml of TRIzol[®] solution. Samples are then incubated at room temperature for 10-15 minutes to allow for cell membrane dissociation. Samples are then centrifuged at 12,000 x g for 10mins at 4°C. The supernatant is then transferred to a fresh tube taking care not to remove any liquid from the interphase. 200µl of chloroform is then added per 1ml of TRIzol[®] used initially. The eppendorf tubes are shaken vigorously by hand for 15secs and left at room temperature for 2-3 mins. Samples are then centrifuged at 12,000 x g for 15mins at 4°C. The colourless upper (aqueous) phase is transferred into a fresh tube. During RNA precipitation, an equal volume of isopropanol is added, mixed well and transferred to -20°C for 1hr. The samples are then centrifuged at 12,000 x g for 20mins at 4°C. RNA is now pelleted at the bottom of the tube. As much supernatant as possible is removed without disturbing the pellet. 1ml of ice cold 75% ethanol in DEPC treated water is added, sample is vortexed and re-centrifuged at 12,000 x g for 20mins at 4°C. The supernatant is then removed and the pellet is washed with ethanol and centrifuged once again. Supernatant is finally removed and the pellet left to air dry for 10-15 mins. Once most ethanol has evaporated, the pellets are dissolved in DEPC treated or nuclease free water approx 30-50µl and stored at -80°C.

1.4.2 DNA extraction

The Maxwell[®] 16 DNA purification robot kits by Promega were used for for DNA isolation from both blood and tissue samples. The sample was collected in 200µl of elution buffer and centrifuged to pellet the beads. Samples were then aliquoted into separate 100µl volumes and stored at -20°C.

1.4.3 Spectrophotometry

The Nanodrop[®] UV spectrophotometer is used for analysis. 1.6µl sample is placed on the pedestal after using an appropriate blank. The machine subsequently forms a column of fluid through which the absorbance of the sample is measured, particularly at the 260nm, 280nm and 230nm wavelengths. RNA and DNA samples should give a 260/280 ratio between 1.8 and 2.

1.4.4 Gel Electrophoresis

A common method used to assess the integrity of total RNA is to run an aliquot of the RNA sample on a denaturing agarose gel stained with ethidium bromide (EtBr). Intact total RNA will have a sharp, clear 28S and 18S rRNA band in eukaryotic tissue. The 28S rRNA band should be approximately twice as intense as the 18S rRNA band. This 2:1 ratio (28S:18S) is a good indication that the RNA is completely intact. Partially degraded RNA will have a smeared appearance, will lack the sharp rRNA bands, or will not exhibit the 2:1 ratio of high quality RNA. Completely degraded RNA will appear as a very low molecular weight smear. Inclusion of RNA size markers on the gel will allow the size of any bands or smears to be determined and will also serve as a good control to ensure the gel was run properly.

Gel construction (1%) for control of RNA degradation involves making a 0.5x TBE Buffer in the following quantity: 950 ml d H₂O + 50 ml 10xTBE. 100 ml of this is then poured into beaker and 1g of Agarose added (per 100mls of 0.5x TBE Buffer). The beaker is then placed in the microwave for 1 min+ 30 sec+ 30 sec. Ethidium bromide (10mg/ml) is added to the gel solution (5µl for every 100 ml of gel). The solution is allowed to cool in the beaker for 20 minutes. As crystals start to form, hot gel solution is poured into the chamber for setting. The remaining 900ml of 0.5xTBE Buffer is used for the running chamber.

1.4.5 DNase Treatment

(Promega RQ1 RNase-Free DNase[®])

Prior to the conversion of mRNA to cDNA, it is necessary to perform DNase treatment to remove all remaining genomic DNA. Per 4µg of RNA, 1µl of DNase is added together

with 1.5µl of buffer DNase and 0.5µl of RNase inhibitor (RNase out) (The latter is necessary in order to de-activate any remaining enzymes capable of degrading RNA in the sample). The sample is made up to 30µl with DEPC treated water and placed at 37°C for 30mins. 1µl of STOP solution is then added per tube. This solution inhibits DNase. Subsequently, the sample is placed at 65°C for 10mins and immediately on ice. Nanodrop is then repeated.

1.4.6 cDNA Synthesis

(Roche Transcriptor Reverse Transcriptase)

After purification of RNA, conversion to cDNA is necessary in order to proceed to q-PCR. For this a standard manufacturer's protocol is used comprising an initial 1µg of RNA (DNase treated), 1.2µl of Random Hexamers and Xµl of H₂O (nuclease free) to make a total of 13µl volume. This is mixed carefully and pulse spun. Samples are then placed at 65°C x 10mins (Biometra Thermal Cycler[®]) and following this, immediately on ice. 0.5µl of RNase out, 0.5µl of Transcriptor[®] Reverse Transcriptase, 2µl of dNTP and 4µl of 5xRT Buffer are added to make a total of 20µl volume. The eppendorf is mixed and pulse spun. The following cycles are undertaken: 25°C for 10mins, 55°C for 30mins, 85°C for 5mins and 4°C for 10mins. Samples are stored at -20°C until further use.

1.4.7 Taqman RT-PCR

Taqman RT-PCR is a cDNA-specific 5' nuclease assay for quantitatively detecting RT-PCR products using a non-extendable oligonucleotide hybridisation probe. The probe is labelled with a reporter fluorescein dye, 6-carboxy-fluorescein (FAM), at the 5' end and a quencher fluorescent dye, 6-carboxy-tetramethyl-rhodamine (TAMRA), at the 3' end. When the probe is intact, the reporter dye emission is quenched due to the physical proximity of the reporter and quencher fluorescent dyes. During the extension phase of the PCR cycle, the nucleolytic activity of the Taq DNA polymerase cleaves the hybridisation probe and releases the reporter dye from the probe. With each cycle of PCR amplification there is an increase in fluorescence emission which is monitored in real-time using the ABI Prism 7700 sequence detector.

The sequence detector is a combination thermal cycler, laser and detection software system that automates 5' nuclease-based detection and quantitation of nucleic acid sequences. A computer algorithm compares the amount of reporter dye emission (R_{n+}) with the quenching dye emission (R_{n-}) during the PCR amplification, generating a ΔR_n value (R_{n+}/R_{n-}). The ΔR_n value reflects the amount of hybridised probe that has been degraded. The algorithm fits an exponential function to the mean ΔR_n values of the last three data points for every PCR extension cycle, generating an amplification plot.

Taqman RT-PCR was performed for CDKN2A and simultaneously performed using primer/probe sets for hypoxanthine phosphoribosyltransferase (HPRT), housekeeping genes used as internal references. The amplification of the endogenous control allowed us to standardise the amount of RNA in each reaction.

A threshold was set at a point where this amplification appeared linear. The resultant threshold cycle number (Ct) for both of these genes was recorded for each sample. This allowed Ct values to be normalized to the endogenous housekeeping gene.

The comparative Ct method of calculating gene expression was then performed. This involved comparing the Ct values of the samples of interest with a control or calibrator such as a non-treated sample or RNA from normal human tissue. The comparative Ct method is also known as the $2^{-\Delta\Delta Ct}$ method, where $\Delta\Delta Ct = \Delta Ct_{\text{Sample}} - \Delta Ct_{\text{Reference}}$. Here, $\Delta Ct_{\text{Sample}}$ is the Ct value for any sample normalized to the endogenous housekeeping gene ($Ct_{\text{Sample}} - Ct_{\text{Housekeeping gene}}$) and $\Delta Ct_{\text{Reference}}$ is the Ct value for the calibrator also normalized to the endogenous housekeeping gene ($Ct_{\text{Reference}} - Ct_{\text{Housekeeping gene}}$).

For the $\Delta\Delta Ct$ calculation to be valid, the amplification efficiencies of the target and the endogenous reference housekeeping gene must be approximately equal. This can be established by looking at how $\Delta Ct_{\text{Sample}}$ varies with template dilution. If the plot of cDNA dilution versus $\Delta Ct_{\text{Sample}}$ is close to zero, it implies that the efficiencies of the target and housekeeping genes are very similar.

The primers used for CDKN2A and HPRT qPCR are listed below followed by a diagrammatic representation of the steps involved in the real-time Taqman PCR reaction is presented in Figure 1.7 [Adapted from Applied Biosystems Taqman Manual]

HPRT

Forward Primer (5/-CTTGCTCGAGATGTGATGAAG-3/),

Reverse Primer (5/-CAGCAGGTCAGCAAAGAATTTATAG-3/),

Probe (5/-FAM-ATCACATTGTAGCCCTCTGTGTGCTCAAGGTAMRA-3/)

CDKN2A

Forward Primer (5/-CATAGATGCCGCGGAAGG-3/),

Reverse Primer (5/-CCCGAGGTTTCTCAGAGC-3/),

Probe (5/-FAM-CCTCAGACATCCCCGATTG-TAMRA-3/)

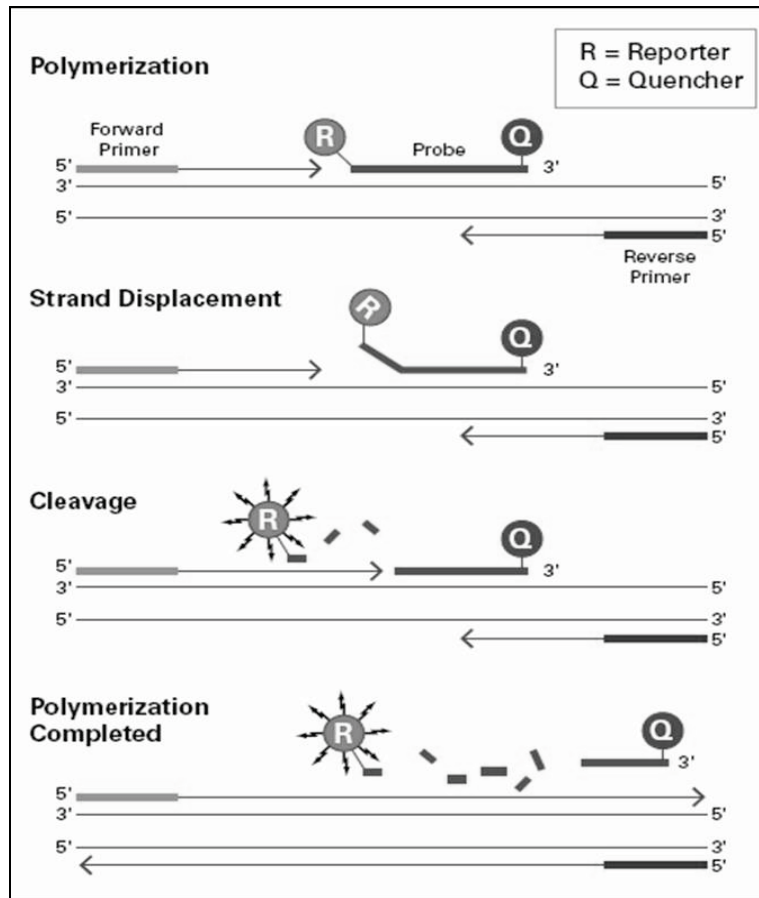


Figure 1.7 Real time Taqman PCR reaction

1. The primers and probe anneal to the cDNA transcript. There is no fluorescence because the reporter dye emission is quenched
2. The primers are extended during the extension phase of the PCR cycle
3. The 5'-3' exonuclease activity of the DNA polymerase cleaves the hybridised probe and releases the reporter dye emission resulting in an increase in reporter fluorescent dye emission
4. The primers continue to be extended until polymerisation of the amplicon is complete. (Adapted from AB Taqman[®] Gene Expression User Manual 2012)

1.4.8 Telomere Assay Protocol

(Roche Light Cycler 480[®])

For this assay 35ng of DNA was required per well. Each sample was assayed in triplicate in both the telomere and 36B4 reference plates. To each well 5 μ l of DNA was added (7ngDNA/ μ l). In total 35 μ l was made (245ng DNA) of each sample (7x5 μ l 6 wells for two plates plus 1 well extra). DNA was diluted in nuclease free H₂O. Before aliquoting the DNA it was heated to 65^oC for 10 minutes then vortexed and centrifuged briefly to ensure it was thoroughly resuspended. Samples were stored at 4^oC until required. For absolute quantification analyses, serial dilutions of a standard with known concentration were used to create a standard curve. The standard curve (reference DNA) was then used to determine the relative telomere lengths of the the unknown samples ratio of telomere repeat copy number to single gene copy number. The methodology adopted is based on Cawthon's technique first described in 2002 (223). (Our standard was chosen to be a young healthy male PhD student and was used for all previous and subsequent telomere analyses in the laboratory) The ratio of telomere repeat copy number to single gene copy number of the unknown sample is compared to that of our reference DNA (standard) to give the T/S ratio. Indeed, T/S = 1 when the unknown DNA is identical to the reference DNA in its ratio of telomere repeat copy number to single gene copy number. The crossing point (CP – the point at which the fluorescence of a sample rises above the background fluorescence) of the standards and the samples was in fact used to calculate relative DNA concentrations. As with the samples, each standard was assayed in triplicate in both the telomere and 36B4 plates. The DNA concentration of the standards for this assay ranged from 100ng to 3.125ng, they were prepared by serial dilution (1:2). To each well 5 μ l of standard DNA was added. A reference positive control (calibrator) was required in each plate. The concentration of this sample should fall within the range of the standard curve (approximately half way). Therefore for this assay 50ng of DNA was required per well for the reference positive control. As with the samples, the reference sample was assayed in triplicate in both the telomere and 36B4 plates. To each well 5 μ l (10ng/ μ l) of reference DNA was added. Therefore 35 μ l (350ng) of reference sample was needed (7x5 μ l 6 wells for two plates plus 1 well extra). DNA was diluted in nuclease free H₂O. Before aliquoting the DNA, it was heated to 65^oC for 10 minutes then vortexed and centrifuged briefly to ensure DNA was thoroughly resuspended. Samples were stored at 4^oC until required.

The following sequence of telomere primers were used:

Telo 1 Sequence (5' to 3')

CGG TTT GTT TGG GTT TGG GTT TGG GTT TGG GTT TGG GTT

Telo 2 Sequence (5' to 3')

GGC TTG CCT TAC CCT TAC CCT TAC CCT TAC CCT TAC CCT

The following sequence of 36B4 primers were used:

36B4d Sequence (5' to 3')

CCC ATT CTA TCA TCA ACG GGT ACA A

36b4u Sequence (5' to 3')

CAG CAA GTG GGA AGG TGT AAT CC

Master Mix Preparation utilised the SYBR Green I Master from Roche. The kit contains 2x SYBR Green I Master Mix and H₂O PCR Grade. The only other reagents that needed to be added to the master mix were the primers. The total reaction volume per well is 20µl; 5µl of this is the sample/standard DNA therefore the remaining 15µl is comprised of the master mix. Consequently the total volume of master mix required is 1500µl (96 wells x 15µl plus 4 extra wells). The master mix is prepared as indicated in Table 1.1:

Reagent	Master mix TEL		Reagent	Master mix 36 B4	
	Vol reqd per well(µl)	Vol reqd for 100 wells(µl)		Vol reqd per well(µl)	Vol Reqd for 100 wells(µl)
2x master mix	10	1000	2x master mix	10	1000
Telo 1	0.75	75	36B4d	0.4	40
Telo 2	0.75	75	36B4u	0.4	40
H2O	3.5	350	H2O	4.2	420
total	15	1500	total	15	1500

Table 1.1 Mastermix preparation

The table shows the mastermix preparation for both telomere and 36B4 plates. Per well total reaction volume = 20µl

As indicated in Table 1.2, in each plate there were 6 standards, a reference sample (SC positive control), a no template control (negative control – no DNA is added to this well only master mix. The purpose of this is to make sure that there is no contamination of any reagents) and 24 unknown samples. Plate layout was as follows:

	1	2	3	4	5	6	7	8	9	10	11	12	
telomere & 36B4	A	SD1	SD1	SD1	1	1	1	9	9	9	17	17	17
	B	SD2	SD2	SD2	2	2	2	10	10	10	18	18	18
	C	SD3	SD3	SD3	3	3	3	11	11	11	19	19	19
	D	SD4	SD4	SD4	4	4	4	12	12	12	20	20	20
	E	SD5	SD5	SD5	5	5	5	13	13	13	21	21	21
	F	SD6	SD6	SD6	6	6	6	14	14	14	22	22	22
	G	SC	SC	SC	7	7	7	15	15	15	23	23	23
	H	ntc	ntc	ntc	8	8	8	16	16	16	24	24	24

Table 1.2 Plate layout of both telomere and 36B4 plates

All standards/samples were heated to 95oC for 5 minutes and then transferred to ice. The plate was wrapped in foil to protect it from light and centrifuged at ~2000rpm for 2 minutes. Various stages of heating and cooling are undertaken in the Light Cycler RT-PCR machine. Conditions are different for both telomere (Table 1.3) and 36B4 plates (Table 1.4).

Program Name		Heat Start (HS)			
Cycles		1	Analysis Mode		None
Target (oC)	Acquisition Mode	Hold (hh:mm:ss)	Ramp (oC/s)	Rate	Acquisitions (per oC)
95	None	00:10:00	4.4		

Program Name		Amplification (Amp)			
Cycles		30	Analysis Mode		Quantification
Target (oC)	Acquisition Mode	Hold (hh:mm:ss)	Ramp (oC/s)	Rate	Acquisitions (per oC)
95	None	00:00:05	4.4		
59	None	00:00:10	2.2		
72	Single	00:02:00	4.4		

Program Name		Melt			
Cycles		1	Analysis Mode		Melting Curves
Target (oC)	Acquisition Mode	Hold (hh:mm:ss)	Ramp (oC/s)	Rate	Acquisitions (per oC)
95	None	00:00:30	4.4		
65	None	00:00:30	2.2		
95	Continuous	00:02:00	0.29		2

Program Name		Cool			
Cycles		1	Analysis Mode		None
Target (oC)	Acquisition Mode	Hold (hh:mm:ss)	Ramp (oC/s)	Rate	Acquisitions (per oC)
40	None	00:00:10	2.2		

Table 1.3 Roche Lightcycler® Telomere Running Conditions

Program Name		Heat Start (HS)			
Cycles		1	Analysis Mode		None
Target (oC)	Acquisition Mode	Hold (hh:mm:ss)	Ramp (oC/s)	Rate	Acquisitions (per oC)
95	None	00:05:00	4.4		

Program Name		Amplification (Amp)			
Cycles		35	Analysis Mode		Quantification
Target (oC)	Acquisition Mode	Hold (hh:mm:ss)	Ramp (oC/s)	Rate	Acquisitions (per oC)
95	None	00:00:05	4.4		
58	None	00:00:15	2.2		
72	Single	00:00:15	4.4		

Program Name		Melt			
Cycles		1	Analysis Mode		Melting Curves
Target (oC)	Acquisition Mode	Hold (hh:mm:ss)	Ramp (oC/s)	Rate	Acquisitions (per oC)
95	None	00:00:30	4.4		
65	None	00:00:30	2.2		
95	Continuous	00:02:00	0.29		2

Program Name		Cool			
Cycles		1	Analysis Mode		None
Target (oC)	Acquisition Mode	Hold (hh:mm:ss)	Ramp (oC/s)	Rate	Acquisitions (per oC)
40	None	00:00:10	2.2		

Table 1.4 Roche Lightcycler® 36B4 Running Conditions

1.4.9 Statistics

Data analyses were performed using SPSS statistical package version 17. The adjusted R^2 was used to indicate the extent to which the dependant variable (eGFR) is explained by the independent variable in question. The association was deemed to be statistically significant if the p value < 0.05 (ANOVA). Prior to multivariate regression, preliminary analysis was conducted to ensure no violation of the assumptions of normality, linearity and multicollinearity. Any missing values were removed by listwise deletion. Bonferroni's adjustment was used to calculate the exact p value for the multivariate models.

1.4.10 Ethics

This is an ongoing prospective study which has been approved by the Regional Ethics Committee of the North Glasgow NHS Trust. Donors from the national pool donated their organs for transplantation. The recipient of the organ provided pre-operative written informed consent for tissue analysis and scientific research. Samples were anonymised and subsequently analyzed.

1.5 Renal Database

The author was responsible for maintaining an up to date renal database of all donor kidney tissue samples taken during renal transplantation at the Transplant Unit, Western Infirmary, Glasgow. After appropriate ethics was obtained from the local Research and Development department, time zero, pre implantation biopsies were removed as a wedge or needle biopsy and placed into RNA Later at -20°C . Samples were then transferred to the laboratory for genetic analysis. Results from final analysis was inputted into an extensive database containing several details regarding both donor and recipient characteristics. These parameters included: degree of HLA mismatch, Cold Ischaemic Time, Mode of Death, Donor co morbidities, type of immunosuppression, rates of rejection, serum creatinine and eGFR calculations at 6 months, 1 year, 2 years and 5 years post transplant. Information was updated on a regular basis and statistical analysis was performed using Statistical Package for the Social Sciences (SPSS), version 17. The primary outcome measured throughout this thesis focused on the relationship between BoAs and renal

function as measured by serum creatinine and eGFR and UPCR at several time points. Secondary outcomes including rates of delayed graft function, effect of angiotensin converting enzyme inhibitors/angiotensin II receptor blockers and variations of immunosuppression were also analysed in various statistical methods.

1.6 Study Population

The global study population is representative of the national UK deceased donor pool. A total of 133 transplant patients were included which were performed in the Western Infirmary, Glasgow between March 2008 and July 2011. All transplants were followed up for post-operative clinical data. Telomere length was calculated for 43 transplanted kidneys. A separate group (n=33) yielded CDKN2A expression. There were 15 matched samples as a result of small biopsy specimens allowing RNA or DNA to be obtained separately and not together. Table 1.5 shows the demographic data for the CDKN2A and telomere groups. Patients, in whom genetic data was not available, were included in the global cohort for clinical analysis. The primary causes of end stage renal disease (ESRF) in the recipients were hypertensive nephropathy, diabetic nephropathy, Adult Polycystic Kidney Disease (APKD), chronic pyelonephritis/reflux disease, IgA nephropathy and the glomerulonephritides. The immunosuppressive regimen consisted primarily of basiliximab at induction and day 4 with a maintenance regime consisting of tacrolimus, mycophenolate mofetil and prednisolone.

1.7 Results

1.7.1 Demographics, Biological Age and Donor Chronological Age

Prior to analysing the predictive power of biomarkers of ageing on renal function, data were validated by determining the association between telomere length and CDKN2A. A Pearson correlation between the two revealed no statistical significance ($p=0.87$, $n=15$).

Telomere length and CDKN2A were then separately correlated with donor chronological age. Telomere length was shown to inversely correlate with chronological age ($p=0.036$,

CC=-0.242, Figure 1.8a), while CDKN2A levels positively associated with increasing chronological age ($p < 0.001$, CC=0.597, Figure 1.8b). These findings indicate that CDKN2A is more robustly associated with the chronological ageing process in kidney tissue when compared to telomere length as seen by a stronger correlation coefficient (CC). There was no difference in demographic and clinical data between both CDKN2A and telomere groups (Table 1.5).

	CDKN2A n=33 Mean (SD)	Telomere n=43 Mean (SD)	p value
Donor Gender** (male/female)	15/18	20/23	0.589
Donor Age**	48.0 (15.7)	51.8 (15.51)	0.189
DCD/DBD organ*	4/29	9/34	0.677
Mismatch at all A,B,DR Loci* (yes/no)	8/25	10/33	0.607
Recipient Age**	50.6 (12.7)	49.7 (12.6)	0.344
Cold Ischaemic Time**	15.5 (3.9)	13.9 (4.0)	0.267

** Unpaired t-Test

* Fisher's exact test

Table 1.5 Demographics

Demographic and important clinical parameters were compared between the separate CDKN2A group and the telomere group. There were no significant differences between the two groups which would account for the different correlations with renal function.

1.7.2 BoA and Correlation with Renal Function Post-Transplant

Pearson correlation showed a significant association between shortening telomere length and deteriorating eGFR at 6 months and at 1 year post-transplant ($p=0.038$ & $p=0.041$, Figure 1.9). However, increasing levels of CDKN2A expression were associated with decreasing eGFR levels at 6 months and 1 year post-transplant ($p=0.020$ & $p=0.012$, Figure 1.10).

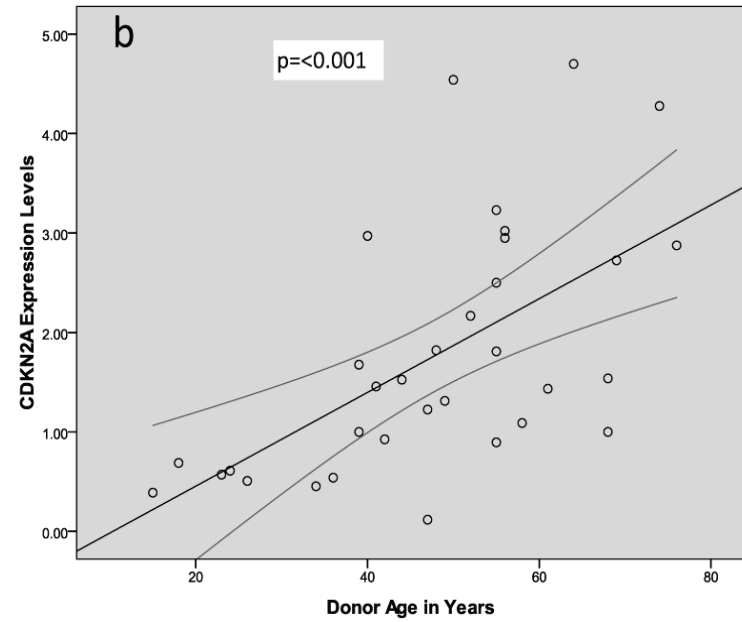
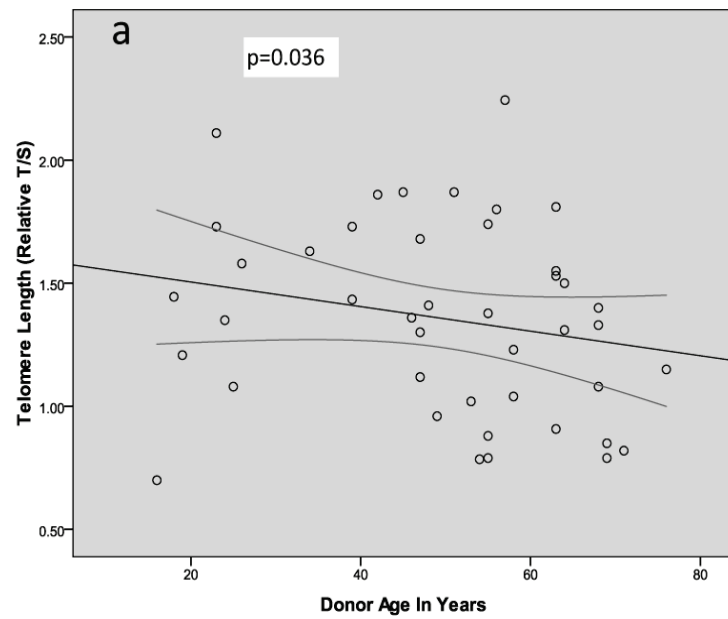


Figure 1.8 Scatter plots showing the correlation between biomarkers of ageing and donor chronological age

a. Negative correlation between Donor Chronological Age and Telomere Length. $n=43$, CC: -0.242 , $p = 0.036$

b. Positive correlation between Donor Chronological Age and CDKN2A. $n=33$, CC: 0.597 , $p<0.001$

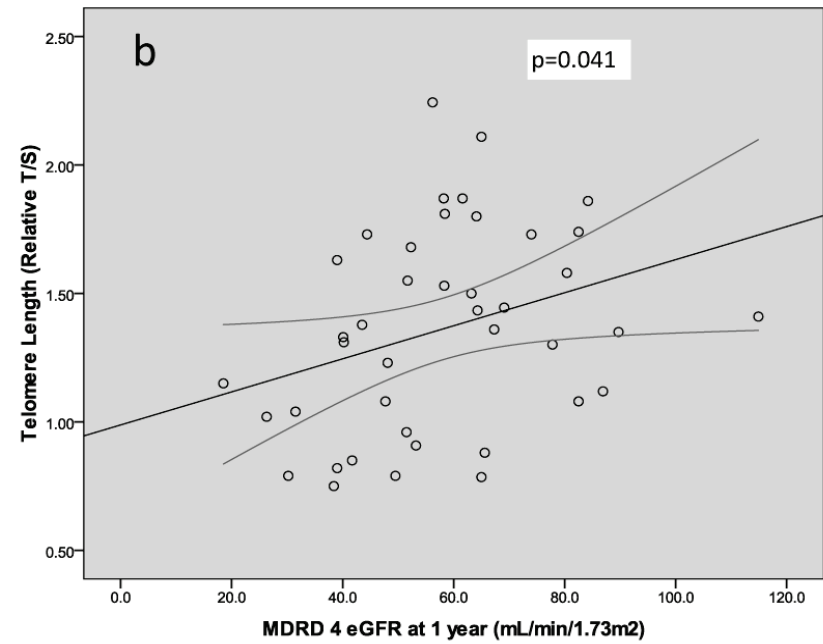
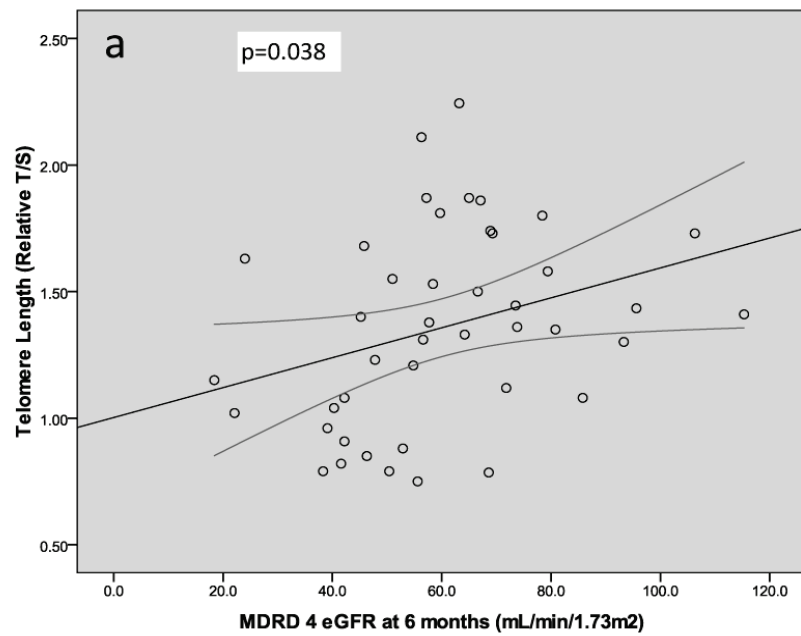


Figure 1.9 Scatter plots showing the relationship between telomere length and renal function, as measured by MDRD 4 eGFR

a. Telomere Length vs MDRD 4 eGFR at 6 months: n=43, CC: 0.317, p =0.038

b. Telomere Length vs MDRD 4 eGFR at 1 year: n=41, CC: 0.320, p =0.041

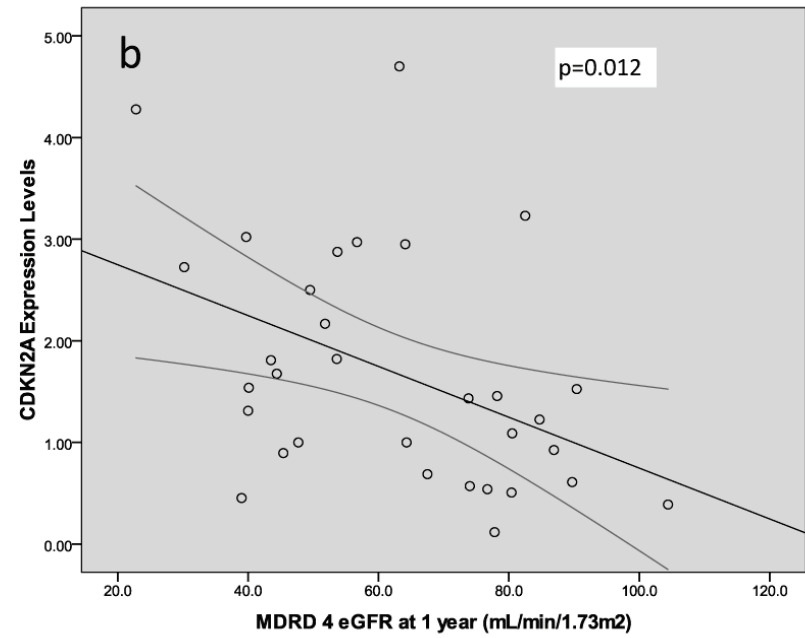
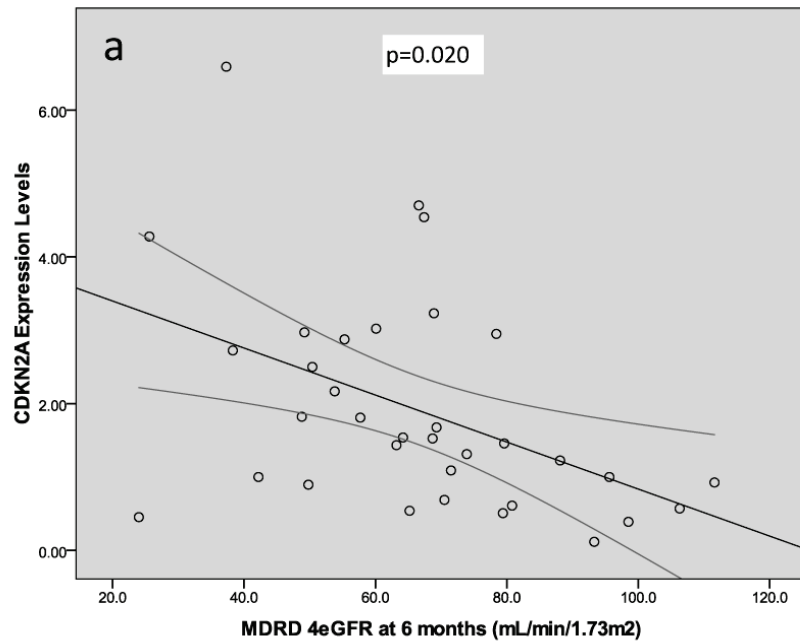


Figure 1.10 Scatterplots showing the relationship between CDKN2A and renal function, as measured by MDRD 4 eGFR

- a. CDKN2A vs MDRD 4 eGFR at 6 months. n=33, CC: -0.403, p=0.020
- b. CDKN2A vs MDRD 4 eGFR at 1 year. n=32, CC: -0.439, p=0.012

1.7.3 Biological Age and Serum Creatinine

Bivariate correlations of BoAs and serum creatinine show varied results. When analysing CDKN2A with serum creatinine, there was no significant association at 6 months but this changed at 1 year, when the two displayed strong statistical correlations as shown below:

CDKN2A Expression vs Serum Creatinine at 6 months:- Pearson Correlation coefficient 0.261, n=33, p=0.142

CDKN2A Expression vs Serum Creatinine at 1 year:- Pearson Correlation coefficient 0.418, n=32, p=0.017

Telomere length displayed strong associations at both time points as shown. There was a significant relationship at 6 months which was not seen with CDKN2A:

Telomere Length vs Serum Creatinine at 6 months:- Pearson Correlation coefficient = - 0.362, n=43, p=0.017

Telomere Length vs Serum Creatinine at 1 year:- Pearson Correlation coefficient= - 0.413, n=41, p=0.007

1.7.4 Biological Age and UPCR

The quantification of tubular and/or glomerular damage was gauged using the Urinary Protein Creatinine Ratio – UPCR (mg/mmol) at routine clinic follow up visits. In accordance with NICE guidelines a value of more than 50 mg/mmol was classified as significant proteinuria. There was a significant relationship between CDKN2A and UPCR at 6 months (p=0.012, CC:0.44, n=32) and at 1 year (p=0.036, CC:0.42, n=25) consolidating the hypothesis that increased levels of CDKN2A reflect increased cellular damage at both tubular and glomerular level. This finding is associated with impaired clearance at the glomerulus (higher serum creatinine and lower eGFR) as shown above. There were no associations between telomere length and UPCR.

1.7.5 ECD Kidneys and DCA vs Renal Function

Since donor chronological age is a strong contributor to the ECD criteria and has been used as the “Gold standard” in determining organ quality over the years, a separate individual analysis has also been undertaken (Table 1.6). Both donor age and ECD kidneys show strong significant univariate associations with both renal function (up to 5 years post transplant) and tubulo-glomerular damage (up to 2 years post transplant). There is also a significant inverse correlation with recipient White Cell Count up to 2 years post transplant.

Variable	Donor Chronological Age			Extended Criteria Donor		
	n	r	p-value	n	z	p-value
SC 6 months	132	0.29	0.001	125	-3.32	0.001
eGFR 6 months	120	-0.36	<0.001	118	-4.08	<0.001
UPCR 6 months	107	0.28	0.003	105	-3.62	<0.001
SC 1 year	123	0.35	<0.001	114	-3.59	<0.001
eGFR 1year	104	-0.48	<0.001	103	-4.66	<0.001
UPCR 1year	86	0.31	0.004	85	-3.04	0.002
SC 2 years	85	0.42	<0.001	80	-2.83	0.005
eGFR 2 years	72	-0.56	<0.001	72	-3.87	<0.001
UPCR 2 years	54	0.33	0.016	54	-2.89	0.004
SC 5 years	38	0.42	0.008	38	-2.12	0.034
eGFR 5 years	37	-0.51	0.001	37	-2.77	0.006
UPCR 5 years	24	0.15	ns	24	-1.77	ns

SC: Serum Creatinine
eGFR: MDRD 4 eGFR
r: Correlation Coefficient
z: Mann-Whitney U z coefficient

Table 1.6 DCD and ECD correlations with renal function and glomerular damage (SC, eGFR and UPCR)

Correlation for Donor Chronological Age (DCA) and Extended Criteria Donor (ECD) kidneys with renal function (SC & eGFR) and tubulo-glomerular damage (UPCR). DCA and ECD status accurately predict post transplant renal function up to 5 years whilst a significant correlation with UPCR is seen up to 2 years post transplant.

1.7.6 ECD Kidneys and DCA vs Post-operative WCC

Interestingly, a significant inverse correlation was seen between the donor chronological age and ECD status with recipient WCC (Table 1.7). The association holds for ECD kidneys at 6 months, 1 year and 2 years whilst Donor Age holds at 1 and 2 years

Variable	Donor Chronological Age			Extended Criteria Donor		
	n	r	p-value	n	z	p-value
WCC 6 months	120	-0.15	ns	118	-3.00	0.003
WCC 1 year	104	-0.24	0.015	103	-2.53	0.011
WCC 2 years	71	-0.27	0.023	71	-1.99	0.046

r: Correlation Coefficient

z: Mann-Whitney U z coefficient

Table 1.7 Correlation between DCA and ECD kidneys with WCC at 6 months, 1 year and 2 years.

The hypothesis underlying an inverse correlation relies on the relationship between increasing immunosuppression and its effect on total WCC. It is postulated that increasing DCA or ECD kidneys with a larger bioage have larger amounts of cellular and extracellular inflammation (a result of increased wear and tear). This leads to worsening renal function post transplantation due possibly to increased episodes of rejection which may even be sub clinical. As a consequence increasing doses of immunosuppressive agents are generally administered to counteract the deterioration in renal function with a consequent fall in WCC. Another possibility is a direct drop in WCC as a result of the systemic inflammatory response syndrome (SIRS).

The relationship between CDKN2A and WCC with respect to the above approaches significance at 1 yr (p=0.051) but there is no relationship at 6 months and 2 years. This implicates that there are other factors other than bioage that are contributing to the postulated inflammatory state

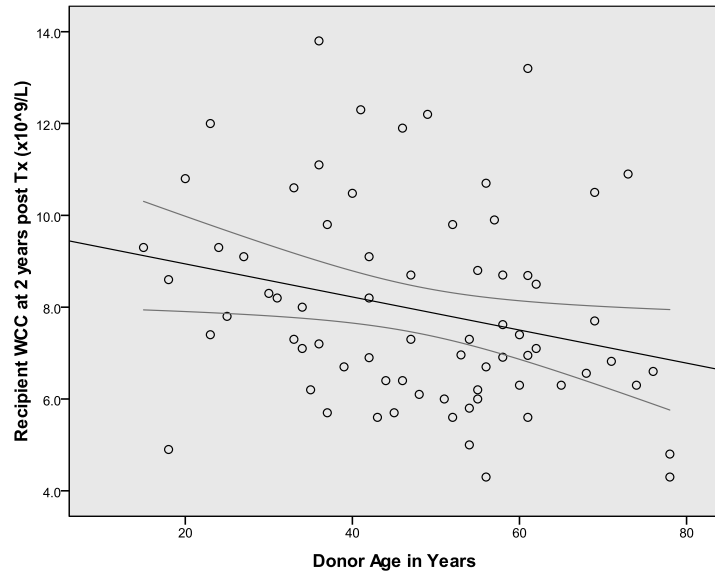


Figure 1.11 The relationship between WCC at 2 years and DCA n=71, $CC: -0.27, p: 0.023$

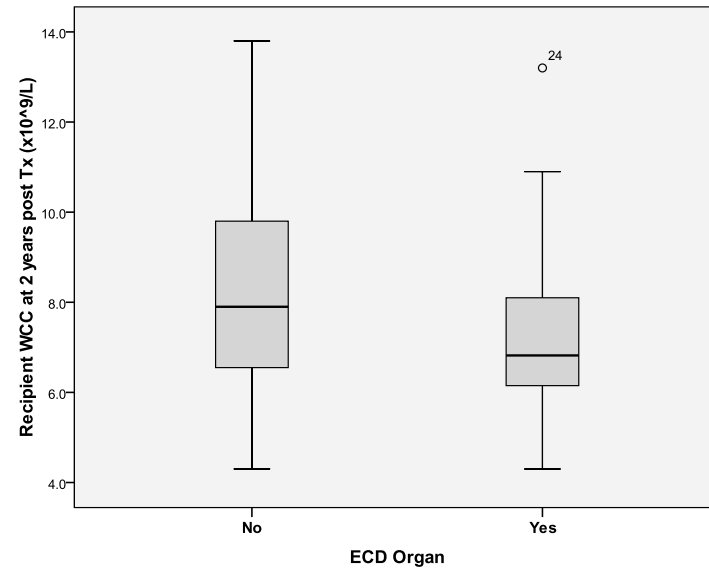


Figure 1.12 Boxplot depicting a significantly lower WCC in ECD kidneys at 2 years. n=71, $z: -1.99, p: 0.046$

Variable	Delayed Graft Function			≥ 1 Rejection Episodes		
	n	z	p-value	n	z	p-value
SC 6 months	120	-2.68	0.007	113	-3.54	<0.001
eGFR 6 months	121	-3.62	<0.001	113	-3.39	0.001
UPCR 6 months	108	-2.009	0.045	100	-1.30	ns
SC 1 year	105	-3.24	0.001	103	-3.50	<0.001
eGFR 1year	105	-3.50	<0.001	103	-3.37	0.001
UPCR 1year	87	-1.10	ns	85	-2.06	0.039
SC 2 years	72	-2.74	0.006	71	-3.36	0.001
eGFR 2 years	72	-3.04	0.002	71	-3.21	0.001
UPCR 2 years	54	-2.51	0.012	53	-2.51	0.012
SC 5 years	38	-1.75	ns	37	-2.89	0.04
eGFR 5 years	37	-2.08	0.037	36	-2.43	0.015
UPCR 5 years	24	-2.57	0.009	23	-2.12	0.034

SC: Serum Creatinine
eGFR: MDRD 4 eGFR
z: Mann-Whitney U z coefficient

Table1.8 Association between DGF and rejection episodes with renal function up to 5 years.

Note that both DGF and 1 or more episodes of rejection are associated with worse renal function and increased tubulo-glomerular damage (UPCR) up to 5 years post transplantation

1.7.7 CDKN2A, Delayed Graft Function and Rejection

Increased expression of CDKN2A in pre-implantation biopsies was significantly associated with DGF (MWU, p=0.032). Although somewhat underpowered, median CDKN2A expression levels in patients with DGF were compared with those grafts that showed primary function (DGF CDKN2A mean expression = 2.61 (SD 0.56, n=6) vs

primary function CDKN2A mean expression = 1.61 (SD 1.30, n=27)). DGF in itself was significantly correlated with graft rejection episodes (Fisher's exact test, n=113, p=0.001). This data suggests that high levels of CDKN2A are linked to increased allograft immunogenicity resulting in increased rejection episodes in the long term and may also play a role in the aetiology of DGF through a similar mechanism.

A total of 112 patients with rejection data were analysed. Biopsy proven evidence of acute rejection was present in 25.0% (n=28) of the total. All such grafts were viable at 6 months with a median eGFR of 39.05 ml/min/1.73m² (SD 17.16) however, there was 1 graft failure at 1 year, with a median eGFR for all other grafts (n=27) of 39.70 ml/min/1.73m² (SD18.09). There was no direct statistical relationship between CDKN2A and rejection itself (p=0.741)

1.7.8 Univariate Regression Analysis

Univariate linear regression was used in order to assess the individual predictive power of multiple variables on eGFR, serum creatinine and UPCR. Each variable was used to predict function at both 6 months (Table 1.9) and 1 year (Table 1.10) post-transplantation. The results indicated that CDKN2A, ECD, and donor chronological age were the strongest univariate predictors for eGFR. Telomere length in contrast displayed a poorer predictive ability in general. As expected, other clinical variables that are included in ECD criteria (donor age, donor hypertension, death by CVA but not high serum creatinine) significantly predicted eGFR at both timelines. Interestingly, there was a small but significant association for recipients who suffered any form of glomerulonephritis (GN) resulting in end stage renal failure. Recipients with ESRF second to GN displayed poorer renal function at both timelines (MWU - 6 months p=0.05, 1 year p=0.04). The adjusted R² indicates the extent to which the dependant variable (Serum Creatinine, MDRD 4 eGFR or UPCR) is explained by the model. The model was deemed to be statistically significant if the p value <0.05 (ANOVA). Important univariate associations displayed in Table 1.9 and 1.10 include:

6 months: Donor chronological age predicted 14.3% of the variability in eGFR whilst ECD kidney category predicted 12.1%. CDKN2A predicted 13.5% of the eGFR, whilst telomere length predicted 7.9%.

1 year: Donor chronological age predicted 21.4% of the eGFR whilst ECD kidney category predicted 17.4%. CDKN2A predicted 16.6% of the eGFR, whilst telomere length remained at 7.9%.

Variable	Serum Creatinine			MDRD 4 eGFR			UPCR		
	n	Adjusted R ²	p-value	n	Adjusted R ²	p-value	n	Adjusted R ²	p-value
CDKN2A expression	33	0.038	ns	33	0.135	0.020	32	0.005	ns
Telomere Length	43	0.110	0.017	43	0.079	0.038	36	-0.009	ns
Donor Chronological Age	132	0.029	0.029	120	0.143	<0.001	107	0.014	ns
GN in recipient	112	0.021	ns	112	0.029	0.040	99	-0.006	ns
ECD Kidney	125	0.020	ns	118	0.121	<0.001	105	0.062	0.006
Donor Hypertension	107	0.002	ns	107	0.051	0.011	94	-0.008	ns
CVA in Donor	123	-0.001	ns	111	0.057	0.007	98	0.022	ns
Donor pre-retrieval Creatinine > 133µMol/L	121	-0.004	ns	110	-0.008	ns	98	0.050	0.015
Mismatch at A, B and DR Loci	114	-0.008	ns	114	-0.009	ns	102	0.008	ns
Previous Transplant	132	0.021	ns	120	0.000	ns	108	0.009	ns
Cold Ischaemic Time	126	0.015	ns	114	0.019	ns	102	0.013	ns
Donor Sex	133	0.015	ns	120	-0.001	ns	108	-0.008	ns
DCD/DBD	63	0.000	ns	63	-0.003	ns	53	-0.017	ns

GN: Glomerulonephritis
DCD: Donation after Cardiac Death
DBD: Donation after Brain Death
CVA: Cerebro Vascular Accident
ECD: Extended Criteria Donor

Table 1.9 Univariate linear regression analysis at 6 months

The table shows the predictive power of CDKN2A, Telomere length and other relevant clinical variables on renal function as measured by serum creatinine, eGFR and UPCR at 6 months. Note the superior predictive strength of CDKN2A, DCA and ECD Kidneys on eGFR in particular.

Variable	Serum Creatinine			MDRD 4 eGFR			UPCR		
	n	Adjusted R ²	p-value	n	Adjusted R ²	p-value	n	Adjusted R ²	p-value
CDKN2A expression	32	0.147	0.017	32	0.166	0.012	27	-0.040	ns
Telomere Length	41	0.149	0.007	41	0.079	0.041	32	-0.033	ns
Donor Chronological Age	123	0.066	0.002	104	0.214	<0.001	86	0.030	ns
GN in recipient	105	0.013	ns	105	0.028	0.048	87	-0.007	ns
ECD Kidney	114	0.062	0.004	103	0.174	<0.001	85	0.046	0.027
Donor Hypertension	100	0.034	0.036	100	0.069	0.005	82	-0.012	ns
CVA in Donor	114	0.010	ns	95	0.075	0.004	78	0.016	ns
Donor pre-retrieval Creatinine > 133µMol/L	113	-0.007	ns	95	-0.011	ns	79	0.094	0.004
Mismatch at A, B and DR Loci	98	-0.010	ns	98	-0.010	ns	80	0.008	ns
Previous Transplant	123	0.018	ns	104	0.000	ns	86	0.023	ns
Cold Ischaemic Time	117	0.014	ns	98	0.014	ns	80	0.007	ns
Donor Sex	124	0.012	ns	105	-0.009	ns	87	-0.012	ns
DCD/DBD	49	0.008	ns	49	0.001	ns	36	-0.019	ns

GN: Glomerulonephritis
DCD: Donation after Cardiac Death
DBD: Donation after Brain Death
CVA: Cerebro Vascular Accident
ECD: Extended Criteria Donor

Table 1.10 Univariate linear regression analysis at 1 year

The table shows the predictive power of CDKN2A, Telomere length and other relevant clinical variables on renal function at 1 year. Note again the superiority of CDKN2A over telomere length in particular. The strength of donor chronological age and ECD kidney status is more pronounced at this point, explaining 21.4% and 17.4% of the eGFR. Only ECD kidney status is able to significantly predict all 3 variables at 1 year.

The results derived from the above tables indicate that CDKN2A is a significant univariate predictor for eGFR and serum creatinine at 1 year. It is the stronger predictor of the two BoAs. The strongest clinical variables to challenge CDKN2A are ECD kidney status and Donor Chronological Age. Interestingly, donor chronological age is able to challenge ECD kidney status and CDKN2A in predicting eGFR, but falls short of being able to contribute to the quantity of proteinuria (UPCR) at both 6 months and 1 year. ECD Kidneys on the other hand together with impaired serum creatinine is able to predict UPCR at both timelines.

Since the aim of this thesis was to suggest an accurate pre-transplant scoring system for kidneys prior to implantation, the relationship of post operative factors such as delayed graft function, rejection and other post-operative variables were omitted from both the univariate and multivariate analysis.

1.7.9 Multivariate Regression Analysis

Proceeding from univariate linear regression models, several predictors were selected into a multivariate linear regression analysis model using renal function as the dependant variable. For simplicity, only the MDRD 4 eGFR was used as the dependant variable for renal function. Preliminary analysis was conducted to ensure no violation of the assumptions of normality, linearity and multicollinearity. Any missing values were removed by pairwise deletion. Models were created for both six month and one year timelines and included three principle pre-transplant variables. The covariates were based on CDKN2A and the stronger clinical univariate predictors: ECD and presence or absence of glomerulonephritis in the recipient. Since donor hypertension, donor chronological age and death by CVA are already included under ECD criteria, they were not included as separate covariates in the model. The addition of telomere length to any model severely weakened it's associations with renal function resulting in a statistically insignificant outcome. This supports the hypothesis that although telomere length is the "gold standard" biomarker of ageing, it's importance in predicting renal function is somewhat diminished or (if used in the context of Baker and Sprott) insignificant. A total of two models were formulated at 6 months and 1 year timelines with a p-value of <0.017 taken to be statistically significant using Bonferroni's correction. At 6 months, the model approached statistical significance (p=0.021) as outlined in Table 1.11. Statistical significance was

reached at 1 year where the model predicted 27.1% of the eGFR (Adjusted R² 0.271, n=31, p=0.008 ANOVA) with respective individual contributions outlined in Table 1.12.

Independent Variable	Standardised Coefficients (Beta)	p-value
CDKN2A	-0.397	0.034
ECD Kidney	-0.211	0.233
Recipient Glomerulonephritis	-0.293	0.088

Table 1.11 Multivariate model outcome for eGFR at 6 months.

Multivariate model outcome for eGFR at 6 months. The model approaches statistical significance using the strict Bonferroni correction (p=0.021)

Independent Variable	Standardised Coefficients (Beta)	p-value
CDKN2A	-0.428	0.019
ECD Kidney	-0.236	0.166
Recipient Glomerulonephritis	-0.311	0.061

Table 1.12 Multivariate model outcome for eGFR at 1 year.

Multivariate model outcome for eGFR at 1 year. The model explains 27.1% of the eGFR (p=0.008)

1.8 Discussion

1.8.1 CDKN2A – most robust BoA in modern era

The results demonstrate that the pre-transplant expression of two independent BoAs correlates with renal function post-transplant. Greater biological age, as determined by shorter telomere length, or higher relative CDKN2A expression, correlated with poorer post-transplant function. This is in keeping with observations in the field. Classically, organs from older donors show poorer function post-transplant and have a decreased lifespan. Although this holds true in most cases, there are times when such organs perform very well and last beyond their life expectancy. The results indicate that such variation in organ function could be attributed to the difference in biological age. The data also indicates that pre-transplant CDKN2A expression is the strongest biomarker of renal function up to 1 year post-operatively. When used in the context of Baker and Sprott's criterion, CDKN2A appears to be significantly more robust as a BoA than telomere length. The latter may be viewed as an effective but imprecise BoA. Distinguishing between age-related telomere attrition and disease-related attrition is difficult (221). Using both together as a composite measure, alongside chronological age, should be of further benefit in this context. Clinical translation of this should be straightforward, as the methodology is readily adaptable to implementation when the organ is undergoing cross-match.

In comparison to previous studies, the estimated Glomerular Filtration Rate (eGFR) was used primarily as a marker for renal function. It is traditionally considered to be the best overall index of renal function in health and disease (37) and the National Kidney Foundation now recommends the MDRD 4 to estimate the GFR and better detect early onset kidney disease. Although the eGFR is considered to be the best overall index of renal function, it is relatively insensitive at detecting early renal disease and does not correlate well with tubular dysfunction (32;38).

McGlynn et al and Koppelstaetter et al have previously shown that CDKN2A is stronger than donor chronological age (DCA) at predicting post transplant function when serum creatinine is used as the marker for renal function. The results of this thesis at 1 year post-op confirm this finding (Table 1.10). However, when eGFR is used to measure renal

function, DCA seemed to have a better predictive power than CDKN2A in univariate linear regression analysis (Table 1.10). Further results from univariate regression analysis revealed that the predictive power of CDKN2A on eGFR was almost equal to that of ECD kidney criteria (Tables 1.9 and 1.10). In multivariate analysis, the only statistically significant contribution to both models is CDKN2A, indicating its predictive superiority in this limited cohort.

Despite increasing efforts by the transplant community to increase the availability of donor organs, there remains a significant shortfall with several thousand patients dying on the waiting list each year. The introduction of ECD kidneys has thus improved the quantitative discrepancy of the problem but we are still a distance from achieving satisfactory targets. Novel techniques of organ discrimination are therefore of huge importance in this respect. With the standard incorporation of biomarkers in assessing organ quality pre-operatively, it would seem logical that transplantation would be safer and an increase in the number of kidney transplants would subsequently ensue. CDKN2A is also related to DGF (Section 1.6.7) which in itself is associated with poorer graft performance and decreased long term survival (224;225). The reason for this remains to be determined, but may relate to biologically older organs being less tolerant to physical stress and requiring more time to recover from peri-transplant ischaemia reperfusion injury.

Why CDKN2A expression levels, in this study, have been observed to be a stronger biomarker of ageing than telomere length remains to be proven. Both fulfil the Baker and Sprott criterion, but the weakness of telomere length in predicting functional capacity in a solid organ is apparent. A contributory factor may be the extent of inter individual variation in telomere length at a given chronological age (13;221;226). The data is thus consistent with that of Koppelstaetter et al (2008), who previously demonstrated that telomere length was inferior to CDKN2A in determining variability on post-transplant serum creatinine levels in renal allografts. Inter-individual variation in CDKN2A expression at a given chronological age has not been fully determined, though increased expression of CDKN2A at the cellular level, remains a robust marker of a senescent state and its elevated expression is coincident with a reduction in cellular proliferation (180). In essence, its expression may be viewed as an 'off switch' for the cell and hence the degree of inter-individual variation observed with telomere length, is not expected to be as great. These observations have direct relevance for any future strategies employing biomarkers of ageing either clinically, or epidemiologically. Telomere length is currently used widely in

this context. The University of Glasgow is currently evaluating CDKN2A similarly, in large epidemiological studies, to evaluate its robustness with greater analytical power.

1.8.2 CDKN2A, SASP and rejection

One potential risk of high CDKN2A expression in the allograft is that it may pre-dispose to immune phenomenon (rejection episodes). Leakage of cell internal epitopes coincident with the senescence associated secretory phenotype (SASP) will result in new epitopes being exposed to the recipient immune system, as a direct function of the number of senescent cells in the donor organ. The SASP is associated with the secretion of growth factors and proteases that participate in wound healing, attractants for immune cells that kill pathogens and proteins that mobilize stem or progenitor cells. Thus, the SASP may also serve to communicate cellular damage/dysfunction to the surrounding tissue and stimulate repair, if needed (113;114). Some SASP proteins, in conjunction with cell surface ligands and adhesion molecules expressed by senescent cells, eventually attract immune cells that kill and clear senescent cells. A related manifestation of the senescent phenotype is the expression of micro-RNAs. CDKN2 associated micro-RNA expression profile in 'zero hour' pre-transplant renal allograft biopsies is also linked to clinicopathological and functional characteristics post-transplant. Evidence in support of this has recently been forthcoming as indicated above.

1.8.3 CDKN2A based pre-transplant scoring system

Based on current findings relating to the predictive power of CDKN2A on eGFR, it would follow that a scoring system incorporating biological markers would provide additional information for patients and clinicians during the organ selection process. Reference is made to larger studies such as the one in use by the OPTN in the US for deceased donor kidneys based on ten pre-transplant covariates, the Kidney Donor Risk Index (227). Undoubtedly, this novel scoring system adds a vital tool to the allograft allocation process. Importantly however, it does not include reference to biological age which may be viewed as an essential parameter of modernised scoring systems. In addition, the study itself showed similar results with age matching alone allowing for the possibility of a simpler scoring technique with equal efficacy. A 4 tier categorical scoring system is therefore

proposed, based on biological age of the graft and ECD (*M Gingell-Littlejohn et al, PLOS One 2013*). Allografts are classified Category I to Category IV based on a straight forward assessment outlined below, with Category I allografts predicting better performance than Category 4 (Table 6)

Category I	SCD Kidney and CDKN2A expression levels < 1.8
Category II	SCD Kidney and CDKN2A expression levels > 1.8
Category III	ECD Kidney and CDKN2A expression levels < 1.8
Category IV	ECD Kidney and CDKN2A expression levels > 1.8

Table 1.13 A donor risk classification based on ECD and CDKN2A

Suggested Donor Kidney Classification system incorporating CDKN2A as the biomarker of ageing and ECD kidney criteria. (SCD – Standard Criteria Donors, ECD – Extended Criteria Donors). Predicted kidney function and incidence of graft failure increases with higher category placement. (Adapted from: M Gingell-Littlejohn et al, PLOS One 2013)

The mean value for CDKN2A gene expression (1.8) was used as the cut-off value in the scoring system. Moreover, it can be seen from the scatter plots of CKDN2A vs eGFR at 1 year that renal function deteriorates significantly at CDKN2A expression levels above 1.8. ECD kidneys occupy both category III and category IV in this pre-transplant scoring tool meaning that ECD status carries a poorer prognosis than CDKN2A itself. The allocation of CDKN2A to a higher tier in this scoring system would require further studies to strengthen the correlations observed above. Since DCA forms part of ECD criteria, it was not used as

a single determinant of transplant function in multivariate analysis or the categorical scoring system.

1.9 Conclusion

A further benefit from these data, is that strategies to mitigate the rate of biological ageing applied to living donors would be expected to have an impact on post-transplant outcomes. Reduction of psychological and psychosocial stress and improved lifestyle via changes to diet and exercising might readily be considered (226;228;229). Biomarkers, specifically CDKN2A, may well expand the field of octogenarian donation for example, by discriminating organs with “less miles on the clock”. Larger multicentre studies are needed to strengthen the hypothesis and the proposed scoring system suggested in this thesis. It is envisaged that the biomarker CDKN2A will be integrated into a similar, robust and validated pre-transplant scoring system for all kidneys and other transplanted organs in the near future. Unfortunately, there remains a significant shortfall of organs across all transplant specialties, with several thousand patients dying on the waiting list each year. The introduction of ECD kidneys has improved the quantitative discrepancy of supply and demand but we are still a distance from achieving satisfactory targets. Novel techniques of organ discrimination are therefore of critical importance in this respect. With the standard incorporation of biomarkers in assessing organ quality pre-operatively, it would seem logical that transplantation would be safer and an increase in the number of kidney transplants would subsequently ensue. Genetic testing can be done in approximately four hour turnaround time and this would have minimal effect on the total cold ischaemic time of most transplants.

Chapter 2

PHENOTYPIC CHARACTERISATION OF THE AS/AGU MUTANT RAT

2.1 Introduction

2.1.1 AS/AGU PKC γ mutation

The mutant rat sub-strain (AS/AGU) arose spontaneously as a result of a specific single gene mutation in a colony of Albino Swiss (AS) rats in the Laboratory of Human Anatomy, Glasgow University (230). It was initially characterised as giving rise to a movement disorder phenotype, which was shown to be primarily attributable to age-dependent progressive loss of dopaminergic neurones of the substantia nigra pars compacta, as occurs in Parkinson's Disease (231)

The mutation was identified by positional cloning as a loss of function mutation in the gene encoding the protein kinase PKC γ (232). PKC γ is a member of an important family of cell signalling molecules with a wide range of functions in various cell types. This knowledge enhances the importance of this strain, as it provides a defined molecular change from which all subsequent physiological and pathological changes derive. Subsequently, the strain was demonstrated to display accelerated ageing in the kidney (P Shiels pers com., University of Glasgow). This strain has subsequently been regarded as a unique model of diseases of ageing and organ dysfunction. In particular, with evidence for premature renal senescence, the strain is an ideal model for renal dysfunction and transplant related pathologies. Furthermore, it is pertinent to neurodegeneration of the basal ganglia and/or aminergic systems such as Parkinson's disease (for which there is no similar laboratory model), Multiple Systems Atrophy, Supranuclear Palsy etc.

The accelerated ageing resulting from the PKC gamma mutation engenders a state of elevated oxidative stress in affected cells, tissues and organs, which predisposes to subsequent pathology (233). This is pertinent to renal dysfunction, in particular to transplant related pathologies, such as delayed graft function, late graft dysfunction as well as the poorer performance of marginal and older, donor organs. All these aspects of renal

transplantation are affected by biological ageing (234-237). Recent human and rodent data on senescence associated genes, particularly CDKN2A, match the accelerated ageing phenotype in the AS/AGU rat (231;238-243). This has been shown primarily in the renal and central nervous system. Phenotypic characterisation of the renal pathway however (with validated GFR studies) has never been described in detail. The aim of this chapter is thus to primarily support the genetic data on the AS/AGU rat with respect to premature deterioration in renal function and translate this into a validated animal model. The animal model comprises control AS and mutated AS/AGU rats. The classic inulin infusion technique was utilised as this is the gold standard measurement of GFR in animals. The response to IR injury was also measured between the two strains in this chapter. The use of anti-ischaemic compounds was directed on AS rats only and is explained in more detail in Chapter 3. Indeed, the testing of novel anti-ischaemic compounds in a model that is an excellent surrogate for human renal transplantation, is aimed at addressing the need to enhance organ half life. Any agents tested in these circumstances, will be evaluated with direct translation to a human setting. It is hoped that this will impact on the availability of useful organs for transplantation, their preservation time prior to transplantation, organ half life and subsequent performance post-transplant. Addressing any of these factors will help alleviate the shortfall in available donor organs, with direct patient and health care benefits. Significantly, the use of the AS/AGU and its parent strain will offer a longitudinal component to the study of BoAs.

2.1.2 Physiological calculation of renal blood flow and GFR

Since renal function depends on the clearance of the plasma by the functioning nephron, the blood flow to the kidneys is of natural importance. The measurement of renal blood flow (RBF) and more importantly, the glomerular filtration rate (GFR) are essential in the analysis and description of renal function. Characterization of the rat model was based on GFR studies for which the concept of clearance is inevitably introduced. Clearance is defined as the volume of plasma which is cleared of substance in unit time. The units of clearance are volume/time, usually ml/min.

$$C_x = U_x V / P_x$$

Where C_x is the clearance of x, U_x is the urine concentration of x, P_x is the plasma concentration of x and V is the urine flow (ml/min). The formula can also be expressed in terms of the units of measurement:

$$C_x = U_x \text{ (mg/ml)} \times V \text{ (ml/min)} / P_x \text{ (mg/ml)}$$

Clearance in itself actually represents a theoretical volume of plasma which is completely cleared of substance x, in 1 minute, because in reality no aliquot of plasma is completely cleared of any substance by its passage through the kidney. Nevertheless, the clearance formula has considerable usefulness in renal physiology and for assessing renal function in disease. Clearance of inulin as described below is used to measure GFR (whilst p-aminohippuric acid is used to measure the renal blood flow) and therefore it is imperative to understand the technical requirements for accurate clearance measurements. Since the plasma concentration of substance x must be known accurately, it must either be constant or changing in a predictable way so that an accurate average concentration can be calculated. Therefore, clearance measurements are only suitable for the steady state determinations of GFR and RBF and cannot be used when transient changes are occurring. An additional requirement is that urine flow must be adequate to collect sufficient amounts for the assay in the clearance period.

2.1.3 Inulin clearance and the measurement of true GFR

The most precise measurement of renal function in mammals is the physiological measurement of Glomerular Filtration Rate (GFR), obtained with a substance called inulin (244). Inulin is an uncharged polyfructose molecule with an average molecular weight of ~5000 and is not bound to plasma proteins. It is not a normal constituent of the body, but can be injected or infused intravenously in order to measure the inulin clearance. After passing freely through the glomerulus inulin travels down the tubule without being subtracted, added, synthesized or metabolized by the tubular cells (245). This is essential because once plasma concentrations have reached a steady state, the quantity that is excreted in the urine per unit time will be equal to that which is filtered through the glomerulus.

The amount of inulin excreted per minute is $U_{in}V$, i.e the urinary inulin concentration, U_{in} (mg/ml) multiplied by the urine flow, V (ml/min), and therefore is the amount which

entered the nephrons by being contained in filtered plasma. The volume of plasma from which the amount $U_{in}V$ mg/min of inulin was derived must therefore have been:

$$U_{in}V / P_{in}$$

And this is the clearance formula, where P_{in} is the plasma concentration (mg/ml). Thus the inulin clearance is equal to the glomerular filtration rate (GFR). The inulin clearance measurement (and hence the GFR measurement) is independent of the plasma inulin concentration.

In humans, the normal inulin clearance (GFR) is 125ml/min per 1.73m² body surface area. Even taking into account body surface area, GFR is low in infants and decreases in old age. On a day to day basis however, the GFR is remarkably constant in man. Variations in excretion of water and solutes depend on changes in tubular reabsorption and secretion, not on GFR changes. Because inulin is not a normal constituent of the body, and measurements of inulin therefore involve inulin infusions, it is rarely used clinically. In humans therefore, “Gold standard” GFR is computed from the clearance of injected, radioactive exogenous markers (the iodothalamate clearance) and is associated with little bias (246). In clinical practice however, GFR usually is not measured directly because of the cost, invasiveness, and possible radioactive exposure associated with the procedures. Alternatively, eGFR is computed from serum concentrations of endogenous markers, such as serum creatinine.

2.1.4 Serum Creatinine Clearance and estimated GFR (eGFR)

Renal function in man is estimated using plasma concentrations of creatinine, a byproduct of muscle metabolism. It is freely filtered by the glomerulus, but also actively secreted by the peritubular capillaries in very small amounts such that creatinine clearance overestimates actual GFR by 10-20%. This margin of error is acceptable in humans considering the ease with which creatinine clearance is measured. Unlike precise GFR measurements involving constant infusions of inulin, creatinine is already at a steady-state concentration in the blood and so measuring creatinine clearance is much less cumbersome in practise. Plasma creatinine concentration does not appreciably rise until 50–75% of kidney function is lost (247), and is therefore not an accurate index of acute renal function change. Furthermore, recent reports indicate that estimates of creatinine clearance in

humans do not reflect true renal function in many circumstances such as declining renal function, body fluid expansion, spinal cord injury, normal aging, renal transplant, and following administration of certain drugs (248-252).

Estimation of glomerular filtration rate is important in assessing and following up renal function as serum creatinine is not reliable enough in reflecting the true glomerular filtration rate (253-255). The performance of the modification of diet in renal disease study group (MDRD) and Cockcroft-Gault formula have been extensively assessed in native kidneys. The Nankivell formula was developed specifically for assessing glomerular filtration of the transplanted kidney (256). Gaspari et al (257) have shown the effectiveness of the MDRD formula and its superiority to Nankivell and Cockcroft Gault equations. Similarly, a rise in serum cystatin C levels have been shown to predict renal function more accurately than serum creatinine(258;259).

2.2 Hypothesis

- i.** Biomarkers of ageing can be exploited in animal models to investigate events associated with ischaemia-reperfusion.
- ii.** The mutant AS/AGU rat possesses inferior renal function to its parent strain when matched for age.
- iii.** The mutant AS/AGU strain is less resistant to the effects of IR Injury and hence may serve as the perfect animal model to characterise ECD kidneys in-vivo.
- iv.** This model can be used to assess interventions using anti-ischaemic compounds for benefit in reducing the harmful short and long term effects of ischaemia-reperfusion injury on the kidney.

2.3 Aims

- i. Can the genetic data (showing increased renal senescence in the mutant AS/AGU strain over its parent strain) be reproduced in an animal model to show a phenotypically valid difference between the two strains?
- ii. Is the mutant strain less tolerant to IR Injury?
- iii. Can this model serve as a platform for the testing of anti-ischaemic compounds?

2.4 Methods

2.4.1 Animal Groups and Housing

The experiments were carried out on both male and female rats. Both control - Albino Swiss (AS) and mutant - Albino Swiss/Anatomy Glasgow University (AS/AGU) were fed a standard diet and tap water *ad libitum*. Animals were housed in the Joint Research Facility – University of Glasgow under standardized conditions in plastic-metal cages, light-dark cycle 12/12 hours, temperature 22 +/-2 °C, humidity 50 +/-5 %.

2.4.2 Preparation of FITC-Inulin Solution

Flourescein Isothiocyanate Inulin (FITC-Inulin) (Sigma-Aldrich) was used for GFR experiments and the fluorescence of urine and plasma was calculated spectrofluorometrically using the fluorescence microplate reader BIO-TEK *flx-800*. The emission and absorbance wavelengths were 495nm and 530nm respectively. This technique offers high sensitivity and can detect concentrations of FITC down to 1µg/ml in tissue fluid. Measurements of fluorescence in the urine and plasma provided quantitative data on the filtration process across the glomerulus, which was then calculated according to the equation:

$$\text{GFR} = \text{UV/P}$$

Where U= Urinary Inulin Fluorescence, V= Urine volume, P= Plasma Inulin Fluorescence

0.2% w/v FITC Inulin solution was made by dissolving 40mg of FITC Inulin in 20mls of 0.9% Physiological Saline Solution (Baxter Pharmaceuticals). 1% FITC Inulin w/v was also made by dissolving 10mg FITC Inulin per ml of 0.9% Physiological Saline Solution. The solutions were warmed in a water bath to facilitate dissolution and dialysed with physiological saline overnight through a 1Kda semi permeable membrane in order to remove any unbound Fluorescein (Gebaflex 1Kda dialysis tubes). Dialysis tubes were protected from light to avoid disassociation prior to infusion.

2.4.3 Experimental Design and Surgical Technique

The animals were weighed and subsequently anaesthetised using Isoflurane for induction of at a concentration of 4% in Oxygen. An intraperitoneal injection of Inactin (Thiobutabarbital sodium salt hydrate, Sigma Aldrich) (100g/ml) was subsequently administered at a dose of 1ml/kg. If the animal showed signs of arousal, then it was additionally maintained on isoflurane 0.5-1 % in 1L/min Oxygen. A heated surgical table was utilised to maintain body temperature of the animal at 37°C.

The femoral vessels were then exposed in animals weighing more than 280 grams (the common iliac vessels were utilised for smaller animals). Fine bore polyethylene tubing (Smiths Medical) (0.96mm) was inserted into the vein under microscopic vision and secured in place using 3/0 silk sutures. A bolus of 0.4mls 1% FITC Inulin was administered via a 1ml syringe with a 23 gauge needle, which fitted exactly into the polyethylene tubing emerging from the vessel. An intravenous infusion of 0.2% FITC Inulin was subsequently commenced at a rate of 3mls/hr using a programmable syringe pump (World Precision Instruments – NE300). A similar sized cannula was then inserted into the accompanying artery and a sample of 0.4 mls blood is removed from the animal. This was centrifuged at 5000rpm for 10 minutes and the plasma transferred to a 200µl eppendorf for storage up to 72 hours at 4°C. The arterial line was flushed with heparin /saline (1%/0.9%) with a v/v ratio of 1:5 so as to maintain patency. Laboratory biochemical analysis was then performed on the stored plasma sample for multiple parameters as indicated in the text below (Companion Animal Diagnostics, University of Glasgow).

A midline laparotomy was then made and the ureters of each kidney identified and ligated distally. A fine microcatheter (0.61mm) was inserted into each ureter and secured using 3/0 silk sutures. Urine was collected from each kidney into a separate tube at 30 minute

intervals and a blood sample (80µl) was taken simultaneously. The 30 minute interval blood samples were spun at 11,000 rpm for 8 minutes and the plasma aliquoted into a fresh eppendorf taking care not to remove any of the interphase. After every blood sample, the arterial line was flushed with heparin/saline.

Equilibrium is reached in the plasma, when the amount of FITC inulin infused is equal to filtration by the kidneys. Several initial experiments indicated that equilibrium is established between 60-120 minutes after the 0.4ml whole blood sample is obtained for laboratory analysis (data not shown). A 0.4ml volume of whole blood is needed (to give approximately 200µl plasma for laboratory biochemical analysis) which results in temporary elevated plasma inulin levels, disturbing equilibration phase. 30 minute sampling is maintained for up to 3 hours in order to ensure a steady state of plasma inulin from which to calculate individual kidney GFR.

Subsequently, the kidney pedicle of the left kidney was dissected in order to clearly display the renal artery and vein and a vascular occluding clamp was applied for exactly 10 minutes. This produced a recoverable injurious state (primarily Acute Tubular Necrosis – ATN) lasting approximately 30-40 minutes (information based on several preliminary tests). Urine samples were then collected at 15 minute intervals post clamp release in order to quantitatively characterize the animal's response to ischaemia-reperfusion (IR) injury. A maximum of two hours of urine collection post clamping was performed.

The procedure was terminated at approximately 6 hours from initiation of anaesthesia by Schedule 1 killing. Tissues were immediately placed in 10% formalin for future histological analysis, RNA Later[®] for genetic expression analysis and liquid nitrogen for immunohistochemistry.

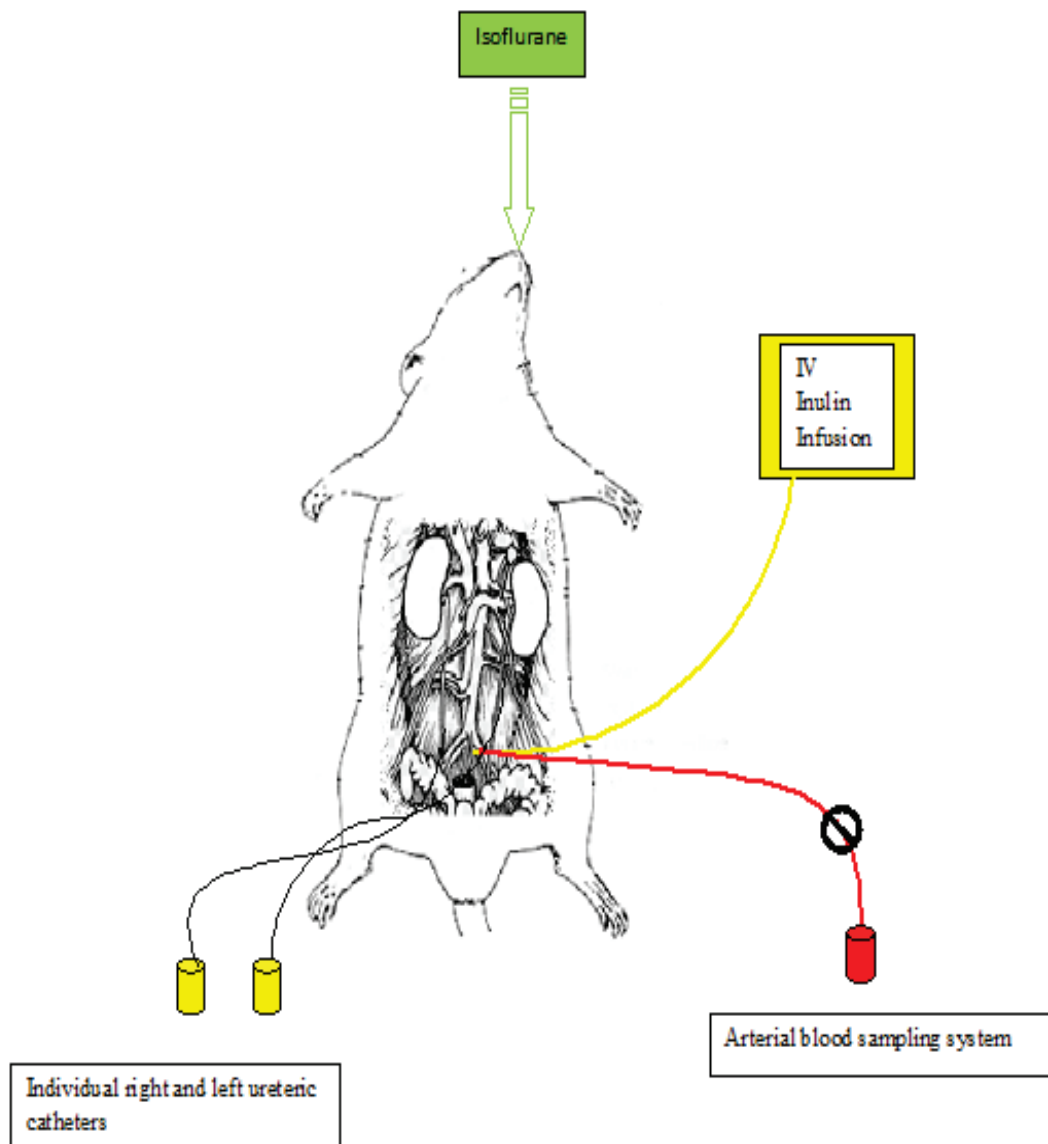


Figure 2.1 Depiction of surgical setup

Rat Model Clearance study depicting the surgical setup in characterizing the renal phenotype of the AS/AGU mutant. Note cannulation of individual ureters to assess function of both kidneys. Also note cannulation of left femoral or iliac vessels to allow infusion of inulin and repeated arterial blood sampling.

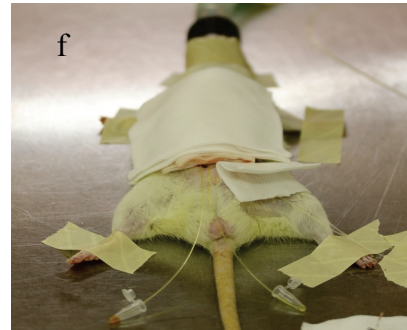
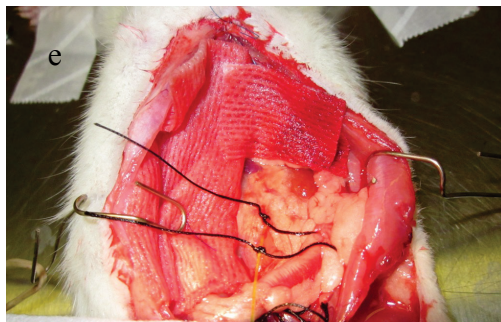
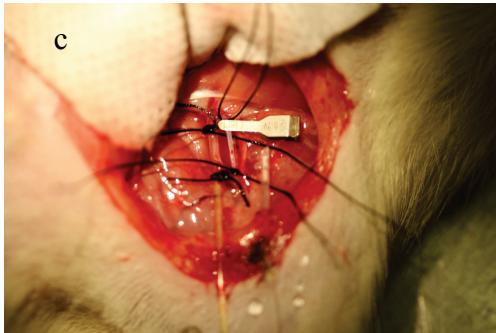
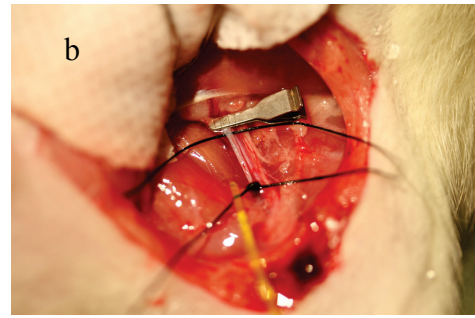


Figure 2.2 Images of surgical technique

Dissection and cannulation of the left femoral vessels and ureters. The groin is dissected and the femoral vessels are exposed beneath the inguinal ligament (a). The vein is carefully dissected from the artery and a clamp is placed proximally. A venotomy is made and the primed cannula containing inulin and is ready to be introduced (b). The venous cannula is introduced and the artery is subsequently dissected. Similarly, a clamp is placed proximally and an arteriotomy is made to allow the passage of a cannula for repeat blood sampling (c & d). The ureters of both kidneys are then cannulated. Here, the left kidney is visible with a cannula inserted into the ureter (e). The procedure continues with minimal physiological disturbance and the urine is collected in separate eppendorfs (f)

2.4.4 GFR Analytical Technique

Urine from each 30 minute interval was immediately measured on table using a Gilsons pipette in a reverse manner so as to give an accurate measurement of volume per unit time per kidney. After a gentle spin to remove sediment, a 10 μ l aliquot per sample was then transferred to a single well in the fluorescent plate (Thermo-Scientific F96 Microwell Plates). 40 μ l of 500mM HEPES buffer solution (dissolved 59.6g of HEPES in 500 ml of deionized water and adjusted pH to 7.4 using 10N NaOH) was then added to the sample to make up a total well volume of 50 μ l. This stage is necessary since fluorescence of urine or plasma may vary across a pH range (260) (Fig 2.3). The process is repeated for all urine and separated plasma samples, such that for each time point during the experiment there is a plasma fluorescence value (assayed in triplicate), a urine fluorescence value and an accurate urine volume per kidney. The unclamped kidney serves as an internal control for the experiment. (See Table 2.1)

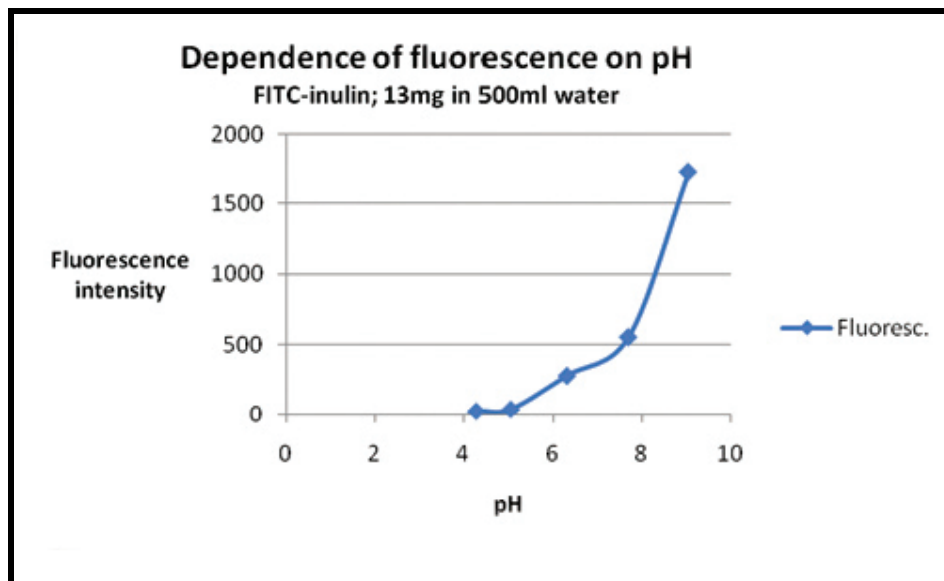


Figure 2.3 Dependence of FITC Inulin fluorescence on pH

Dependence of fluorescence of FITC-Inulin in the range pH 4-9 (Adapted from FITC Inulin manual - TdB Consultancy)

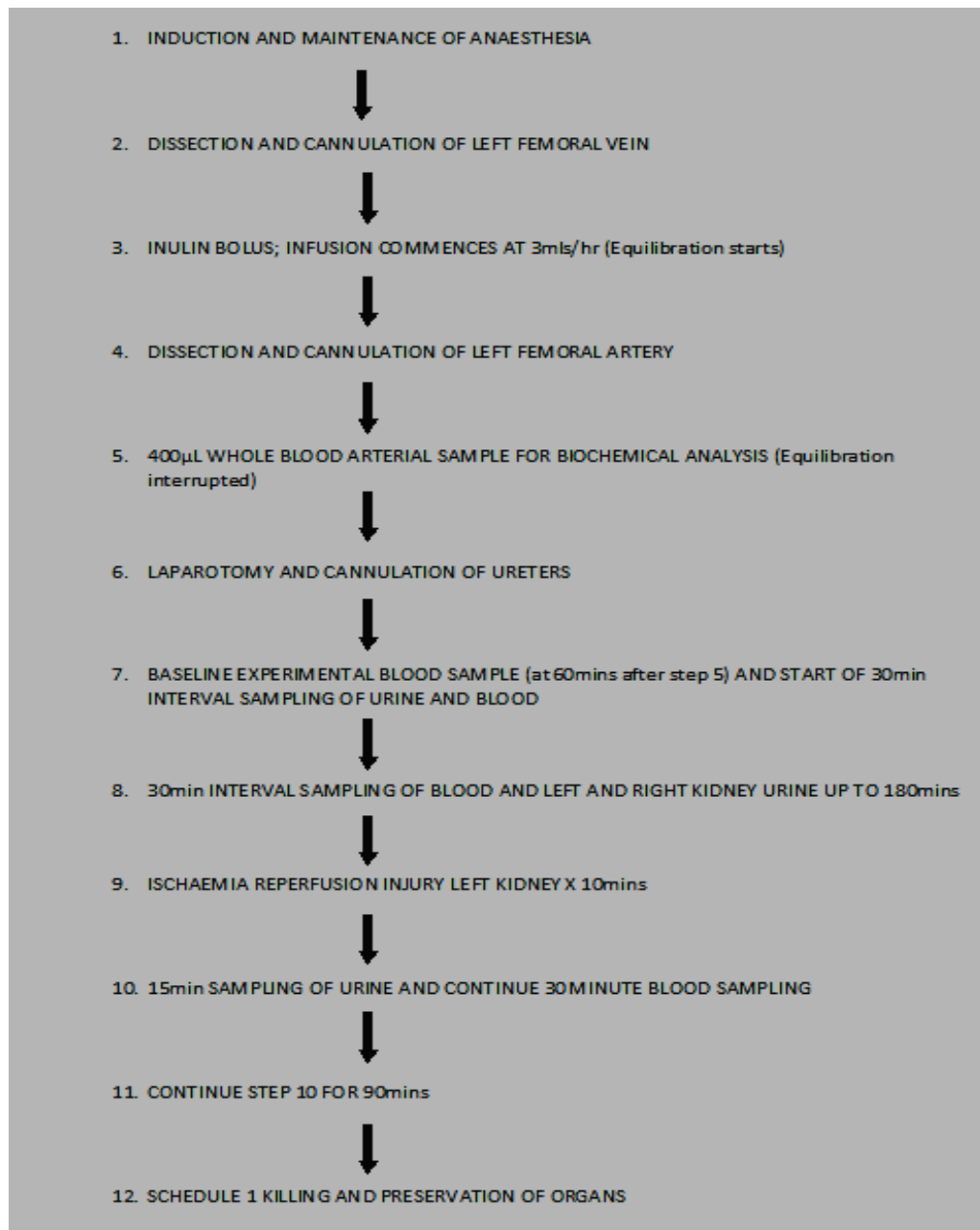


Fig 2.4 Schematic representation of operative methods

The twelve steps shown above were standard protocol for all GFR/IR Injury experiments

Time Point	Time in mins post analysis sample	Plasma 1	Plasma 2	Plasma 3	Plasma Average	Urine FL Rt Kidney	Urine FL Lt Kidney	Urine Vol Rt Kidney	Urine Vol Lt Kidney
Baseline									
1									
2									
3									
4									
5									

Table 2.1 Rodent GFR experimental documentation

The table was used for every GFR experiment documented. Note how the final plasma concentrations of FITC (column 6) is an average of 3 individual readings whenever possible (columns 3-5). This is because it is essential to have reached *plasma* equilibrium before determining GFR. Baseline sample is the first sample (usually 60-90mins) from which GFR analysis commences. FL=Flourescence, Rt=right, Lt=left

2.4.5 GFR and IR Injury Studies - Initial Testing Phase

Prior to official GFR studies, a period of initial testing addressing critical experimental conditions was undertaken. Factors to be determined included:

- Rate of FITC Inulin decomposition after preparation
- Ideal concentration of FITC Inulin infusion
- Ideal concentration for FITC Inulin bolus
- Ability to tolerate a 3ml/hr infusion for 6 hours without adverse physiological effects
- Time before equilibrium of 0.2 % FITC in rodent plasma with a 3ml/hr infusion?

A total of 24 animals were utilised for actual GFR experiments. A further 6 animals (not included in this thesis) were used for preliminary testing described above. With the period of experimentation for one animal lasting approximately 10 hours (7 hours surgery & preparation, 3 hours analysis), the total time of testing approached 300 hours. Initial experiments using FITC Inulin by Qi et al (261) showed that dialysis through a semi-permeable membrane is necessary to remove unbound inulin prior to experimentation and that the process should last for approximately 12hrs. Based on initial fluorescence readings, the amount of unbound inulin removed through this process was calculated as being between 0.2% and 0.4%. The ideal concentration which allowed for stability of FITC Inulin in solution for up to 24 hours at 4°C was approximately to 2% w/v. Higher concentrations of FITC Inulin especially above 10% form precipitates on standing, since inulin tends to form crystalline aggregates (FITC Inulin – TdB consultancy). Despite refrigeration and a dark environment, there was a 8.94% reduction in fluorescence over 7 days and therefore most FITC Inulin solutions were prepared 24-48 hrs in advance.

A total of 16 animals from the GFR cohort above were analysed for IR studies. This is because urine urea and SG parameters were commenced after having started GFR studies.

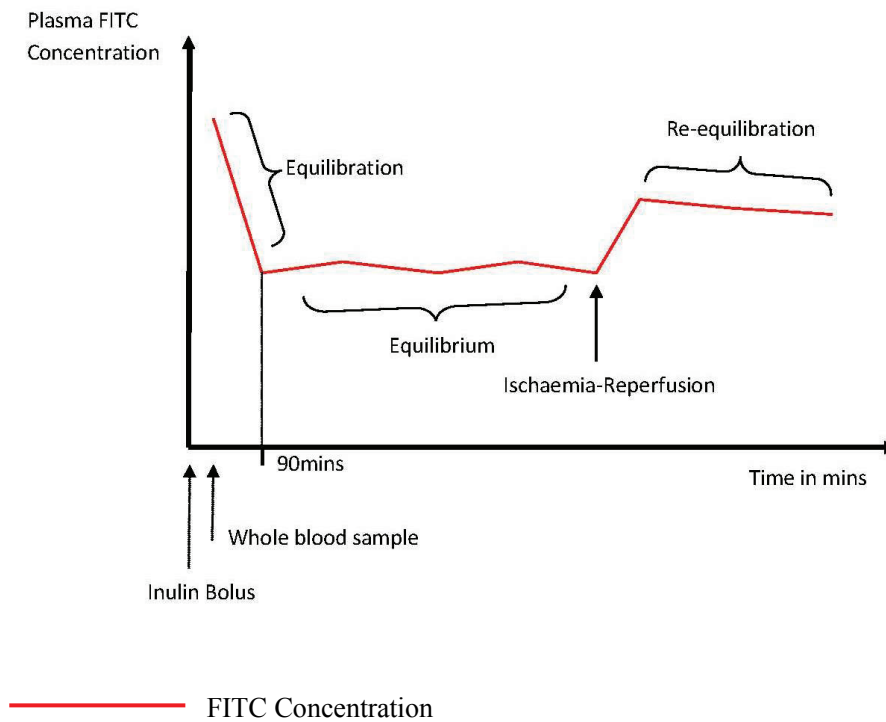


Figure 2.5 Graphical representation of plasma FITC Inulin concentration through a typical experiment

Line graph depicting plasma FITC concentration over time with steady equilibrium phase achieved. Initial bolus of 0.4mls 1% FITC tends to overshoot the eventual equilibrium concentrations in the plasma. This is compounded by the removal of a whole blood sample after arterial cannulation. This results in a smaller circulating blood volume which is replaced by the constant infusion of 0.2% FITC Inulin which has a background fluorescence value of approximately 7000. Note how plasma FITC level increases post clamping due to decreased excretion from the renal system setting a new equilibrium until renal function is restored in the damaged kidney at which point baseline Inulin concentration begins to approach its pre clamping levels.

Both male and female rats were used. 12 control AS rats and 12 mutant AS/AGU rats were analysed for GFR studies, biochemical profile and recovery from a set ischaemic insult to a unilateral kidney. The tables below depict the demographics of the rat population for both the GFR and biochemical studies.

	AS (Control) n=12	AS/AGU (Mutant) n=12
Male	6	7
Female	6	5
Mean Age (Months)	10	9.8
Mean Weight (grams)	311.50	306.08

Table 2.2 Demographics of rodent population for GFR studies (n=24)

2.4.6 Biochemical Serum and Urine Analysis

An extended biochemical kidney profile was performed on both AS (control) and mutant (AS/AGU) strains on whole blood samples. To increase the power in this arm of the experiment, blood was also taken from other animals due to be sacrificed by a schedule 1 killing. Urine from each animal was also sampled by aspirating the urinary bladder. The analysis was performed on 200µl of separated plasma via an automated laboratory process at Glasgow University, Veterinary Diagnostic Services. Blood samples were measured with the automated Olympus AU5400 analyser. The urine specific gravity was measured with a refractometer at room temperature. The variables sampled were:

Plasma: Sodium, Potassium, Sodium/Potassium Ratio, Chloride, Calcium, Phosphate, Urea, Creatinine, Cholesterol, Total Protein, Albumin, Globulin, Albumin/Globulin ratio

Urine: Specific Gravity, Protein, Creatinine, Protein/Creatinine ratio.

	AS (Control) n=37	AS/AGU (Mutant) n=27
Male	21	15
Female	16	12
Mean Age (Months)	8.6	8.8
Mean Weight (grams)	319.8	309.8

Table 2.3 Demographics of rodent population for biochemical studies (n=64)

2.4.7 Immunohistochemical analysis for bio-age in rat kidney

Renal tissue from 6 animals (n=3 AS, n=3 AS/AGU) were subject to immunohistochemical (IHC) analysis to monitor for the presence of apoptosis – TUNEL assay and lipofuscin SA β Gal together with the presence of senescence proteins p16 and p21. The kidneys were cut processed, stained and scanned for HistoPath scoring (i.e clinically based scoring). All stained sections were doubled scored by two judges. The absolute difference between individual histoscores was lower than 50 in the majority (96%) of cases, which proved the reliability of the ratings for both judges.

2.4.8 TUNEL assay protocol

(Chemicon, ApopTag Plus Peroxidase *In Situ* Apoptosis Detection Kit S7101)

Dewaxing and rehydration - 2 x 2 mins in Xylene (Dewaxing), 2 x 2 mins 100% alcohol (Rehydration), 2 mins 90% alcohol, 2 mins 70% alcohol and final rinse in water.

Preparation of 20 μ g/ml Proteinase K solution in PBS (Dilute 200 μ g/ml stock solution). 100 μ l is required per kidney slide - Sections were ringed with DAKO pen to create a barrier and proteinase K solution was added to the slide and incubated at 25oC for 15 minutes (humidified chamber to ensure constant temperature). Then, proteinase K solution was removed and slides were washed twice in dH₂O for 2 minutes.

Preparation of 3% H₂O₂ in dH₂O (40mls H₂O₂ in 360mls dH₂O) – slides were treated with H₂O₂ for 5 mins at room temperature (on stirrer) and then washed twice in water for 5 minutes. 75µl of equilibration buffer was added to the slide and incubated at 25oC for 10 minutes (in a humidified chamber).

Preparation of working strength TdT Enzyme (70% Reaction Buffer : 30% TdT Enzyme). 55µl is required per slide - equilibration buffer was tapped from the slide and applied 55µl of working strength enzyme. Incubation at 37°C for 1hour (humidified). For negative control TdT enzyme was not added equilibration buffer left on slide.

Preparation of working strength stop/wash buffer (1ml stop/wash buffer : 34mls dH₂O) - slides were placed in a coplin jar/staining dish with stop/wash buffer and agitated for 15 seconds, then washed for 10 minutes on a stirrer at room temperature (RT).

Removal of aliquot of anti-digoxigenin conjugate from stock, 65µl is required per slide, and then warmed to room temperature - slides were washed three times in TBS for 1 minute on stirrer at RT. Anti-digoxigenin was applied to slides (65µl) and incubated at 25oC for 30 minutes (humidified chamber). Slides were washed four times in TBS for 2 minutes on stirrer at RT.

Preparation of working strength peroxidase substrate (1:50 DAB Substrate : DAB dilution buffer i.e 60µls DAB Substrate : 3mls DAB dilution buffer). 75µl DAB needed per slide – application of peroxidase substrate to slide and incubation at RT for 10 minutes. Slides were washed in running water for 10 minutes.

Haematoxylin Counterstain – Slides were stained in Harris haematoxylin for 1 minute, rinsed in running water and inserted into scots tap water substitute (for 1minute, care was taken with respect to intensity of blue colour) and finally rinsed again in running water

Dehydrate and mounting: 1 min 70% alcohol, 1 min 90% alcohol, 2 x 1 min 100% alcohol, 2 x 1 min xylene, mount in DPX

2.4.9 SA-Beta-Gal Staining on Tissue Sections

Tissue Fixation: Slides are incubated in 95% Ethanol for 10 minutes then allowed to dry in air and stored at 4 °C until required.

Reagent Preparation - For SA-Beta-Gal staining, two solutions are required: one pH4 solution and one pH6 solution. The pH4 solution acts as a positive control as it should stain all cells blue in colour. The reagents required for both solutions are the same:

- Potassium Ferricyanide (400mM)
- Potassium Ferrocyanide (400mM)
- Magnesium Chloride (MgCl₂ 200mM)
- Sodium Chloride (NaCl 1500mM)
- Citric Acid (800mM)
- Sodium Phosphate (800mM)

All solutions are prepared in PBS. MgCl₂, NaCl, Citric Acid, Sodium Phosphate are all stored at 4°C. Potassium Ferricyanide and Potassium Ferrocyanide are stored in aliquots at -20°C

	MW	Conc Reqd		Vol Soln Reqd	Amt Reqd (g)
Potassium Ferricyanide(400mM)	329.2	400	mM	5000	0.6584
Potassium Ferrocyanide(400mM)	422.4	400	mM	5000	0.8448
MgCl ₂ (200 mM)	203.31	200	mM	4000	0.162648
NaCl in 1X PBS	58.44	1500	mM	40000	3.5064
Citric acid	294.1	800	mM	30000	7.0584
Sodium Phosphate	142	800	mM	30000	3.408

Table 2.4 Reagents used in SA-Beta-Gal Staining

pH4 and pH6 solution preparation – Next step involved preparing the Citric Acid (400mM)/Sodium Phosphate (400mM) pH4 and Citric Acid (400mM)/Sodium Phosphate (400mM) pH6 solutions: equal volumes of citric acid (800mM) and Sodium Phosphate (800mM) were added to two beakers. One beaker made to pH4 and the other to pH6.

The final SA-Beta-Gal solutions were prepared as follows:

		pH6	
		Total Volume Reqd =30mls	
μL/slide	Ingredients	Final Conc (per 1ml)	Required Volume
20	xl -Gal (50mg/ml)	1mg	600ul
12.5	Potassium Ferricyanide(400mM)	5mM	375ul
12.5	Potassium Ferrocyanide(400mM)	5mM	375ul
10	MgCl ₂ (200 mM)	2mM	300ul
100	NaCl (1500mM)	150mM	3000ul
100	Citric acid (400 mM)/ Sodium Phosphate (400mM) PH 6.0	40mM	3000ul
	PBS		22350ul
		pH4 +ve control	
		Total Volume Reqd =10mls	
μL/slide	Ingredients	Final Conc (per 1ml)	Required Volume
20	xl -Gal (50mg/ml)	1mg	200ul
12.5	Potassium Ferricyanide(400mM)	5mM	125ul
12.5	Potassium Ferrocyanide(400mM)	5mM	125ul
10	MgCl ₂ (200 mM)	2mM	100ul
100	NaCl (1500mM)	150mM	1000ul
100	Citric acid (400 mM)/ Sodium Phosphate (400mM) PH 4.0	40mM	1000ul
	PBS		7450ul

Table 2.5 Final SA-Beta-Gal solutions at pH4 and pH6

Tissue Rehydration – tissue allowed to warm up to room temperature and rehydrated in DPBS for 10 minutes.

SA-Beta-Gal Staining – Hydrophobic barrier with DAKO pen followed by 200μls of pH6 solution to each slide with the exception of the positive control. To the positive control slide 200μls of the pH4 solution was added. Slides placed in an incubation tray and incubated at 37oC for ~48 hours.

Counterstaining with Nuclear Fast Red Solution was prepared as follows - 25g of Aluminium Potassium Sulphate Dodecahydrate (Sigma #237086) was dissolved in 500ml

dH₂O. 0.5g of Nuclear Fast Red (Sigma #60700) added to this solution and heated to dissolve. Filter and removal of SA-b-Gal solution from slides. Washed in running water and slides placed in Nuclear Fast Red Solution for 30 seconds. Again washed in running water.

Dehydrating and mounting slides – Slides incubated in 70% alcohol for 1 minute, 90% alcohol for 1 minute, 100% alcohol for 2x1 minute, xylene for 2x1 minute. Sections mounted onto coverslips with DPX.

2.4.10 IHC using MOUSE p16 Antibody F-12

(Santa Cruz # sc-1661 Mouse Monoclonal Ab)

Tissues were fixed in 95% Ethanol for 10mins, then allowed to air dry and warm up to room temperature. Subsequently, tissues were rehydrated in PBS for 5 minutes. Sections were then treated with 3% H₂O₂ for 10minutes on a stirrer (40mls 30% H₂O₂ – 360mls dH₂O). Sections then washed in running water. Slides dried and barrier formed with DAKO pen. M.O.M Mouse blocking reagent prepared by adding 2 drops of Blocking Reagent stock solution to 2.5mls TBS. 200µls of blocking reagent added to slide and incubated at 37°C for 1 hour. Slides were then washed for 2 x 2 minutes in TBS. Preparation of M.O.M Diluent – Addition of 300µls protein concentrate to 3.75mls TBS. 1^o Antibody prepared using a 1:100 dilution in M.O.M diluents and addition of 200µls M.O.M diluent to each slide. Slides incubated for 5 minutes at RT and M.O.M diluent removed from slides. 200µls 1^o Ab added to each slide. For the negative control only M.O.M diluent was used. Slides were then incubated in primary antibody at 4 ° C overnight.

Slides were then washed for 2x2mins in TBS and M.O.M Biotinylated Anti-Mouse IgG reagent prepared by adding 10µls Biotinylated Anti-Mouse IgG Reagent to 2.5mls M.O.M diluent. 200µls of Biotinylated Anti-Mouse IgG Reagent was added to each slide and they were incubated for 5 minutes at RT. The Biotinylated Anti-Mouse IgG Reagent was removed and slides washed 2x2 minutes in TBS.

VECTASTAIN Elite ABC Reagent prepared by adding 2 drops of *Reagent A* to 2.5mls TBS, mixed and added to 2 drops of *Reagent B*. This had to sit for thirty minutes before use and then 200µls of VECTASTAIN Elite ABC Reagent was added to each slide.

Incubation was for 5 minutes at RT. VECTASTAIN Elite ABC Reagent removed and slides washed for 2x5 minutes in TBS.

DAB substrate (Vector, Sk-4100) prepared by adding 5ml of distilled water to 2 drops of buffer stock and mixed, 4 drops of DAB stock and mixed, 2 drops of hydrogen peroxide and mixed. Sections incubated with DAB substrate at room temperature until colour developed (approx 10 minutes). Slides were then washed in running water for 10 minutes and stained in Harris haematoxylin for 1 minute, rinsed in running water, turned blue with scots tap water substitute and lastly rinsed in running water. Dehydration and mounting of slides: 1 min 70% alcohol, 1 min 90% alcohol, 2 x 1 min 100% alcohol, 2 x 1 min xylene, sections mounted onto coverslips with DPX.

2.4.11 IHC using MOUSE p21 Antibody C-19

(Santa Cruz # sc-397 Rabbit anti Mouse)

Tissues were fixed in 95% Ethanol for 10mins, then allowed to air dry and warm up to room temperature. Subsequently, tissues were rehydrated in PBS for 5 minutes. Sections were then treated with 3% H₂O₂ for 10minutes on a stirrer (40mls 30% H₂O₂ – 360mls dH₂O). Sections then washed in running water. Slides dried and barrier formed with DAKO pen. Blocking solution prepared: 20% Goat Serum in TBS (needed 200µls solution per slide). Section were covered with 200µls blocking solution and incubated for 1 hour at 37oC – use incubator. Blocking solution was blotted from the section and incubated in primary antibody at 4 ° C overnight (1:100 in antibody diluent (DAKO, S0809) for the negative control, only antibody diluent was used). Antibody was removed from the section and slides washed for 2x5mins in TBS. Secondary antibody was prepared – Goat anti Rabbit secondary (DAKO, P0448), 1:200 in 20% Goat Serum in TBS solution. Sections incubated with secondary antibody for 30 mins at 37oC and slides washed for 2x5mins in TBS. DAB substrate (DAKO DAB REAL #K5007) was prepared (200µls per slide). 1X Substrate Buffer : 50X DAB + Chromagen (i.e for 5ml solution, 500µls DAB Chromagen was added to 4500µls DAB Substrate Buffer). Sections were incubated with substrate at room temperature until colour developed (10 minutes). Slides were then washed in running water for 10 minutes and stained in Harris haematoxylin for 1 minute, rinsed in running water, turned blue with scots tap water substitute and lastly rinsed in running

water. Dehydration and mounting of slides: 1 min 70% alcohol, 1 min 90% alcohol, 2 x 1 min 100% alcohol, 2 x 1 min xylene, sections mounted onto coverslips with DPX.

2.5 Results

2.5.1 GFR Validation

In order to validate the GFR results, a graph of total GFR (ml/min) vs body weight was plotted (Fig 2.6). As would be expected, this shows increasing values of GFR as rodent body weight increases (R^2 Linear = 0.533), implicating that total rodent GFR results were following a reliable trend.

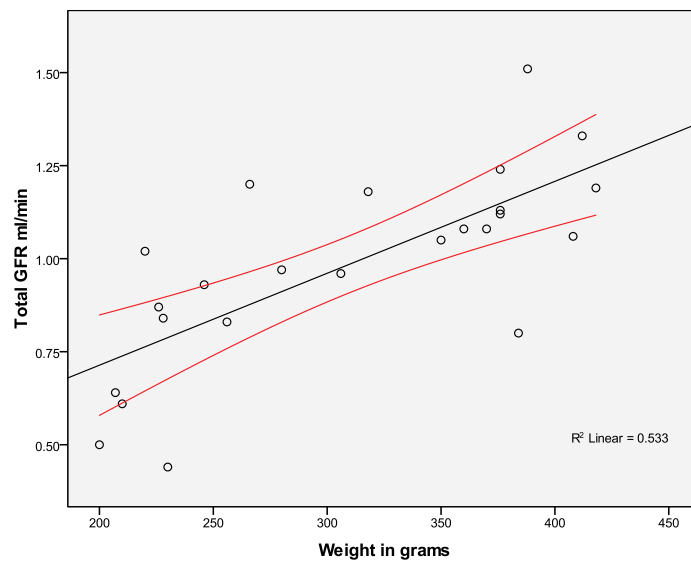


Figure 2.6 Scatterplot showing the expected increase in GFR with weight for both AS and mutant strains (n=24)

As indicated above, the GFR in the rodent population varies significantly with weight ($p = <0.001$). The increasing size of the kidney in larger animals is associated with greater nephron mass and hence greater filtration rates. It follows that unless rats involved in the experiments were all of identical size, then figures for GFR will be skewed by weight. To compensate for this confounding variable, all GFR variables were corrected to 100 grams of body weight (bw).

Strain	Age in Months	Weight (gr)	Sex	Total GFR ml/min	Split Right ml/min	Split Left ml/min	GFR/100gr bw
AS	4.9	228	F	0.84	0.48	0.36	0.37
AS/AGU	4.5	210	F	0.61	0.34	0.27	0.29
AS	5.1	226	F	0.87	0.48	0.39	0.38
AS/AGU	4.7	200	F	0.5	0.26	0.24	0.25
AS	5.6	220	F	1.02	0.52	0.50	0.46
AS/AGU	5.2	207	F	0.64	0.4	0.24	0.31
AS	6	360	M	1.08	0.6	0.49	0.30
AS/AGU	5.5	306	M	0.96	0.47	0.49	0.31
AS	6.2	350	M	1.05	0.59	0.46	0.30
AS/AGU	5.5	318	M	1.18	0.6	0.58	0.37
AS/AGU	7.5	230	F	0.44	0.22	0.22	0.19
AS	7.4	256	F	0.83	0.43	0.40	0.32
AS	7.9	280	F	0.97	0.45	0.52	0.35
AS/AGU	8.7	246	F	0.93	0.5	0.43	0.38
AS/AGU	15.6	376	M	1.24	0.69	0.55	0.33
AS	14.7	266	F	1.2	0.62	0.58	0.45
AS	15.1	370	M	1.08	0.53	0.55	0.29
AS/AGU	16.5	384	M	0.8	0.43	0.37	0.21
AS	15.6	418	M	1.19	0.63	0.56	0.28
AS/AGU	16.5	412	M	1.33	0.71	0.62	0.32
AS	15.7	388	M	1.51	0.73	0.79	0.39
AS/AGU	16.8	408	M	1.06	0.65	0.41	0.26
AS	15.8	376	M	1.13	0.63	0.51	0.30
AS/AGU	11.7	376	M	1.12	0.65	0.47	0.30

Table 2.6 Results of GFR analysis

Database extract of results from GFR experiments showing details of total, split and corrected GFR/100gr bw.(AS n=12, AS/AGU n=12)

	AS	AS/AGU
Mean GFR ml/min/100gr bw	0.3492	0.2933
SD	0.0617	0.0577
SEM	0.0178	0.0167
N	12	12

Table 2.7 GFR comparison between strains

Results of students t-test analysis to compare mean GFR between the two strains. A statistically significant difference between strains holds (p=0.032)

eGFR / 100g bw (ml/min)	AS ♂	AS ♀	AS/AGU ♂	AS/AGU ♀
Mean	0.31	0.39	0.30	0.28
Std Error of Mean	0.016	0.023	0.019	0.031
Range	0.11	0.14	0.16	0.19
Minimum	0.28	0.32	0.21	0.19
Maximum	0.39	0.46	0.37	0.38

Table 2.8 Mean GFR between female and male strains

2.5.2 Parallel Strain Analysis

Figure 2.7 shows a symmetrical increase in GFR between both strains with increasing age. The scatterplots with a line of best fit indicate that even at a young age there is a difference in total GFR between the two strains, with GFR consistently lower in the mutant rats. As expected, the GFR increases with age/weight however the values for AS/AGU mutant are consistently lower.

When GFR is corrected for body weight, it is possible to visualise the age related decline in GFR. This is shown in Figure 2.8 where both strains show an equal rate of deterioration in GFR with age. The graph indicates that the mutant strain shows a compromised GFR pattern from a young age which persists into adulthood and declines at the same rate as the parent strain. The difference in the corrected GFR/100g body weight between the two strains was statistically significant (t-test, n=24) ($p=0.0321$, 95% CI 0.0052 - 0.1064).

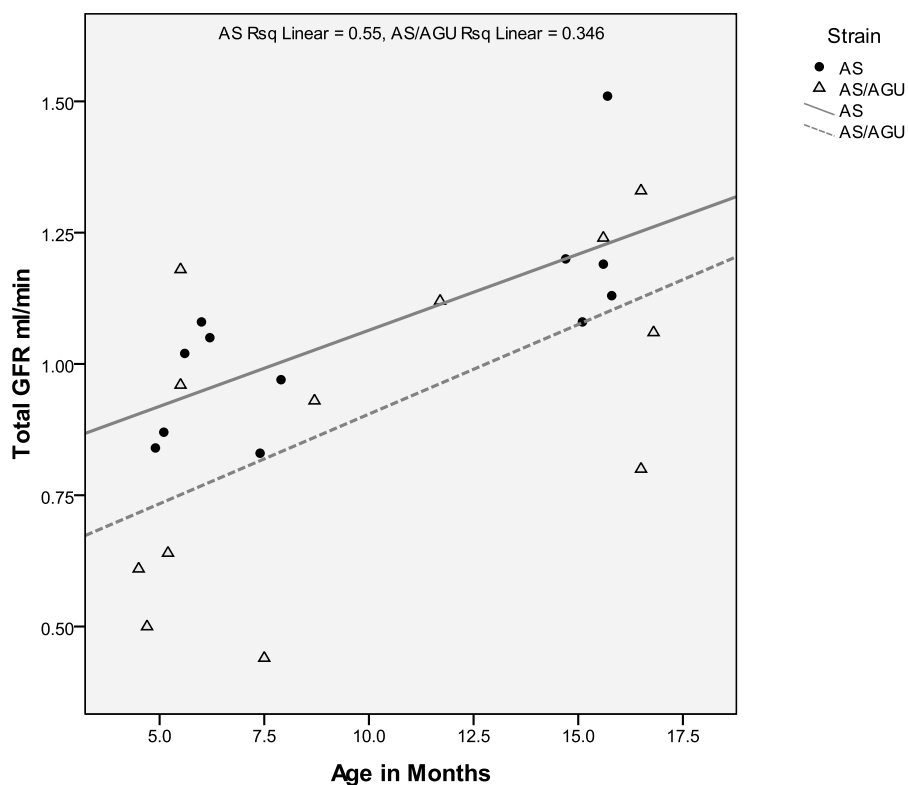


Figure 2.7 Total GFR difference between control and mutant strain

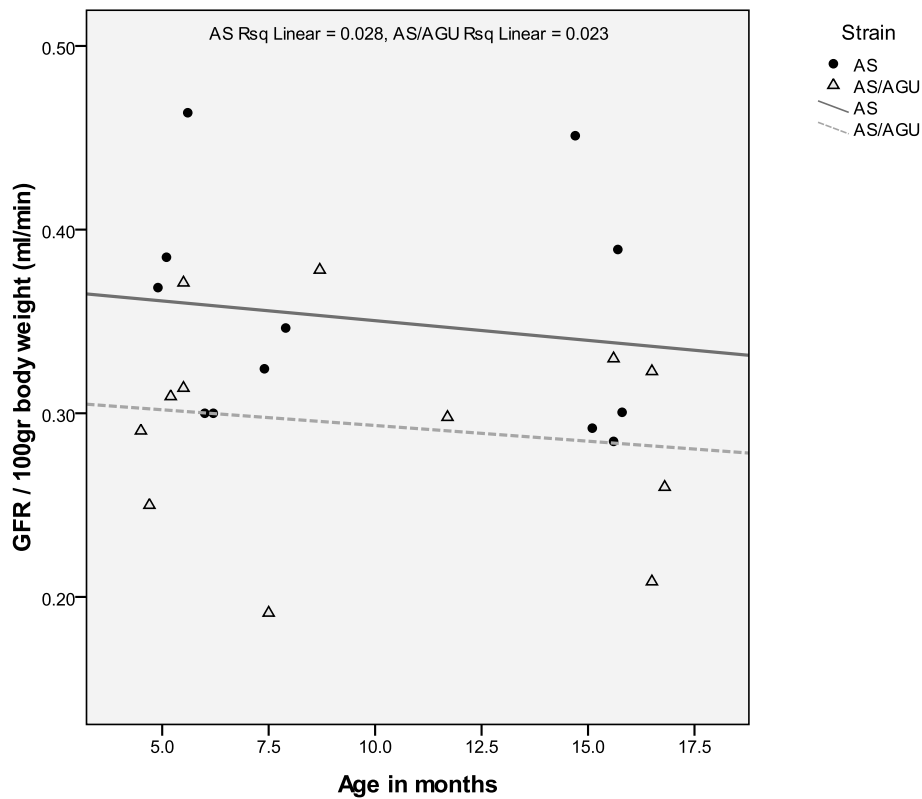


Figure 2.8 Corrected GFR difference between control and mutant strain

Calculations based on the line of best fit in Figure 2.8 show that at 5 months of age, the corrected GFR for AS strain was 0.36ml/min whilst that for the AS/AGU strain was 0.30ml/min. Similarly at 17.5 months of age, the AS strain GFR was 0.34ml/min whilst that of the mutant AS/AGU was 0.28ml/min. These results confirm a superior GFR for AS rats at both time points however, the rate of decline of GFR is equal between both strains – 0.02ml/min/100gr bw over a period 12.5 months. There is no data to deduce whether the decline in GFR occurs at 0 to 5 months of age or whether the mutant strain possesses an intrinsically lower GFR from birth.

2.5.3 Biochemical Analysis

The results of a comprehensive biochemical analysis between the two strains is outlined below. The table incorporates number of animals sampled per group, mean value, standard deviation and the p value for comparison of significance between the two groups (t-test)

A significant difference in plasma urea concentrations and urinary creatinine between the strains was observed. Mutant AS/AGU displayed higher plasma urea and lower urinary creatinine than the control strain. Other parameters did not appear to differ between the two strains however there was variability in cholesterol levels with mutant strains possessing higher levels than the control strain, this difference approaching statistical significance ($p=0.066$)

Parameter	AS			AS/AGU			p value (t-test)
	n	mean	SD	n	mean	SD	
Sodium (mmol/L)	35	146.45	3.96	27	145.29	3.8	0.224
Potassium (mmol/L)	27	5.12	1.19	26	5.23	1.09	0.287
Chloride (mmol/L)	35	104.01	7.75	27	103.34	5.02	0.454
Calcium (mmol/L)	31	2.63	0.41	27	2.63	0.29	0.619
Phosphate (mmol/L)	36	3.01	0.68	27	2.89	0.47	0.827
Urea (mmol/L)	34	7.14	1.53	27	8.68	1.97	0.002
Creatinine (μ mol/L)	36	47.28	8.27	27	45.52	10.49	0.808
Cholesterol (mmol/L)	34	2.81	0.81	27	3.09	0.82	0.066
Total Protein (g/L)	32	62.53	15.1	27	61.04	10.72	0.982
Albumin (g/L)	30	29.83	6.77	27	29.74	5.21	0.931
Glucose (mmol/L)	11	9.1	0.72	10	8.83	0.60	0.368
Urine SG	13	0.97	0.28	10	1.04	0.01	0.436
Urine Protein (g/L)	11	451.64	351.58	13	409.00	413.02	0.790
Urine Creatinine (μ mol/L)	11	11,299.27	3,621.70	13	8,168.54	3,599.89	0.046
Urine Urea (mmol/L)	8	637.87	157.59	9	513.55	243.28	0.237
UPCR	13	4.01	4.28	13	3.44	2.41	0.697

Table 2.9 Biochemical differences between AS and AS/AGU rats

An extensive panel of biochemical parameters was tested on plasma pertaining to both strains. Samples were machine analysed at the University of Glasgow – Veterinary Diagnostic Services. Note the statistical difference in plasma urea concentration and urinary creatinine (bold). Changes in plasma cholesterol levels show a strong trend between the two strains.

2.5.4 Subgroup Analysis – Sex Differences

A subgroup analysis for sex differences showed that in both groups analysed as a whole (AS + AS/AGU), male rats had a significantly lower serum albumin (mean F = 32.29g/L vs mean M = 27.97, $p = 0.007$) and had significantly much increased levels of proteinuria (mean F = 173.00g/L vs mean M = 644.77g/L, $p = <0.001$) with significantly higher UPCr than their female counterparts (mean F = 5.73 vs mean M = 1.39, $p = <0.001$). The difference in serum urea between female and male rats approached significance, with females possessing higher concentrations (mean F = 8.36 mmol/L vs mean M = 7.42 mmol/L, $p = 0.054$)

2.5.5 Ischaemia Reperfusion Injury Studies

Ischaemia Reperfusion Injury (IRI) was performed on a unilateral kidney following a period of GFR testing. Any ischaemic insult to the kidneys would alter the equilibrium state of plasma in the circulation. The mean time needed for a steady plasma concentration of inulin following the removal of 400 μ L of blood for laboratory analysis was 103mins (SD 30.5mins). Due to easier access to the left kidney pedicle, one or two vascular clamps were placed for sufficient time to allow injury and adequate recovery (anuria/oliguria/polyuria) within the experimental time period. The maximum clamp time for this was established to be 10 minutes. Preliminary studies showed that further ischaemia resulted in prolonged periods of anuria whilst shorter insults did not induce the required IRI. The urine specific gravity and urine urea concentration before and after clamping of the selected kidney were used to biochemically deduce the functional recovery and extent of injury. This was supplemented with immunohistochemical analysis for senescence associated proteins SA β Gal, p16, p21 and TUNEL assay for extent of apoptosis in the damaged renal tissue. In this way, IR injury is assessed in triplicate – physiologically, genetically and morphologically.

2.5.6 Global Urine Analysis

In both groups (AS+AS/AGU, n=16) analysed as a whole using the 2 sided student t-test, there was a significant difference between pre and post IRI urine urea concentration (mean pre-IRI urea concentration 572.25mmol/L, mean post-IRI urea concentration

381.88mmol/L, p=0.012). However, a significant difference in urine specific gravity was not observed (mean pre-IRI urine SG 1.047; mean post-IRI urine SG 1.042, p=0.160). The latter is most likely related to suboptimal measurements for urine SG, since scale readings on the refractometer were maximally limited to 1.050 with many readings marginally surpassing the limit described. Of the latter two parameters therefore, the urine urea concentration is taken as the more precise biochemical measurement of IRI. To further enhance the accuracy of this test and control for changes in plasma urea between the groups, the urine/plasma urea ratio pre and post IRI was additionally calculated. Pre and post IRI mean urine urea/plasma ratio for both AS+AS/AGU rats shows a statistically significant difference (mean pre IRI ratio = 1.59, mean post IRI ratio = 3.02, p=0.03).

The same was repeated between strains to ascertain whether the mutant shows biochemical changes indicating that it is less tolerant to IRI than the control. Table 2.10 shows the results of urine SG and urine urea concentrations for both groups and individual AS and mutant AS/AGU rats.

Strain	Mean SG pre IRI	Mean SG post IRI	Diff	p value	Mean Urea pre IRI mmol/L	Mean Urea post IRI mmol/L	Diff mmol/L	p value
AS + AS/AGU	1.047	1.042	0.005	0.160	572.25	381.88	190.37	0.012
AS	1.051	1.042	0.009	0.106	637.88	444.25	193.63	0.086
AS/AGU	1.045	1.041	0.004	0.700	513.55	326.44	187.11	0.068

Table 2.10 Urine Biochemical changes in response to IR injury

The table shows mean changes in urine specific gravity (SG) and urine urea concentration for total cohort (n=16) and both mutant (n=8) and control (n=8) rats before and after ischaemia reperfusion injury (IRI). Diff = Difference between mean pre and post values

2.5.7 Individual Strain Urine Analysis

When analysing the individual strain biochemical response to IRI (Table 2.10), there was no difference between pre and post IRI mean urine SG in either AS rats ($p=0.106$, $n=8$) or AS/AGU rats ($p=0.700$, $n=8$) (t-test). In addition, there is no significant difference between pre and post IRI mean urine urea concentration for AS rats ($p=0.086$) and neither for AS/AGU rats ($p=0.068$) (t-test).

The calculated pre and post IRI urine/plasma urea ratio for AS rats shows no statistical significant difference (pre IRI mean ratio = 1.32, post IRI mean ratio = 2.69, $p=0.100$). The same is true for AS/AGU strain (pre IRI mean ratio = 1.86, post IRI mean ratio = 3.35, $p=0.166$). The urine/plasma urea ratio was used to correct for a statistically significant difference in plasma urea concentration between the strains, yet still give an indication of the extent of tubular function post IRI. A higher ratio is synonymous with worsening tubular function and the results may indeed be clinically relevant as they indicate poorer recovery in the mutant strains tubular function post IR injury.

2.5.8 Immunohistochemistry

Tables 2.12 to 2.15 summarise the results of staining for senescence proteins in animals exposed to IR injury. The tables show the p value following analysis of Ischaemia/Reperfusion against control kidneys. In each table, the first column (AS) shows the p value in each cell of IR vs Control for Nuclear, Cytoplasmic and *combined* Nuclear + Cytoplasmic scoring (Mann-Whitney U Test). TUNEL and SA β GAL showed no differences, however there were differences in p16 and p21 expression in the mutant AS/AGU rat.

Strain	Age in Months	Weight (gr)	Sex	Ischaemic Insult Left / Right Kidney	Clamp Time (mins)	Time to reach plasma steady state* (mins)	Urine SG pre IRI	Urine SG post IRI	Urine Urea pre IRI	Urine Urea post IRI	UP Urea pre IRI	UP Urea post IRI
AS	4.9	228	F	Left	5	60	ND	ND	ND	ND	ND	ND
AS/AGU	4.5	210	F	Left	5	90	ND	ND	ND	ND	ND	ND
AS	5.1	226	F	Left	5	70	ND	ND	ND	ND	ND	ND
AS/AGU	4.7	200	F	Right	5	60	ND	ND	ND	ND	ND	ND
AS	5.6	220	F	Left	8	85	>1.050	1.042	ND	ND	ND	ND
AS/AGU	5.2	207	F	Left	8	95	>1.050	1.052	ND	ND	ND	ND
AS	6	360	M	Left	12	110	1.058	1.055	808	570	107.73	76
AS/AGU	5.5	306	M	Left	12	120	ND	ND	ND	ND	ND	ND
AS	6.2	350	M	Left	10	140	1.048	1.049	729	570	86.79	67.86
AS/AGU	5.5	318	M	Right	10	90	1.056	1.048	941	475	104.56	52.78
AS/AGU	7.5	230	F	Right	10	150	>1.050	1.054	710	281	72.45	28.67
AS	7.4	256	F	Left	10	65	>1.050	1.036	539	171	50.37	15.98
AS	7.9	280	F	Left	10	85	1.053	1.02	494	142	58.81	16.90
AS/AGU	8.7	246	F	Left	10	135	1.051	1.016	451	92	49.02	10.00
AS/AGU	15.6	376	M	Left	10	140	1.043	1.049	470	529	65.28	73.47
AS	14.7	266	F	ND	ND	(255)	ND	ND	ND	ND	ND	ND
AS	15.1	370	M	Left	10	130	>1.050	>1.050	790	870	123.44	135.94
AS/AGU	16.5	384	M	Left	10	70	1.04	1.042	253	232	34.19	31.35
AS	15.6	418	M	Left	10	80	>1.050	>1.050	802	588	112.96	82.82
AS/AGU	16.5	412	M	Left	10	100	1.032	1.028	276	299	40.59	43.97
AS	15.7	388	M	Left	10	150	1.054	1.05	473	400	57.68	48.78
AS/AGU	16.8	408	M	Left	10	105	1.034	1.032	235	189	39.83	32.03
AS	15.8	376	M	Left	10	150	1.042	1.028	468	243	73.13	37.97
AS/AGU	11.7	376	M	Left	10	90	>1.050	>1.050	717	523	89.63	65.38

Table 2.11 IR Injury Urine Biochemical data

*Time to reach plasma inulin equilibrium after removing 400microL sample from animal

()Difficulty cannulating femoral artery resulted in a delay in obtaining blood samples

ND – Not determined
SG – Specific Gravity
UP – Urine / Plasma

Note: Urine SG and Urine Urea not obtained on first 4 experiments

TUNEL	AS			AS/AGU			AS + AS/AGU		
	C n=3	I/R n=3	p value	C n=3	I/R n=3	p value	C n=6	I/R n=6	p value
Nuclear	68	95	0.12	72	97	0.13	70	96	<u>0.025</u>
Cytoplasm	31	38	0.18	31	41	0.51	31	40	0.13
Nuclear + Cytoplasm	50	67	0.31	52	69	0.42	51	68	0.17

C=Control

I/R= Ischaemia/Reperfusion

Table 2.12 TUNEL IHC – Control vs IR Injured Kidneys

Neither AS nor AS/AGU rats showed any significant change in staining patterns however there was a significant difference in the overall AS + AS/AGU nuclear staining between I/R and control kidneys $p=0.025$. Each value represents the mean score from both judges individual calculation of the 3 animals per group. When comparing uninjured kidneys in AS and AS/AGU groups, there is no difference in the quantity of apoptosis or indeed p16 expression, p21 expression and SA β GAL as seen in the tables below.

SA β GAL	AS			AS/AGU			AS + AS/AGU		
	C n=3	I/R n=3	p value	C n=3	I/R n=3	p value	C n=6	I/R n=6	p value
Nuclear	1	0	0.12	0	1	0.38	1	1	0.67
Cytoplasm	6	11	1.0	5	16	0.37	6	14	0.57
Nuclear + Cytoplasm	4	6	0.44	3	9	0.45	4	8	0.93

C=Control

I/R= Ischaemia/Reperfusion

Table 2.13 SA β GAL IHC Results – Control vs IR Injured Kidneys

No significant changes relating to SA β GAL was observed in either group.

p16	AS			AS/AGU			AS + AS/AGU		
	C n=3	I/R n=3	p value	C n=3	I/R n=3	p value	C n=6	I/R n=6	p value
Nuclear	56	51	0.82	32	54	0.51	44	53	0.63
Cytoplasm	23	29	0.40	18	38	<u>0.046</u>	21	34	<u>0.029</u>
Nuclear + Cytoplasm	40	40	0.93	25	46	<u>0.024</u>	33	43	0.19

C=Control

I/R= Ischaemia/Reperfusion

Table 2.14 p16 IHC Results – Control vs IR Injured Kidneys

Increased expression of the p16 protein was present in mutant rat kidneys exposed to IR injury particularly in the cytoplasm. Similar changes were not observed in the AS rat indicating a possible degree of increased tolerance to IR when compared to its AS/AGU counterpart.

p21	AS			AS/AGU			AS + AS/AGU		
	C n=3	I/R n=3	p value	C n=3	I/R n=3	p value	C n=6	I/R n=6	p value
Nuclear	61	82	0.28	52	73	<u>0.046</u>	57	78	0.11
Cytoplasm	42	45	0.82	33	79	0.83	38	62	0.63
Nuclear + Cytoplasm	52	64	0.75	43	76	0.42	48	70	0.42

C=Control

I/R= Ischaemia/Reperfusion

Table 2.15 p21 IHC Results – Control vs IR Injured Kidneys

Expression of p21 was statistically more evident in the nucleus of the mutant strain undergoing IR Injury. The same change was not present in AS animals undergoing a similar insult. This consolidates findings in table 2.14.

2.6 Discussion

2.6.1 GFR and Renal Function

The discovery of the mutant AS/AGU rat substrain was initially prompted by an unsteady movement disorder in a colony of AS rats. Studies by Payne, Davies and colleagues at the University of Glasgow discovered several associated pathological features including impaired cerebral glucose uptake and a parkinsonian gait due to loss of dopaminergic neurones of the substantia nigra pars compacta (231). The latter was found to be attributed to a PKC γ mutation in the AS/AGU colony (238).

Unpublished data by Wright et al. showed that in addition to enhanced neurodegeneration, the mutant rat strain also displayed genetic evidence of premature renal senescence. Progressing further, the work in this thesis is aimed at physiologically characterizing the renal phenotype of the mutant strain with GFR, biochemistry, immunohistochemistry and the response to ischaemia-reperfusion injury (IRI) as confirmed by the IHC studies presented.

A nephron is a single functioning unit of a kidney and comprises the glomerulus, bowman's capsule and associated tubules. Formation of urine begins at the glomerulus itself with the generation of a plasma ultrafiltrate. The rate of formation of this ultrafiltrate (glomerular filtration rate or GFR) has become a mainstay for evaluating renal function and monitoring the progression of kidney disease in humans (262;263).

Thus, the GFR is arguably one of the most important parameters in human physiology and plays a fundamental role in nephrology. In both clinical practice and research, comparisons of GFR between and within subjects are of vital importance. Other markers of renal function are similarly important clinically although there are inherent limitations to the use of so called "dynamic equilibrium" markers such as serum creatinine and cystatin C. The serum creatinine itself varies considerably with muscle mass and protein intake whilst it is claimed that cystatin C is generated at a constant rate and thus is superior to serum creatinine as a marker of GFR. Indeed, cystatin C correlates with GFR more precisely than serum creatinine does (264). However, cystatin C has also been shown to be associated, independently of glomerular filtration rate, with inflammation, glucocorticoids, thyroid function, obesity, smoking, diabetes, age, sex, and race (265;266). Cystatin C is helpful for

diagnosing CKD, but, similar to serum creatinine, one needs to be aware of the causes of modest elevations.

Because GFR varies with weight and height, it is important that GFR comparisons include some adjustment for body size. The traditional adjustment method in humans has been to divide GFR by body-surface area (BSA) and to standardize it to 1.73 m^2 (267). During the animal studies described, GFR values were standardised to 100 grams body weight. GFR studies in this thesis were performed via a classical inulin infusion technique. A bolus of 0.4ml inulin was administered in order to saturate plasma inulin concentration and attempt to reduce the time taken for equilibration. Indeed, as can be seen in Figure 2.5 the inulin concentration initially overshoot steady state value and gradually reduced to equilibrium. This is disrupted by bloodletting for laboratory analysis. The explanation for this lies in the reduction of blood volume during the procedure which is promptly replaced by FITC from the infusion pump at a background fluorescence of 7000. A rate of 3mls/hr was chosen as this maintained a well filled state and ensured that hypotension was not a confounding variable in the studies. This is evidenced by uninjured kidney urine output and previous initial experiments (5 animals) together with recommendations by experts in the field of rodent renal research (Dilworth, Clancy and colleagues; University of Manchester).

GFR validation studies proved that actual GFR values would increase with weight of the animal. This step acted as an internal control for subsequent experiments and provided reassurance that the method of GFR calculation was correct and fit for further experimental evaluation between strains. Since each kidney was catheterised individually, an independent value for GFR was obtained enabling accurate calculations for total and split GFR per kidney. Parallel strain analysis however provided an essential conclusion to the original hypothesis of this thesis. It is shown in Figures 2.7 and 2.8 that from the youngest animal specimens examined, there is a difference in both total GFR and corrected GFR between strains. Biochemically, a significant difference in plasma urea concentration and urinary creatinine between the strains was observed. Mutant rats displayed higher plasma urea ($p=0.002$) and lower urine creatinine ($p=0.026$)

2.6.2 The possible role of Protein Kinase C in explaining differences in GFR

Since the AS/AGU mutant is known to possess the PKC γ mutation, it may be that the difference in renal function between the two strains is explained by a difference in PKC γ

expression. Although Payne and colleagues determined the mutation to affect central dopamine neurotransmission in rats (231), there has been no evidence to support as yet the possible contribution of PKC γ to the inferior values of GFR observed in the AS/AGU strain.

The parallel strain analysis (Figs 2.7, 2.8) indicated that at the youngest age analysed (i.e. 4.5 months), there is a statistically significant difference in GFR between the two strains. This means that the mutant strain is possibly undergoing sub-optimal organogenesis in-utero resulting in decreased filtration mass. Alternatively, there is a rapid descent in renal function from birth to the earliest analysis point at 4.5 months. Should the latter be the case, one would expect a continuous decline in renal function, thereby increasing the difference in GFR between the two strains as they age and a graph showing 2 lines of best fit diverging from each other. Instead, the difference observed in renal function, present at 4 to 5 months, remains constant throughout the lifetime of the two strains. This maintained difference is statistically significant and scientifically relevant, as this indicates that the PKC γ gene is a possible target for amelioration/deterioration of kidney function. Further studies establishing renal function before and after loss of PKC γ gene function are therefore of clinical relevance.

The role of protein kinase C (PKC) in kidney organogenesis has in fact been described previously. From early stages of development, ureteric bud branching is one of the most important processes in renal organogenesis, and reciprocal induction by ureteric bud and metanephric mesenchymal cells is important for ureteric bud branching and mesenchyme-to-epithelial conversion (268). For signal transduction mechanisms in various biologic processes and in controlling gene expression during organ development, PKC, a serine/threonine kinase, is recognized as a key enzyme (269). In addition, it is involved in the regulation of growth and differentiation during development. Kidney development is governed by proliferation, differentiation, and apoptosis. Several isoforms of PKC are expressed during kidney development, and it has been shown that inhibition of PKC by a sphingolipid product, ceramide, interferes with nephron formation (poor branching of ureteric buds) and induces apoptosis in the developing kidney (270).

PKC is also involved in regulation of the growth and differentiation of many other organs during development, and so far, expression of PKC-alpha, -delta, and -zeta in the developing kidney has been detected by Northern blot analysis (271).

The group of classical or conventional PKC (cPKC) consists of the α , β I, β II and γ isoforms, all of which depend on calcium, or its analogue phorbol 12-myristate 13-acetate, and in most cases phosphatidylserine for activation. Tissue homeostasis is of course dependent on the balance between cell proliferation and cell death. An imbalance can result in diseases linked with unwanted apoptosis or unwanted cell growth. PKC appears to also have a role in both processes, not only by stimulating cell cycling and proliferation but also by stimulating apoptosis. The conventional PKCs (of which PKC γ is a member) are predominantly anti-apoptotic, being principally involved in promoting cell survival and proliferation (272). It is plausible to assume that inactivation (or impairment) of PKC γ leads to decreased cell survival and augmented rates of apoptosis resulting in decreased tissue biomass. However, its role in the mediation of ischaemia reperfusion injury is still unclear.

2.6.3 Urea Transport

In mammals, urea is the predominant end-product of nitrogen metabolism and plays a central role in the urinary concentrating mechanism. Urea accumulation in the renal medulla is critical to the ability of the kidney to concentrate urine to an osmolality greater than systemic plasma. Urea formed in the liver via the urea cycle enters the circulation and is freely filtered by the kidney. The amount of filtered urea excreted is regulated and depends on the physiological status of the animal. Protein restriction causes a decrease in the fraction of filtered urea excreted (273;274). This response reduces the loss of nitrogen from the body and serves to maintain plasma urea concentration, which would otherwise decrease in direct proportion to the lowering of nitrogen intake (275-279). Studies have suggested that the decrease in urea excretion with low protein intake is a result of increased urea absorption from the collecting ducts (278;280). In agreement, measurements in isolated perfused inner medullary collecting ducts (IMCD) show an increase in urea transport in the initial IMCD after dietary protein restriction (279;281).

Regulation of urea transport forms an integral part of the urinary concentrating mechanism. During antidiuresis, increased plasma vasopressin stimulates a rapid increase in urea transport in the IMCD allowing urea to enter the medullary interstitium (282). Increasing urea transport in the IMCD in conjunction with Na,K,2Cl cotransport in the thick ascending limb of the loop of Henle (283) enables the establishment and maintenance of

the hypertonic medulla which, in turn, provides the osmotic gradient required for water reabsorption (284). Urea absorbed in the IMCD is furthermore secreted into thin ascending and descending limbs and descending vasa recta in a process called urea recycling. This recycling pathway limits urea diffusion from the inner medulla allowing the maintenance of the corticopapillary osmotic gradient. The IMCD (285) and the descending vasa recta (286;287) have been recently shown to contain several urea transporters.

Several hypotheses are discussed as to why the mutant AS/AGU rats may in fact possess a higher plasma urea concentration. Firstly, the difference could be due to a mild, chronic form of dehydration (The AS/AGU mutant displays a particular dental development abnormality. The two lower incisors tend to overgrow and thicken resulting in a form of inhibition to normal feeding habits) This may lead to changes in the baseline level of vasopressin and physiological mechanisms to preserve blood urea concentrations so as to maintain a reserve of urea to enable urine to be concentrated should the need arise. Another reason for the elevated plasma urea in the mutant rat could be a higher metabolic rate resulting in increased protein catabolism and increased urea formation. This will explain, not only higher plasma urea concentrations, but also the difference in weight between the two strains. It is possible that the mutation in PKC affects thyroid status, however this would be accompanied by other clinical signs such as over-activity and impaired sleeping patterns which were not seen in the mutant strain. Also, thyroid function tests were not performed to prove this and such a theory is only speculative. A third theory to explain the increase in plasma urea is simply a lower intrinsic GFR in the mutant. Urea is freely filtered at the glomerulus and the serum urea concentration may be used as an index of the glomerular filtration rate (GFR). However, a number of non-renal factors also affect the serum urea concentration e.g. a high protein diet. There is also significant reabsorption of urea from the lumen of the nephron by passive diffusion (this is primarily the reason why serum creatinine is considered a better test of renal function in a clinical setting). The amount of urea reabsorbed in the nephron increases at high serum urea concentrations e.g. in renal failure, or if the flow rate through the nephron is reduced e.g. dehydration. Comparison of the degree of elevation between the serum urea and the serum creatinine concentration is useful in differentiating between pre-renal and intrinsic renal failure. In pre-renal failure the serum urea is disproportionately higher than the serum creatinine, whereas in intrinsic renal failure they rise in parallel. Thus, one reason to criticise this theory is the fact that no difference in serum creatinine between the strains was observed and this indicates that the changes in renal function between the strains may be too small to

be detected by serum and urine biochemical analysis alone. The relative proportion of muscle mass is small in rodents when compared to humans. This raises questions as to the diagnostic accuracy of creatinine with such animals in a similar way to humans in a cachexic state. Since creatinine is a product of muscle metabolism, smaller organisms would have little variation in plasma creatinine levels and it would take increasing GFR derangement in order to show an appropriate rise in serum creatinine. A final theory to explain serum urea differences relates to specific urea transporters in the nephrons as explained below.

2.6.4 Mammalian Urea Transporters

The majority of mammals consume diets that are high in protein. Under most circumstances, this dietary protein intake greatly exceeds that which is necessary for the support of anabolic processes. Excess protein is catabolized by the liver, which results in the formation of large amounts of urea by the ornithine-urea cycle. Urea is freely filterable by the kidney and the excretion of this urea constitutes a large osmotic load to the kidney. Most solutes excreted in such large amounts would obligate large amounts of water excretion by causing an osmotic diuresis.

In mammals, there are two urea transporter genes: UT-A (SLC14A2) and UT-B (SLC14A1). Multiple protein isoforms derived from each gene are produced by alternative splicing and alternative promoters (288). Along the nephron, the specialized urea transporters UT-A1, UT-A2, UT-A3, and UT-B are involved in complex urea reabsorption and recycling pathways that allow large amounts of urea to be excreted without obligating water excretion (Figure 2.9)

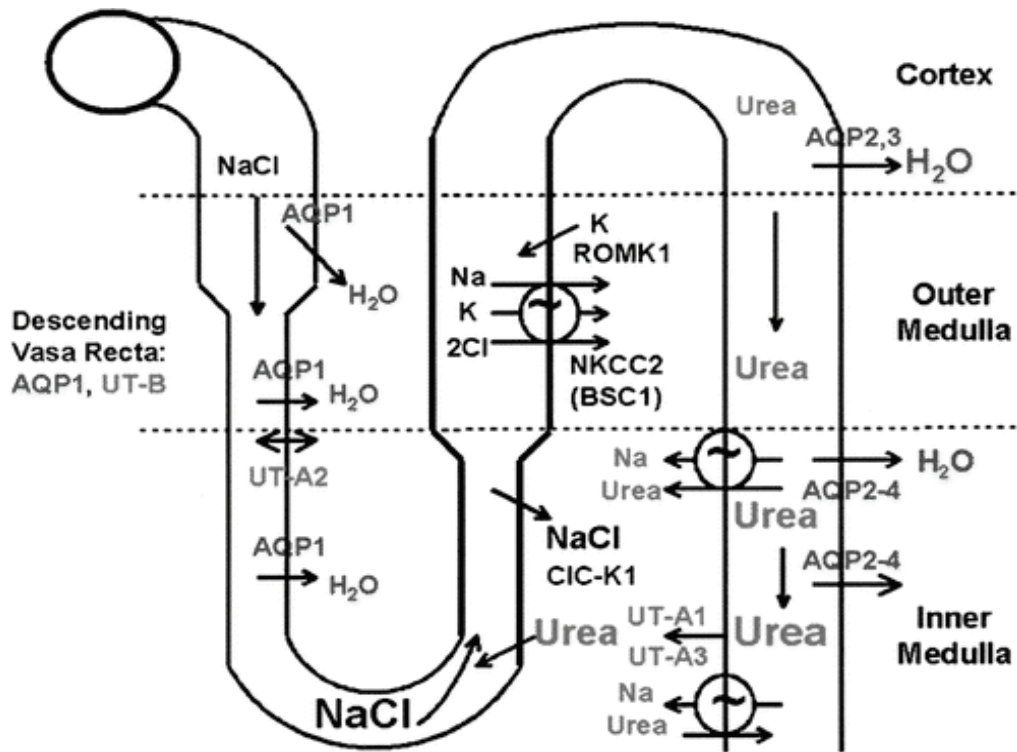


Figure 2.9 Mammalian urea transporters

Diagram showing the location of the major transport proteins involved in the urine concentrating mechanism in the outer and inner medulla. UT, urea transporter; AQP, aquaporin; NKCC/BSC, Na-K-2Cl cotransporter; ROMK, renal outer medullary K channel, CIC-K1, chloride channel. Adapted from Sands JM. Mammalian urea transporters. *Annu Rev Physiol* 2003;65:543-66.

Urea transporter A1 (AT-A1) transports urea across the apical membrane into the intracellular space of luminal cells in the inner medullary collecting duct of the kidneys. UT-1 is activated by ADH, but is a passive transporter. It reabsorbs up to 40% of the original filtered load of urea (288). UT-A2 transports urea across the apical membrane into the luminal space of cells in the thin descending loop of Henle. UT-A3 transports urea into the interstitium of the Inner Medullary Collecting Duct. UT-A4 has been detected in rat but not mouse kidney medulla and UT-A5 is not expressed in the kidney but in the testis.

UT-A1 and UT-A3 contain several sites for phosphorylation by protein kinase A (PKA), as well as PKC and tyrosine kinase. In the inner medullary collecting duct, increases in intracellular calcium and activation of PKC mediate hyperosmolality-stimulated urea permeability (289;290), whereas increases in cAMP mediate vasopressin-stimulated urea permeability (291). Thus both hyperosmolality and vasopressin rapidly increase urea permeability, but they do so via different second messenger pathways.

UT-B protein is expressed in erythrocytes and vasa recta (292-294), suggesting that urea transport in erythrocytes and descending vasa recta occurs via UT-B protein. Studies of microcirculatory exchange between ascending and descending vasa recta indicates that urea transporters (UT-B) are necessary to counterbalance the effect of aquaporin-1 water channels in the descending vasa recta, i.e., in the absence of UT-B, the efficiency of small solute trapping within the renal medulla is decreased, slowing the efficiency of countercurrent exchange and urine-concentrating ability (295;296). Consistent with this hypothesis, urea recycling is impaired in the vasa recta of UT-B knockout mice (108). Thus the production of maximally concentrated urine requires UT-B protein expression in erythrocytes (297;298) and in descending vasa recta (295;296).

A statistically significant difference in urinary creatinine was also observed with the control AS strain excreting larger quantities compared with its AS/AGU counterpart. The difference may be related to the larger muscle mass of the control strain and the greater GFR in the parent strain. A difference in serum cholesterol levels was also observed approaching statistical significance ($p=0.066$) with mutant strains possessing a higher serum levels. The hepatic mobilisation and metabolism of the cholesterol pathway is complex and beyond the scope of this thesis. Serum levels could however be impaired by the mutant PKC mutation resulting in a hypercholesterolaemic state.

Subgroup analysis with respect to urinary protein and serum albumin shows increased UPCr / proteinuria in male rats over females. The result holds true when the analysis is performed for all control and mutant rats ($p<0.001$). The most common cause of proteinuria in adults is diabetic nephropathy, however a total of 21 animals were tested with random serum glucose samples and no difference was observed between control (mean 9.1mmol/L) and mutant (mean 8.83mmol/L). Individual glucose samples reflected a euglycaemic state in all animals. Proteinuria, more specifically albuminuria is one of the first signs of kidney damage. The presence of excess protein in the urine indicates either an insufficiency of absorption or impaired filtration. With severe proteinuria,

general hypoproteinaemia can develop which results in diminished oncotic pressure. Symptoms of diminished oncotic pressure may include ascites, oedema and hydrothorax which were never observed in any of the rat species. It is not possible to ascertain a clear cause for this finding without formal histological analysis and indeed histopathology to characterise interstrain or intersex differences in both normal and IR states was not performed. It is however a point of interest in future related experimental work.

2.6.5 IR Studies - Urine Biochemistry

Ischaemia reperfusion is a pathological condition characterised by an initial restriction of blood supply to an organ followed by the subsequent restoration of perfusion and the re-establishment of oxygenation. It results in a severe imbalance of metabolic supply and demand, causing tissue hypoxia. Eventual restoration of blood flow and oxygenation is frequently associated with an exacerbation of tissue injury and a profound inflammatory response termed reperfusion injury.

During the laboratory experiments for this project, animals were given a standard 10 minute ischaemic insult to a unilateral kidney following completion of formal GFR studies. This amount of IR injury generally allowed for intra-operative recovery of urine output from the damaged kidney within 30 to 90 minutes. Urine specific gravity together with urine urea concentration was analysed from the injured kidney before and after the timed insult which inevitably resulted in a degree of generalised tubular dysfunction. The aim of this was to help characterise the degree of renal injury via urine biochemistry and perform a comparison between mutant and control rats. The renal damage was also measured with IHC staining techniques.

When tubular dysfunction is established, damage to the tubular cells impairs the adjustment of the composition and volume of urine in several ways. Firstly, the countercurrent mechanism may be impaired, water reabsorption is reduced and large volumes of dilute urine are passed. Secondly, the tubules cannot secrete hydrogen ion and therefore cannot reabsorb bicarbonate normally and cannot acidify the urine. Thirdly, reabsorption of sodium and exchange mechanisms involving sodium are impaired and the urine contains an inappropriately high concentration of sodium relative to the state of hydration. Failure of sodium reabsorption in the proximal tubule contributes to impairment of water reabsorption at this site. Potassium reabsorption in the proximal tubule is also

impaired and potassium depletion may occur. Lastly, reabsorption of glucose, phosphate, urate and amino acids is impaired and there is often glycosuria, phosphaturia and generalised aminoaciduria. Uraemia may occur if fluid and electrolyte depletion causes renal circulatory insufficiency. Thus the effects of acute tubular dysfunction on serum plasma include a metabolic acidosis with low plasma bicarbonate, hypokalaemia, hypophosphataemia, hypouricaemia, haemoconcentration (if fluid deplete) and a normal plasma urea unless dehydration sets in. The effects on the urine are polyuria, inappropriately low osmolality and specific gravity and inappropriately low urea concentration. In most cases there is mild proteinuria and casts are present in the urine

2.6.6 IR Studies - Urine Urea and Specific Gravity

In order to estimate the degree of damage to the renal tubules, the pre and post ischaemia reperfusion urea and SG were measured from the clamped kidney. The hypothesis in this thesis is that the mutant AS/AGU rat displays an advanced senescence phenotype and would be intrinsically less tolerant to the stress of any ischaemic insult. It would also in theory recover over a longer period of time from a standard insult. The specific gravity (which is directly proportional to urine osmolality and reflects solute concentration) measures urine density, or the ability of the kidney to concentrate or dilute the urine over that of plasma. Damage to the kidney's tubules affects the ability of the kidney to re-absorb water. As a result, the urine remains dilute and this is reflected in a low specific gravity.

Analysis of urine urea in both groups as a whole (AS + AS/AGU) showed a significant difference in concentration with post ischaemia urine containing a lower concentration of urea ($p=0.012$). The changes in the control AS group showed a decrease in urea concentration post IR injury with a trend towards significance ($p=0.086$) whilst there was a decrease in urea with a trend towards statistical significance in the mutant AS/AGU group ($p=0.068$). With impaired ischaemic tolerance resulting in a higher degree of acute tubular necrosis (ATN), the secretion of urea into the distal convoluted tubule is increasingly impaired, as is the ability to reabsorb water into the systemic circulation. The result is more dilute urine and lower urine urea concentrations.

The urine/plasma urea ratio may be seen as a more accurate figure as it takes into account the difference in plasma urea concentration between the two strains. Outcome of urine specific gravity testing shows a decrease in SG post IR injury reflecting a degree of tubular

damage as indicated in the preceding text, however results were not statistically significant in either of the groups studied and there was difficulty measuring urine SG above 1.050 on the refractometer. In all urine biochemical analyses performed, there was a change between pre and post IR injury ratios that did not reach statistical significance. This is possibly due to the relatively smaller numbers in each group (n=8 per group). As is noted here, the numbers for the above IRI studies are smaller per group when compared to the GFR studies (GFR n=12 / group vs IRI n=8 / group) because biochemical urine testing commenced at a slightly later period.

2.6.7 IR Studies - Immunohistochemistry

Together with the biochemical analysis of serum and urine, renal tissue sections from six animals were subject to immunohistochemical staining to monitor for the presence of proteins p16 and p21. In addition, the extent of apoptosis was gauged using the TUNEL assay and SA β Gal for accumulation of the biomarker of senescence – lipofuscin. The animals were sacrificed by Schedule 1 technique approximately 120 minutes +/- 30 mins following the release of clamps and the organs were immediately placed in liquid Nitrogen. This implies that any tissue changes noticed during the IR injury experiments were allowed to take place within the aforementioned time frame between clamp release and animal sacrifice. A brief description of the physiological, genetic and molecular mechanisms involved in IR injury is therefore warranted to enable a better understanding of the results.

A wide range of pathological processes contribute to ischaemia reperfusion injury. Hypoxia is associated with impaired endothelial cell barrier function (299) due to decreases in adenylate cyclase activity and intracellular cAMP levels with a concomitant increase in vascular permeability and leakage (300). In addition, IR injury leads to the activation of cell death programs, including apoptosis (nuclear fragmentation, plasma membrane blebbing, cell shrinkage and loss of mitochondrial membrane potential and integrity), autophagy-associated cell death (cytoplasmic vacuolization, loss of organelles and accumulation of vacuoles with membrane whorls) and necrosis (progressive cell and organelle swelling, plasma membrane rupture and leakage of proteases and lysosomes into the extracellular compartment) (301) At this point some cells may choose to enter a state of senescence (Figure 2.10)

The ischaemic period in particular is associated with significant alterations in the transcriptional control of gene expression (transcriptional reprogramming). For example, ischaemia is associated with an inhibition of oxygen sensing prolylhydroxylase (PHD) enzymes because they require oxygen as a cofactor. Hypoxia-associated inhibition of PHD enzymes leads to the post-translational activation of hypoxia and inflammatory signalling cascades, which control the stability of the transcription factors hypoxia-inducible factor (HIF) and nuclear factor- κ B (NF- κ B) (302), respectively. Despite successful reopening of the vascular supply system, an ischaemic organ may not immediately regain its perfusion (no reflow phenomenon). Moreover, reperfusion injury is characterized by autoimmune responses, including natural antibody recognition of neoantigens and subsequent activation of the complement system (autoimmunity) (303). Despite the fact that ischaemia and reperfusion typically occurs in a sterile environment, activation of innate and adaptive immune responses occurs and contributes to injury, including activation of pattern-recognition receptors such as Toll-like receptors (TLRs) and inflammatory cell trafficking into the diseased organ (innate and adaptive immune activation) (304).

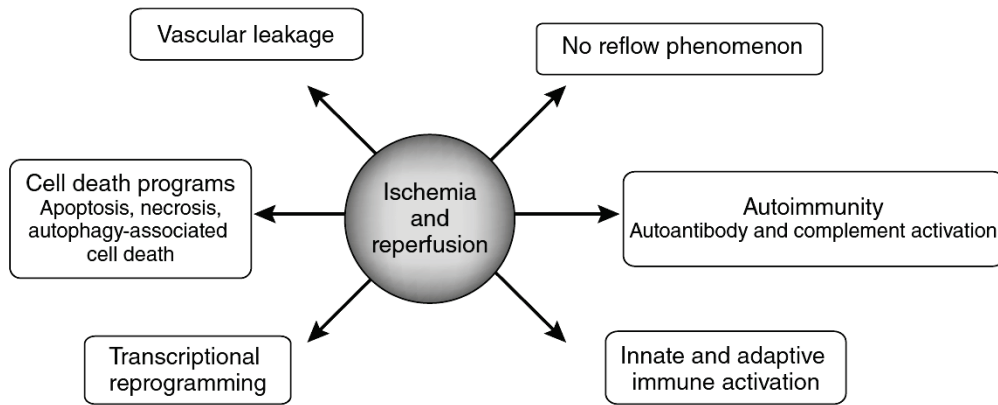


Figure 2.10 Biological processes implicated in IR Injury

The effects of IR injury are multiple and not completely understood. The inflammatory response to “sterile” injury has many similarities to that observed in microbial infections. Tissue hypoxia during the ischaemic period results in the transcriptional activation of inflammatory gene programmes. Such mechanisms are dependent on Toll-like receptor (TLR) – dependant stabilisation of the transcription factor NF- κ B. TLR 4 in particular may have a detrimental role in mediating kidney injury and has been implicated in early graft failure. NF- κ B itself is a protein complex that controls DNA transcription. It is found in almost all animal cell types in response to stress, infection and other stressors. It plays a key role in regulating the immune response to infection and has been linked to cancer and autoimmune diseases. Dendritic cells and macrophages play an important role in the innate and adaptive immune response of acute IR injury. They are key initiators, potentiators and effectors of innate immunity in kidney IRI and induce injury either through inflammatory signals to other effector cells or directly through the release of soluble mediators. In addition, dendritic cells (potent antigen presenting cells) contribute to the innate immune response by activating NKT cells and promoting inflammation (Adapted from: Eltzschig HK, Eckle T. Ischemia and reperfusion--from mechanism to translation. Nat Med 2011.)

When damage accumulates irreversibly, mitotic cells from renewable tissues rely on either of two mechanisms to avoid replication. They can permanently arrest the cell cycle (cellular senescence) or trigger cell death programs. Apoptosis is the best-described form of programmed cell death, but autophagy, (a lysosomal degradation pathway essential for homeostasis) may contribute to cell death too. Unlike mitotic cells, postmitotic cells like neurons or cardiomyocytes cannot become senescent since they are already terminally differentiated. The fate of these cells entirely depends on their ability to cope with stress.

Autophagy then operates as a major homeostatic mechanism to eliminate damaged organelles, long-lived or aberrant proteins and superfluous portions of the cytoplasm.

As described in chapter 1, the following mechanism in response to cellular stress is paramount to the work performed in this thesis and merits further discussion. Cellular senescence actually refers to the arrest in the G1 phase of the cell cycle of continuously proliferating cells, in response to stress that puts them at risk of malignant transformation (305). Senescent cells adopt a flattened, enlarged morphology and exhibit specific molecular markers like SA β GAL, senescence-associated heterochromatin foci and the accumulation of lipofuscin granules (306;307). There are many stimuli leading to the senescent state. Among them, telomere shortening, DNA damage and oxidative stress are the best described (305;308). In spite of the diversity of these stimulatory signals, they only converge onto two major effector pathways: the p53 pathway and the pRB pathway (figure 2.11). In normal conditions, the tumour suppressor protein p53 is constitutively targeted to proteasome-mediated degradation by MDM2, but upon mitogenic stress or DNA damage, MDM2 activity is suppressed and functional p53 is able to activate the cyclin dependent kinase inhibitor p21 which stops the cell cycle. In the second pathway, the retinoblastoma protein pRB is activated by p16 after cellular stress or DNA damage and then binds to members of the E2F family of transcription factors, known to regulate cell cycle progression (309;310). The two pathways manifest ample crosstalk in the control of cellular senescence, and can also overlap with death pathways (311;312).

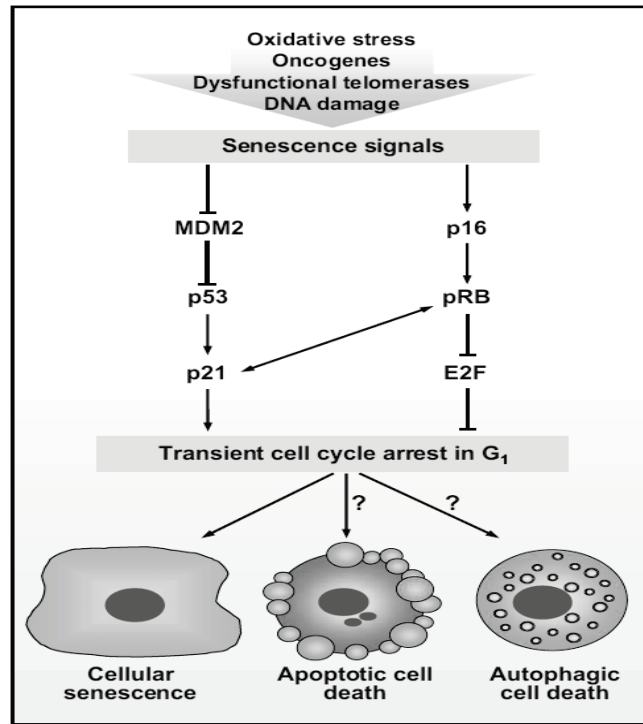


Figure 2.11 Outcomes of the p16 and p21 cellular pathways

When dividing cells are exposed to genetic stress, the cell cycle must be arrested immediately to ensure the integrity of the DNA and/or the cell cycle control. To prevent an unscheduled entry into S-phase, the activity of the Cyclin-CDK complex is suppressed by an association with CDK inhibitors. Dependent on the extent of the damage, the cell must determine whether to arrest the cell cycle and enter senescence, repair the DNA, or to enter the apoptosis/autophagy pathway. (Adapted from Vicencio JM, Galluzzi L, Tajeddine N, Ortiz C, Criollo A, Tasdemir E, et al. Senescence, apoptosis or autophagy? When a damaged cell must decide its path--a mini-review. *Gerontology* 2008.)

IHC analysis of kidneys exposed IR injury show significant changes in levels of p16 and p21 protein expression primarily in the mutant AS/AGU strain. AS rats showed no difference between control and IR subjected kidneys. Closer to the IR insult (i.e earlier in the senescence cycle), one would expect to see higher levels of p21 which would eventually give way to p16 for maintenance of the senescence state. Indeed, after

senescence is achieved, p21 declines considerably to an amount that was consistent with a reversible arrest earlier in the lifespan. P16 increases as p21 declines and reduces the number of targets for p21 through its inhibitory effect on cyclin D1-Cdk4/6 complex formation. Elevated p16 is critical to maintain the senescent cell cycle arrest as p21 declines from its maximum at the initiation of senescence. Studies on *replicative* senescence outline two events : an increase in p21 that is driven by the “mitotic clock” and an upregulation of p16 as part of a program of differentiation that is turned on in senescent cells. First, the progressive age-dependent accumulation of p21 suggests that it occurs as a consequence of replication- related processes such as telomere shortening (313), DNA demethylation (314), and the effects of DNA damage (315;316). It results in inactivation of all G1 cyclin-Cdks, such that pRb fails to be phosphorylated, E2F transcription factors are not released, late-G1 genes necessary for DNA synthesis are not expressed, and the cells become irreversibly arrested in G1 phase (317). In parallel, an efficient G1 block may also be assured by inactivation of proliferative cell nuclear antigen (PCNA) by association with p21 and cyclin D1. Second, at senescence a program of differentiation is initiated that involves the accumulation of p16, as well as changes in the morphology, size, and functional attributes of the cells (318-325). The concomitant decline of p21 from its peak in early senescence could occur owing to decay of the replication-related signals that drove its increase as the cells were aging. Consequently, in late senescent cells Cdk inactivation and the cell cycle arrest are maintained through the combined effect of p16 and p21.

One of the most widely used methods for detecting DNA damage *in situ* is TdT-mediated dUTP-biotin nick end labeling (TUNEL) staining (326). TUNEL staining was initially described as a method for staining cells that have undergone programmed cell death, or apoptosis and exhibit the biochemical hallmark of apoptosis—internucleosomal DNA fragmentation(327-331). TUNEL staining relies on the ability of the enzyme terminal deoxynucleotidyl transferase to incorporate labeled dUTP into free 3'-hydroxyl termini generated by the fragmentation of genomic DNA into low molecular weight double-stranded DNA and high molecular weight single stranded DNA. Results for the 6 animals (and 12 kidneys) analysed for such changes showed a global difference in nuclear staining ($p=0.025$) as shown in Table 2.12, although there was no inter or intra-strain difference with this particular assay. It could be concluded therefore that under the above experimental conditions, molecular changes with respect to DNA fragmentation and apoptosis are not primarily observed.

A similar association was seen with the biomarker of ageing SA β GAL (Table 2.13) - a hydrolase enzyme that catalyses the hydrolysis of β - galactosides into monosaccharides in senescent cells. Staining with this method showed no significant difference across all groups. In addition (as was observed with the TUNEL assay) there was no difference between IR exposed kidneys and controls. This finding does not conform with similar experiments within our laboratory and is reflective of a relatively short IR injury time being insufficient to produce statistically significant differences with these markers. It is also reflective of the lack of relative sensitivity of these particular markers. The increase in cellular lysosomal content in ageing cells is thought to be caused by the accumulation of non-degradable intracellular macromolecules and organelles in autophagic vacuoles (332). In vivo, this process is manifested by the accumulation of lipofuscin in ageing post-mitotic cells (333). Also, these secondary lysosomes are loaded with non-degradable material that are not available for further digestion of macromolecules, forcing cells to synthesise more primary lysosomes in an attempt to continue with normal cellular function. Most of the newly formed primary lysosomes appear to fuse with these lipofuscin-containing acidic vacuoles, contributing further to their increase in size and content of hydrolytic enzymes (332).

P16 staining however, proved different in that both interstrain and intrastrain differences were observed (Table 2.14). In all three groups (Nuclear, Cytoplasm and Nuclear + Cytoplasm) there were no intra-strain differences observed for AS rats. With the AS/AGU strain we observe a significant difference in cytoplasmic staining ($p=0.046$) but not nuclear. When nuclear and cytoplasmic staining are analysed together there is again a significant intrastrain difference for the AS/AGU rat ($p=0.024$). The analysis of both strains together shows a difference in cytoplasmic staining between IR kidneys and control. The results drawn from p16 staining therefore implicate that following IR injury to rat kidneys for a period of 10 minutes, there is a significant increase in p16 protein present in the AS/AGU renal cell cytoplasm within a mean period of 105 minutes (range 75-135 mins). The reason for cytoplasm predominant p16 has only recently come to light and is of relatively new scientific interest (334). Classically, the only function attributed to p16 has been cell cycle regulation and this function takes place in the nucleus. There is however, considerable evidence that certain tumours exhibit significant p16 levels in the cytoplasm (335). In addition, cytoplasmic p16 has been associated with tumour progression and prognosis in certain kinds of neoplasms such as breast cancer, where the presence of p16 was preferentially confined to the nucleus in fibroadenoma and nuclear/cytoplasmic or

exclusively cytoplasmic in carcinoma (336;337) Other similar changes have been seen in colorectal cancers (336;338;339), astrocytomas and uterine leiomyomas (340-342) and gastrointestinal stromal tumours (343). Proteomic and post-translational studies have been performed in an attempt to clarify the function of p16 in the cytoplasm. These studies have shown that p16 is expressed in the cytoplasm and the nucleus, depending on post-translational modifications or its capability to form a complex with other proteins (344). Nevertheless, further work is needed to elucidate the molecular mechanisms involving cytoplasmic location of p16, its functions and its connection with oncogene-induced senescence and failure of the p16 tumour suppressor function. In essence, as occurs with other proteins involved in cell cycle regulation, p16 localization in the cytoplasm may represent an alternative mechanism for modulating different pathways, instead of simply a way to inactivate the cell cycle control function.

With p21 staining there was a similar pattern between strains i.e there were no significant changes observed in the nuclear or cytoplasmic AS control strain (Table 2.15). However, in contrast to p16, there was a significant change in nuclear p21 levels (but not cytoplasmic) for the AS/AGU strain ($p=0.04$). This further supports findings that the AS/AGU strain is less resilient to ischaemia reperfusion insults and that (as in p16) within a mean period of 105 minutes, a visible change in p21 levels are observed. The reasons behind these findings may indeed be related to the ageing phenotype displayed by the AS/AGU rat and may be related somehow to the PKC γ mutation although further genomic and proteomic studies are necessary to further clarify this association. The mechanisms which regulate the cellular localisation of p21 in different cell types are not yet clear. Recently, evidence has accumulated that the cyclin kinase inhibitor, p21, is a multifunctional cell cycle-regulatory molecule that contributes to the regulation of apoptosis, as well as associating and inhibiting Cyclin-CDKs or proliferating cell nuclear antigen (PCNA) (345). It has been shown to protect cells from apoptosis when exposed to hydrogen peroxide (346;347) and also protects cells from cytokine induced apoptosis (348;349). In contrast, a number of reports suggest that p21 possesses pro-apoptotic functions under certain conditions in specific systems (350-353). Again, the mechanism by which p21 can regulate the apoptotic pathway is not well understood. While cell cycle inhibition by p21 is a nuclear event (since p21 binds and inhibits CDKs and/or PCNA in the nuclei), the regulation of apoptosis may be a nuclear or cytoplasmic event, or both. Since there are differing apoptosis signal cascades, one induced by DNA damage and

another being the death signal from the cell membrane or cell organelle, various regulatory points in the apoptosis signal cascades exist. Thus, the influence and activity of p21 on the apoptosis signal cascade may depend on the cell type or the cell conditions.

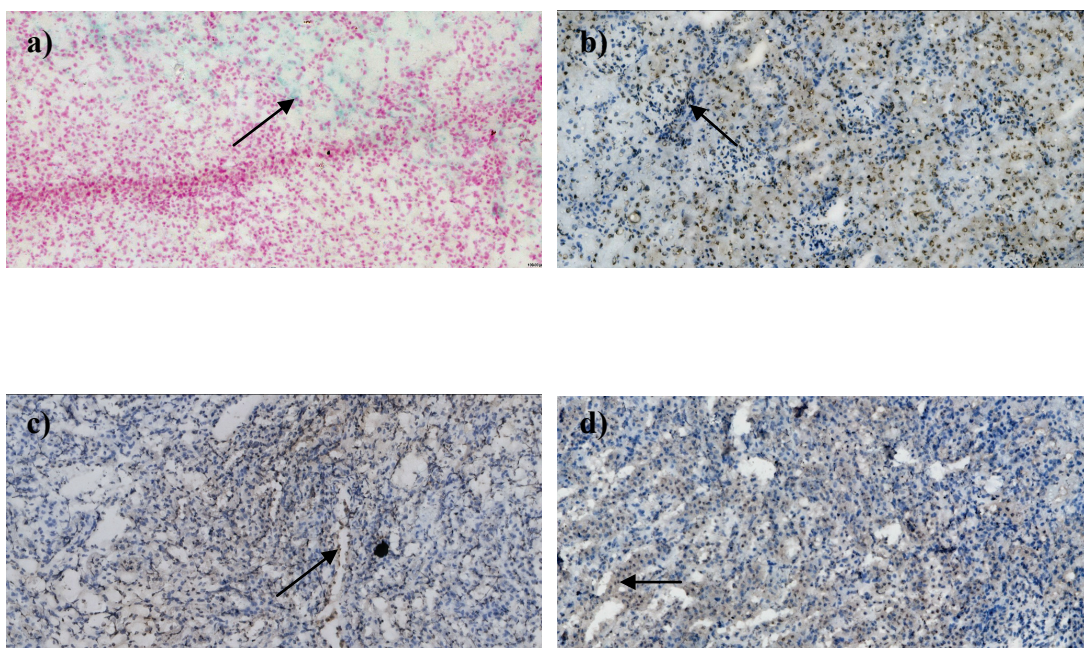


Figure 2.12 Immunohistochemical staining for senescence markers

Immunohistochemistry showing staining patterns in kidney parenchyma at 20x magnification. Arrows mark: a) Very weak SA β GAL pattern was seen in all experimental subjects. b) TUNEL assay revealing dark staining in kidney cells exposed to IR injury. The difference between IR and control kidneys was not statistically significant here c) p16 staining is evident in tubular cells entering senescence d) p21 showing a similar staining pattern in cells exposed to the ischaemic insult described.

2.7 Conclusion

The AS/AGU mutant rat is shown to possess several characteristics which make it a suitable model to study the effects of senescence and ischaemia reperfusion injury on renal tissue. Firstly, the strain displays an inferior GFR at all age groups when corrected for body weight. This is most likely related to decreased functional nephrons mass (as a result of premature senescence) associated with the premature ageing process and is in keeping with unpublished data from Wright et al (University of Glasgow). In addition the mutant strain has a higher serum urea and a lower urinary creatinine, which further reflect its impaired renal function. Reasons for such differences in its biochemistry and senescent state are not entirely clear but may be related to the PKC γ mutation which itself plays a crucial role in several signal transduction cascades. A more complete understanding of the functions of individual PKC isoforms in the kidney, and further development of isoform-specific inhibitors or gene therapy will be necessary for the future treatment of cellular dysregulation in renal disease.

IR injury experiments have shown that the AS/AGU rat is also ideal for testing ischaemia related senescent changes and provides a model more reminiscent of the condition of extended criteria kidneys in human transplantation than current rodent models. The studies indicate that the AS/AGU strain shows immunohistochemical evidence of impaired tolerance to moderate levels of IR injury. It displays a relatively prompt cell protection/senescent mechanism, demonstrated by higher p16 and p21 expression in the cytoplasm and nucleus when recovering from an ischaemic insult. Indeed, no such immunohistochemical changes were observed in the parent AS strain. Further studies with a larger number of animals, lengthier ischaemic times and transplantation itself would be beneficial to support these findings. Moreover, the addition of formal histological analysis including electron microscopy would be of additional value in further characterizing the phenotype of this uniquely mutated rodent.

We have seen in the first chapter of this thesis that donor chronological age is a key predictor of DGF and renal function suggesting that strategies to protect biologically aged kidneys from transplant associated injury would prolong graft survival and improve observed renal function. This inevitably results in improved quality of life and patient survival, eventually resulting in significant health economic benefit due to reduced morbidity and hospitalization. These studies are the platform on which we can eventually

provide a reliable and objective molecular test to identify kidneys that will respond poorly to ischaemia reperfusion and thus benefit most from protective translational strategies.

Chapter 3

ISCHAEMIA REPERFUSION INJURY AND ANTI-ISCHAEMIC COMPOUNDS – AN EXPERIMENTAL ANIMAL MODEL

3.1 Introduction

Acute kidney injury (AKI) refers to a complex disorder that comprises multiple causative factors and occurs in a variety of settings with varied clinical manifestations that range from a minimal but sustained elevation in serum creatinine to anuric renal failure. AKI sustained during temporary interruption of blood supply to kidneys as occurs in experimental ischaemia reperfusion (IR), mimics to a certain extent the damage sustained during cold ischaemic time in kidney transplantation. In transplantation however, a cascade of events besides the IR injury phase itself contributes to global graft injury. In DBD donors for example, the pre-retrieval phase is notoriously associated with a cascade of events such as complement activation and cytokine release leading to microvascular injury and tubular necrosis.

Even when retrieved under ideal circumstances i.e live donation, the graft endures at least a modest ischaemic insult. During deceased donation, the inflammatory mechanisms are triggered during the pre-retrieval process and further inevitable injury occurs during the longer preservation period. In all cases, injury is then exacerbated as warm host blood circulates the organ with initiation of host innate and adaptive immune response and no reflow phenomena. Recognition of the importance of these injuries to long-term graft survival continues to gain intense interest among scientists and clinicians in a race to determine optimal countermeasure strategies. Several groups have published results on specific compounds or biological agents, which have been shown to influence the effects of IR injury. However, such experiments have been mostly limited to in vitro cell lines and/or small mammal experiments. Examples of such include endothelin receptor antagonist which inhibits the potent vasoconstrictor effect of endothelin (354), PARP (355) and Caspase (356) inhibitors which work as anti apoptotic agents, complement (357;358) and interleukin receptor antagonists (359;360) which function as anti-inflammatories and erythropoietin working as both an anti-inflammatory and anti-apoptotic agent (361).

3.1.1 mTOR inhibitors and AZ-6

This chapter focuses on the use of a specific compound (AZ-6) in an animal model to establish its effect on renal physiology when injected intravenously before or after a predetermined length of ischaemia reperfusion injury. Physiological outcomes i.e serum creatinine values and weight were also determined for intravenous injection and no IR injury in a separate arm. AZ-6 is an mTOR inhibitor (provided by the pharmaceutical company Astra Zeneca) identified previously, through blinded testing and ranking in vitro of 11 separate novel chemical entities (NCE), as the best NCE to mitigate the effects of oxidative damage in primary human renal epithelial cells (Moullisova et al in preparation). The choice of compound was based on its ability to minimize the effects of an oxidative insult on cellular biological age, as measured by CDKN2A expression in both Human Diploid Fibroblasts (HDF) and Human Renal Epithelial Cells (HREpi). These data indicated that this compound might mitigate the acceleration of bio-ageing induced by acute stress and could therefore be utilised in further trials relating to transplantation associated ischaemic injury. Whilst much of the work relating to this compound revolves around the effects on bio-age, the chapter focuses on experimental design, surgical technique, animal housing and testing such compounds in vivo, relative to any future clinical translation in man.

The first mTOR inhibitor was discovered in 1975 when researchers discovered that a bacterium *Streptomyces hygroscopicus* produced an antifungal, later called Rapamycin (362). Further studies revealed that Rapamycin itself did not only have antifungal properties but also significantly suppressed the immune system by blocking G1 to S phase in T-Lymphocytes and hence it's widespread use in transplantation today (363). mTOR, also known as mammalian target of rapamycin (or FK506) is actually a serine/threonine protein kinase that also regulates protein synthesis, cell survival and cell motility (364). Much of the literature in transplantation, related to the use of mTOR inhibitors regards calcineurin inhibitor (CNI) sparing regimes (365-367). CNI's are notorious for causing long term chronic allograft nephropathy (and hence may contribute to decreased long term graft survival) but till today, these agents are still in use as first line immunosuppressive drugs together with steroids and anti-metabolite agents such as mycophenolate mofetil. mTOR signalling is aberrantly activated in many human cancers and has a central role in the regulation of cancer cell growth by control of the initiation of mRNA translation into protein. Aberrant activation of mTOR is thought to occur in ~50% of human malignancies

(368). A possible mechanism is increased activation of Akt (protein kinase B) arising from the loss of tumour suppressor gene PTEN (phosphatase and tensin homologue) function. Such loss is observed in many cancers including renal cell carcinoma (369).

The mTOR signalling pathway is highly complex and detail of this would deviate from the full purpose of this thesis. However, a brief explanation is merited on the basis of its central role as a proposed therapeutic agent in the experimental animal groups. mTOR exists in the form of two molecular complexes, mTORC1 and mTORC2, but only the former is generally susceptible to inhibition by rapamycin analogues. The two best characterised pathways lying downstream of mTOR are mediated by ribosomal protein S6 kinase (S6K1) and by eukaryotic initiation factor binding protein (4EBP1). Activation of either PI3K and/or Akt and/or loss of PTEN suppressor function results in activation of S6K1 and 4EBP1 by mTOR kinase. mTOR inhibitors bind with high affinity to a cytoplasmic protein FKBP-12 to form a complex that interacts with mTOR kinase. This blocks downstream signalling events, affecting the synthesis of cell cycle regulators such as cyclin D and decreasing hypoxia-inducible transcription factor (HIF) expression. It is mainly through the synthesis of HIFs that mTOR controls the production of proteins involved in angiogenesis (e.g. VEGF) and in other responses that increase supplies of nutrients and energy for growing cells (Figure 3.1)

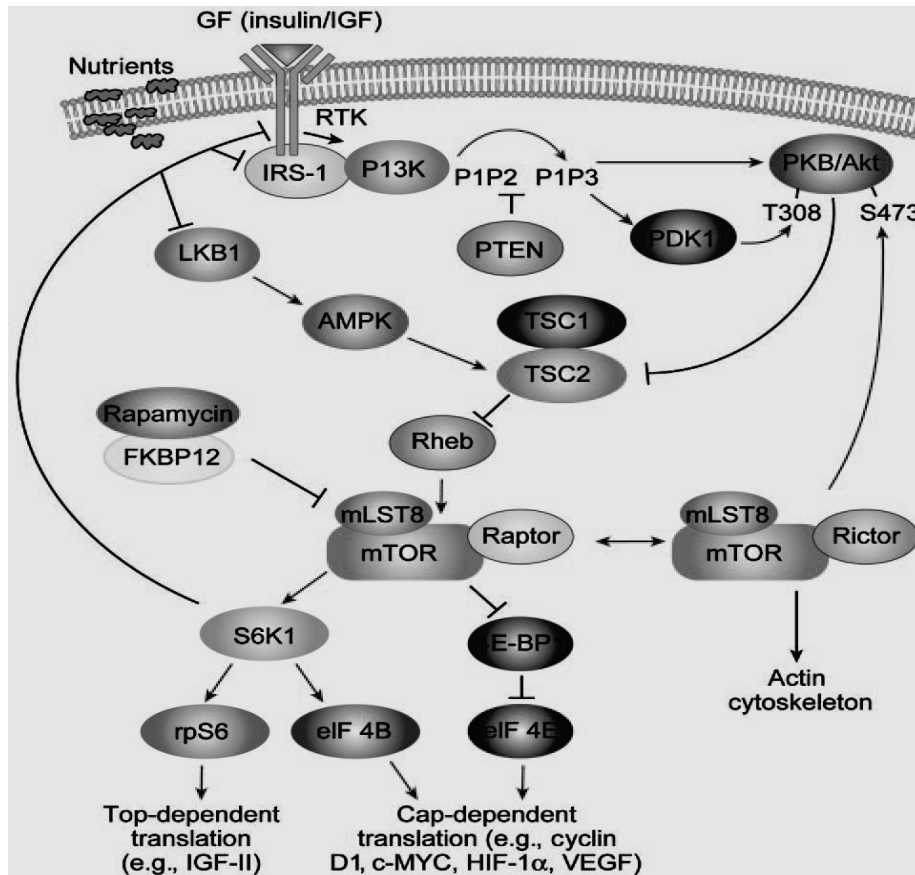


Figure 3.1 A model of mTOR signalling cascade and its function

This diagram outlines how mTOR integrates nutrient and growth factor-derived signaling inputs to regulate translation initiation. Mitogen signaling to RTKs activates PI3K and Akt. Akt is phosphorylated on T308 by PDK1 and by mTORC2 (consisting of mTOR, mLST8, and rictor) on S473, leading to its full activation, which in turn phosphorylates TSC2, leading to activation of Rheb GTPase and mTORC1 (consisting of mTOR, mLST8, and raptor) activation. The energy-sensing pathway (i.e., through amino acids and ATP) is linked to mTOR signaling through LKB1. LKB1 activates AMPK, which in turn activates TSC1/2, leading to mTORC1 inhibition. Activation of mTORC1 phosphorylates S6K1 and 4E-BP1 and leads to release of 4E-BP1 from eIF-4E, which play fundamental roles in top-dependent and cap-dependent translation, respectively. mTORC1 initiates a negative feedback loop to modulate Akt activity through S6K1. (Adapted from Wan X, Helman LJ. The biology behind mTOR inhibition in sarcoma. *Oncologist* 2007 Aug;12(8):1007-18)

3.2 Hypothesis

- iv. Biomarkers can be exploited in animal models to investigate events associated with ischaemia-reperfusion.
- v. Such a model can be used to assess interventions using anti-ischaemic compounds for benefit in reducing the harmful short and long term effects of ischaemia-reperfusion injury on the kidney
- vi. mTOR inhibitors show a promising role in the reduction of IR injury when administered systemically at the time of injury

3.3 Aims

- i. Can we match *in vitro* experiments to reduce or minimize cellular stress in the face of IR injury *in vivo* within a suitable animal model?
- ii. Can the effect of such a compound (AZ-6) on renal tissue, be determined biochemically and/or genetically + immunohistochemically using markers validated *in vivo* in Chapter 1

3.4 Methods

3.4.1 Animal Groups and Housing

The experiments were carried out on both male and female Albino Swiss rats aged between 6 and 9 months and weighing between 218 grams and 412 grams. Nutrition consisted of a standard rodent diet and tap water *ad libitum*. Animals were housed in the Joint Research Facility – University of Glasgow under standardized conditions in plastic-metal cages, light-dark cycle 12/12 hours, temperature 22 +/-2 °C, humidity 50 +/-5 %. The study was approved by the University's Ethics committee.

3.4.2 Experimental Design and Surgical Technique

There were 5 separate groups of animals with n=4 per group. Each group consisted of 2 male and 2 female rats: Group I: Nephrectomy only, Group II: Nephrectomy / Contralateral 30 minute IR Injury, Group III: Nephrectomy / AZ-6, Group IV: Nephrectomy / pre IR injury AZ-6 / Contralateral 30 minute IR Injury, Group V: Nephrectomy / post IR injury AZ-6 / Contralateral 30 minute IR Injury (Table 3.1).

The animals were anaesthetised using Isoflurane for induction of anaesthesia at a concentration of 4% in Oxygen. The animal was then maintained on Isoflurane 0.5% in Oxygen. A heated surgical table was utilised to maintain body temperature of the animal at 37°C. A subcutaneous injection of buprenorphine at 0.05mg/kg was administered upon induction and a 22G cannula was inserted into the tail vein (when required) at this stage. The cannula was flushed with 0.5ml of unfractionated heparin to maintain patency. Group III and group IV received an IV injection of AZ-6 at this stage. The dose for AZ-6 treatment was estimated at 0.8 µmol/kg of body weight after extrapolation from *in vitro* tests and after consultation with Astra Zeneca. The drug was dissolved in normal saline and 1% DMSO and administered i.v. (tail vein).

The animal's abdomen was shaved and subsequently prepped and draped in a sterile manner using Chlorhexidine solution. A midline laparotomy was performed and the bowels displaced medially to display the pedicle of the right kidney, which was subsequently ligated using a prolene 5/0 tie. The kidney was then freed from its ligamentous attachments including the ureter, removed from the animal and placed in liquid Nitrogen. The ureter was then ligated at its distal end. Haemostasis was achieved in all procedures with virtually no blood loss. Attention was then focused on the left kidney pedicle where the vein and artery were displayed with both blunt and sharp dissection. A haemostatic clamp was placed over both artery and vein in groups II, IV and V at specified time points during the procedure for a period of 30 minutes. Upon release of the clamp, adequate observation of reperfusion to the kidney was mandatory in order to proceed with recovery. The abdomen was subsequently closed with 3/0 silk to the muscular layer and to the skin. The animal was recovered in standard heated and carpeted cages for a period of 1-2 hours and each rat received a 2ml subcutaneous injection of normal saline. During the post-operative period up to sacrifice on day 10, the animals were weighed on a daily basis and blood samples were obtained at day 3, 6 and 10 via the tail vein under minimal sedation. A 300µl sample was obtained and subsequently spun down at 3000rpm for

10mins. The plasma was removed (approx 100µl) and stored at 5°C for up to 5 days. Analysis for plasma creatinine was via an automated laboratory process at Glasgow University, Veterinary Diagnostic Services using the automated Olympus AU5400 analyser. Although it was not the case with any of the animals in this study, weight loss exceeding more than 20% of the original body weight was an indication to sacrifice prematurely. There were no operative or post-operative deaths, however 2 animals (1 in Group III and another in Group V) required a repeat laparotomy during the recovery period because of pallor and suspected intra-abdominal bleeding. A washout was performed in both cases with visible clot in between small bowel loops but no obvious bleeding point identified. Animals were sacrificed by schedule 1 killing on day 10 at which point a blood sample was taken by cardiac puncture. The animals organs i.e lung, heart, liver and left kidney were subsequently frozen in liquid nitrogen for subsequent IHC analysis with similar organ biopsies stored in RNA Later[®] for gene expression analysis.

The reason for performing nephrectomy in all groups was to avoid confounding results in creatinine values by a contralateral unaffected kidney. As explained earlier in chapter 2, creatinine in itself is not the ideal marker for subtle changes in GFR and clearance studies using inulin are otherwise better suited. The caveat to this however is that the GFR studies performed in our lab can only be performed on animals with no recovery. We therefore used the serum creatinine estimations in this part of the study as a guide for further genetic and proteomic studies.

GROUP	PROCEDURE
I	Nephrectomy only (sham)
II	IR Injury
III	AZ-6
IV	IR injury + AZ6 pre
V	IR injury + AZ-6 post

Table 3.1 The five separate groups used in the animal model

All animals received a right sided nephrectomy. IR Injury was of 30 minute duration in all groups

Group	Sex	Day 3		Day 6		Day 10		WEIGHT in grams (Days post-op)										
		Creat	Adj Creat	Creat	Adj Creat	Creat	Adj Creat	0	1	2	3	4	5	6	7	8	9	10
I	M	69	18.25	59	15.53	61	15.68	404	396	377	378	377	385	384	380	380	388	389
	M	53	15.32	49	13.92	57	15.70	368	363	349	346	355	353	355	352	359	358	363
	F	61	25.52	56	23.83	52	21.67	250	249	242	239	242	240	236	235	237	240	240
	F	57	23.46	55	23.40	53	22.08	254	253	248	243	240	239	238	235	239	237	240
II	M	81	27.74	56	19.18	60	20.27	312	302	289	292	-	-	-	292	296	296	296
	F	68	29.57	57	25.00	56	24.35	232	224	224	230	-	-	-	228	230	230	230
	M	78	22.81	-	-	53	15.41	356	352	339	342	-	-	-	338	338	338	344
	F	85	37.95	61	26.99	52	22.81	242	238	227	224	-	-	-	226	226	226	228
III	M	100	29.59	58	16.57	58	16.11	370	352	340	338	340	347	350	344	352	354	360
	F	73	32.88	66	30.00	66	30.00	230	230	222	222	222	221	220	215	218	220	220
	M	90	28.85	63	20.19	54	16.98	318	320	306	312	310	310	312	307	312	318	318
	F	79	36.57	61	27.48	61	25.85	232	232	218	216	218	219	222	220	228	232	236
IV	M	58	16.20	54	15.25	53	14.80	372	360	360	358	352	354	354	354	354	354	358
	F	100	42.37	66	28.45	54	23.48	246	242	234	236	230	232	232	230	228	228	230
	F	117	51.77	71	31.42	61	26.07	238	234	226	226	220	224	226	226	228	234	234
	M	82	22.91	64	17.68	58	15.68	390	384	368	358	352	356	362	362	360	364	370
V	M	119	38.39	68	21.25	53	16.06	360	354	334	310	308	311	320	320	324	328	330
	F	-	-	67	27.69	54	22.13	258	256	250	248	248	242	242	245	244	244	244
	F	95	42.41	75	34.09	57	25.91	236	232	224	224	223	220	220	223	222	224	220
	M	89	24.45	62	16.85	49	13.17	382	384	368	364	368	366	368	364	365	368	372

Table 3.2 Details of the group demographics, weight, individual creatinine values and adjusted creatinine/100gr body weight

3.5 Results

3.5.1 Biochemical Analysis

The mean baseline creatinine was calculated from a representative cohort of 20 AS rats in an extended research database and was found to be $47.3\mu\text{Mol/l}$ with the mean weight being 313.6 grams. The corrected mean baseline serum creatinine per 100 grams body weight was $15.08\mu\text{Mol/l}$ and was used as the baseline value in all groups. Serum creatinine values were determined at 3 three time points post IR injury – Days 3, 6 and 10. The animals were sacrificed by schedule 1 killing on the 10th post operative day.

Although the serum creatinine is not an ideal marker for quantifying renal damage, it served as a valuable initial test on which to base further experimental – genetic and immunohistochemical analysis. The serum creatinine is usually unaffected until roughly 50% of kidney function is lost. Initial testing shows that there was a significant difference between the mean (body weight corrected/100gr) baseline creatinine of untreated animals ($n=20$) vs those in Group I that received a right sided nephrectomy at day 3 (diff=5.01; $p=0.04$). However, the data show that there is some form of compensatory renal hypertrophy up to day 6 when significant differences between the two groups is lost (diff=3.55; $p=0.15$). A similar finding is seen at day 10 (diff=3.16; $p=0.18$).

Tables 3.3, 3.4 and 3.5 below show the mean corrected creatinine values for all groups of animals at days 3,6 and 10. Figure 3.2 shows a clustered graph depicting information in the three tables above with 1SD error bars. There were two missing creatinine values due to technical sampling errors (Day 3 Group V and Day 6 Group II), which meant that mean values were calculated on 3 animals in the respective group.

DAY 3	Group I	Group II	Group III	Group IV	Group V
N	4	4	4	4	3*
Mean	20.64	29.50	31.97	33.29	35.08
Std. Error of Mean	2.34	3.14	1.77	8.27	5.44
Std. Deviation	4.68	6.29	3.53	16.55	9.42

*Missing data

Table 3.3 Creatinine values at Day 3

Peak creatinine values are seen on day 3 and are highest in Group V. There is a statistically significant increase in creatinine for group III (AZ-6 only) ($p < 0.01$) and Group V (AZ-6 post) ($p = 0.04$) when compared to sham operation in Group I. The difference approaches significance in Group II (IR Injury only) ($p = 0.06$). There is no difference however in Group IV (AZ-6 pre) ($p < 0.19$) indicating a possible protective effect of AZ-6 on renal tissue in the face of ischaemia reperfusion injury when administered pre-operatively.

DAY 6	Group I	Group II	Group III	Group IV	Group V
N	4	3*	4	4	4
Mean	19.17	23.72	23.54	23.19	24.97
Std. Error of Mean	2.59	2.35	3.14	3.96	3.77
Std. Deviation	5.18	4.06	6.27	7.93	7.54

*Missing data

Table 3.4 Creatinine values at Day 6

Creatinine values begin to normalise and approach Group I levels. As indicated in table 3.6, there is no significant difference in creatinine values between Groups II to V when compared to Group I at this point indicating that recovery is more or less equal between the groups independent of AZ-6 administration or IR injury.

DAY 10	Group I	Group II	Group III	Group IV	Group V
N	4	4	4	4	4
Mean	18.78	20.69	22.23	20.00	19.31
Std. Error of Mean	1.79	1.96	3.40	2.81	2.88
Std. Deviation	3.57	3.92	6.79	5.61	5.76

Table 3.5 Creatinine values at Day 10

Creatinine values further approach those seen in Group I, with a similar pattern to Day 6. Still, there is no significant difference between creatinine levels in Group II to V when compared to Group I. Although not significant statistically, creatinine levels in Group IV and V were closest to those of the control Group I.

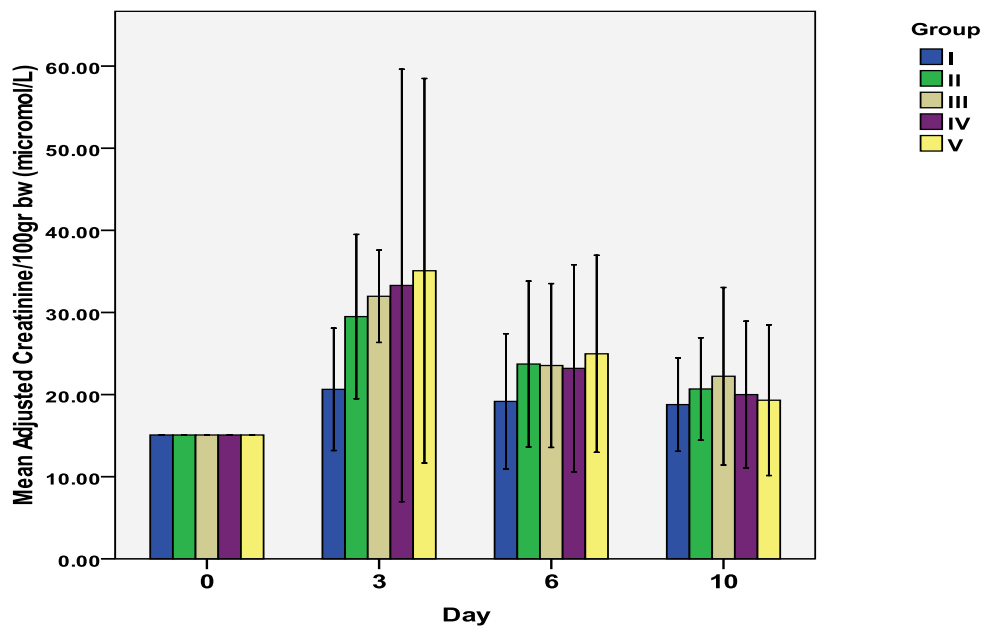


Figure 3.2 Clustered Bar Graph with 95% CI error bars

The graph gives a better depiction of the mean adjusted creatinine values in each group at different time points. The mean corrected creatinine of $15.08\mu\text{Mol/l}$ is used for all Groups at Day 0, although this time point is just a reference point and not actually utilised in the study.

		Change in Mean Corrected Creatinine vs Group I (Nephrectomy only)	p value
Group II	Day 3	8.87	0.06
	Day 6	3.92	0.27
	Day 10	1.93	0.49
Group III	Day 3	11.33	<0.01
	Day 6	4.39	0.32
	Day 10	3.55	0.40
Group IV	Day 3	12.67	0.19
	Day 6	4.03	0.43
	Day 10	1.23	0.72
Group V	Day 3	12.79	0.04
	Day 6	5.8	0.25
	Day 10	0.54	0.87

Table 3.7 Changes in corrected creatinine compared to Group I

This table confirms the findings presented in earlier results and shows the absolute change in corrected serum creatinine when compared to Group I (Nephrectomy only). Note that the largest differences in creatinine occur at day 3 where statistical differences exist in Groups III and V (unpaired t-test). The statistically non-significant result in Group IV Day 3 is possibly due to high standard deviation and standard error of the mean. There are no other significant time points at any other days

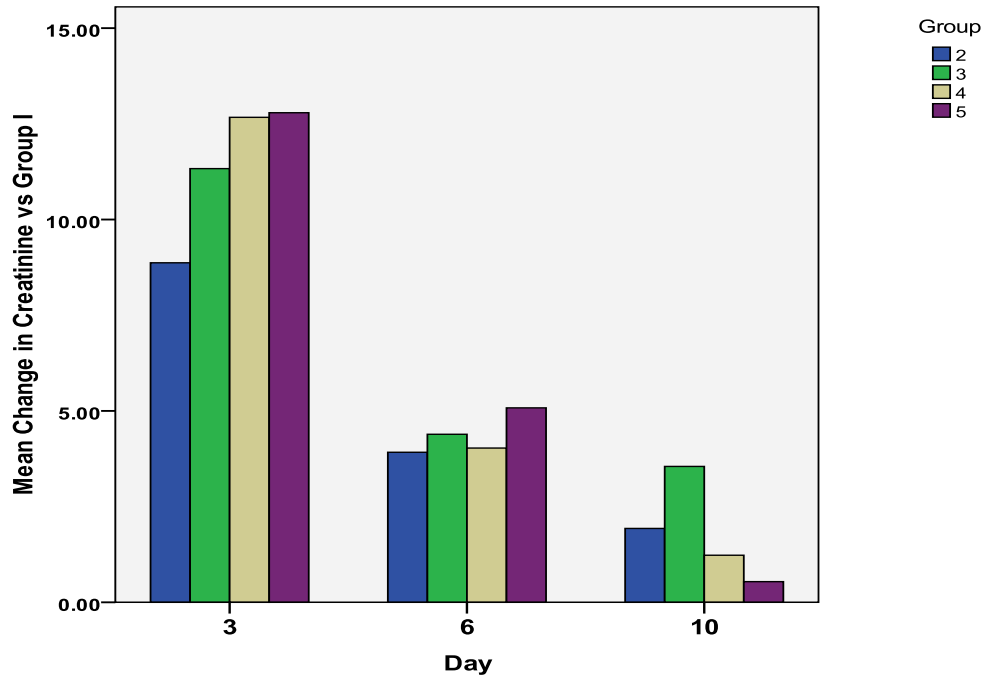


Figure 3.3 Changes in corrected creatinine compared to Group I

The graph depicts more clearly the changes in serum creatinine when compared to the control Group I. Initial significant changes, at day 3 are seen in Groups III ($p < 0.01$) and V ($p = 0.04$). Despite the graph showing very similar bar lengths to those in Group V, mean change was not significant, possibly due to high SEM + SD in the group. It is also interesting to note that the most rapid decline in creatinine levels occurs fastest in Group V where the graph shows only very minimal change from control creatinine at Day 10. The difference in creatinine is not significant when compared to Group I, meaning that pre-IR injury state is reached. The same result, however is seen in all groups at Day 10 and therefore neither treatment arm is the more valid

		Change in Mean Corrected Creatinine vs Group II (Nephrectomy + IR Injury)	p value
Group IV	Day 3	3.79	0.68
	Day 6	0.52	0.92
	Day 10	0.70	0.84
Group V	Day 3	5.56	0.38
	Day 6	1.24	0.80
	Day 10	1.39	0.70

Table 3.7 Changes in corrected creatinine compared to Group II (control)

The table shows that when Group II (Nephrectomy and IR Injury) is used as the control, there is no difference in biochemical recovery rates over 10 days when using AZ-6 either before or after the ischaemic insult is applied.

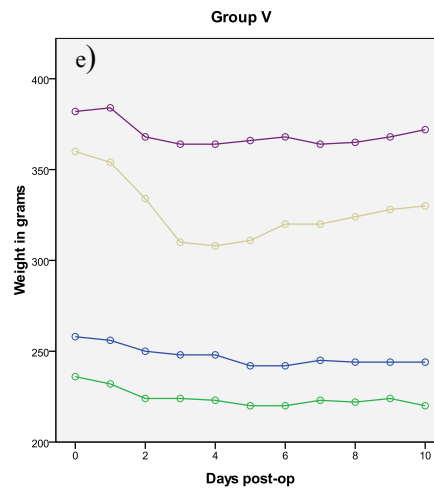
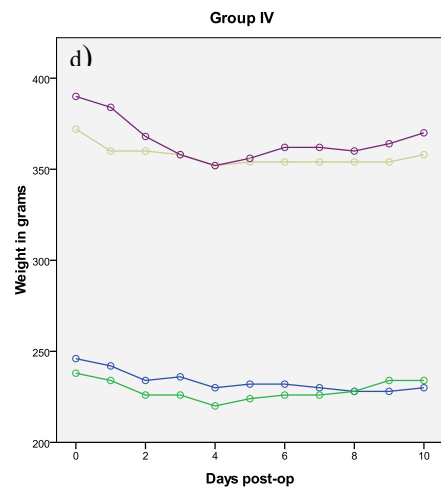
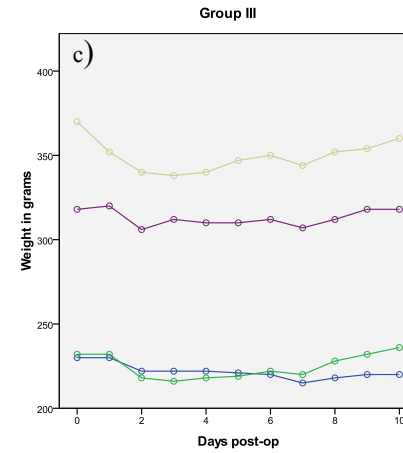
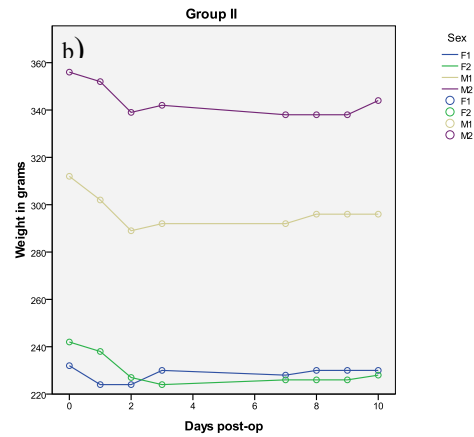
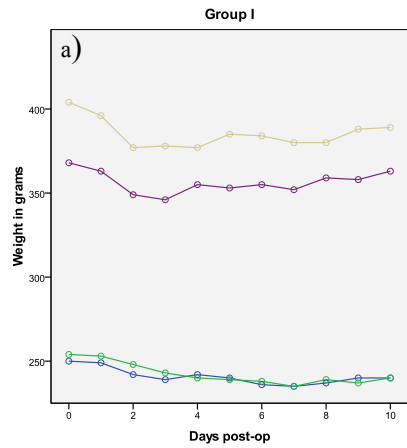


Figure 3.4a-e. Weight recordings for experimental groups I-V

The graphs show a clear distinction between female and male weights in all groups (n=2 male and n=2 female/group). A clear demonstration of the acute stress response to surgery with increased catabolism and weight loss evident, particularly in the first 3 post-operative days. Marked weight loss is evident in Group III, M1 and Group V, M1 both of which underwent a repeat exploratory laparotomy from the recovery area.

3.5.2 Bioage Genetic Expression and Immunohistochemical Staining

(The following subsection is adapted from work performed by Dr V. Moulisova PhD)

Prior to In vivo animal model testing, AZ-6 was selected from several compounds tested in vitro on HDFs (Human Diploid Fibroblasts) and on HREpi (Human Renal Epithelial Cells) in the presence and absence of an oxidative challenge. It displayed a protective effect on CDKN2A expression in both cell lines compared to control in both stress and no stress conditions (Figure 3.5).

3.5.3 Gene Expression Analysis Assays

Total RNA was extracted from human cells and rat kidney tissues using standard Trizol method, concentrations were measured on NanoDrop. After DNase treatment with RQ1 DNase (Promega), the concentration of RNA samples was measured again to keep the same amount of RNA for the reverse transcription step. RNaseOUT™ Recombinant Ribonuclease Inhibitor (Invitrogen) was used during all procedures with RNA. Transcriptor reverse transcriptase (Roche) was used for synthesizing the cDNA; per 100 µl of reverse transcription reaction, 1.6 µg and 2.5 µg of RNA was used in experiments with human cells and rat tissue, respectively. All cDNA samples were kept in -20°C until used for TaqMan qPCR. For single qPCR reactions with human cell samples, 16 ng of cDNA was amplified in total volume of 10 µl, and each reaction mix consisted of a specific TaqMan probe (10 nM for 18S, 200 nM for HPRT1 and CDKN2A), a set of forward and reverse primers (360 nM for 18S, 300 nM for HPRT1 and CDKN2A) and 2x concentrated TaqMan Universal Master Mix (Roche).

The sequences for primers and probes for housekeeping genes (18S rRNA and HPRT1), and for CDKN2A are listed below:

18S rRNA Forward: 5'- TTG ACT CAA CAC GGG AAA CC-3', 18S rRNA Reverse: 5'- CGT TCT TAG TTG GTG GAG CG-3', UPL probe No. 77: 5'-GGTGGTGG-3'; HPRT1 Forward: 5'-CTT GCT CGA GAT GTG ATG AAG G-3', HPRT1 Reverse: 5'-CAG CAG GTC AGC AAA GAA TTT ATA G-3', Probe: 5'-FAM-ATC ACA TTG TAG CCC TCT

GTG TGC TCA AGG-TAMRA-3'; CDKN2A Forward: 5'-CAT AGA TGC CGC GGA AGG T-3', CDKN2A Reverse: 5'-CCC GAG GTT TCT CAG AGC CT-3', Probe: 5'-FAM-CCT CAG CAT CCC CGA TTG AAA GAA CC-TAMRA-3'.

For single Q-PCR reactions with rat kidney samples, 25 ng of cDNA was amplified in total volume of 10 μ l, and each reaction mix consisted of 2x concentrated TaqMan Universal Master Mix (Roche), and 20x concentrated individual validated TaqMan assay from Applied Biosystems (Rn01527840, Rn00580664, and Rn00589996 primer-probe mix for HPRT1, CDKN2A, and CDKN1A, resp.). For rat and human samples, quantitative PCRs were done on LightCycler[®] 480 Real-Time PCR System (Roche) and AB 7500 Fast Real-Time PCR System (Applied Biosystems), respectively.

Custom designed TaqMan Low Density Array (TLDA) cards with 32 Gene Expression Assay targets pre-loaded into each of the wells were used for human cell samples. For one port, reaction mix in total volume of 110 μ l contained 170 ng cDNA and 2x TaqMan Universal Master Mix (Roche). TLDA cards were run on AB 7500 Fast Real-Time PCR System (Applied Biosystems). For analyses, manufacturer's software together with MicroSoft Excel and GraphPad Prism software was used.

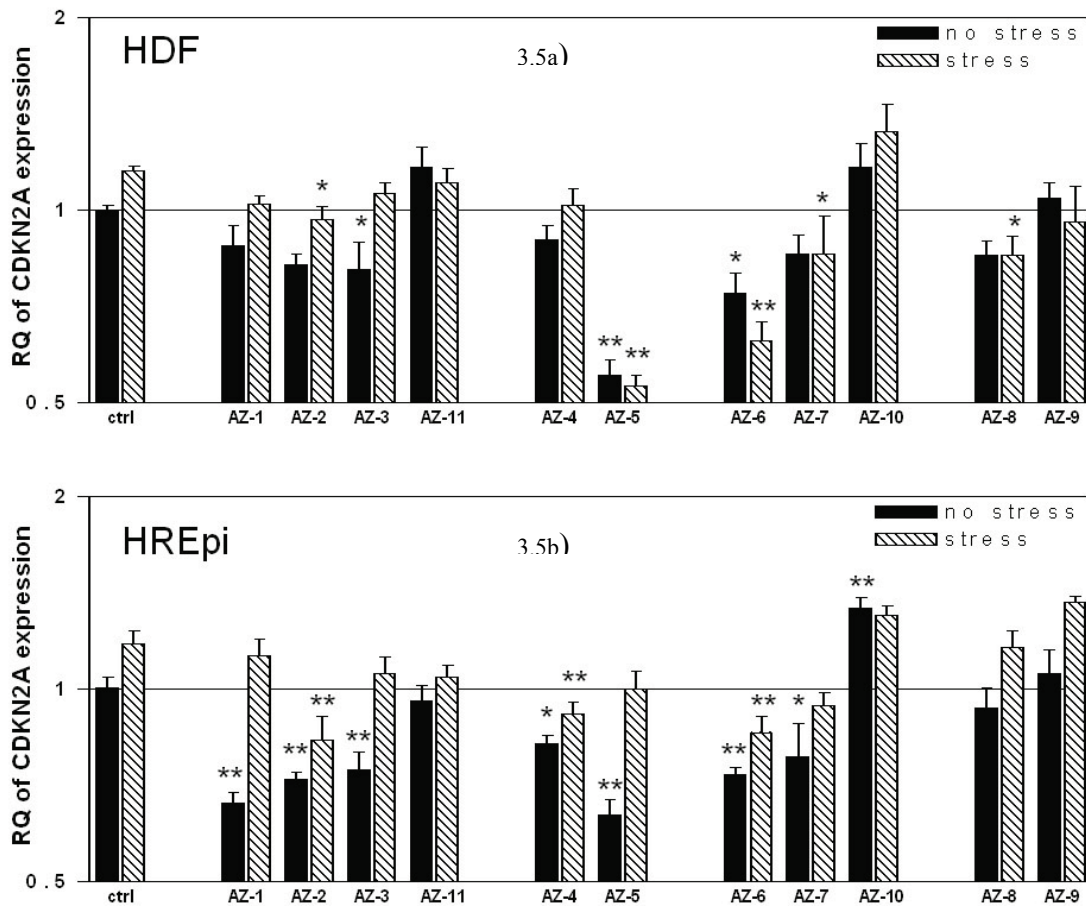


Figure 3.5 Compound treatment effects on CDKN2A transcriptional expression in two human primary cell types, a) HDF and b) HREpi.

Relative quantification is displayed as a fold change from control non-stressed cells. Values higher than 1 represent increased expression, values lower than 1 signify decreased expression. Statistical analysis was performed individually for nonstressed (black) and stressed cells (striped bars) by one-way ANOVA with Dunnett's post-test; samples were compared to controls; * where $P < 0.05$, ** where $P < 0.01$. (Adapted from: Anti-ageing Effects of mTOR Inhibition by a Reduction of Oxidative Stress in the Kidney. Vladimíra Moulisová et al. Aging and Diseases of Aging Conference, Tokyo, Japan. October 2012. Poster.)

During In vivo testing AZ-6 was able to counteract the effects of acute cellular stress following IRI as determined by CDKN1A expression levels (Figure 3.6).

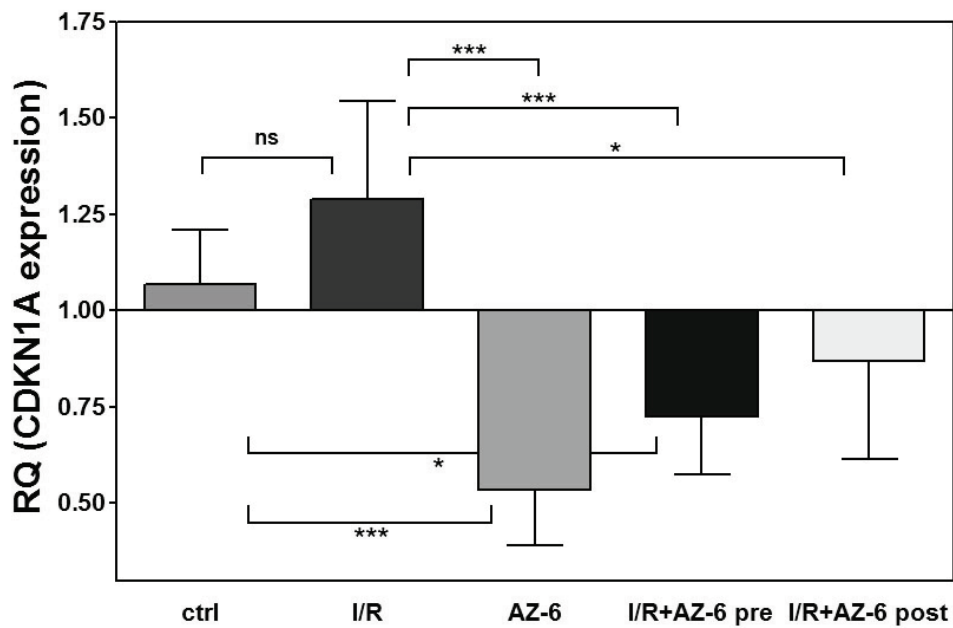


Figure 3.6 Expression levels for CDKN1A in rat kidney ischemia model with or without AZ-6 treatment

All values are means with SD; ns = non-significant; * = significant difference with $P < 0.05$; ** = significant difference with $P < 0.01$; *** = significant difference with $P < 0.001$ (Adapted from: Anti-ageing Effects of mTOR Inhibition by a Reduction of Oxidative Stress in the Kidney. Vladimíra Moulisová et al. Aging and Diseases of Aging Conference, Tokyo, Japan. October 2012. Poster.)

During IHC analysis for p16 and p21 protein, AZ-6 offered significant protection to the kidney in the face of IR injury as determined by decreased levels of expression in the treated groups relative to the controls.

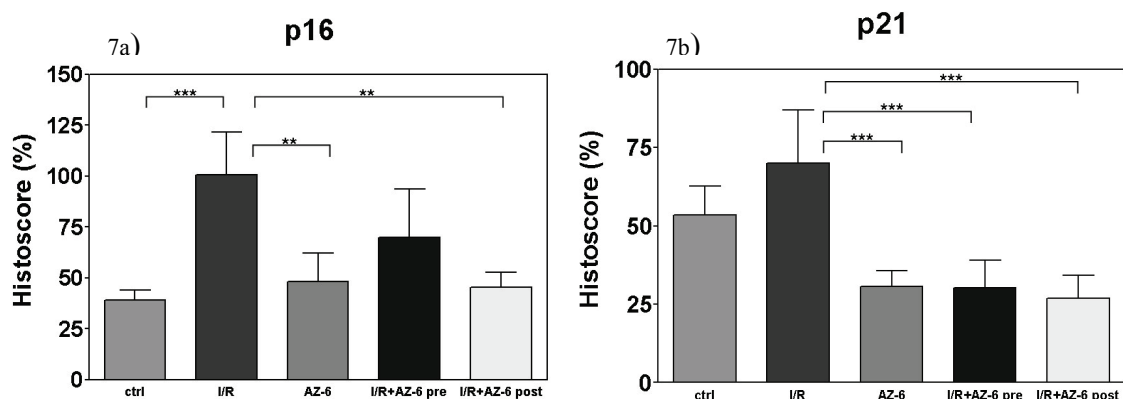


Figure 3.7a) p16 and Figure 3.7b) p21 Histocore

Nuclear histoscores for p16 and p21 proteins in rat kidney tissue sections. * = significant difference with $P < 0.05$; ** = significant difference with $P < 0.01$; *** = significant difference with $P < 0.001$. (Adapted from: Anti-ageing Effects of mTOR Inhibition by a Reduction of Oxidative Stress in the Kidney. Vladimíra Moulisová et al. Aging and Diseases of Aging Conference, Tokyo, Japan. October 2012. Poster.)

3.6 Discussion

3.6.1 Biochemical response to AZ-6

The data presented give a clear indication about the efficacy of AZ-6 in reducing the adverse effects of IR injury on renal tissue. The results are more robust in the genetic and IHC analysis however, the initial experiments involving serial creatinine and body weight measurements bring to light several important conclusions. Firstly, the results show that AZ-6 is a safe compound when administered as an intravenous preparation in the recommended dose of $0.8 \mu\text{mol/kg}$ of body weight and all animals survived the experimental 10 day phase. There were 2 post operative complications related to bleeding (1 male rat in Group III and 1 male rat in group V). It is difficult to conclude for certain whether such spontaneous bleeds were secondary to the administered compound itself or iatrogenic. The impression of the author performing these experiments is that AZ-6 does induce a temporary coagulopathic state leading to the possibility of spontaneous haemorrhages. This is consolidated by the fact that re-laparotomy could not isolate a particular bleeding point per se. Secondly, it is interesting to note that at day 10 the groups that approximated control serum creatinine more closely were those that received IR injury

and AZ-6. This observation is not statistically significant however in the face of results obtained in genetic analysis and IHC, this finding would make sense and may be of clinical relevance. Importantly however, the group that received AZ-6 only (Group III) possessed the highest creatinine values at day 10. This observation is minimal and not statistically significant from other groups however, it could be that AZ-6 may not provide the anticipated “nephroprotective” effect as measured by serum creatinine in an unstressed situation. It follows therefore, that the IR injury in itself is necessary for the maximal nephroprotective ability of AZ-6. This could be in part associated with the reperfusion process that results in release of NO and other chemokines into the circulation resulting in improved tissue and cellular penetration of the compound.

3.6.2 mTOR Inhibitors and Renal Function

Most studies related to mTOR nephrotoxicity have been centred on the original drug Sirolimus (Rapamycin). Sirolimus is not usually a first line immunosuppressive agent in the UK although it is commonly used when intolerance to mycophenolate or tacrolimus is observed. The perfect immunosuppressive agent would be able to suppress the immune response whilst simultaneously avoiding toxicity of any form. Despite excellent immunosuppressive capabilities, these agents have an incessant list of reported side effects of which nephrotoxicity is almost always reported. Immunosuppressive agents have a narrow therapeutic index and a broad availability in patient response necessitating serum level drug monitoring. Sirolimus exposure leads primarily to cell-cycle arrest in the early G1 phase of T and B lymphocytes (370;371)

There are conflicting reports in the literature as to the nephroprotective vs nephrotoxic effects of sirolimus in the acute injury phase in particular. In the longer term, it is well known to be minimally nephrotoxic after renal and solid organ transplantation (372;373) and prevents acute rejection by inhibition of cytokine and growth factor-mediated lymphocyte proliferation, especially the proliferation and clonal expansion of interleukin-2 stimulated T lymphocytes (374). Importantly, other cells are also a direct target of this drug, including endothelial, smooth muscle, mesangial and renal tubular cells (375-377).

Sirolimus however, has also been linked with high levels of proteinuria (second to decreased tubular protein reabsorption, increased VEGF secretion and podocyte dysregulation), cast nephropathy, ARF in association with myoglobinuria and delayed graft

function. Liberthal et al reported that rapamycin inhibits growth factor induced proliferation of cultured proximal tubular cells and supports their apoptosis by blocking the survival effects of the same growth factors (374). Accordingly, sirolimus impaired recovery from experimental acute renal failure induced by renal artery occlusion due to the combined effects of increased tubular cell loss (apoptosis) and inhibition of regenerative proliferation. These effects were attributable to the inhibition of p70 S6 kinase (374). Thus, during periods of renal allograft injury, sirolimus may be harmful due to its negative effects on tubular cell regeneration and survival [(374;375)]. The same may be true at the glomerular level in inflammatory states that require intact cell proliferation for repair and/or compensatory mechanisms (376). Other authors have shown that both sirolimus and its successor everolimus are able to limit infarction and apoptosis in heart muscle and preserve renal function after IR injury in rats (378;379). Low doses of everolimus have also been shown to limit proteinuria in rats affected by nephrotic syndrome (380)

3.6.3 CDKN1A and CDKN2A

Most of the genetic expression data presented in this chapter is based on the theory put forward in the first chapter of this thesis. Renal ischaemia reperfusion injury is known to shorten telomeres and upregulate stress-induced genes, such as the cyclin-dependent kinase (CDK) inhibitor 1A. CDKN1A is the gene responsible for encoding the p21 protein, a cell cycle regulator that has been reported at increased levels after stress events and senescence associated changes in the kidney, and is considered as a marker of cellular stress. CDKN2A provides later onset correlated changes with CDKN1A in renal tissue subject to ischaemia (235).

As can be seen in Figure 3.6 there was a statistically significant decrease in CDKN1A gene expression in both IR groups treated with AZ-6 (Groups IV and V) in comparison to the IR group without treatment (Group II). There was also a further decrease in CDKN1A expression in Group III, the non ischaemic control group. The results therefore indicate that AZ-6 reduces cellular stress even in the absence of IR injury and shows a protective effect when the kidney has been exposed to IR injury and treated with AZ-6 either before or after the ischaemic insult. These results were also strengthened in the IHC analysis where kidneys undergoing treatment with AZ-6 demonstrated less p21 and p16 staining when compared to controls in Group II undergoing an ischaemic insult only. Results for

p21 IHC actually showed a significant difference between all AZ-6 groups and control IR injury group Figure 3.7a, whilst for p16 there was a difference between control group and Groups III and V but not Group IV (Figure 3.7b) where AZ-6 was administered prior to the IR insult. The results indicate therefore that AZ-6 is preventing to a certain extent, renal cells from entering a state of senescence, maintaining ultimately their functional capacity and contributing to an improved renal clearance. During the dynamic senescence process, a programme of differentiation is initiated that involves the accumulation of p16 as well as changes in the morphology, size and attributes of the cells (320). After senescence is achieved, p21 declines considerably to an amount that was consistent with a reversible arrest earlier in the lifespan. p16 also increases as p21 declines and reduces the number of targets for p21 through its inhibitory effect on cyclin D1-Cdk4/6 complex formation (381;382). The low levels of staining present for both p21 and p16, when compared to controls is a valid observation that AZ-6 is preventing cells from entering the senescent state and thus retain maximal functional capacity.

The experimental model presented gives good insight into the tolerability of the compound AZ-6. At the recommended dose of 0.8µmol/kg there were no mortalities, although at day 3 there seemed to be a rise in serum creatinine with AZ-6 administration alone. This however needs to be confirmed with further trials as a high standard deviation and SEM was observed. There were 2 morbidities from what was clinically judged to be a coagulopathy concerning 2 animals that were found to have significant post operative ooze requiring a relaparotomy and washout with no actual bleeding point found. There is no evidence in the literature associating mTOR inhibitors with a coagulopathic state and neither with decreased platelet function. In fact rapamycin has been shown to be prothrombotic through its effects on platelet aggregation enhancement (383). The weights of the animals receiving only AZ-6 (Group III) remained constant throughout the post-operative period when correcting for the initial catabolic decline in response to surgery. This is further evidence as to the tolerability of the compound in the unstressed state. In animals receiving IR injury and AZ-6, there were no significant changes in weight from Day 0 when compared to sacrifice at day 10. The model tested creatinine values at 3,6 and 10 days based on a preliminary literature review into animal model testing. It is clearly seen however that the rise in creatinine in these animals is greatest at day 3 with creatinine values at 6 and 10 days being almost equal.

3.6.4 Telomere Length and CDKN2A synchrony

It is clear that critically short telomeres result in apoptosis, cell senescence, and chromosomal instability in tissue culture and animal models. Most telomeric studies are based upon, and have found associations between peripheral blood telomere length with diseases of aging (385) and longevity (386). Tissue surrogate markers, such as peripheral blood leukocytes (PBL), sputum, and buccal cells, can be easily and inexpensively collected and TL in these tissues may be a potential tool to screen individuals for their future risk of cancer or end organ damage (synchrony). Indeed there have been many studies to date that have analysed TL in surrogate tissues in relation to cancer risk, however the results are disappointingly inconsistent with positive, negative or null associations mostly from retrospective case controlled studies (387). Hodes et al (388) present a plausible hypothesis regarding the variability of surrogate tissue TL predicting cancer risk. They state that when TL in PBL become critically shortened due to exposure to risk factors, they may in turn trigger compensatory mechanisms, such as increased telomerase activity and an alternative non-telomerase-based mechanism lengthening telomeres that maintain TL integrity. This is in contrast to our general understanding of shortening telomeres with environmental stressors. In addition, an inherent problem when examining PBL TL is that different subtypes of PBL may possess differing TL and in fact, most studies examine a pool of mixed blood leukocytes (387).

The literature for CDKN2A leukocyte synchrony in relation to longevity is very sparse and this is probably because CDKN2A is a marker of oxidative stress at organ level only. In addition, there are almost no studies relating the association of CKN2A expression as a surrogate for peripheral organ quality. However, there are very few studies comparing the synchrony of CDKN2A with the onset of cancer. In fact, epigenetics, particularly DNA methylation at gene promoter regions for p16, has recently been reported to play a role in the development of gastric carcinoma (389). Shiels lab at the University of Glasgow is currently correlating PBL and renal allograft CDKN2A and TL in pre and post perfusion timelines of recipients undergoing kidney transplantation. This will be one of the first studies to show a possible dynamic association of organ and PBL bioage. The implications of finding a surrogate marker for end organ damage are vast and will have an enormous economic impact, particularly in relation to patient safety and quality of care.

3.6.5 Model Testing, Biological Ageing and Novel Clinical Entities

As shown in this work, bioage is a key determinant of cellular responses to stress and can be seen as an essential tool in providing information about safety and suitability for experimental compounds and NCEs. Bioage therefore can be used as a screen for NCEs in the context of healthy tissue and that which is diseased or exposed to increasing levels of stress. It can also be used to address inter-individual responses to treatment or disease. An NCE is a molecule developed by a particular pharmaceutical company or laboratory, in the early drug discovery stage, which after undergoing clinical trials may translate into a drug that could be a cure for some particular disease. Synthesis of an NCE is the first step in the process of drug development.

Many different intrinsic and extrinsic factors may induce ageing and associated diseases of ageing (e.g. oxidative stress, inflammation, genetic modulators, telomere attrition, mitochondrial dysfunction and nutritional differences). Assessing their impact is not straightforward, as human ageing is a heterogeneous gradual and complex process for which very few validated biomarkers exist and many of which do not translate well from model organisms (221). Biological ageing (i.e. ageing at the level of the cell, tissue, organ and organism) is thus not well understood.

Health status (whether at organ level or individual level) is classically based on chronological age and this is still widely used as a determinant of organ quality in clinical transplantation. Using biological age in order to override the predictive capacity of chronological age requires very sensitive and specific markers. There are indeed very few validated biomarkers in the literature that fulfil Baker and Sprott's 1988 criteria of which CDKN2A and telomere length were primarily studied in this thesis. Telomere length has proven to be a significantly weaker biomarker and is lost in multivariate analysis primarily because of inter-individual variation in telomere length which is subject to various socio-economic and lifestyle confounding factors. Also, as published by Shiels et al, it is difficult to extrapolate cellular observations to the organ and organism as a whole and in addition, telomere biology is slightly different between species (4;221)

The ability of a cell to optimally respond to stressful stimuli is dependent on its ability to sense the damage and respond accordingly, in the face of the metabolic and oxidative conditions at that time. It has been postulated that one way in which this critical cellular

response can be dealt with is via the concept of the MTR trinity. This is composed of mitochondrion, telomere & ribosome biogenesis. Through this triad critical DNA damage is sensed by the telomere nucleo-protein complex which also plays a role in effector mechanisms such as senescence. Energy production and apoptosis are facilitated by mitochondria, as well as the requisite protein synthetic pathways which are controlled via ribosomal DNA (165;226;384)

The evaluation of cellular stress responses is paramount to many NCE testing protocols. Most cytotoxicity testing for such NCEs typically assess extreme toxicity i.e cell death and are less able to detect subtle damage in which the cell may eventually enter a state of senescence or even neoplasia. An inherent problem when interpreting NCE testing is that studies involving small mammals e.g mice and rats, do not always correlate with human responses to such compounds. Attempts to overcome these shortfalls have used gene array, proteomic and metabolic analyses to match in vitro and in vivo data sets and to cross compare responses in different species.

The studies performed by Shiels laboratory (Moulisova et al. in prep) has sought to utilize a novel approach to NCE (AZ-6) testing in human cells. Instead of utilizing immortalised or conditionally immortalised cell lines, studies were conducted on fibroblasts and renal epithelial cells (primary cells) in order to closely characterise and mimic as much as possible, the human cell stress response system with validated BoAs such as CDKN2A. Thus, the use of such a model incorporates to a greater degree the efficacy of NCE testing and accounts for greater inter individual variation in health and disease settings. It is thus shown that bioage has an important role in determining NCE safety and can be used as a basis for studying future compounds both in vitro and in vivo.

3.7 Conclusion

Initial biochemistry and robust genetic testing have shown that AZ-6 can modulate cellular stress responses in the face of IR injury both in-vitro and in vivo. Remarkably, bioage as measured by CDKN1A / CDKN2A and their precursor proteins p21 / p16 is ameliorated when compared with suitable controls. Future studies on similar animal models engaging the use of serum creatine as a preliminary marker for end organ damage would be better suited utilising additional creatinine values at 24, 48 and 72 hours, serum urea and cystatin

C. The dosing of AZ-6 is also of primary importance for future studies. A single dose was given to each animal at a particular time point, however repeated doses or alterations in concentrations of AZ-6 are a possibility. The model could be extended to rodent transplantation, where an extra factor – cold preservation will be tested in addition to IR injury. It's efficacy in the prevention of allograft rejection will be of significant interest.

General Summary

With the current crisis of organ shortage and an increasing number of dialysis patients, studies directed at ameliorating such a substantial organ discrepancy are of considerable importance to the transplant community. The use of extended criteria donation has helped to compensate the disparity of organs however, we are still a long way from achieving satisfactory targets. Still there are many organs from older donors that are discarded primarily on the basis of chronological age. It is here that biological age may display a crucial role in allowing the transplant team to characterize donor organs with greater accuracy. Indeed both biological and chronological age are very closely related and ECD criteria are based very much on the latter, albeit with other clinical variables. However the biomarker of ageing CDKN2A which is suitably represented by Baker and Sprott's criteria, displays closer variabilities with post-operative transplant function, at least up to one year. Telomere length known as the "Gold standard" biomarker of ageing does not display as robust a role in predicting organ function as CDKN2A. The classification of organs represented in this text from category I-IV serves merely as a guide to future studies and is yet to be validated in larger clinical trials. It is however a simple and rapid assessment tool. (*Gingell-Littlejohn et al PLOS One 2013*)

Relatively advanced cellular senescence was displayed in the mutant AS/AGU rat kidney when compared to the parent AS strain. This was exploited in a unique animal model to study the effects of ischaemia reperfusion injury on the mutant kidney, hence mimicking to a certain degree the transplant related injuries in ECD kidneys. Although ischaemic times in the model were moderate in nature, there was nonetheless a difference in the tolerance to IR injury between parent and mutant strain as evidenced by increased p16 and p21 staining in AS/AGU rats. Such a model therefore is exclusive in that interventions to improve ECD

renal function post-transplantation can accurately and conveniently be represented and studied at a pre-clinical level.

Anti-ischaemic compounds have been the subject of much debate over the years, however a single “Holy Grail” compound able to completely abolish the injurious effects of IR injury has never been elicited. mTOR inhibitors however, display several cellular effects and act as potent immunosuppressants. They (AZ-6) have also been shown to partially mediate the detrimental effects of IR injury on the native kidneys of AS rats in a specifically designed animal model as shown. Further studies encompassing transplanted kidneys from mutant AS/AGU rats exposed to such a promising agent would be of undoubted importance to the clinical field of transplantation, potentially leading to immeasurable economic and patient benefits.

Acknowledgements

I would like to especially thank my supervisors Professor Paul Shiels and Mr Marc Clancy for their continuous support over the years. In addition, I would like to thank my adviser Dr Joanne Edwards, Dr Liane McGlynn for her help with the telomere RT-PCR analysis, Dr Dagmara McGuinness for providing CDKN2A expression values on a subset of kidney biopsies and Mr Alan McIntyre for his technical assistance. I would also like to thank the Darlinda Charitable Trust for Renal Research and the Cunningham Trust. In addition, Astra Zeneca for supporting the work in the final chapter of this project together with Dr Vladimira Moulisova for her meticulous genetic / IHC analyses and Mr Henry Whalen’s surgical contribution. All work was approved by the University of Glasgow Ethics committee in conjunction with the UK Home Office and additionally supported by the renal failure and transplant fund, Western Infirmary, Glasgow.

References

- (1) Joosten SA, van H, V, Nolan CE, Borrias MC, Jardine AG, Shiels PG, et al. Telomere shortening and cellular senescence in a model of chronic renal allograft rejection. *Am J Pathol* 2003 Apr;162(4):1305-12.
- (2) Melk A, Schmidt BM, Vongwiwatana A, Rayner DC, Halloran PF. Increased expression of senescence-associated cell cycle inhibitor p16INK4a in deteriorating renal transplants and diseased native kidney. *Am J Transplant* 2005 Jun;5(6):1375-82.
- (3) Melk A, Schmidt BM, Takeuchi O, Sawitzki B, Rayner DC, Halloran PF. Expression of p16INK4a and other cell cycle regulator and senescence associated genes in aging human kidney. *Kidney Int* 2004 Feb;65(2):510-20.
- (4) Shiels PG, Jardine AG. Dolly, no longer the exception: telomeres and implications for transplantation. *Cloning Stem Cells* 2003;5(2):157-60.
- (5) Halloran PF, Melk A, Barth C. Rethinking chronic allograft nephropathy: the concept of accelerated senescence. *J Am Soc Nephrol* 1999 Jan;10(1):167-81.
- (6) Melk A, Halloran PF. Cell senescence and its implications for nephrology. *J Am Soc Nephrol* 2001 Feb;12(2):385-93.
- (7) Yarlagadda SG, Coca SG, Garg AX, Doshi M, Poggio E, Marcus RJ, et al. Marked variation in the definition and diagnosis of delayed graft function: a systematic review. *Nephrol Dial Transplant* 2008 Sep;23(9):2995-3003.
- (8) Mayer G, Persijn GG. Eurotransplant kidney allocation system (ETKAS): rationale and implementation. *Nephrol Dial Transplant* 2006 Jan;21(1):2-3.
- (9) Morris PJ, Johnson RJ, Fuggle SV, Belger MA, Briggs JD. Analysis of factors that affect outcome of primary cadaveric renal transplantation in the UK. HLA Task Force of the Kidney Advisory Group of the United Kingdom Transplant Support Service Authority (UKTSSA). *Lancet* 1999 Oct 2;354(9185):1147-52.
- (10) Perico N, Codreanu I, Caruso M, Remuzzi G. Hyperuricemia in kidney transplantation. *Contrib Nephrol* 2005;147:124-31.
- (11) Moers C, Smits JM, Maathuis MH, Treckmann J, van GF, Napieralski BP, et al. Machine perfusion or cold storage in deceased-donor kidney transplantation. *N Engl J Med* 2009 Jan 1;360(1):7-19.
- (12) Quiroga I, McShane P, Koo DD, Gray D, Friend PJ, Fuggle S, et al. Major effects of delayed graft function and cold ischaemia time on renal allograft survival. *Nephrol Dial Transplant* 2006 Jun;21(6):1689-96.

- (13) Koppelstaetter C, Schratzberger G, Perco P, Hofer J, Mark W, Ollinger R, et al. Markers of cellular senescence in zero hour biopsies predict outcome in renal transplantation. *Aging Cell* 2008 Aug;7(4):491-7.
- (14) McGlynn LM, Stevenson K, Lamb K, Zino S, Brown M, Prina A, et al. Cellular senescence in pretransplant renal biopsies predicts postoperative organ function. *Aging Cell* 2009 Feb;8(1):45-51.
- (15) Becker TY. Use of Marginal Donors in Kidney Transplantation. 2011. Ref Type: Generic
- (16) Randhawa P. Role of donor kidney biopsies in renal transplantation. *Transplantation* 2001 May 27;71(10):1361-5.
- (17) de Fijter JW, Mallat MJ, Doxiadis II, Ringers J, Rosendaal FR, Claas FH, et al. Increased immunogenicity and cause of graft loss of old donor kidneys. *J Am Soc Nephrol* 2001 Jul;12(7):1538-46.
- (18) Ojo AO, Hanson JA, Meier-Kriesche H, Okechukwu CN, Wolfe RA, Leichtman AB, et al. Survival in recipients of marginal cadaveric donor kidneys compared with other recipients and wait-listed transplant candidates. *J Am Soc Nephrol* 2001 Mar;12(3):589-97.
- (19) Lee CM, Scandling JD, Pavlakis M, Markezich AJ, Dafoe DC, Alfrey EJ. A review of the kidneys that nobody wanted: determinants of optimal outcome. *Transplantation* 1998 Jan 27;65(2):213-9.
- (20) Port FK, Bragg-Gresham JL, Metzger RA, Dykstra DM, Gillespie BW, Young EW, et al. Donor characteristics associated with reduced graft survival: an approach to expanding the pool of kidney donors. *Transplantation* 2002 Nov 15;74(9):1281-6.
- (21) Metzger RA, Delmonico FL, Feng S, Port FK, Wynn JJ, Merion RM. Expanded criteria donors for kidney transplantation. *Am J Transplant* 2003;3 Suppl 4:114-25.
- (22) Levey AS. Measurement of renal function in chronic renal disease. *Kidney Int* 1990 Jul;38(1):167-84.
- (23) Perrone RD, Madias NE, Levey AS. Serum creatinine as an index of renal function: new insights into old concepts. *Clin Chem* 1992 Oct;38(10):1933-53.
- (24) Cockcroft DW, Gault MH. Prediction of creatinine clearance from serum creatinine. *Nephron* 1976;16(1):31-41.
- (25) Sawyer WT, Canaday BR, Poe TE, Webb CE, Gal P, Joyner PU, et al. Variables affecting creatinine clearance prediction. *Am J Hosp Pharm* 1983 Dec;40(12):2175-80.
- (26) Bjornsson TD, Cocchetto DM, McGowan FX, Verghese CP, Sedor F. Nomogram for estimating creatinine clearance. *Clin Pharmacokinet* 1983 Jul;8(4):365-9.

- (27) Taylor GO, Bamgboye EA, Oyediran AB, Longe O. Serum creatinine and prediction formulae for creatinine clearance. *Afr J Med Med Sci* 1982 Dec;11(4):175-81.
- (28) Gates GF. Creatinine clearance estimation from serum creatinine values: an analysis of three mathematical models of glomerular function. *Am J Kidney Dis* 1985 Mar;5(3):199-205.
- (29) Jelliffe RW. Letter: Creatinine clearance: bedside estimate. *Ann Intern Med* 1973 Oct;79(4):604-5.
- (30) Hallynck T, Soep HH, Thomis J, Boelaert J, Daneels R, Fillastre JP, et al. Prediction of creatinine clearance from serum creatinine concentration based on lean body mass. *Clin Pharmacol Ther* 1981 Sep;30(3):414-21.
- (31) Kampmann J, Siersbaek-Nielsen K, Kristensen M, Hansen JM. Rapid evaluation of creatinine clearance. *Acta Med Scand* 1974 Dec;196(6):517-20.
- (32) K DOQI. Clinical Practice guidelines for chronic kidney disease: evaluation, classification and stratification. 2013. Ref Type: Generic
- (33) Coresh J, Astor BC, Greene T, Eknoyan G, Levey AS. Prevalence of chronic kidney disease and decreased kidney function in the adult US population: Third National Health and Nutrition Examination Survey. *Am J Kidney Dis* 2003 Jan;41(1):1-12.
- (34) McClellan WM, Knight DF, Karp H, Brown WW. Early detection and treatment of renal disease in hospitalized diabetic and hypertensive patients: important differences between practice and published guidelines. *Am J Kidney Dis* 1997 Mar;29(3):368-75.
- (35) Remuzzi G, Ruggenti P, Perico N. Chronic renal diseases: renoprotective benefits of renin-angiotensin system inhibition. *Ann Intern Med* 2002 Apr 16;136(8):604-15.
- (36) Obrador GT, Ruthazer R, Arora P, Kausz AT, Pereira BJ. Prevalence of and factors associated with suboptimal care before initiation of dialysis in the United States. *J Am Soc Nephrol* 1999 Aug;10(8):1793-800.
- (37) Levey AS. A simplified equation to predict GFR from serum creatinine. 2013. Ref Type: Generic
- (38) Levey AS, Coresh J, Balk E, Kausz AT, Levin A, Steffes MW, et al. National Kidney Foundation practice guidelines for chronic kidney disease: evaluation, classification, and stratification. *Ann Intern Med* 2003 Jul 15;139(2):137-47.
- (39) Levey AS, Coresh J, Balk E, Kausz AT, Levin A, Steffes MW, et al. National Kidney Foundation practice guidelines for chronic kidney disease: evaluation, classification, and stratification. *Ann Intern Med* 2003 Jul 15;139(2):137-47.

- (40) Shin M. ABO Incompatible Kidney Transplantation-Current Status and Uncertainties. 2013. Ref Type: Generic
- (41) Hayflick L, Moorhead PS. The serial cultivation of human diploid cell strains. *Exp Cell Res* 1961 Dec;25:585-621.
- (42) Miura T, Mattson MP, Rao MS. Cellular lifespan and senescence signaling in embryonic stem cells. *Aging Cell* 2004 Dec;3(6):333-43.
- (43) CAMPISI J. Cellular Senescence; when bad things happen to bad cells. 2013. Ref Type: Generic
- (44) Shay JW, Roninson IB. Hallmarks of senescence in carcinogenesis and cancer therapy. *Oncogene* 2004 Apr 12;23(16):2919-33.
- (45) Bodnar AG, Ouellette M, Frolkis M, Holt SE, Chiu CP, Morin GB, et al. Extension of life-span by introduction of telomerase into normal human cells. *Science* 1998 Jan 16;279(5349):349-52.
- (46) Harley CB, Futcher AB, Greider CW. Telomeres shorten during ageing of human fibroblasts. *Nature* 1990 May 31;345(6274):458-60.
- (47) d'Adda di FF, Reaper PM, Clay-Farrace L, Fiegler H, Carr P, Von ZT, et al. A DNA damage checkpoint response in telomere-initiated senescence. *Nature* 2003 Nov 13;426(6963):194-8.
- (48) Herbig U, Jobling WA, Chen BP, Chen DJ, Sedivy JM. Telomere shortening triggers senescence of human cells through a pathway involving ATM, p53, and p21(CIP1), but not p16(INK4a). *Mol Cell* 2004 May 21;14(4):501-13.
- (49) Rodier F, Coppe JP, Patil CK, Hoeijmakers WA, Munoz DP, Raza SR, et al. Persistent DNA damage signalling triggers senescence-associated inflammatory cytokine secretion. *Nat Cell Biol* 2009 Aug;11(8):973-9.
- (50) Takai H, Smogorzewska A, de LT. DNA damage foci at dysfunctional telomeres. *Curr Biol* 2003 Sep 2;13(17):1549-56.
- (51) Dimri GP, Itahana K, Acosta M, Campisi J. Regulation of a senescence checkpoint response by the E2F1 transcription factor and p14(ARF) tumor suppressor. *Mol Cell Biol* 2000 Jan;20(1):273-85.
- (52) Lin AW, Barradas M, Stone JC, van AL, Serrano M, Lowe SW. Premature senescence involving p53 and p16 is activated in response to constitutive MEK/MAPK mitogenic signaling. *Genes Dev* 1998 Oct 1;12(19):3008-19.
- (53) Serrano M, Lin AW, McCurrach ME, Beach D, Lowe SW. Oncogenic ras provokes premature cell senescence associated with accumulation of p53 and p16INK4a. *Cell* 1997 Mar 7;88(5):593-602.
- (54) Zhu J, Woods D, McMahon M, Bishop JM. Senescence of human fibroblasts induced by oncogenic Raf. *Genes Dev* 1998 Oct 1;12(19):2997-3007.

- (55) Bartkova J, Rezaei N, Liontos M, Karakaidos P, Kletsas D, Issaeva N, et al. Oncogene-induced senescence is part of the tumorigenesis barrier imposed by DNA damage checkpoints. *Nature* 2006 Nov 30;444(7119):633-7.
- (56) Di MR, Fumagalli M, Cicalese A, Piccinin S, Gasparini P, Luise C, et al. Oncogene-induced senescence is a DNA damage response triggered by DNA hyper-replication. *Nature* 2006 Nov 30;444(7119):638-42.
- (57) Mallette FA, Ferbeyre G. The DNA damage signaling pathway connects oncogenic stress to cellular senescence. *Cell Cycle* 2007 Aug 1;6(15):1831-6.
- (58) Beausejour CM, Krtolica A, Galimi F, Narita M, Lowe SW, Yaswen P, et al. Reversal of human cellular senescence: roles of the p53 and p16 pathways. *EMBO J* 2003 Aug 15;22(16):4212-22.
- (59) Dirac AM, Bernards R. Reversal of senescence in mouse fibroblasts through lentiviral suppression of p53. *J Biol Chem* 2003 Apr 4;278(14):11731-4.
- (60) Hayflick L. THE LIMITED IN VITRO LIFETIME OF HUMAN DIPLOID CELL STRAINS. *Exp Cell Res* 1965 Mar;37:614-36.
- (61) Dimri GP, Lee X, Basile G, Acosta M, Scott G, Roskelley C, et al. A biomarker that identifies senescent human cells in culture and in aging skin in vivo. *Proc Natl Acad Sci U S A* 1995 Sep 26;92(20):9363-7.
- (62) Lee BY, Han JA, Im JS, Morrone A, Johung K, Goodwin EC, et al. Senescence-associated beta-galactosidase is lysosomal beta-galactosidase. *Aging Cell* 2006 Apr;5(2):187-95.
- (63) Alcorta DA, Xiong Y, Phelps D, Hannon G, Beach D, Barrett JC. Involvement of the cyclin-dependent kinase inhibitor p16 (INK4a) in replicative senescence of normal human fibroblasts. *Proc Natl Acad Sci U S A* 1996 Nov 26;93(24):13742-7.
- (64) Brenner AJ, Stampfer MR, Aldaz CM. Increased p16 expression with first senescence arrest in human mammary epithelial cells and extended growth capacity with p16 inactivation. *Oncogene* 1998 Jul 16;17(2):199-205.
- (65) Hara E, Smith R, Parry D, Tahara H, Stone S, Peters G. Regulation of p16CDKN2 expression and its implications for cell immortalization and senescence. *Mol Cell Biol* 1996 Mar;16(3):859-67.
- (66) Stein GH, Drullinger LF, Soulard A, Dulic V. Differential roles for cyclin-dependent kinase inhibitors p21 and p16 in the mechanisms of senescence and differentiation in human fibroblasts. *Mol Cell Biol* 1999 Mar;19(3):2109-17.
- (67) Narita M, Nunez S, Heard E, Narita M, Lin AW, Hearn SA, et al. Rb-mediated heterochromatin formation and silencing of E2F target genes during cellular senescence. *Cell* 2003 Jun 13;113(6):703-16.

- (68) Acosta JC, O'Loghlen A, Banito A, Guijarro MV, Augert A, Raguz S, et al. Chemokine signaling via the CXCR2 receptor reinforces senescence. *Cell* 2008 Jun 13;133(6):1006-18.
- (69) Coppe JP, Patil CK, Rodier F, Sun Y, Munoz DP, Goldstein J, et al. Senescence-associated secretory phenotypes reveal cell-nonautonomous functions of oncogenic RAS and the p53 tumor suppressor. *PLoS Biol* 2008 Dec 2;6(12):2853-68.
- (70) Coppe JP, Patil CK, Rodier F, Krtolica A, Beausejour CM, Parrinello S, et al. A human-like senescence-associated secretory phenotype is conserved in mouse cells dependent on physiological oxygen. *PLoS One* 2010;5(2):e9188.
- (71) Kuilman T, Michaloglou C, Vredeveld LC, Douma S, van DR, Desmet CJ, et al. Oncogene-induced senescence relayed by an interleukin-dependent inflammatory network. *Cell* 2008 Jun 13;133(6):1019-31.
- (72) Hanahan D, Weinberg RA. The hallmarks of cancer. *Cell* 2000 Jan 7;100(1):57-70.
- (73) Beausejour CM, Krtolica A, Galimi F, Narita M, Lowe SW, Yaswen P, et al. Reversal of human cellular senescence: roles of the p53 and p16 pathways. *EMBO J* 2003 Aug 15;22(16):4212-22.
- (74) Bond JA, Wyllie FS, Wynford-Thomas D. Escape from senescence in human diploid fibroblasts induced directly by mutant p53. *Oncogene* 1994 Jul;9(7):1885-9.
- (75) Chen Z, Trotman LC, Shaffer D, Lin HK, Dotan ZA, Niki M, et al. Crucial role of p53-dependent cellular senescence in suppression of Pten-deficient tumorigenesis. *Nature* 2005 Aug 4;436(7051):725-30.
- (76) Collins CJ, Sedivy JM. Involvement of the INK4a/Arf gene locus in senescence. *Aging Cell* 2003 Jun;2(3):145-50.
- (77) Hara E, Tsurui H, Shinozaki A, Nakada S, Oda K. Cooperative effect of antisense-Rb and antisense-p53 oligomers on the extension of life span in human diploid fibroblasts, TIG-1. *Biochem Biophys Res Commun* 1991 Aug 30;179(1):528-34.
- (78) Jacobs JJ, de LT. Significant role for p16INK4a in p53-independent telomere-directed senescence. *Curr Biol* 2004 Dec 29;14(24):2302-8.
- (79) Ohtani N, Yamakoshi K, Takahashi A, Hara E. The p16INK4a-RB pathway: molecular link between cellular senescence and tumor suppression. *J Med Invest* 2004 Aug;51(3-4):146-53.
- (80) Oren M. Decision making by p53: life, death and cancer. *Cell Death Differ* 2003 Apr;10(4):431-42.

- (81) Rodier F, Campisi J, Bhaumik D. Two faces of p53: aging and tumor suppression. *Nucleic Acids Res* 2007;35(22):7475-84.
- (82) Schmitt CA, Fridman JS, Yang M, Lee S, Baranov E, Hoffman RM, et al. A senescence program controlled by p53 and p16INK4a contributes to the outcome of cancer therapy. *Cell* 2002 May 3;109(3):335-46.
- (83) Shay JW, Pereira-Smith OM, Wright WE. A role for both RB and p53 in the regulation of human cellular senescence. *Exp Cell Res* 1991 Sep;196(1):33-9.
- (84) Ventura A, Kirsch DG, McLaughlin ME, Tuveson DA, Grimm J, Lintault L, et al. Restoration of p53 function leads to tumour regression in vivo. *Nature* 2007 Feb 8;445(7128):661-5.
- (85) Xue W, Zender L, Miething C, Dickins RA, Hernando E, Krizhanovsky V, et al. Senescence and tumour clearance is triggered by p53 restoration in murine liver carcinomas. *Nature* 2007 Feb 8;445(7128):656-60.
- (86) Collado M, Serrano M. Senescence in tumours: evidence from mice and humans. *Nat Rev Cancer* 2010 Jan;10(1):51-7.
- (87) Balducci L, Ershler WB. Cancer and ageing: a nexus at several levels. *Nat Rev Cancer* 2005 Aug;5(8):655-62.
- (88) Campisi J. Cancer and ageing: rival demons?. *Nat Rev Cancer* 2003 May;3(5):339-49.
- (89) Erusalimsky JD, Kurz DJ. Cellular senescence in vivo: its relevance in ageing and cardiovascular disease. *Exp Gerontol* 2005 Aug;40(8-9):634-42.
- (90) Jeyapalan JC, Ferreira M, Sedivy JM, Herbig U. Accumulation of senescent cells in mitotic tissue of aging primates. *Mech Ageing Dev* 2007 Jan;128(1):36-44.
- (91) Melk A, Kittikowit W, Sandhu I, Halloran KM, Grimm P, Schmidt BM, et al. Cell senescence in rat kidneys in vivo increases with growth and age despite lack of telomere shortening. *Kidney Int* 2003 Jun;63(6):2134-43.
- (92) Paradis V, Youssef N, Dargere D, Ba N, Bonvoust F, Deschatrette J, et al. Replicative senescence in normal liver, chronic hepatitis C, and hepatocellular carcinomas. *Hum Pathol* 2001 Mar;32(3):327-32.
- (93) Wang C, Jurk D, Maddick M, Nelson G, Martin-Ruiz C, Von ZT. DNA damage response and cellular senescence in tissues of aging mice. *Aging Cell* 2009 Jun;8(3):311-23.
- (94) Bavik C, Coleman I, Dean JP, Knudsen B, Plymate S, Nelson PS. The gene expression program of prostate fibroblast senescence modulates neoplastic epithelial cell proliferation through paracrine mechanisms. *Cancer Res* 2006 Jan 15;66(2):794-802.

- (95) Krtolica A, Parrinello S, Lockett S, Desprez PY, Campisi J. Senescent fibroblasts promote epithelial cell growth and tumorigenesis: a link between cancer and aging. *Proc Natl Acad Sci U S A* 2001 Oct 9;98(21):12072-7.
- (96) Bartholomew JN, Volonte D, Galbiati F. Caveolin-1 regulates the antagonistic pleiotropic properties of cellular senescence through a novel Mdm2/p53-mediated pathway. *Cancer Res* 2009 Apr 1;69(7):2878-86.
- (97) Bhatia B, Multani AS, Patrawala L, Chen X, Calhoun-Davis T, Zhou J, et al. Evidence that senescent human prostate epithelial cells enhance tumorigenicity: cell fusion as a potential mechanism and inhibition by p16INK4a and hTERT. *Int J Cancer* 2008 Apr 1;122(7):1483-95.
- (98) Liu D, Hornsby PJ. Senescent human fibroblasts increase the early growth of xenograft tumors via matrix metalloproteinase secretion. *Cancer Res* 2007 Apr 1;67(7):3117-26.
- (99) Maier B, Gluba W, Bernier B, Turner T, Mohammad K, Guise T, et al. Modulation of mammalian life span by the short isoform of p53. *Genes Dev* 2004 Feb 1;18(3):306-19.
- (100) Tyner SD, Venkatachalam S, Choi J, Jones S, Ghebranious N, Igelmann H, et al. p53 mutant mice that display early ageing-associated phenotypes. *Nature* 2002 Jan 3;415(6867):45-53.
- (101) Hinkal GW, Gatza CE, Parikh N, Donehower LA. Altered senescence, apoptosis, and DNA damage response in a mutant p53 model of accelerated aging. *Mech Ageing Dev* 2009 Apr;130(4):262-71.
- (102) Leong WF, Chau JF, Li B. p53 Deficiency leads to compensatory up-regulation of p16INK4a. *Mol Cancer Res* 2009 Mar;7(3):354-60.
- (103) Su X, Cho MS, Gi YJ, Ayanga BA, Sherr CJ, Flores ER. Rescue of key features of the p63-null epithelial phenotype by inactivation of Ink4a and Arf. *EMBO J* 2009 Jul 8;28(13):1904-15.
- (104) Yamakoshi K, Takahashi A, Hirota F, Nakayama R, Ishimaru N, Kubo Y, et al. Real-time in vivo imaging of p16Ink4a reveals cross talk with p53. *J Cell Biol* 2009 Aug 10;186(3):393-407.
- (105) Zhang J, Pickering CR, Holst CR, Gauthier ML, Tlsty TD. p16INK4a modulates p53 in primary human mammary epithelial cells. *Cancer Res* 2006 Nov 1;66(21):10325-31.
- (106) Esiri MM. Ageing and the brain. *J Pathol* 2007 Jan;211(2):181-7.
- (107) Bahar R, Hartmann CH, Rodriguez KA, Denny AD, Busuttill RA, Dolle ME, et al. Increased cell-to-cell variation in gene expression in ageing mouse heart. *Nature* 2006 Jun 22;441(7096):1011-4.

- (108) Drummond-Barbosa D. Stem cells, their niches and the systemic environment: an aging network. *Genetics* 2008 Dec;180(4):1787-97.
- (109) Freund A, Orjalo AV, Desprez PY, Campisi J. Inflammatory networks during cellular senescence: causes and consequences. *Trends Mol Med* 2010 May;16(5):238-46.
- (110) Chung HY, Cesari M, Anton S, Marzetti E, Giovannini S, Seo AY, et al. Molecular inflammation: underpinnings of aging and age-related diseases. *Ageing Res Rev* 2009 Jan;8(1):18-30.
- (111) Franceschi C, Capri M, Monti D, Giunta S, Olivieri F, Sevini F, et al. Inflammaging and anti-inflammaging: a systemic perspective on aging and longevity emerged from studies in humans. *Mech Ageing Dev* 2007 Jan;128(1):92-105.
- (112) Baker DJ, Wijshake T, Tchkonian T, LeBrasseur NK, Childs BG, van de Sluis B, et al. Clearance of p16Ink4a-positive senescent cells delays ageing-associated disorders. *Nature* 2011 Nov 10;479(7372):232-6.
- (113) Jun JI, Lau LF. The matricellular protein CCN1 induces fibroblast senescence and restricts fibrosis in cutaneous wound healing. *Nat Cell Biol* 2010 Jul;12(7):676-85.
- (114) Krizhanovsky V, Yon M, Dickins RA, Hearn S, Simon J, Miething C, et al. Senescence of activated stellate cells limits liver fibrosis. *Cell* 2008 Aug 22;134(4):657-67.
- (115) Orjalo AV, Bhaumik D, Gengler BK, Scott GK, Campisi J. Cell surface-bound IL-1alpha is an upstream regulator of the senescence-associated IL-6/IL-8 cytokine network. *Proc Natl Acad Sci U S A* 2009 Oct 6;106(40):17031-6.
- (116) Taganov KD, Boldin MP, Chang KJ, Baltimore D. NF-kappaB-dependent induction of microRNA miR-146, an inhibitor targeted to signaling proteins of innate immune responses. *Proc Natl Acad Sci U S A* 2006 Aug 15;103(33):12481-6.
- (117) Gourtsoyiannis N, Prassopoulos P, Cavouras D, Pantelidis N. The thickness of the renal parenchyma decreases with age: a CT study of 360 patients. *AJR Am J Roentgenol* 1990 Sep;155(3):541-4.
- (118) Fliser D, Zeier M, Nowack R, Ritz E. Renal functional reserve in healthy elderly subjects. *J Am Soc Nephrol* 1993 Jan;3(7):1371-7.
- (119) Fliser D, Franek E, Joest M, Block S, Mutschler E, Ritz E. Renal function in the elderly: impact of hypertension and cardiac function. *Kidney Int* 1997 Apr;51(4):1196-204.
- (120) Fuiano G, Sund S, Mazza G, Rosa M, Caglioti A, Gallo G, et al. Renal hemodynamic response to maximal vasodilating stimulus in healthy older subjects. *Kidney Int* 2001 Mar;59(3):1052-8.

- (121) Berg UB. Differences in decline in GFR with age between males and females. Reference data on clearances of inulin and PAH in potential kidney donors. *Nephrol Dial Transplant* 2006 Sep;21(9):2577-82.
- (122) Cusack BJ. Pharmacokinetics in older persons. *Am J Geriatr Pharmacother* 2004 Dec;2(4):274-302.
- (123) Young A. Ageing and physiological functions. *Philos Trans R Soc Lond B Biol Sci* 1997 Dec 29;352(1363):1837-43.
- (124) Wetzels JF, Kiemeney LA, Swinkels DW, Willems HL, den HM. Age- and gender-specific reference values of estimated GFR in Caucasians: the Nijmegen Biomedical Study. *Kidney Int* 2007 Sep;72(5):632-7.
- (125) Fehrman-Ekholm I, Skeppholm L. Renal function in the elderly (>70 years old) measured by means of iohexol clearance, serum creatinine, serum urea and estimated clearance. *Scand J Urol Nephrol* 2004;38(1):73-7.
- (126) Esposito C, Plati A, Mazzullo T, Fasoli G, De MA, Grosjean F, et al. Renal function and functional reserve in healthy elderly individuals. *J Nephrol* 2007 Sep;20(5):617-25.
- (127) Robertson KD, Jones PA. Tissue-specific alternative splicing in the human INK4a/ARF cell cycle regulatory locus. *Oncogene* 1999 Jul 1;18(26):3810-20.
- (128) Der G, Batty GD, Benzeval M, Deary IJ, Green MJ, McGlynn L, et al. Is telomere length a biomarker for aging: cross-sectional evidence from the west of Scotland?. *PLoS One* 2012;7(9):e45166.
- (129) Allsopp RC, Vaziri H, Patterson C, Goldstein S, Younglai EV, Futcher AB, et al. Telomere length predicts replicative capacity of human fibroblasts. *Proc Natl Acad Sci U S A* 1992 Nov 1;89(21):10114-8.
- (130) Blackburn EH. Structure and function of telomeres. *Nature* 1991 Apr 18;350(6319):569-73.
- (131) Palm W, de LT. How shelterin protects mammalian telomeres. *Annu Rev Genet* 2008;42:301-34.
- (132) Griffith JD, Comeau L, Rosenfield S, Stansel RM, Bianchi A, Moss H, et al. Mammalian telomeres end in a large duplex loop. *Cell* 1999 May 14;97(4):503-14.
- (133) van SB, Smogorzewska A, de LT. TRF2 protects human telomeres from end-to-end fusions. *Cell* 1998 Feb 6;92(3):401-13.
- (134) Celli GB, de LT. DNA processing is not required for ATM-mediated telomere damage response after TRF2 deletion. *Nat Cell Biol* 2005 Jul;7(7):712-8.

- (135) van SB, de LT. Control of telomere length by the human telomeric protein TRF1. *Nature* 1997 Feb 20;385(6618):740-3.
- (136) Sfeir A, Kosiyatrakul ST, Hockemeyer D, MacRae SL, Karlseder J, Schildkraut CL, et al. Mammalian telomeres resemble fragile sites and require TRF1 for efficient replication. *Cell* 2009 Jul 10;138(1):90-103.
- (137) Kim SH, Kaminker P, Campisi J. TIN2, a new regulator of telomere length in human cells. *Nat Genet* 1999 Dec;23(4):405-12.
- (138) Bae NS, Baumann P. A RAP1/TRF2 complex inhibits nonhomologous end-joining at human telomeric DNA ends. *Mol Cell* 2007 May 11;26(3):323-34.
- (139) Sarthy J, Bae NS, Scrafford J, Baumann P. Human RAP1 inhibits non-homologous end joining at telomeres. *EMBO J* 2009 Nov 4;28(21):3390-9.
- (140) Baumann P, Cech TR. Pot1, the putative telomere end-binding protein in fission yeast and humans. *Science* 2001 May 11;292(5519):1171-5.
- (141) Ye JZ, Hockemeyer D, Krutchinsky AN, Loayza D, Hooper SM, Chait BT, et al. POT1-interacting protein PIP1: a telomere length regulator that recruits POT1 to the TIN2/TRF1 complex. *Genes Dev* 2004 Jul 15;18(14):1649-54.
- (142) Liu D, Safari A, O'Connor MS, Chan DW, Laegeler A, Qin J, et al. PTPN22 interacts with POT1 and regulates its localization to telomeres. *Nat Cell Biol* 2004 Jul;6(7):673-80.
- (143) Hockemeyer D, Sfeir AJ, Shay JW, Wright WE, de LT. POT1 protects telomeres from a transient DNA damage response and determines how human chromosomes end. *EMBO J* 2005 Jul 20;24(14):2667-78.
- (144) Wu L, Multani AS, He H, Cosme-Blanco W, Deng Y, Deng JM, et al. Pot1 deficiency initiates DNA damage checkpoint activation and aberrant homologous recombination at telomeres. *Cell* 2006 Jul 14;126(1):49-62.
- (145) Hockemeyer D, Palm W, Else T, Daniels JP, Takai KK, Ye JZ, et al. Telomere protection by mammalian Pot1 requires interaction with Tpp1. *Nat Struct Mol Biol* 2007 Aug;14(8):754-61.
- (146) Hockemeyer D, Daniels JP, Takai H, de LT. Recent expansion of the telomeric complex in rodents: Two distinct POT1 proteins protect mouse telomeres. *Cell* 2006 Jul 14;126(1):63-77.
- (147) Loayza D, de LT. POT1 as a terminal transducer of TRF1 telomere length control. *Nature* 2003 Jun 26;423(6943):1013-8.
- (148) Wang F, Podell ER, Zaug AJ, Yang Y, Baciuc P, Cech TR, et al. The POT1-TPP1 telomere complex is a telomerase processivity factor. *Nature* 2007 Feb 1;445(7127):506-10.

- (149) Xin H, Liu D, Wan M, Safari A, Kim H, Sun W, et al. TPP1 is a homologue of ciliate TEBP-beta and interacts with POT1 to recruit telomerase. *Nature* 2007 Feb 1;445(7127):559-62.
- (150) Campisi J. Replicative senescence: an old lives' tale?. *Cell* 1996 Feb 23;84(4):497-500.
- (151) Harley CB. Telomere loss: mitotic clock or genetic time bomb?. *Mutat Res* 1991 Mar;256(2-6):271-82.
- (152) Melk A, Halloran PF. Cell senescence and its implications for nephrology. *J Am Soc Nephrol* 2001 Feb;12(2):385-93.
- (153) Artandi SE, DePinho RA. Telomeres and telomerase in cancer. *Carcinogenesis* 2010 Jan;31(1):9-18.
- (154) Eisenberg DT. An evolutionary review of human telomere biology: the thrifty telomere hypothesis and notes on potential adaptive paternal effects. *Am J Hum Biol* 2011 Mar;23(2):149-67.
- (155) Benetos A, Gardner JP, Zureik M, Labat C, Xiaobin L, Adamopoulos C, et al. Short telomeres are associated with increased carotid atherosclerosis in hypertensive subjects. *Hypertension* 2004 Feb;43(2):182-5.
- (156) Brouillette S, Singh RK, Thompson JR, Goodall AH, Samani NJ. White cell telomere length and risk of premature myocardial infarction. *Arterioscler Thromb Vasc Biol* 2003 May 1;23(5):842-6.
- (157) Cawthon RM, Smith KR, O'Brien E, Sivatchenko A, Kerber RA. Association between telomere length in blood and mortality in people aged 60 years or older. *Lancet* 2003 Feb 1;361(9355):393-5.
- (158) Fitzpatrick AL, Kronmal RA, Kimura M, Gardner JP, Psaty BM, Jenny NS, et al. Leukocyte telomere length and mortality in the Cardiovascular Health Study. *J Gerontol A Biol Sci Med Sci* 2011 Apr;66(4):421-9.
- (159) Fuster JJ, Andres V. Telomere biology and cardiovascular disease. *Circ Res* 2006 Nov 24;99(11):1167-80.
- (160) Samani NJ, Boulby R, Butler R, Thompson JR, Goodall AH. Telomere shortening in atherosclerosis. *Lancet* 2001 Aug 11;358(9280):472-3.
- (161) Carrero JJ, Shiels PG, Stenvinkel P. Telomere biology alterations as a mortality risk factor in CKD. *Am J Kidney Dis* 2008 Jun;51(6):1076-7.
- (162) Carrero JJ, Stenvinkel P, Fellstrom B, Qureshi AR, Lamb K, Heimbürger O, et al. Telomere attrition is associated with inflammation, low fetuin-A levels and high mortality in prevalent haemodialysis patients. *J Intern Med* 2008 Mar;263(3):302-12.

- (163) Nawrot TS, Staessen JA, Gardner JP, Aviv A. Telomere length and possible link to X chromosome. *Lancet* 2004 Feb 14;363(9408):507-10.
- (164) Robertson T, Batty GD, Der G, Green MJ, McGlynn LM, McIntyre A, et al. Is telomere length socially patterned? Evidence from the West of Scotland Twenty-07 Study. *PLoS One* 2012;7(7):e41805.
- (165) Sklavounou E, Hay A, Ashraf N, Lamb K, Brown E, Mac IA, et al. The use of telomere biology to identify and develop superior nitronone based anti-oxidants. *Biochem Biophys Res Commun* 2006 Aug 25;347(2):420-7.
- (166) Busuttill RA, Rubio M, Dolle ME, Campisi J, Vijg J. Oxygen accelerates the accumulation of mutations during the senescence and immortalization of murine cells in culture. *Aging Cell* 2003 Dec;2(6):287-94.
- (167) Dickson MA, Hahn WC, Ino Y, Ronfard V, Wu JY, Weinberg RA, et al. Human keratinocytes that express hTERT and also bypass a p16(INK4a)-enforced mechanism that limits life span become immortal yet retain normal growth and differentiation characteristics. *Mol Cell Biol* 2000 Feb;20(4):1436-47.
- (168) Drayton S, Peters G. Immortalisation and transformation revisited. *Curr Opin Genet Dev* 2002 Feb;12(1):98-104.
- (169) Farwell DG, Shera KA, Koop JI, Bonnet GA, Matthews CP, Reuther GW, et al. Genetic and epigenetic changes in human epithelial cells immortalized by telomerase. *Am J Pathol* 2000 May;156(5):1537-47.
- (170) Forsyth NR, Evans AP, Shay JW, Wright WE. Developmental differences in the immortalization of lung fibroblasts by telomerase. *Aging Cell* 2003 Oct;2(5):235-43.
- (171) Jarrard DF, Sarkar S, Shi Y, Yeager TR, Magrane G, Kinoshita H, et al. p16/pRb pathway alterations are required for bypassing senescence in human prostate epithelial cells. *Cancer Res* 1999 Jun 15;59(12):2957-64.
- (172) Jones CJ, Kipling D, Morris M, Hepburn P, Skinner J, Bounacer A, et al. Evidence for a telomere-independent "clock" limiting RAS oncogene-driven proliferation of human thyroid epithelial cells. *Mol Cell Biol* 2000 Aug;20(15):5690-9.
- (173) Kiyono T, Foster SA, Koop JI, McDougall JK, Galloway DA, Klingelutz AJ. Both Rb/p16INK4a inactivation and telomerase activity are required to immortalize human epithelial cells. *Nature* 1998 Nov 5;396(6706):84-8.
- (174) Naka K, Tachibana A, Ikeda K, Motoyama N. Stress-induced premature senescence in hTERT-expressing ataxia telangiectasia fibroblasts. *J Biol Chem* 2004 Jan 16;279(3):2030-7.
- (175) Ramirez RD, Morales CP, Herbert BS, Rohde JM, Passons C, Shay JW, et al. Putative telomere-independent mechanisms of replicative aging reflect inadequate growth conditions. *Genes Dev* 2001 Feb 15;15(4):398-403.

- (176) Ramirez RD, Herbert BS, Vaughan MB, Zou Y, Gandia K, Morales CP, et al. Bypass of telomere-dependent replicative senescence (M1) upon overexpression of Cdk4 in normal human epithelial cells. *Oncogene* 2003 Jan 23;22(3):433-44.
- (177) Robles SJ, Adami GR. Agents that cause DNA double strand breaks lead to p16INK4a enrichment and the premature senescence of normal fibroblasts. *Oncogene* 1998 Mar 5;16(9):1113-23.
- (178) Serrano M, Blasco MA. Putting the stress on senescence. *Curr Opin Cell Biol* 2001 Dec;13(6):748-53.
- (179) Sherr CJ, DePinho RA. Cellular senescence: mitotic clock or culture shock?. *Cell* 2000 Aug 18;102(4):407-10.
- (180) Krishnamurthy J, Ramsey MR, Ligon KL, Torrice C, Koh A, Bonner-Weir S, et al. p16INK4a induces an age-dependent decline in islet regenerative potential. *Nature* 2006 Sep 28;443(7110):453-7.
- (181) Krishnamurthy J, Torrice C, Ramsey MR, Kovalev GI, Al-Regaiey K, Su L, et al. Ink4a/Arf expression is a biomarker of aging. *J Clin Invest* 2004 Nov;114(9):1299-307.
- (182) Liu Y, Sanoff HK, Cho H, Burd CE, Torrice C, Ibrahim JG, et al. Expression of p16(INK4a) in peripheral blood T-cells is a biomarker of human aging. *Aging Cell* 2009 Aug;8(4):439-48.
- (183) Nielsen GP, Stemmer-Rachamimov AO, Shaw J, Roy JE, Koh J, Louis DN. Immunohistochemical survey of p16INK4A expression in normal human adult and infant tissues. *Lab Invest* 1999 Sep;79(9):1137-43.
- (184) Ressler S, Bartkova J, Niederegger H, Bartek J, Scharffetter-Kochanek K, Jansen-Durr P, et al. p16INK4A is a robust in vivo biomarker of cellular aging in human skin. *Aging Cell* 2006 Oct;5(5):379-89.
- (185) Zindy F, Quelle DE, Roussel MF, Sherr CJ. Expression of the p16INK4a tumor suppressor versus other INK4 family members during mouse development and aging. *Oncogene* 1997 Jul 10;15(2):203-11.
- (186) Huschtscha LI, Reddel RR. p16(INK4a) and the control of cellular proliferative life span. *Carcinogenesis* 1999 Jun;20(6):921-6.
- (187) Serrano M, Hannon GJ, Beach D. A new regulatory motif in cell-cycle control causing specific inhibition of cyclin D/CDK4. *Nature* 1993 Dec 16;366(6456):704-7.
- (188) Stott FJ, Bates S, James MC, McConnell BB, Starborg M, Brookes S, et al. The alternative product from the human CDKN2A locus, p14(ARF), participates in a regulatory feedback loop with p53 and MDM2. *EMBO J* 1998 Sep 1;17(17):5001-14.

- (189) Kamb A, Gruis NA, Weaver-Feldhaus J, Liu Q, Harshman K, Tavtigian SV, et al. A cell cycle regulator potentially involved in genesis of many tumor types. *Science* 1994 Apr 15;264(5157):436-40.
- (190) Koh J, Enders GH, Dynlacht BD, Harlow E. Tumour-derived p16 alleles encoding proteins defective in cell-cycle inhibition. *Nature* 1995 Jun 8;375(6531):506-10.
- (191) Lukas J, Parry D, Aagaard L, Mann DJ, Bartkova J, Strauss M, et al. Retinoblastoma-protein-dependent cell-cycle inhibition by the tumour suppressor p16. *Nature* 1995 Jun 8;375(6531):503-6.
- (192) Medema RH, Herrera RE, Lam F, Weinberg RA. Growth suppression by p16ink4 requires functional retinoblastoma protein. *Proc Natl Acad Sci U S A* 1995 Jul 3;92(14):6289-93.
- (193) Serrano M, Gomez-Lahoz E, DePinho RA, Beach D, Bar-Sagi D. Inhibition of ras-induced proliferation and cellular transformation by p16INK4. *Science* 1995 Jan 13;267(5195):249-52.
- (194) Shapiro GI, Park JE, Edwards CD, Mao L, Merlo A, Sidransky D, et al. Multiple mechanisms of p16INK4A inactivation in non-small cell lung cancer cell lines. *Cancer Res* 1995 Dec 15;55(24):6200-9.
- (195) Stone S, Dayananth P, Kamb A. Reversible, p16-mediated cell cycle arrest as protection from chemotherapy. *Cancer Res* 1996 Jul 15;56(14):3199-202.
- (196) Serrano M, Lee H, Chin L, Cordon-Cardo C, Beach D, DePinho RA. Role of the INK4a locus in tumor suppression and cell mortality. *Cell* 1996 Apr 5;85(1):27-37.
- (197) Goldstein AM, Fraser MC, Struewing JP, Hussussian CJ, Ranade K, Zametkin DP, et al. Increased risk of pancreatic cancer in melanoma-prone kindreds with p16INK4 mutations. *N Engl J Med* 1995 Oct 12;333(15):970-4.
- (198) Hussussian CJ, Struewing JP, Goldstein AM, Higgins PA, Ally DS, Sheahan MD, et al. Germline p16 mutations in familial melanoma. *Nat Genet* 1994 Sep;8(1):15-21.
- (199) Kamb A, Shattuck-Eidens D, Eeles R, Liu Q, Gruis NA, Ding W, et al. Analysis of the p16 gene (CDKN2) as a candidate for the chromosome 9p melanoma susceptibility locus. *Nat Genet* 1994 Sep;8(1):23-6.
- (200) Whelan AJ, Bartsch D, Goodfellow PJ. Brief report: a familial syndrome of pancreatic cancer and melanoma with a mutation in the CDKN2 tumor-suppressor gene. *N Engl J Med* 1995 Oct 12;333(15):975-7.
- (201) Reznikoff CA, Yeager TR, Belair CD, Savelieva E, Puthenveetil JA, Stadler WM. Elevated p16 at senescence and loss of p16 at immortalization in human papillomavirus 16 E6, but not E7, transformed human uroepithelial cells. *Cancer Res* 1996 Jul 1;56(13):2886-90.

- (202) Sherr CJ. Cancer cell cycles. *Science* 1996 Dec 6;274(5293):1672-7.
- (203) Clarke AR, Purdie CA, Harrison DJ, Morris RG, Bird CC, Hooper ML, et al. Thymocyte apoptosis induced by p53-dependent and independent pathways. *Nature* 1993 Apr 29;362(6423):849-52.
- (204) Lowe SW, Ruley HE, Jacks T, Housman DE. p53-dependent apoptosis modulates the cytotoxicity of anticancer agents. *Cell* 1993 Sep 24;74(6):957-67.
- (205) el-Deiry WS, Tokino T, Velculescu VE, Levy DB, Parsons R, Trent JM, et al. WAF1, a potential mediator of p53 tumor suppression. *Cell* 1993 Nov 19;75(4):817-25.
- (206) Harper JW, Adami GR, Wei N, Keyomarsi K, Elledge SJ. The p21 Cdk-interacting protein Cip1 is a potent inhibitor of G1 cyclin-dependent kinases. *Cell* 1993 Nov 19;75(4):805-16.
- (207) Xiong Y, Hannon GJ, Zhang H, Casso D, Kobayashi R, Beach D. p21 is a universal inhibitor of cyclin kinases. *Nature* 1993 Dec 16;366(6456):701-4.
- (208) Fairweather DS, Fox M, Margison GP. The in vitro lifespan of MRC-5 cells is shortened by 5-azacytidine-induced demethylation. *Exp Cell Res* 1987 Jan;168(1):153-9.
- (209) Chen Q, Fischer A, Reagan JD, Yan LJ, Ames BN. Oxidative DNA damage and senescence of human diploid fibroblast cells. *Proc Natl Acad Sci U S A* 1995 May 9;92(10):4337-41.
- (210) Fraga CG, Shigenaga MK, Park JW, Degan P, Ames BN. Oxidative damage to DNA during aging: 8-hydroxy-2'-deoxyguanosine in rat organ DNA and urine. *Proc Natl Acad Sci U S A* 1990 Jun;87(12):4533-7.
- (211) Bayreuther K, Rodemann HP, Hommel R, Dittmann K, Albiez M, Francz PI. Human skin fibroblasts in vitro differentiate along a terminal cell lineage. *Proc Natl Acad Sci U S A* 1988 Jul;85(14):5112-6.
- (212) Kumazaki T, Robetorye RS, Robetorye SC, Smith JR. Fibronectin expression increases during in vitro cellular senescence: correlation with increased cell area. *Exp Cell Res* 1991 Jul;195(1):13-9.
- (213) Millis AJ, Hoyle M, McCue HM, Martini H. Differential expression of metalloproteinase and tissue inhibitor of metalloproteinase genes in aged human fibroblasts. *Exp Cell Res* 1992 Aug;201(2):373-9.
- (214) Mitsui Y, Schneider EL. Relationship between cell replication and volume in senescent human diploid fibroblasts. *Mech Ageing Dev* 1976 Jan;5(1):45-56.
- (215) West MD, Pereira-Smith OM, Smith JR. Replicative senescence of human skin fibroblasts correlates with a loss of regulation and overexpression of collagenase activity. *Exp Cell Res* 1989 Sep;184(1):138-47.

- (216) DAVIES DF, SHOCK NW. Age changes in glomerular filtration rate, effective renal plasma flow, and tubular excretory capacity in adult males. *J Clin Invest* 1950 May;29(5):496-507.
- (217) Macia-Nunez. *Physiology of the healthy aging kidney*. 2013. Ref Type: Generic
- (218) Rowe JW, Andres R, Tobin JD, Norris AH, SHOCK NW. The effect of age on creatinine clearance in men: a cross-sectional and longitudinal study. *J Gerontol* 1976 Mar;31(2):155-63.
- (219) Lindeman RD, Tobin J, SHOCK NW. Longitudinal studies on the rate of decline in renal function with age. *J Am Geriatr Soc* 1985 Apr;33(4):278-85.
- (220) Mather KA, Jorm AF, Parslow RA, Christensen H. Is telomere length a biomarker of aging? A review. *J Gerontol A Biol Sci Med Sci* 2011 Feb;66(2):202-13.
- (221) Shiels PG. Improving precision in investigating aging: why telomeres can cause problems. *J Gerontol A Biol Sci Med Sci* 2010 Aug;65(8):789-91.
- (222) Rando TA. Epigenetics and aging. *Exp Gerontol* 2010 Apr;45(4):253-4.
- (223) Cawthon RM. Telomere measurement by quantitative PCR. *Nucleic Acids Res* 2002 May 15;30(10):e47.
- (224) Sanfilippo F, Vaughn WK, Spees EK, Lucas BA. The detrimental effects of delayed graft function in cadaver donor renal transplantation. *Transplantation* 1984 Dec;38(6):643-8.
- (225) Koning OH, Ploeg RJ, van Bockel JH, Groenewegen M, van der Woude FJ, Persijn GG, et al. Risk factors for delayed graft function in cadaveric kidney transplantation: a prospective study of renal function and graft survival after preservation with University of Wisconsin solution in multi-organ donors. European Multicenter Study Group. *Transplantation* 1997 Jun 15;63(11):1620-8.
- (226) Shiels PG, McGlynn LM, MacIntyre A, Johnson PC, Batty GD, Burns H, et al. Accelerated telomere attrition is associated with relative household income, diet and inflammation in the pSoBid cohort. *PLoS One* 2011;6(7):e22521.
- (227) Rao PS, Schaubel DE, Guidinger MK, Andreoni KA, Wolfe RA, Merion RM, et al. A comprehensive risk quantification score for deceased donor kidneys: the kidney donor risk index. *Transplantation* 2009 Jul 27;88(2):231-6.
- (228) Ornish D, Lin J, Daubenmier J, Weidner G, Epel E, Kemp C, et al. Increased telomerase activity and comprehensive lifestyle changes: a pilot study. *Lancet Oncol* 2008 Nov;9(11):1048-57.
- (229) Shiels PG. CDKN2A might be better than telomere length in determining individual health status. *BMJ* 2012;344:e1415.

- (230) Clarke DJ, Payne AP. Neuroanatomical characterization of a new mutant rat with dopamine depletion in the substantia nigra. *Eur J Neurosci* 1994 May 1;6(5):885-8.
- (231) Payne AP, Campbell JM, Russell D, Favor G, Sutcliffe RG, Bennett NK, et al. The AS/AGU rat: a spontaneous model of disruption and degeneration in the nigrostriatal dopaminergic system. *J Anat* 2000 May;196 (Pt 4):629-33.
- (232) Craig NJ, Duran Alonso MB, Hawker KL, Shiels P, Glencorse TA, Campbell JM, et al. A candidate gene for human neurodegenerative disorders: a rat PKC gamma mutation causes a Parkinsonian syndrome. *Nat Neurosci* 2001 Nov;4(11):1061-2.
- (233) Toussaint O, Medrano EE, von ZT. Cellular and molecular mechanisms of stress-induced premature senescence (SIPS) of human diploid fibroblasts and melanocytes. *Exp Gerontol* 2000 Oct;35(8):927-45.
- (234) Carrero JJ, Stenvinkel P, Fellstrom B, Qureshi AR, Lamb K, Heimbürger O, et al. Telomere attrition is associated with inflammation, low fetuin-A levels and high mortality in prevalent haemodialysis patients. *J Intern Med* 2008 Mar;263(3):302-12.
- (235) Joosten SA, van H, V, Nolan CE, Borrias MC, Jardine AG, Shiels PG, et al. Telomere shortening and cellular senescence in a model of chronic renal allograft rejection. *Am J Pathol* 2003 Apr;162(4):1305-12.
- (236) McGlynn LM, Stevenson K, Lamb K, Zino S, Brown M, Prina A, et al. Cellular senescence in pretransplant renal biopsies predicts postoperative organ function. *Aging Cell* 2009 Feb;8(1):45-51.
- (237) Shiels PG, Jardine AG. Dolly, no longer the exception: telomeres and implications for transplantation. *Cloning Stem Cells* 2003;5(2):157-60.
- (238) Craig NJ, Duran Alonso MB, Hawker KL, Shiels P, Glencorse TA, Campbell JM, et al. A candidate gene for human neurodegenerative disorders: a rat PKC gamma mutation causes a Parkinsonian syndrome. *Nat Neurosci* 2001 Nov;4(11):1061-2.
- (239) Goldberg MS, Fleming SM, Palacino JJ, Cepeda C, Lam HA, Bhatnagar A, et al. Parkin-deficient mice exhibit nigrostriatal deficits but not loss of dopaminergic neurons. *J Biol Chem* 2003 Oct 31;278(44):43628-35.
- (240) Goldberg MS, Pisani A, Haburcak M, Vortherms TA, Kitada T, Costa C, et al. Nigrostriatal dopaminergic deficits and hypokinesia caused by inactivation of the familial Parkinsonism-linked gene DJ-1. *Neuron* 2005 Feb 17;45(4):489-96.
- (241) Heid CA, Stevens J, Livak KJ, Williams PM. Real time quantitative PCR. *Genome Res* 1996 Oct;6(10):986-94.
- (242) Kitada T, Pisani A, Karouani M, Haburcak M, Martella G, Tschertner A, et al. Impaired dopamine release and synaptic plasticity in the striatum of parkin-/- mice. *J Neurochem* 2009 Jul;110(2):613-21.

- (243) Sklavounou E, Hay A, Ashraf N, Lamb K, Brown E, Mac IA, et al. The use of telomere biology to identify and develop superior nitrone based anti-oxidants. *Biochem Biophys Res Commun* 2006 Aug 25;347(2):420-7.
- (244) Levey AS. Measurement of renal function in chronic renal disease. *Kidney Int* 1990 Jul;38(1):167-84.
- (245) Stanton BAaBMK. Elements of renal function. In: *Physiology*, edited by R. M. Berne and M. N. Levy. St.Louis, MO: Mosby-Year Book, 1993, p. 719–753. 2012. Ref Type: Generic
- (246) Dowling TC, Frye RF, Fraley DS, Matzke GR. Comparison of iothalamate clearance methods for measuring GFR. *Pharmacotherapy* 1999 Aug;19(8):943-50.
- (247) Finco DR, Duncan JR. Evaluation of blood urea nitrogen and serum creatinine concentrations as indicators of renal dysfunction: a study of 111 cases and a review of related literature. *J Am Vet Med Assoc* 1976 Apr 1;168(7):593-601.
- (248) Beck CL, Pucino F, Carlson JD, Silbergleit IL, Strommen GL, Fenelon JC, et al. Evaluation of creatinine clearance estimation in an elderly male population. *Pharmacotherapy* 1988;8(3):183-8.
- (249) Freysz M, Lafleur P, Dupont G, Guillard JC, d'Athis P, Escousse A, et al. Comparison of creatinine and inulin clearances in multiple trauma. *Biomed Pharmacother* 1990;44(3):175-80.
- (250) Malmrose LC, Gray SL, Pieper CF, Blazer DG, Rowe JW, Seeman TE, et al. Measured versus estimated creatinine clearance in a high-functioning elderly sample: MacArthur Foundation Study of Successful Aging. *J Am Geriatr Soc* 1993 Jul;41(7):715-21.
- (251) Mohler JL, Ellison MF, Flanigan RC. Creatinine clearance prediction in spinal cord injury patients: comparison of 6 prediction equations. *J Urol* 1988 Apr;139(4):706-9.
- (252) Takabatake T, Ohta H, Ishida Y, Hara H, Ushioji Y, Hattori N. Low serum creatinine levels in severe hepatic disease. *Arch Intern Med* 1988 Jun;148(6):1313-5.
- (253) Walser M, Drew HH, LaFrance ND. Creatinine measurements often yielded false estimates of progression in chronic renal failure. *Kidney Int* 1988 Sep;34(3):412-8.
- (254) Ross EA, Wilkinson A, Hawkins RA, Danovitch GM. The plasma creatinine concentration is not an accurate reflection of the glomerular filtration rate in stable renal transplant patients receiving cyclosporine. *Am J Kidney Dis* 1987 Aug;10(2):113-7.
- (255) Kasiske BL, Vazquez MA, Harmon WE, Brown RS, Danovitch GM, Gaston RS, et al. Recommendations for the outpatient surveillance of renal transplant

- recipients. American Society of Transplantation. *J Am Soc Nephrol* 2000 Oct;11 Suppl 15:S1-86.
- (256) Nankivell BJ, Gruenewald SM, Allen RD, Chapman JR. Predicting glomerular filtration rate after kidney transplantation. *Transplantation* 1995 Jun 27;59(12):1683-9.
- (257) Gaspari F, Ferrari S, Stucchi N, Centemeri E, Carrara F, Pellegrino M, et al. Performance of different prediction equations for estimating renal function in kidney transplantation. *Am J Transplant* 2004 Nov;4(11):1826-35.
- (258) Roos JF, Doust J, Tett SE, Kirkpatrick CM. Diagnostic accuracy of cystatin C compared to serum creatinine for the estimation of renal dysfunction in adults and children--a meta-analysis. *Clin Biochem* 2007 Mar;40(5-6):383-91.
- (259) Dharnidharka VR, Kwon C, Stevens G. Serum cystatin C is superior to serum creatinine as a marker of kidney function: a meta-analysis. *Am J Kidney Dis* 2002 Aug;40(2):221-6.
- (260) Lorenz JN, Gruenstein E. A simple, nonradioactive method for evaluating single-nephron filtration rate using FITC-inulin. *Am J Physiol* 1999 Jan;276(1 Pt 2):F172-F177.
- (261) Qi Z, Whitt I, Mehta A, Jin J, Zhao M, Harris RC, et al. Serial determination of glomerular filtration rate in conscious mice using FITC-inulin clearance. *Am J Physiol Renal Physiol* 2004 Mar;286(3):F590-F596.
- (262) Kasiske BL and Keane WF. *Laboratory Assessment of Renal Disease: Clearance, Urinalysis and Renal Biopsy*. Saunders; 1996.
- (263) Meneton P, Ichikawa I, Inagami T, Schnermann J. Renal physiology of the mouse. *Am J Physiol Renal Physiol* 2000 Mar;278(3):F339-F351.
- (264) Rule AD, Bergstralh EJ, Slezak JM, Bergert J, Larson TS. Glomerular filtration rate estimated by cystatin C among different clinical presentations. *Kidney Int* 2006 Jan;69(2):399-405.
- (265) Knight EL, Verhave JC, Spiegelman D, Hillege HL, de ZD, Curhan GC, et al. Factors influencing serum cystatin C levels other than renal function and the impact on renal function measurement. *Kidney Int* 2004 Apr;65(4):1416-21.
- (266) Stevens LA, Schmid CH, Greene T, Li L, Beck GJ, Joffe MM, et al. Factors other than glomerular filtration rate affect serum cystatin C levels. *Kidney Int* 2009 Mar;75(6):652-60.
- (267) McIntosh JF, Moller E, Van Slyke DD. STUDIES OF UREA EXCRETION. III: The Influence of Body Size on Urea Output. *J Clin Invest* 1928 Dec;6(3):467-83.
- (268) Saxen L, Lehtonen E. Embryonic kidney in organ culture. *Differentiation* 1987;36(1):2-11.

- (269) Livingston BT, Wilt FH. Phorbol esters alter cell fate during development of sea urchin embryos. *J Cell Biol* 1992 Dec;119(6):1641-8.
- (270) Serlachius E, Svennilson J, Schalling M, Aperia A. Protein kinase C in the developing kidney: isoform expression and effects of ceramide and PKC inhibitors. *Kidney Int* 1997 Oct;52(4):901-10.
- (271) Ostlund E, Mendez CF, Jacobsson G, Fryckstedt J, Meister B, Aperia A. Expression of protein kinase C isoforms in renal tissue. *Kidney Int* 1995 Mar;47(3):766-73.
- (272) Musashi M, Ota S, Shiroshita N. The role of protein kinase C isoforms in cell proliferation and apoptosis. *Int J Hematol* 2000 Jul;72(1):12-9.
- (273) Meijer AJ, Lamers WH, Chamuleau RA. Nitrogen metabolism and ornithine cycle function. *Physiol Rev* 1990 Jul;70(3):701-48.
- (274) Nielsen S, DiGiovanni SR, Christensen EI, Knepper MA, Harris HW. Cellular and subcellular immunolocalization of vasopressin-regulated water channel in rat kidney. *Proc Natl Acad Sci U S A* 1993 Dec 15;90(24):11663-7.
- (275) Schmidt-Nielsen B, Barrett JM, Graves B, Crossley B. Physiological and morphological responses of the rat kidney to reduced dietary protein. *Am J Physiol* 1985 Jan;248(1 Pt 2):F31-F42.
- (276) Knepper MA, Danielson RA, Saidel GM, Johnston KH. Effects of dietary protein restriction and glucocorticoid administration on urea excretion in rats. *Kidney Int* 1975 Nov;8(5):303-15.
- (277) Schmidt-Nielsen B. Urea excretion in mammals. *Physiol Rev* 1958 Apr;38(2):139-68.
- (278) Lassiter WE, Mylle M, Gottschalk CW. Micropuncture study of urea transport in rat renal medulla. *Am J Physiol* 1966 May;210(5):965-70.
- (279) Isozaki T, Verlander JW, Sands JM. Low protein diet alters urea transport and cell structure in rat initial inner medullary collecting duct. *J Clin Invest* 1993 Nov;92(5):2448-57.
- (280) Ullrich KJ, Rumrich G, Schmidt-Nielsen B. Urea transport in the collecting duct of rats on normal and low protein diet. *Pflugers Arch Gesamte Physiol Menschen Tiere* 1967;295(2):147-56.
- (281) Isozaki T, Gillin AG, Swanson CE, Sands JM. Protein restriction sequentially induces new urea transport processes in rat initial IMCD. *Am J Physiol* 1994 May;266(5 Pt 2):F756-F761.
- (282) Sands JM, Nonoguchi H, Knepper MA. Vasopressin effects on urea and H₂O transport in inner medullary collecting duct subsegments. *Am J Physiol* 1987 Nov;253(5 Pt 2):F823-F832.

- (283) Gamba G, Miyanoshita A, Lombardi M, Lytton J, Lee WS, Hediger MA, et al. Molecular cloning, primary structure, and characterization of two members of the mammalian electroneutral sodium-(potassium)-chloride cotransporter family expressed in kidney. *J Biol Chem* 1994 Jul 1;269(26):17713-22.
- (284) Sands JM, Kokko JP. Countercurrent system. *Kidney Int* 1990 Oct;38(4):695-9.
- (285) Chou CL, Knepper MA. Inhibition of urea transport in inner medullary collecting duct by phloretin and urea analogues. *Am J Physiol* 1989 Sep;257(3 Pt 2):F359-F365.
- (286) Pallone TL, Work J, Myers RL, Jamison RL. Transport of sodium and urea in outer medullary descending vasa recta. *J Clin Invest* 1994 Jan;93(1):212-22.
- (287) Pallone TL. Characterization of the urea transporter in outer medullary descending vasa recta. *Am J Physiol* 1994 Jul;267(1 Pt 2):R260-R267.
- (288) Fenton RA, Knepper MA. Urea and renal function in the 21st century: insights from knockout mice. *J Am Soc Nephrol* 2007 Mar;18(3):679-88.
- (289) Gillin AG, Star RA, Sands JM. Osmolarity-stimulated urea transport in rat terminal IMCD: role of intracellular calcium. *Am J Physiol* 1993 Aug;265(2 Pt 2):F272-F277.
- (290) Kato A, Klein JD, Zhang C, Sands JM. Angiotensin II increases vasopressin-stimulated facilitated urea permeability in rat terminal IMCDs. *Am J Physiol Renal Physiol* 2000 Nov;279(5):F835-F840.
- (291) Star RA, Nonoguchi H, Balaban R, Knepper MA. Calcium and cyclic adenosine monophosphate as second messengers for vasopressin in the rat inner medullary collecting duct. *J Clin Invest* 1988 Jun;81(6):1879-88.
- (292) Hu MC, Bankir L, Michelet S, Rousselet G, Trinh-Trang-Tan MM. Massive reduction of urea transporters in remnant kidney and brain of uremic rats. *Kidney Int* 2000 Sep;58(3):1202-10.
- (293) Timmer RT, Klein JD, Bagnasco SM, Doran JJ, Verlander JW, Gunn RB, et al. Localization of the urea transporter UT-B protein in human and rat erythrocytes and tissues. *Am J Physiol Cell Physiol* 2001 Oct;281(4):C1318-C1325.
- (294) Xu Y, Olives B, Bailly P, Fischer E, Ripoche P, Ronco P, et al. Endothelial cells of the kidney vasa recta express the urea transporter HUT11. *Kidney Int* 1997 Jan;51(1):138-46.
- (295) Edwards A, Pallone TL. Facilitated transport in vasa recta: theoretical effects on solute exchange in the medullary microcirculation. *Am J Physiol* 1997 Apr;272(4 Pt 2):F505-F514.
- (296) Edwards A, Pallone TL. A multiunit model of solute and water removal by inner medullary vasa recta. *Am J Physiol* 1998 Apr;274(4 Pt 2):H1202-H1210.

- (297) Sands JM, Gargus JJ, Frohlich O, Gunn RB, Kokko JP. Urinary concentrating ability in patients with Jk(a-b-) blood type who lack carrier-mediated urea transport. *J Am Soc Nephrol* 1992 Jun;2(12):1689-96.
- (298) Macey RI, Yousef LW. Osmotic stability of red cells in renal circulation requires rapid urea transport. *Am J Physiol* 1988 May;254(5 Pt 1):C669-C674.
- (299) Ogawa S, Gerlach H, Esposito C, Pasagian-Macaulay A, Brett J, Stern D. Hypoxia modulates the barrier and coagulant function of cultured bovine endothelium. Increased monolayer permeability and induction of procoagulant properties. *J Clin Invest* 1990 Apr;85(4):1090-8.
- (300) Ogawa S, Koga S, Kuwabara K, Brett J, Morrow B, Morris SA, et al. Hypoxia-induced increased permeability of endothelial monolayers occurs through lowering of cellular cAMP levels. *Am J Physiol* 1992 Mar;262(3 Pt 1):C546-C554.
- (301) Hotchkiss RS, Strasser A, McDunn JE, Swanson PE. Cell death. *N Engl J Med* 2009 Oct 15;361(16):1570-83.
- (302) Eltzschig HK, Carmeliet P. Hypoxia and inflammation. *N Engl J Med* 2011 Feb 17;364(7):656-65.
- (303) Carroll MC, Holers VM. Innate autoimmunity. *Adv Immunol* 2005;86:137-57.
- (304) Chen GY, Nunez G. Sterile inflammation: sensing and reacting to damage. *Nat Rev Immunol* 2010 Dec;10(12):826-37.
- (305) Campisi J, d'Adda di FF. Cellular senescence: when bad things happen to good cells. *Nat Rev Mol Cell Biol* 2007 Sep;8(9):729-40.
- (306) Kurz T, Terman A, Brunk UT. Autophagy, ageing and apoptosis: the role of oxidative stress and lysosomal iron. *Arch Biochem Biophys* 2007 Jun 15;462(2):220-30.
- (307) Itahana K, Campisi J, Dimri GP. Methods to detect biomarkers of cellular senescence: the senescence-associated beta-galactosidase assay. *Methods Mol Biol* 2007;371:21-31.
- (308) van HD, den Reijer PM, Westendorp RG. Ageing or cancer: a review on the role of caretakers and gatekeepers. *Eur J Cancer* 2007 Oct;43(15):2144-52.
- (309) Vaziri H, Benchimol S. Alternative pathways for the extension of cellular life span: inactivation of p53/pRb and expression of telomerase. *Oncogene* 1999 Dec 13;18(53):7676-80.
- (310) Helmbold H, Deppert W, Bohn W. Regulation of cellular senescence by Rb2/p130. *Oncogene* 2006 Aug 28;25(38):5257-62.

- (311) Maddika S, Ande SR, Panigrahi S, Paranjothy T, Weglarczyk K, Zuse A, et al. Cell survival, cell death and cell cycle pathways are interconnected: implications for cancer therapy. *Drug Resist Updat* 2007 Feb;10(1-2):13-29.
- (312) Kapic A, Helmbold H, Reimer R, Klotzsche O, Deppert W, Bohn W. Cooperation between p53 and p130(Rb2) in induction of cellular senescence. *Cell Death Differ* 2006 Feb;13(2):324-34.
- (313) Harley CB, Futcher AB, Greider CW. Telomeres shorten during ageing of human fibroblasts. *Nature* 1990 May 31;345(6274):458-60.
- (314) Fairweather DS, Fox M, Margison GP. The in vitro lifespan of MRC-5 cells is shortened by 5-azacytidine-induced demethylation. *Exp Cell Res* 1987 Jan;168(1):153-9.
- (315) Chen Q, Fischer A, Reagan JD, Yan LJ, Ames BN. Oxidative DNA damage and senescence of human diploid fibroblast cells. *Proc Natl Acad Sci U S A* 1995 May 9;92(10):4337-41.
- (316) Fraga CG, Shigenaga MK, Park JW, Degan P, Ames BN. Oxidative damage to DNA during aging: 8-hydroxy-2'-deoxyguanosine in rat organ DNA and urine. *Proc Natl Acad Sci U S A* 1990 Jun;87(12):4533-7.
- (317) Stein GH, Dulic V. Origins of G1 arrest in senescent human fibroblasts. *Bioessays* 1995 Jun;17(6):537-43.
- (318) Alcorta DA, Xiong Y, Phelps D, Hannon G, Beach D, Barrett JC. Involvement of the cyclin-dependent kinase inhibitor p16 (INK4a) in replicative senescence of normal human fibroblasts. *Proc Natl Acad Sci U S A* 1996 Nov 26;93(24):13742-7.
- (319) Bayreuther K, Rodemann HP, Hommel R, Dittmann K, Albiez M, Francz PI. Human skin fibroblasts in vitro differentiate along a terminal cell lineage. *Proc Natl Acad Sci U S A* 1988 Jul;85(14):5112-6.
- (320) Dimri GP, Lee X, Basile G, Acosta M, Scott G, Roskelley C, et al. A biomarker that identifies senescent human cells in culture and in aging skin in vivo. *Proc Natl Acad Sci U S A* 1995 Sep 26;92(20):9363-7.
- (321) Hara E, Smith R, Parry D, Tahara H, Stone S, Peters G. Regulation of p16CDKN2 expression and its implications for cell immortalization and senescence. *Mol Cell Biol* 1996 Mar;16(3):859-67.
- (322) Kumazaki T, Robetorye RS, Robetorye SC, Smith JR. Fibronectin expression increases during in vitro cellular senescence: correlation with increased cell area. *Exp Cell Res* 1991 Jul;195(1):13-9.
- (323) Millis AJ, Hoyle M, McCue HM, Martini H. Differential expression of metalloproteinase and tissue inhibitor of metalloproteinase genes in aged human fibroblasts. *Exp Cell Res* 1992 Aug;201(2):373-9.

- (324) Mitsui Y, Schneider EL. Relationship between cell replication and volume in senescent human diploid fibroblasts. *Mech Ageing Dev* 1976 Jan;5(1):45-56.
- (325) West MD, Pereira-Smith OM, Smith JR. Replicative senescence of human skin fibroblasts correlates with a loss of regulation and overexpression of collagenase activity. *Exp Cell Res* 1989 Sep;184(1):138-47.
- (326) Gavrieli Y, Sherman Y, Ben-Sasson SA. Identification of programmed cell death in situ via specific labeling of nuclear DNA fragmentation. *J Cell Biol* 1992 Nov;119(3):493-501.
- (327) Arends MJ, Morris RG, Wyllie AH. Apoptosis. The role of the endonuclease. *Am J Pathol* 1990 Mar;136(3):593-608.
- (328) Bortner CD, Oldenburg NB, Cidlowski JA. The role of DNA fragmentation in apoptosis. *Trends Cell Biol* 1995 Jan;5(1):21-6.
- (329) Kerr JF, Wyllie AH, Currie AR. Apoptosis: a basic biological phenomenon with wide-ranging implications in tissue kinetics. *Br J Cancer* 1972 Aug;26(4):239-57.
- (330) Loo DT, Rillema JR. Measurement of cell death. *Methods Cell Biol* 1998;57:251-64.
- (331) Wyllie AH, Kerr JF, Currie AR. Cell death: the significance of apoptosis. *Int Rev Cytol* 1980;68:251-306.
- (332) Brunk U, Terman. *Understanding the Process of Aging: The Roles of Mitochondria, Free Radicals and Antioxidants*. 229-249. 1999. Ref Type: Generic
- (333) Yin D. Biochemical basis of lipofuscin, ceroid, and age pigment-like fluorophores. *Free Radic Biol Med* 1996;21(6):871-88.
- (334) Sawicka M, Pawlikowski J, Wilson S, Ferdinando D, Wu H, Adams PD, et al. The specificity and patterns of staining in human cells and tissues of p16INK4a antibodies demonstrate variant antigen binding. *PLoS One* 2013;8(1):e53313.
- (335) Evangelou K, Bramis J, Peros I, Zacharatos P, Dasiou-Plakida D, Kalogeropoulos N, et al. Electron microscopy evidence that cytoplasmic localization of the p16(INK4A) "nuclear" cyclin-dependent kinase inhibitor (CKI) in tumor cells is specific and not an artifact. A study in non-small cell lung carcinomas. *Biotech Histochem* 2004 Feb;79(1):5-10.
- (336) Di VA, Perdelli L, Banelli B, Salvi S, Casciano I, Gelvi I, et al. p16(INK4a) promoter methylation and protein expression in breast fibroadenoma and carcinoma. *Int J Cancer* 2005 Apr 10;114(3):414-21.
- (337) Milde-Langosch K, Bamberger AM, Rieck G, Kelp B, Loning T. Overexpression of the p16 cell cycle inhibitor in breast cancer is associated with a more malignant phenotype. *Breast Cancer Res Treat* 2001 May;67(1):61-70.

- (338) Dai CY, Furth EE, Mick R, Koh J, Takayama T, Niitsu Y, et al. p16(INK4a) expression begins early in human colon neoplasia and correlates inversely with markers of cell proliferation. *Gastroenterology* 2000 Oct;119(4):929-42.
- (339) Zhao P, Mao X, Talbot IC. Aberrant cytological localization of p16 and CDK4 in colorectal epithelia in the normal adenoma carcinoma sequence. *World J Gastroenterol* 2006 Oct 21;12(39):6391-6.
- (340) Beasley MB, Lantuejoul S, Abbondanzo S, Chu WS, Hasleton PS, Travis WD, et al. The P16/cyclin D1/Rb pathway in neuroendocrine tumors of the lung. *Hum Pathol* 2003 Feb;34(2):136-42.
- (341) Arifin MT, Hama S, Kajiwara Y, Sugiyama K, Saito T, Matsuura S, et al. Cytoplasmic, but not nuclear, p16 expression may signal poor prognosis in high-grade astrocytomas. *J Neurooncol* 2006 May;77(3):273-7.
- (342) O'Neill CJ, McBride HA, Connolly LE, McCluggage WG. Uterine leiomyosarcomas are characterized by high p16, p53 and MIB1 expression in comparison with usual leiomyomas, leiomyoma variants and smooth muscle tumours of uncertain malignant potential. *Histopathology* 2007 Jun;50(7):851-8.
- (343) Haller F, Agaimy A, Cameron S, Beyer M, Gunawan B, Happel N, et al. Expression of p16INK4A in gastrointestinal stromal tumours (GISTs): two different forms exist that independently correlate with poor prognosis. *Histopathology* 2010 Feb;56(3):305-18.
- (344) Nilsson K, Landberg G. Subcellular localization, modification and protein complex formation of the cdk-inhibitor p16 in Rb-functional and Rb-inactivated tumor cells. *Int J Cancer* 2006 Mar 1;118(5):1120-5.
- (345) Gartel AL, Tyner AL. The role of the cyclin-dependent kinase inhibitor p21 in apoptosis. *Mol Cancer Ther* 2002 Jun;1(8):639-49.
- (346) Migliaccio E, Giorgio M, Mele S, Pelicci G, Reboldi P, Pandolfi PP, et al. The p66shc adaptor protein controls oxidative stress response and life span in mammals. *Nature* 1999 Nov 18;402(6759):309-13.
- (347) Kim DK, Cho ES, Lee SJ, Um HD. Constitutive hyperexpression of p21(WAF1) in human U266 myeloma cells blocks the lethal signaling induced by oxidative stress but not by Fas. *Biochem Biophys Res Commun* 2001 Nov 23;289(1):34-8.
- (348) Yan Q, Sage EH. Transforming growth factor-beta1 induces apoptotic cell death in cultured retinal endothelial cells but not pericytes: association with decreased expression of p21waf1/cip1. *J Cell Biochem* 1998 Jul 1;70(1):70-83.
- (349) Javelaud D, Wietzerbin J, Delattre O, Besancon F. Induction of p21Waf1/Cip1 by TNFalpha requires NF-kappaB activity and antagonizes apoptosis in Ewing tumor cells. *Oncogene* 2000 Jan 6;19(1):61-8.

- (350) Fotedar R, Brickner H, Saadatmandi N, Rousselle T, Diederich L, Munshi A, et al. Effect of p21waf1/cip1 transgene on radiation induced apoptosis in T cells. *Oncogene* 1999 Jun 17;18(24):3652-8.
- (351) Shibata MA, Yoshidome K, Shibata E, Jorcyk CL, Green JE. Suppression of mammary carcinoma growth in vitro and in vivo by inducible expression of the Cdk inhibitor p21. *Cancer Gene Ther* 2001 Jan;8(1):23-35.
- (352) Kondo S, Barna BP, Kondo Y, Tanaka Y, Casey G, Liu J, et al. WAF1/CIP1 increases the susceptibility of p53 non-functional malignant glioma cells to cisplatin-induced apoptosis. *Oncogene* 1996 Sep 19;13(6):1279-85.
- (353) Lincet H, Poulain L, Remy JS, Deslandes E, Duigou F, Gauduchon P, et al. The p21(cip1/waf1) cyclin-dependent kinase inhibitor enhances the cytotoxic effect of cisplatin in human ovarian carcinoma cells. *Cancer Lett* 2000 Dec 8;161(1):17-26.
- (354) Jerkic M, Miloradovic Z, Jovovic D, Mihailovic-Stanojevic N, Elena JV, Nastic-Miric D, et al. Relative roles of endothelin-1 and angiotensin II in experimental post-ischaemic acute renal failure. *Nephrol Dial Transplant* 2004 Jan;19(1):83-94.
- (355) Chatterjee PK, Chatterjee BE, Pedersen H, Sivarajah A, McDonald MC, Mota-Filipe H, et al. 5-Aminoisoquinolinone reduces renal injury and dysfunction caused by experimental ischemia/reperfusion. *Kidney Int* 2004 Feb;65(2):499-509.
- (356) Hoglen NC, Chen LS, Fisher CD, Hirakawa BP, Groessl T, Contreras PC. Characterization of IDN-6556 (3-[2-(2-tert-butyl-phenylaminooxalyl)-amino]-propionylamino]-4-oxo-5-(2,3,5,6-tetrafluoro-phenoxy)-pentanoic acid): a liver-targeted caspase inhibitor. *J Pharmacol Exp Ther* 2004 May;309(2):634-40.
- (357) de VB, Kohl J, Leclercq WK, Wolfs TG, van Bijnen AA, Heeringa P, et al. Complement factor C5a mediates renal ischemia-reperfusion injury independent from neutrophils. *J Immunol* 2003 Apr 1;170(7):3883-9.
- (358) de VB, Matthijsen RA, Wolfs TG, van Bijnen AA, Heeringa P, Buurman WA. Inhibition of complement factor C5 protects against renal ischemia-reperfusion injury: inhibition of late apoptosis and inflammation. *Transplantation* 2003 Feb 15;75(3):375-82.
- (359) Deng J, Kohda Y, Chiao H, Wang Y, Hu X, Hewitt SM, et al. Interleukin-10 inhibits ischemic and cisplatin-induced acute renal injury. *Kidney Int* 2001 Dec;60(6):2118-28.
- (360) Patel NS, Chatterjee PK, di PR, Mazzon E, Britti D, De SA, et al. Endogenous interleukin-6 enhances the renal injury, dysfunction, and inflammation caused by ischemia/reperfusion. *J Pharmacol Exp Ther* 2005 Mar;312(3):1170-8.

- (361) Gong H, Wang W, Kwon TH, Jonassen T, Li C, Ring T, et al. EPO and alpha-MSH prevent ischemia/reperfusion-induced down-regulation of AQPs and sodium transporters in rat kidney. *Kidney Int* 2004 Aug;66(2):683-95.
- (362) Vezina C, Kudelski A, Sehgal SN. Rapamycin (AY-22,989), a new antifungal antibiotic. I. Taxonomy of the producing streptomycete and isolation of the active principle. *J Antibiot (Tokyo)* 1975 Oct;28(10):721-6.
- (363) Magnuson B, Ekim B, Fingar DC. Regulation and function of ribosomal protein S6 kinase (S6K) within mTOR signalling networks. *Biochem J* 2012 Jan 1;441(1):1-21.
- (364) Dobashi Y, Watanabe Y, Miwa C, Suzuki S, Koyama S. Mammalian target of rapamycin: a central node of complex signaling cascades. *Int J Clin Exp Pathol* 2011 Jun 20;4(5):476-95.
- (365) Flechner SM, Kobashigawa J, Klintmalm G. Calcineurin inhibitor-sparing regimens in solid organ transplantation: focus on improving renal function and nephrotoxicity. *Clin Transplant* 2008 Jan;22(1):1-15.
- (366) Helal I, Chan L. Steroid and calcineurin inhibitor-sparing protocols in kidney transplantation. *Transplant Proc* 2011 Mar;43(2):472-7.
- (367) Sharif A, Shabir S, Chand S, Cockwell P, Ball S, Borrows R. Meta-analysis of calcineurin-inhibitor-sparing regimens in kidney transplantation. *J Am Soc Nephrol* 2011 Nov;22(11):2107-18.
- (368) Cho D, Signoretti S, Regan M, Mier JW, Atkins MB. The role of mammalian target of rapamycin inhibitors in the treatment of advanced renal cancer. *Clin Cancer Res* 2007 Jan 15;13(2 Pt 2):758s-63s.
- (369) Shin LJ, Seok KH, Bok KY, Cheol LM, Soo PC. Expression of PTEN in renal cell carcinoma and its relation to tumor behavior and growth. *J Surg Oncol* 2003 Nov;84(3):166-72.
- (370) Lorber MI, Basadonna GP, Friedman AL, Lorber KM, Bia MJ, Formica R, et al. The evolving role of tor inhibitors for individualizing posttransplant immunosuppression. *Transplant Proc* 2001 Nov;33(7-8):3075-7.
- (371) McTaggart RA, Gottlieb D, Brooks J, Bacchetti P, Roberts JP, Tomlanovich S, et al. Sirolimus prolongs recovery from delayed graft function after cadaveric renal transplantation. *Am J Transplant* 2003 Apr;3(4):416-23.
- (372) Uhlmann D, Weber T, Ludwig S, Ludwig B, Bartels M, Hauss J, et al. Long-term outcome of conversion to sirolimus monotherapy after liver transplant. *Exp Clin Transplant* 2012 Feb;10(1):30-8.
- (373) Cardinal H, Froidure A, Dandavino R, Daloze P, Hebert MJ, Colette S, et al. Conversion from calcineurin inhibitors to sirolimus in kidney transplant recipients: a retrospective cohort study. *Transplant Proc* 2009 Oct;41(8):3308-10.

- (374) Lieberthal W, Fuhro R, Andry CC, Rennke H, Abernathy VE, Koh JS, et al. Rapamycin impairs recovery from acute renal failure: role of cell-cycle arrest and apoptosis of tubular cells. *Am J Physiol Renal Physiol* 2001 Oct;281(4):F693-F706.
- (375) Smith KD, Wrenshall LE, Nicosia RF, Pichler R, Marsh CL, Alpers CE, et al. Delayed graft function and cast nephropathy associated with tacrolimus plus rapamycin use. *J Am Soc Nephrol* 2003 Apr;14(4):1037-45.
- (376) Fervenza FC, Fitzpatrick PM, Mertz J, Erickson SB, Liggett S, Popham S, et al. Acute rapamycin nephrotoxicity in native kidneys of patients with chronic glomerulopathies. *Nephrol Dial Transplant* 2004 May;19(5):1288-92.
- (377) Marx SO, Jayaraman T, Go LO, Marks AR. Rapamycin-FKBP inhibits cell cycle regulators of proliferation in vascular smooth muscle cells. *Circ Res* 1995 Mar;76(3):412-7.
- (378) Inman SR, Davis NA, Olson KM, Lukaszek VA, McKinley MR, Seminerio JL. Rapamycin preserves renal function compared with cyclosporine A after ischemia/reperfusion injury. *Urology* 2003 Oct;62(4):750-4.
- (379) Khan S, Salloum F, Das A, Xi L, Vetrovec GW, Kukreja RC. Rapamycin confers preconditioning-like protection against ischemia-reperfusion injury in isolated mouse heart and cardiomyocytes. *J Mol Cell Cardiol* 2006 Aug;41(2):256-64.
- (380) Ramadan R, Faour D, Awad H, Khateeb E, Cohen R, Yahia A, et al. Early treatment with everolimus exerts nephroprotective effect in rats with adriamycin-induced nephrotic syndrome. *Nephrol Dial Transplant* 2012 Jun;27(6):2231-41.
- (381) Alcorta DA, Xiong Y, Phelps D, Hannon G, Beach D, Barrett JC. Involvement of the cyclin-dependent kinase inhibitor p16 (INK4a) in replicative senescence of normal human fibroblasts. *Proc Natl Acad Sci U S A* 1996 Nov 26;93(24):13742-7.
- (382) Hara E, Smith R, Parry D, Tahara H, Stone S, Peters G. Regulation of p16CDKN2 expression and its implications for cell immortalization and senescence. *Mol Cell Biol* 1996 Mar;16(3):859-67.
- (383) Babinska A, Markell MS, Salifu MO, Akoad M, Ehrlich YH, Kornecki E. Enhancement of human platelet aggregation and secretion induced by rapamycin. *Nephrol Dial Transplant* 1998 Dec;13(12):3153-9.
- (384) Maxwell F, McGlynn LM, Muir HC, Talwar D, Benzeval M, Robertson T, et al. Telomere attrition and decreased fetuin-A levels indicate accelerated biological aging and are implicated in the pathogenesis of colorectal cancer. *Clin Cancer Res* 2011 Sep 1;17(17):5573-81.
- (385) Oeseburg H, de Boer RA, van Gilst WH, van der Harst P. Telomere biology in healthy aging and disease. *Pflugers Arch* 2010 Jan;459(2):259-68.

- (386) Fitzpatrick AL, Kronmal RA, Kimura M, Gardner JP, Psaty BM, Jenny NS, et al. Leukocyte telomere length and mortality in the Cardiovascular Health Study. *J Gerontol A Biol Sci Med Sci* 2011 Apr;66(4):421-9.
- (387) Hou L, Zhang X, Gawron AJ, Liu J. Surrogate tissue telomere length and cancer risk: shorter or longer?. *Cancer Lett* 2012 Jun 28;319(2):130-5.
- (388) Hodes RJ, Hathcock KS, Weng NP. Telomeres in T and B cells. *Nat Rev Immunol* 2002 Sep;2(9):699-706.
- (389) Al-Moundhri MS, Al-Nabhani M, Tarantini L, Baccarelli A, Rusiecki JA. The prognostic significance of whole blood global and specific DNA methylation levels in gastric adenocarcinoma. *PLoS One* 2010;5(12):e15585.

List of Publications

❖ Book Chapter

1. “Novel Cell Therapies in Transplantation”

Shiels PG, Stevenson K, Gingell-Littlejohn M, Clancy M

Abdominal Organ Transplantation – State of the Art

Editors: Mamode and Kandaswamy

Publisher: Wiley Blackwell

ISBN: 978-1-4443-3432-6

❖ Papers

2. **Pre-transplant CDKN2A Expression in Kidney Biopsies Predicts Renal Function and Is a Future Component of Donor Scoring Criteria**

Marc Gingell Littlejohn, Dagmara McGuinness, Karen Stevenson, David Kingsmore, Marc Clancy, C Koppelstaetter and Paul G Shiels.

PLoS ONE 8(7): e68133. doi:10.1371/journal.pone.0068133

❖ Abstracts

3. **Allograft Biological Age Is Prognostic For Renal Function Post Transplant**

M Gingell-Littlejohn, L McGlynn, MJ Clancy, D Kingsmore, P Shiels.

American Journal of Transplantation. April 2010; Vol 10 (Supp): 441

4. **Donor Biological Age is a Key Predictor of Renal Function post Transplant**

L McGlynn, M Gingell-Littlejohn, MJ Clancy, D Kingsmore, P Shiels.

British Transplant Society. 13th Annual Congress. Abstract Book. March 2010

5. **Pre-transplant markers for post-transplant kidney function based on transcript isoforms of bioageing marker CDKN2**
 Dagmara McGuinness, Liane McGlynn, Marc Gingell-Littlejohn, Marc Clancy and Paul G. Shiels
Kidney International Journal - World Congress of Nephrology 2011, British Transplant Society. 14th Annual Congress. Abstract Book. March 2011

6. **Donor Telomere Length in Pre-implantation Biopsies Is Predictive for Renal Allograft Function at Six Months Post-transplant**
Marc Gingell-Littlejohn, Dagmara McGuinness, Liane M McGlynn, Colin Geddes, David Kingsmore, Marc Clancy, Christian Koppelstaetter and Paul G Shiels
British Transplant Society. 14th Annual Congress. Abstract Book. March 2011

7. **Telomere Length is Associated with Renal Allograft Function in Kidney Transplantation**
Marc Gingell-Littlejohn, Dagmara McGuinness, Liane M McGlynn, David Kingsmore, Marc Clancy, Christian Koppelstaetter, Gert Mayer and Paul G Shiels
American Journal of Transplantation. Vol 11 (Suppl). April 2011

8. **Renal Allograft Function at Six Months Post Transplant Is Associated with Donor Chromosomal Telomere Length**
M Gingell-Littlejohn, D McGuinness, L M McGlynn, DB Kingsmore, M Clancy, C Koppelstaetter, G Mayer and PG Shiels
Transplant International. Vol 24; (Supp 2): 114. Sept 2011.

9. **MicroRNA Regulation of Cellular Bioage Provides a Novel Pre-Transplant Prognostic and Predictive Assessment of Post Transplant Allograft Function**
 D McGuinness, M Gingell-Littlejohn, K Stevenson, D Kingsmore, M Clancy, P G Shiels
Transplant International. Vol 24; (Supp 2): 335. Sept 2011
British Transplant Society. 15th Annual Congress. Abstract Book. February 2012

10. Accelerated Renal Senescent Phenotype in the AS/AGU Rat – A Novel In-vivo Model

Marc Gingell-Littlejohn, Marc J Clancy and Paul G Shiels

British Transplant Society. 15th Annual Congress. Abstract Book. February 2012

American Journal of Transplantation, May 2012, Volume 12, Supplement s3

11. CDKN2A Expression in Pre-implantation Kidney Biopsies is the Single, Strongest Predictive Factor for Post-Transplant Renal Function at 1 year

Marc Gingell Littlejohn, Dagmara McGuinness, Karen Stevenson, David Kingsmore, Marc Clancy and C Koppelstaetter and Paul G Shiels

British Transplant Society. 15th Annual Congress. Abstract Book. February 2012

American Journal of Transplantation, May 2012, Volume 12, Supplement s3

❖ **PRIZES**

1. Allograft Biological Age Is Prognostic For Renal Function Post Transplant

L McGlynn, M Gingell- Littlejohn, MJ Clancy, D Kingsmore, P Shiels

ORAL PRIZE: *West of Scotland Surgical Meeting. October 2010.*

2. CDKN2A Expression in Pre-implantation Kidney Biopsies is the Single, Strongest Predictive Factor for Post-Transplant Renal Function at 1 year

Marc Gingell Littlejohn, Dagmara McGuinness, Karen Stevenson, David Kingsmore, Marc Clancy and C Koppelstaetter and Paul G Shiels

POSTER PRIZE: *American Transplant Congress 2012, Boston, USA*

Pre-Transplant CDKN2A Expression in Kidney Biopsies Predicts Renal Function and Is a Future Component of Donor Scoring Criteria

Marc Gingell-Littlejohn^{1,2}, Dagmara McGuinness¹, Liane M. McGlynn¹, David Kingsmore^{1,2}, Karen S. Stevenson^{1,2}, Christian Koppelstaetter³, Marc J. Clancy^{1,2}, Paul G. Shiels^{1*}

1 University of Glasgow, College of Medical, Veterinary and Life Sciences, Institute of Cancer Sciences, Glasgow, United Kingdom, **2** Transplant Unit, Western Infirmary, Glasgow, United Kingdom, **3** Division of Nephrology, Department of Internal Medicine, Medical University Innsbruck, Innsbruck, Austria

Abstract

CDKN2A is a proven and validated biomarker of ageing which acts as an off switch for cell proliferation. We have demonstrated previously that CDKN2A is the most robust and the strongest pre-transplant predictor of post-transplant serum creatinine when compared to “Gold Standard” clinical factors, such as cold ischaemic time and donor chronological age. This report shows that CDKN2A is better than telomere length, the most celebrated biomarker of ageing, as a predictor of post-transplant renal function. It also shows that CDKN2A is as strong a determinant of post-transplant organ function when compared to extended criteria (ECD) kidneys. A multivariate analysis model was able to predict up to 27.1% of eGFR at one year post-transplant ($p = 0.008$). Significantly, CDKN2A was also able to strongly predict delayed graft function. A pre-transplant donor risk classification system based on CDKN2A and ECD criteria is shown to be feasible and commendable for implementation in the near future.

Citation: Gingell-Littlejohn M, McGuinness D, McGlynn LM, Kingsmore D, Stevenson KS, et al. (2013) Pre-Transplant CDKN2A Expression in Kidney Biopsies Predicts Renal Function and Is a Future Component of Donor Scoring Criteria. PLoS ONE 8(7): e68133. doi:10.1371/journal.pone.0068133

Editor: Jean-Claude Dussaule, INSERM, France

Received: December 7, 2012; **Accepted:** May 26, 2013; **Published:** July 4, 2013

Copyright: © 2013 Gingell-Littlejohn et al. This is an open-access article distributed under the terms of the Creative Commons Attribution License, which permits unrestricted use, distribution, and reproduction in any medium, provided the original author and source are credited.

Funding: This work was supported by Darlinda's Charity for Renal Research (<http://www.darlindascharity.co.uk/>). The funders had no role in study design, data collection and analysis, decision to publish, or preparation of the manuscript.

Competing Interests: The authors have declared that no competing interests exist.

* E-mail: paul.shiels@glasgow.ac.uk

Introduction

Kidney transplantation is the optimum treatment for renal failure but is restricted by donor shortage. A large proportion of End Stage Renal Failure (ESRF) patients must therefore receive alternative replacement therapies in the form of peritoneal dialysis, or haemodialysis. Such treatment results in increasing morbidity particularly affecting the cardiovascular system, a severely reduced lifespan and poorer quality of life. “Extended Criteria Donor” (ECD) kidneys are increasingly used to meet this shortfall in kidney supply.

In accordance with the Organ Procurement and Transplantation Network (OPTN) and United Network for Organ Sharing (UNOS), an Expanded Criteria Donor (ECD) is one which is: [1].

- a. 60 years or over
- b. 50–59 years with at least 2 of the following three medical criteria
 - i. Cerebro-Vascular Accident as the cause of death
 - ii. History of hypertension
 - iii. Pre retrieval creatinine more than 133 $\mu\text{mol/L}$

Although ECD organs incur elevated risks of Delayed Graft Function (DGF) and ultimately have unfavorable long-term outcomes compared with younger donor kidneys, average results

remain far superior to alternative treatment modalities, such as haemodialysis. Some grafts, however, perform poorly – or never function adequately – and thus display Primary Non Function (PNF). The reasons for this phenomenon are unclear, but seem likely to relate to the inability of older kidneys to tolerate and recover from the multiple injurious processes associated with transplantation. In essence, such organs will have more ‘miles on the clock’ and thus not function as well, or last as long. The presence of substantial cellular senescence will make them more susceptible to the effects of transplant-related stresses. [2,3] In general, however, poor function is difficult to predict as many older organs perform adequately despite advanced chronological age. [4,5] Dependent upon the numbers of senescent cells present in an organ, tissue integrity may be impaired and the capacity to withstand stress reduced. Furthermore, senescence-associated upregulation of pro-inflammatory cytokine gene expression may lead to chronic persistent inflammation. We have therefore hypothesised that the biological age of the organ, rather than just its chronological age, may have a major impact on allograft function and that this may be directly relevant to discriminating between ECD organs.

This would imply that the expression of genes involved in cellular processes regulating biological ageing, should provide suitable reporters for investigating such a hypothesis. Indeed, robust and reproducible studies have shown that gene expression of senescence markers in a donor organ (organ bioage), can predict renal function in vivo, irrespective of classical parameters

currently in use, such as donor chronological age and sub optimal pre-retrieval serum creatinine [6,7].

To date, of those putative biomarkers of ageing (BoA) that have been tested, very few meet the Baker and Sprott criteria required for validation. [8] This dictates that a valid BoA must demonstrate variation of sufficient magnitude in short-term longitudinal, or in cross-sectional studies, to be of predictive value within a population or cohort with regard to physiological capacity at a later chronological age, in the absence of disease. [9] Failures include Senescence Associated β Galactosidase (SA- β -GAL), advanced glycation end products and lipofuscin, which were originally supported by substantial in vitro evidence. [10] In vivo, only two BoA have been validated with respect to renal function: Cyclin Dependant Kinase 2A (CDKN2A) and telomere length [6,7].

Telomeres are nucleo-protein complexes at the ends of chromosomes with a DNA component comprising variable lengths of a TTAGGG simple repeat. Their primary role includes maintaining stability and protecting the integrity of chromosomes. [11] In somatic cells telomeric DNA shortens in length as a consequence of the end replication problem. [12] The rate of telomere shortening is directly influenced by oxidative stress. [13] This provides a rationale for using telomere length as a BoA at the cellular level and potentially explains the impact of environmental and lifestyle factors on inter-individual differences in the rate of ageing, [14] though with the caveat that it acts as a proxy for the effects of stress and not causal for it [15].

CDKN2A expression is a key age-related component of senescence in human renal allografts and renal disease. [16,17] CDKN2A expression is elevated as a function of increasing cellular stress and organismal ageing. As such, this typically accompanies the telomere shortening observed during normal human ageing. CDKN2A acts as a tumour suppressor, is a component of STASIS (stress and stimulation induced senescence) [18] and is functionally involved in maintaining cells in a state of growth arrest. It has previously been demonstrated to be a significant pre-transplant predictor of post transplant renal allograft function [6,7,19].

In this study, we have sought to directly compare the expression of CDKN2A and telomere length in pre-implantation, time zero biopsies and correlate this with renal function up to 1 year post-operatively. We have sought to determine associations with donor chronological age and other important clinical variables in both univariate and multivariate regression analysis. Included in this analysis was renal function, assessed using the 4 variable "Modification of Diet in Renal Disease Study Group" formula - MDRD 4 eGFR (ml/min/1.73 m²), referred to as eGFR in the subsequent text. These analyses were designed to provide a basic indication of the importance of each respective BoA and to assess their capacity pre-transplant to predict post-transplant function and any associated adverse clinical characteristics, when used either singly, or in combination. Any indication of suitability in this respect could then be exploited, to provide a simple pre-transplant scoring or classification system by assessing BoA expression in the allograft as it is being cross-matched.

Results

Association between Biological Age and Chronological Age

Prior to analysing the predictive power of biomarkers of ageing on renal function, data were validated by determining the association between telomere length and CDKN2A. A Pearson correlation between the two revealed no statistical significance

($p = 0.87$, $n = 15$). Telomere length and CDKN2A were then separately correlated with donor chronological age. Telomere length was shown to inversely correlate with chronological age ($p = 0.036$, $CC = -0.242$, Figure 1a), while CDKN2A levels positively associated with increasing chronological age ($p < 0.001$, $CC = 0.597$, Figure 1b). These findings indicate that CDKN2A is more robustly associated with the chronological ageing process in kidney tissue when compared to telomere length. There was no difference in demographic and clinical data between both CDKN2A and telomere groups (Table 1).

BoA and Correlation with Renal Function Post-Transplant

Pearson correlation showed a significant association between shortening telomere length and deteriorating eGFR at 6 months and at 1 year post-transplant ($p = 0.038$ & $p = 0.041$, Figure 2). However, increasing levels of CDKN2A expression were associated with decreasing eGFR levels at 6 months and 1 year post-transplant ($p = 0.020$ & $p = 0.012$, Figure 3).

Univariate Linear Regression

Univariate linear regression was used in order to assess the individual predictive power of multiple variables on eGFR. Each variable was used to predict function at both 6 months (Table 2) and 1 year (Table 3) post transplantation. The results indicated that CDKN2A, ECD, and donor chronological age were the strongest univariate predictors for eGFR. Telomere length in contrast displayed a poorer predictive ability in general. As expected, other clinical variables that are included in ECD criteria (donor age, donor hypertension, death by CVA but not high serum creatinine) significantly predicted eGFR at both timelines. Interestingly, there was a small but significant association for recipients who suffered any form of glomerulonephritis (GN) resulting in end stage renal failure. Recipients with ESRF second to GN displayed poorer renal function at both timelines (MWU - 6 months $p = 0.05$, 1 year $p = 0.04$). Important univariate associations displayed in Table 2 and 3 include:

6 months. Donor chronological age predicted 14.3% of the variability in eGFR whilst ECD kidney category predicted 12.1%. CDKN2A predicted 13.5% of the eGFR, whilst telomere length predicted 7.9%.

1 year. Donor chronological age predicted 21.4% of the eGFR whilst ECD kidney category predicted 17.4%. CDKN2A predicted 16.6% of the eGFR, whilst telomere length remained at 7.9%.

Multivariate Linear Regression Analysis

A multivariate regression model encompassing the three principle pre-transplant variables was formulated using eGFR as the dependant variable. The covariates were based on CDKN2A and the stronger clinical univariate predictors: ECD and presence or absence of glomerulonephritis in the recipient. Since donor hypertension, donor chronological age and death by CVA are already included under ECD criteria, they were not included as separate covariates in the model. The addition of telomere length to any model severely weakened its associations with renal function resulting in a statistically insignificant outcome. A total of two models were formulated at 6 months and 1 year timelines with a p-value of < 0.017 taken to be statistically significant using Bonferroni's correction. At 6 months, the model approached statistical significance ($p = 0.021$) as outlined in Table 4. Statistical significance was reached at 1 year where the model predicted 27.1% of the eGFR (Adjusted R² 0.271, $n = 31$, $p = 0.008$ ANOVA) with respective individual contributions outlined in Table 5.

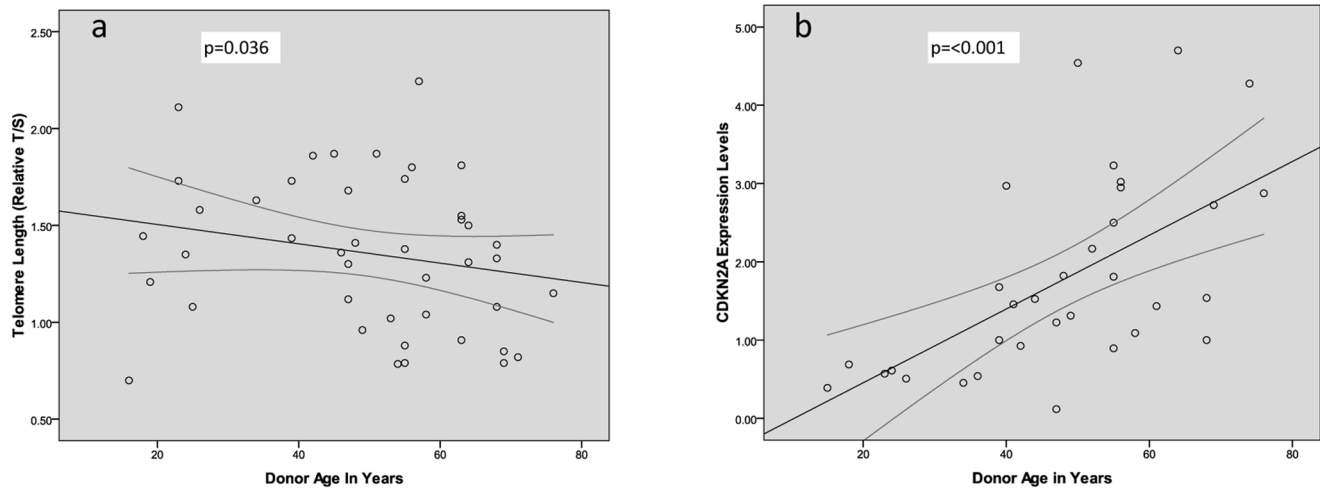


Figure 1. Scatter plots showing the correlation between biomarkers of ageing and donor chronological age. a. Negative correlation between Donor Chronological Age and Telomere Length. $n = 43$, $CC: -0.242$, $p = 0.036$. b. Positive correlation between Donor Chronological Age and CDKN2A. $n = 33$, $CC: 0.597$, $p < 0.001$.

doi:10.1371/journal.pone.0068133.g001

CDKN2A, Delayed Graft Function and Rejection

Increased expression of CDKN2A in pre-implantation biopsies was significantly associated with DGF (MWU, $p = 0.032$). Median CDKN2A expression levels in patients with DGF were compared with those grafts that showed primary function (DGF CDKN2A mean expression = 2.61 (SD 0.56, $n = 6$) vs primary function CDKN2A mean expression = 1.61 (SD 1.30, $n = 27$)). DGF in itself was significantly correlated with graft rejection episodes (Fisher's exact test, $n = 113$, $p = 0.001$). This data suggests that high levels of CDKN2A are linked to increased allograft immunogenicity resulting in increased rejection episodes in the long term and may also play a role in the aetiology of DGF through a similar mechanism.

A total of 112 patients with rejection data were analysed. Biopsy proven evidence of acute rejection was present in 25.0% ($n = 28$) of the total. All such grafts were viable at 6 months with a median eGFR of 39.05 ml/min/1.73 m² (SD 17.16) however, there was 1 graft failure at 1 year, with a median eGFR for all other grafts ($n = 27$) of 39.70 ml/min/1.73 m² (SD 18.09). There was no direct statistical relationship between CDKN2A and rejection itself ($p = 0.741$).

Discussion

We have demonstrated that the pre-transplant expression of two independent BoAs correlates with renal function post-transplant. Greater biological age, as determined by shorter telomere length, or higher relative CDKN2A expression, correlated with poorer post-transplant function [19]. This is in keeping with observations in the field. Classically, organs from older donors show poorer function post-transplant and have a decreased lifespan. Although this holds true in most cases, there are times when such organs perform very well and last beyond their life expectancy. Our results indicate that such variation in organ function could be attributed to the difference in biological age. Our data indicate that pre-transplant CDKN2A expression is the strongest biomarker of renal function up to 1 year post-operatively. When used in the context of Baker and Spratt's criterion, CDKN2A appears to be significantly more robust as a BoA than telomere length. The latter may be viewed as an effective but imprecise BoA. Distinguishing between age-related telomere attrition and disease-related attrition is difficult [8]. Using both together as a composite measure, alongside chronological age, should be of further benefit in this context. Clinical translation of this should be

Table 1. Demographic and important clinical parameters were compared between the separate CDKN2A group and the telomere group.

	CDKN2A $n = 33$ Mean (SD)	Telomere $n = 43$ Mean (SD)	p value
Donor Gender** (male/female)	15/18	20/23	0.589
Donor Age**	48.0 (15.7)	51.8 (15.51)	0.189
DCD/DBD organ*	4/29	9/34	0.677
Mismatch at all A,B,DR Loci* (yes/no)	8/25	10/33	0.607
Recipient Age**	50.6 (12.7)	49.7 (12.6)	0.344
Cold Ischaemic Time**	15.5 (3.9)	13.9 (4.0)	0.267

There were no significant differences between the two groups which would account for the different correlations with renal function (eGFR).

**Unpaired t-Test.

*Fisher's exact test.

doi:10.1371/journal.pone.0068133.t001

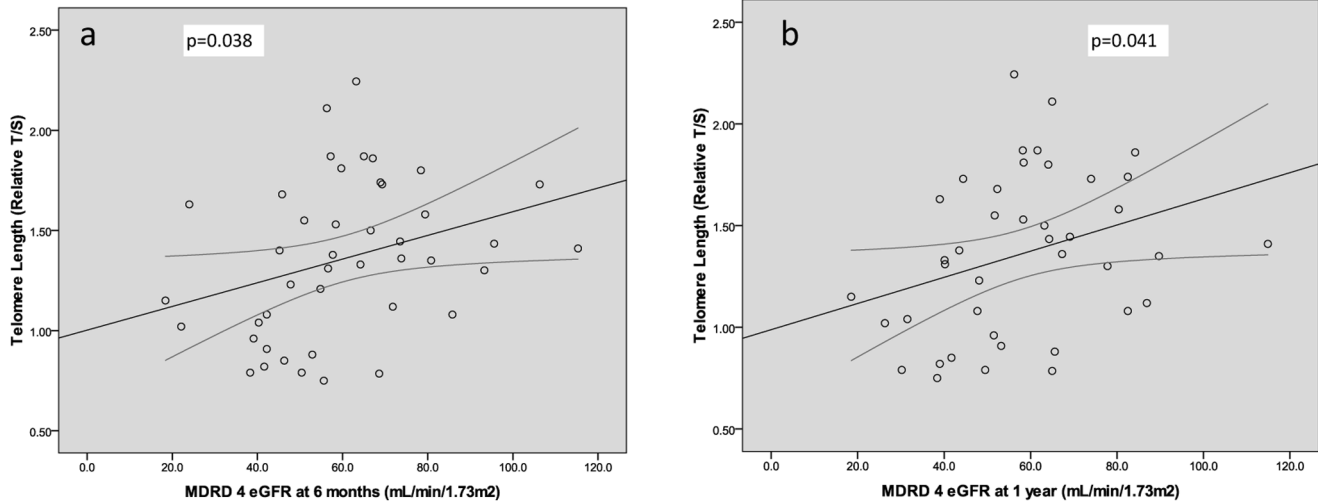


Figure 2. Scatterplots showing the primary significant relationship between telomere length and renal function, as measured by MDRD 4 eGFR at a) 6 months and b) 1 year. a. Telomere Length vs MDRD 4 eGFR at 6 months: $n=43$, $CC: 0.317$, $p=0.038$, b. Telomere Length vs MDRD 4 eGFR at 1 year: $n=41$, $CC: 0.320$, $p=0.041$. doi:10.1371/journal.pone.0068133.g002

straightforward, as our methodology is readily adaptable to implementation when the organ is undergoing cross-match.

In comparison to previous studies, we used the estimated Glomerular Filtration Rate (eGFR) as a marker for renal function as it is traditionally considered the best overall index of function in health and disease. [20] The National Kidney Foundation now recommends the MDRD 4 to estimate the GFR and better detect early onset kidney disease. Although the eGFR is considered to be the best overall index of renal function, it is relatively insensitive at detecting early renal disease and does not correlate well with tubular dysfunction [21,22].

We have previously shown that CDKN2A is stronger than donor chronological age (DCA) at predicting post transplant function when serum creatinine is used as the marker for renal function. [7] However, when eGFR is used to measure renal function, DCA seemed to have a better predictive power than

CDKN2A (Tables 2 and 3). Further univariate regression analysis revealed that the predictive power of CDKN2A on eGFR was almost equal to that of ECD kidney criteria (Tables 2 and 3). In multivariate analysis, the only statistically significant contribution to both models is CDKN2A, indicating its predictive superiority in this limited cohort.

Despite increasing efforts by the transplant community to increase the availability of donor organs, there remains a significant shortfall with several thousand patients dying on the waiting list each year. The introduction of ECD kidneys has improved the quantitative discrepancy of such organs but we are still a distance from achieving satisfactory targets. Novel techniques of organ discrimination are therefore of huge importance in this respect. With the standard incorporation of biomarkers in assessing organ quality pre-operatively, it would seem logical that transplantation would be safer and an increase in

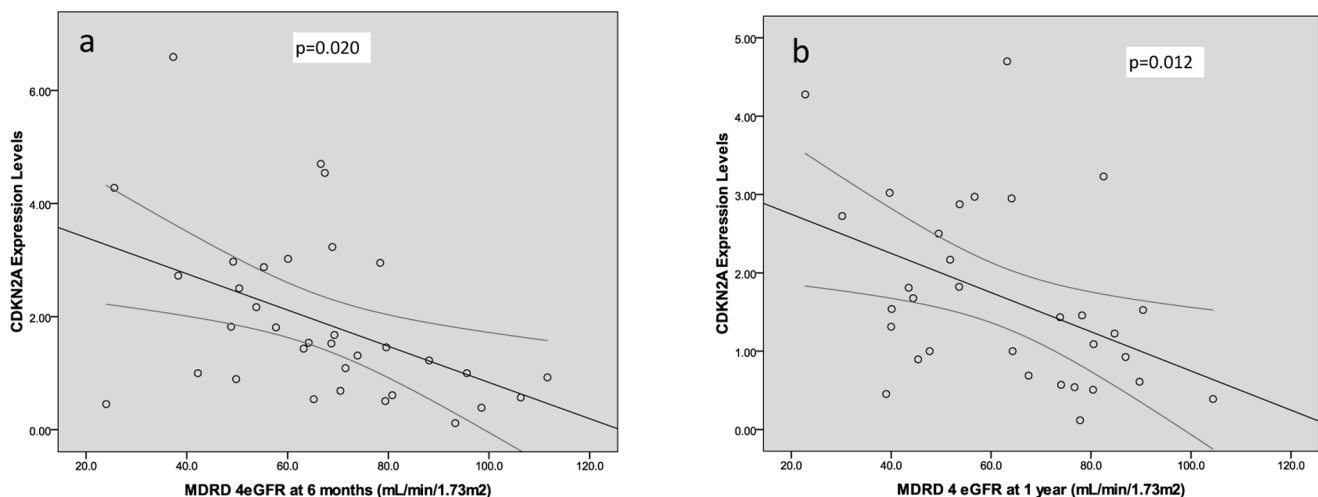


Figure 3. Scatterplots showing the primary significant relationship between CDKN2A and renal function, as measured by MDRD 4 eGFR at a) 6 months and b) 1 year. a. CDKN2A vs MDRD 4 eGFR at 6 months. $n=33$, $CC: -0.403$, $p=0.020$. b. CDKN2A vs MDRD 4 eGFR at 1 year. $n=32$, $CC: -0.439$, $p=0.012$. doi:10.1371/journal.pone.0068133.g003

Table 2. Univariate linear regression analysis showing the predictive power of CDKN2A, telomere length and other relevant clinical variables on renal function at 6 months.

Variable	MDRD 4 eGFR at 6 months		
	n	Adjusted R ²	p-value
CDKN2A expression	33	0.135	0.020
Telomere Length	43	0.079	0.038
Donor Chronological Age	120	0.143	<0.001
GN in recipient	112	0.029	0.040
ECD Kidney	118	0.121	<0.001
Donor Hypertension	107	0.051	0.011
CVA in Donor	111	0.057	0.007
Donor pre-retrieval Creatinine >133 µMol/L	110	-0.008	ns
Mismatch at A, B and DR Loci	114	-0.009	ns
Previous Transplant	120	0.000	ns
Cold Ischaemic Time	114	0.019	ns
Donor Sex	120	-0.001	ns
DCD/DBD	63	-0.003	ns

Note the superior predictive strength of CDKN2A when compared to telomere length. (GN: Glomerulonephritis, DCD: Donation after Cardiac Death, DBD: Donation after Brain Death, CVA: Cerebro Vascular Accident, ECD: Extended Criteria Donor).

doi:10.1371/journal.pone.0068133.t002

the number of kidney transplants would subsequently ensue. CDKN2A is also related to DGF which in itself is associated with poorer graft performance and decreased long term survival. [23,24] The reason for this remains to be determined, but may relate to biologically older organs being less tolerant to physical stress and requiring more time to recover from peri-transplant ischaemia reperfusion injury.

Why CDKN2A expression levels, in this study, have been observed to be a stronger biomarker of ageing than telomere length remains to be proven. Both fulfil the Baker and Sprott criterion, but the weakness of telomere length in predicting functional capacity in a solid organ is apparent. A contributory factor may be the extent of inter individual variation in telomere length at a given chronological age. [6,8,14] Our data are consistent with those of Koppelstaetter et al [6], who previously demonstrated that telomere length was inferior to CDKN2A in determining variability on post-transplant serum creatinine levels in renal allografts. Inter-individual variation in CDKN2A expression at a given chronological age has not been fully determined, though increased expression of CDKN2A at the cellular level, remains a robust marker of a senescent state and its elevated expression is coincident with a reduction in cellular proliferation. [25] In essence, its expression may be viewed as an 'off switch' for the cell and hence the degree of inter-individual variation observed with telomere length, is not expected to be as great. Our observations have direct relevance for any future strategies employing biomarkers of ageing either clinically, or epidemiologically. Telomere length is currently used widely in this context. We are now evaluating CDKN2A similarly, in large epidemiological studies, to evaluate its robustness with greater analytical power.

Based on current findings relating to the predictive power of CDKN2A on eGFR, it would follow that a scoring system incorporating biological markers would provide additional infor-

Table 3. Univariate linear regression analysis showing the predictive power of CDKN2A, telomere length and other relevant clinical variables on renal function at 1 year.

Variable	MDRD 4 eGFR at 1 year		
	n	Adjusted R ²	p-value
CDKN2A expression	32	0.166	0.012
Telomere Length	41	0.079	0.041
Donor Chronological Age	104	0.214	<0.001
GN in recipient	105	0.028	0.048
ECD Kidney	103	0.174	<0.001
Donor Hypertension	100	0.069	0.005
CVA in Donor	95	0.075	0.004
Donor pre-retrieval Creatinine >133 µMol/L	95	-0.011	ns
Mismatch at A, B and DR Loci	98	-0.010	ns
Previous Transplant	104	0.000	ns
Cold Ischaemic Time	98	0.014	ns
Donor Sex	105	-0.009	ns
DCD/DBD	49	0.001	ns

Note again the superiority of CDKN2A over telomere length in particular. (GN: Glomerulonephritis, DCD: Donation after Cardiac Death, DBD: Donation after Brain Death, CVA: Cerebro Vascular Accident, ECD: Extended Criteria Donor).

doi:10.1371/journal.pone.0068133.t003

mation for patients and clinicians during the organ selection process. Reference is made to larger studies such as the one in use by the OPTN in the US for deceased donor kidneys based on ten pre-transplant covariates, the Kidney Donor Risk Index. [26] Undoubtedly, this novel scoring system adds a vital tool to the allograft allocation process. Importantly however, it does not include reference to biological age which may be viewed as an essential parameter of modernised scoring systems. In addition, the study itself showed similar results with age matching alone allowing for the possibility of a simpler scoring technique with equal efficacy. We therefore propose a 4 tier categorical scoring system based on biological age of the graft and ECD. Allografts are classified Category I to Category IV based on a straight forward assessment outlined below, with Category I allografts predicting better performance than Category 4 (Table 6).

The mean value for CDKN2A gene expression (1.8) was used as the cut-off value in the scoring system. Moreover, it can be seen from the scatter plots of CKDN2A vs eGFR at 1 year that renal function deteriorates significantly at CDKN2A expression levels above 1.8. ECD kidneys occupy both category III and category IV

Table 4. Multivariate model outcome for eGFR at 6 months.

Independent Variable	Standardised Coefficients (Beta)	p-value
CDKN2A	-0.397	0.034
ECD Kidney	-0.211	0.233
Recipient Glomerulonephritis	-0.293	0.088

The model approaches statistical significance using the strict Bonferroni correction (p=0.021).

doi:10.1371/journal.pone.0068133.t004

Table 5. Multivariate model outcome for eGFR at 1 year.

Independent Variable	Standardised Coefficients (Beta)	p-value
CDKN2A	-0.428	0.019
ECD Kidney	-0.236	0.166
Recipient Glomerulonephritis	-0.311	0.061

The model explains 27.1% of the eGFR $p=0.008$.
doi:10.1371/journal.pone.0068133.t005

in this pre-transplant scoring tool meaning that ECD status carries a poorer prognosis than CDKN2A itself. The allocation of CDKN2A to a higher tier in this scoring system would require further studies to strengthen the correlations observed above. Since DCA forms part of ECD criteria, it was not used as a single determinant of transplant function in multivariate analysis or the categorical scoring system.

A further benefit from our data, is that strategies to mitigate the rate of biological ageing applied to living donors would be expected to have impact on post-transplant outcomes. Reduction of psychological and psychosocial stress and improved lifestyle via changes to diet and exercising might readily be considered. [14,27,28] Biomarkers, specifically CDKN2A, may well expand the field of octogenarian donation for example, by discriminating organs with “less miles on the clock”. Larger multicentre studies are needed to strengthen the hypothesis and the proposed scoring system suggested in this report. It is envisaged that the biomarker CDKN2A will be integrated into a similar, robust and validated pre-transplant scoring system for all kidneys and other transplanted organs in the near future.

Methods

Ethics

This is an ongoing prospective study which has been approved by the Regional Ethics Committee of the North Glasgow NHS Trust. Donors from the national pool donated their organs for transplantation. The recipient of the organ provided pre-operative written informed consent for tissue analysis and scientific research. Samples were anonymised and subsequently analyzed.

Study Population

The global study population is representative of the national UK deceased donor pool. A total of 120 transplant patients were included which were performed in the Western Infirmary, Glasgow between March 2008 and February 2011. All transplants were followed up for post-operative clinical data. Telomere length was calculated for 43 transplanted kidneys. A separate group ($n=33$) yielded CDKN2A expression. There were 15 matched samples as a result of small biopsy specimens allowing RNA or DNA to be obtained separately and not together. Table 1 shows the demographic data for the CDKN2A and telomere groups. Patients, in whom genetic data was not available, were included in the global cohort for clinical analysis. The primary cause of end stage renal disease (ESRF) in the recipients was Adult Polycystic Kidney Disease (APKD) followed by chronic pyelonephritis/reflux disease, hypertensive nephropathy, IgA nephropathy and the glomerulonephritides. The immunosuppressive regimen consisted primarily of basiliximab at induction and day 4 with a maintenance regime consisting of tacrolimus, mycophenolate mofetil and prednisolone.

Table 6. Suggested Donor Kidney Classification system incorporating CDKN2A as the biomarker of ageing and ECD kidney criteria.

Category I	SCD Kidney and CDKN2A expression levels <1.8
Category II	SCD Kidney and CDKN2A expression levels >1.8
Category III	ECD Kidney and CDKN2A expression levels <1.8
Category IV	ECD Kidney and CDKN2A expression levels >1.8

(SCD – Standard Criteria Donors, ECD – Extended Criteria Donors). Predicted kidney function and incidence of graft failure increases with higher category placement.

doi:10.1371/journal.pone.0068133.t006

Human Renal Biopsies and RNA/DNA Extraction

Renal biopsies were obtained on the surgical backbench via wedge resection or needle biopsy according to the surgeon's preference. All biopsies were obtained from “donation after brain death” (DBD) and “donation after cardiac death” (DCD) donors. All samples were stored in ‘RNA later’ solution (Ambion, Austin, TX, USA) at -20°C until processing. RNA was extracted using Trizol reagent (Invitrogen, Paisley, UK) following manufacturer's guidelines. The Maxwell[®] 16 DNA purification robot kits by Promega were used for for DNA isolation.

Delayed Graft Function (DGF)

DGF was defined as failure of serum creatinine to fall by half within seven days of the transplant, or need for dialysis within seven days of the transplant, except dialysis performed for fluid overload or elevated serum potassium levels [29].

MDRD 4 eGFR

The final value for the eGFR was calculated electronically by a biochemical and clinical database – SERPR. The four variables used in the equation include serum creatinine, age, race and gender [20].

CDKN2A Expression Determination

Relative quantitative real-time PCR (qRT-PCR) was used to estimate mRNA levels corresponding to the candidate senescence associated gene (SAGs) - CDKN2A. Expression levels were measured against a reference HPRT housekeeping gene on an ABI Prism[®] 7700 Sequence Detection System. Sequences of human TaqMan[™] Primer/Probe sets designed by Primer Express algorithm (Applied Biosystems, Austin, TX, USA).

HPRT

Forward Primer (5'–CTTGCTCGAGATGTGATGAAG-3/),

Reverse Primer (5'–CAGCAGGTCAGCAAAGAATTATAG-3/),

Probe (5'–FAM-ATCACATTGTAGCCCTCTGTGTGCTCAAGGTAMRA-3/)

CDKN2A

Forward Primer (5'–CATAGATGCCGCGGAAGG-3/),

Reverse Primer (5'–CCCAGGTTTCTCAGAGC-3/),

Probe (5'–FAM-CCTCAGACATCCCCGATTG-TAMRA-3/)

The comparative threshold cycle method ($\Delta\Delta\text{CT}$) was employed as the method of choice to quantify relative gene expression. The quantification result was transformed to an

exponential value, $2^{-\Delta\Delta Ct}$ [30] where Ct is the threshold cycle, or the cycle when the product was first detected. Before undertaking this quantitative study we demonstrated that the efficiency of amplification of reference (HPRT) and test genes were approximately equal (data not shown).

Telomere Length Determination

Telomere length determination was performed by qPCR using a Roche Light Cycler LC480. Telomere length analyses were performed in triplicate for each sample, using a single-copy gene amplicon primer set (acidic ribosomal phosphoprotein, 36B4) and a telomere-specific amplicon primer set. Quality control parameters employed for the amplifications comprised using a cut off 0.15 for the standard deviation (SD) of the threshold cycle (Ct) for sample replicates. At a SD above 0.15 the sample was reanalysed. The average SD across plates was <0.05 .

Relative telomere length was estimated from Ct scores using the comparative Ct method after confirming that the telomere and control gene assays yielded similar amplification efficiencies. This method determines the ratio of telomere repeat copy number to single copy gene number (T/S) ratio in experimental samples relative to a control sample DNA. This normalised T/S ratio was used as the estimate of relative telomere length (Relative T/S).

TELOMERE

Telo 1 Sequence (5' to 3')

CGG TTT GTT TGG GTT TGG GTT TGG GTT TGG GTT TGG GTT

References

- Metzger RA, Delmonico FL, Feng S, Port FK, Wynn JJ et al (2003) Expanded criteria donors for kidney transplantation. *Am J Transplant* 3 Suppl 4: 114–125. pii].
- Halloran PF, Melk A, Barth C (1999) Rethinking chronic allograft nephropathy: the concept of accelerated senescence. *J Am Soc Nephrol* 10: 167–181.
- Melk A, Halloran PF (2001) Cell senescence and its implications for nephropathy. *J Am Soc Nephrol* 12: 385–393.
- Mayer G, Persijn GG (2006) Eurotransplant kidney allocation system (ETKAS): rationale and implementation. *Nephrol Dial Transplant* 21: 2–3. gfi269 [pii];10.1093/ndt/gfi269 [doi].
- Morris PJ, Johnson RJ, Fuggle SV, Belger MA, Briggs JD (1999) Analysis of factors that affect outcome of primary cadaveric renal transplantation in the UK. HLA Task Force of the Kidney Advisory Group of the United Kingdom Transplant Support Service Authority (UKTSSA). *Lancet* 354: 1147–1152. S0140673699011046 [pii].
- Koppelstaetter C, Schratzberger G, Perco P, Hofer J, Mark W et al (2008) Markers of cellular senescence in zero hour biopsies predict outcome in renal transplantation. *Aging Cell* 7: 491–497. ACE398 [pii];10.1111/j.1474-9726.2008.00398.x [doi].
- McGlynn LM, Stevenson K, Lamb K, Zino S, Brown M et al (2009) Cellular senescence in pretransplant renal biopsies predicts postoperative organ function. *Aging Cell* 8: 45–51. ACE447 [pii];10.1111/j.1474-9726.2008.00447.x [doi].
- Shiels PG (2010) Improving precision in investigating aging: why telomeres can cause problems. *J Gerontol A Biol Sci Med Sci* 65: 789–791. glq095 [pii];10.1093/gerona/glq095 [doi].
- Baker GT III, Sprott RL (1988) Biomarkers of aging. *Exp Gerontol* 23: 223–239.
- Lamb KJ, Shiels PG (2009) Telomeres, ageing and oxidation. *SEB Exp Biol Ser* 62: 117–137.
- Blackburn EH (1991) Structure and function of telomeres. *Nature* 350: 569–573. 10.1038/350569a0 [doi].
- Olovnikov AM (1973) A theory of marginotomy. The incomplete copying of template margin in enzymic synthesis of polynucleotides and biological significance of the phenomenon. *J Theor Biol* 41: 181–190. 0022-5193(73)90198-7 [pii].
- von ZT (2002) Oxidative stress shortens telomeres. *Trends Biochem Sci* 27: 339–344. S0968000402021102 [pii].
- Shiels PG, McGlynn LM, MacIntyre A, Johnson PC, Batty GD (2011) Accelerated telomere attrition is associated with relative household income, diet and inflammation in the pSoBid cohort. *PLoS One* 6: e22521. 10.1371/journal.pone.0022521 [doi];PONE-D-11-07269 [pii].
- von ZT, Martin-Ruiz CM (2005) Telomeres as biomarkers for ageing and age-related diseases. *Curr Mol Med* 5: 197–203.

Telo 2 Sequence (5' to 3')

GGC TTG CCT TAC CCT TAC CCT TAC CCT TAC CCT TAC CCT

36B4

36B4d Sequence (5' to 3')

CCC ATT CTA TCA TCA ACG GGT ACA A

36b4u Sequence (5' to 3')

CAG CAA GTG GGA AGG TGT AAT CC

Statistics

Data analyses were performed using SPSS statistical package version 17. The adjusted R^2 was used to indicate the extent to which the dependant variable (eGFR) is explained by the independent variable in question. The association was deemed to be statistically significant if the p value <0.05 . Prior to multivariate regression, preliminary analysis was conducted to ensure no violation of the assumptions of normality, linearity and multicollinearity. Any missing values were removed by pairwise deletion. Bonferroni's adjustment was used to calculate the exact p value for the multivariate models.

Author Contributions

Conceived and designed the experiments: MGL PGS. Performed the experiments: MGL DM. Analyzed the data: MGL DM LMM. Contributed reagents/materials/analysis tools: MGL DM LMM DK KS CK MJC PGS. Wrote the paper: MGL PSG.

- Melk A, Schmidt BM, Takeuchi O, Sawitzki B, Rayner DC et al (2004) Expression of p16INK4a and other cell cycle regulator and senescence associated genes in aging human kidney. *Kidney Int* 65: 510–520. 10.1111/j.1523-1755.2004.00438.x [doi].
- Melk A, Schmidt BM, Vongwiwatana A, Rayner DC, Halloran PF (2005) Increased expression of senescence-associated cell cycle inhibitor p16INK4a in deteriorating renal transplants and diseased native kidney. *Am J Transplant* 5: 1375–1382. AJT [pii];10.1111/j.1600-6143.2005.00846.x [doi].
- Shay JW, Wright WE (2000) Hayflick, his limit, and cellular ageing. *Nat Rev Mol Cell Biol* 1: 72–76. 10.1038/35036093 [doi];35036093 [pii].
- Lamb K, Stevenson KS, Zino S, MacIntyre A, Kingsmore D et al (2006) Telomere binding protein expression correlates with cold ischemic time and late graft dysfunction in human renal allografts, as a result of accelerated organ senescence. *Neph Dial Trans* 21: 259–260.
- Levey AS, GTKJea (2011) A simplified equation to predict GFR from serum creatinine. *J Am Soc Nephrol* 2000; 11: 155A Abstract.
- K/DOQI clinical practice guidelines for chronic kidney disease: evaluation, classification, and stratification. *Am J Kidney Dis* 39: S1–266. S0272638602093563 [pii].
- Levey AS, Coresh J, Balk E, Kausz AT, Levin A et al (2003) National Kidney Foundation practice guidelines for chronic kidney disease: evaluation, classification, and stratification. *Ann Intern Med* 139: 137–147. 200307150-00013 [pii].
- Sanfilippo F, Vaughn WK, Spees EK, Lucas BA (1984) The detrimental effects of delayed graft function in cadaver donor renal transplantation. *Transplantation* 38: 643–648.
- Koning OH, Ploeg RJ, van Bockel JH, Groenewegen M, van der Woude EJ et al (1997) Risk factors for delayed graft function in cadaveric kidney transplantation: a prospective study of renal function and graft survival after preservation with University of Wisconsin solution in multi-organ donors. *European Multicenter Study Group. Transplantation* 63: 1620–1628.
- Krishnamurthy J, Ramsey MR, Ligon KL, Torrice C, Koh A et al (2006) p16INK4a induces an age-dependent decline in islet regenerative potential. *Nature* 443: 453–457. nature05092 [pii];10.1038/nature05092 [doi].
- Rao PS, Schaubel DE, Guidinger MK, Andreoni KA, Wolfe RA et al (2009) A comprehensive risk quantification score for deceased donor kidneys: the kidney donor risk index. *Transplantation* 88: 231–236. 10.1097/TP.0b013e3181ac620b [doi];00007890-200907270-00013 [pii].
- Ornish D, Lin J, Daubenmier J, Weidner G, Epel E et al (2008) Increased telomerase activity and comprehensive lifestyle changes: a pilot study. *Lancet Oncol* 9: 1048–1057. S1470-2045(08)70234-1 [pii];10.1016/S1470-2045(08)70234-1 [doi].

28. Shiels PG (2012) CDKN2A might be better than telomere length in determining individual health status. *BMJ* 344: e1415.
29. Yarlagadda SG, Coca SG, Garg AX, Doshi M, Poggio E et al (2008) Marked variation in the definition and diagnosis of delayed graft function: a systematic review. *Nephrol Dial Transplant* 23: 2995–3003. gfn158 [pii];10.1093/ndt/gfn158 [doi].
30. Livak KJ, Schmittgen TD (2001) Analysis of relative gene expression data using real-time quantitative PCR and the 2⁻(Delta Delta C(T)) Method. *Methods* 25: 402–408. 10.1006/meth.2001.1262 [doi];S1046-2023(01)91262-9 [pii].

Novel cell therapies in transplantation

Shiels PG, Stevenson KS, Gingell-Littlejohn M and Clancy M

Human organs have a limited capacity for repairing themselves. This capacity declines as a function of increasing chronological age, driven by a cocktail of biological, psychological, and sociological stressors that can accelerate organ degeneration. As a consequence, both transplant recipient survival and donor organ function, are affected by these processes. Novel therapies to tackle this are manifold, but typically limited in effect.

Solid organ transplants replace diseased organs with biologically newer, healthier whole organs, but this strategy is inherently limited. The requirement for an individual with healthy organs to die or to undergo major surgery in order for an organ to be replaced is the central, limiting paradox of whole organ transplantation. Stem cell treatments (*or novel, cell-based therapies if preferred*) represent perhaps the most exciting and most logical approach of the many ways this clinical problem is being addressed. The isolation and propagation of stem cell lines promised a more permanent and potent method of repair or regeneration of damaged tissue or organs. Indeed at the time of James Thomson's description of the first embryonic stem cell lines in 1998 (*Thomson et al 1998*) solid organ transplantation had been established for nearly three decades and the step to having perfect, quality-controlled neo-organs on a shelf ready for surgical implantation appeared small. Initial perceptions have seemingly underestimated the quantum leap from single multipotent stem cell to functioning organ.

The holy grail of cell-based tissue engineering approaches remains the growth of functional (and ideally tolerant) neo-organs, which can spontaneously, or surgically, assimilate into the body and fulfill the role of a diseased organ. Whilst pluripotent cell lines of infinite proliferative capacity have reliably been made to form cardiac myocytes, hepatocytes and many of the different renal specific cell types, few have been directed into a neorgan of adequate function to establish a role in clinical practice and none in the fields currently managed by major abdominal organ transplants.

Therapeutic applications of novel cell lines are far more advanced in immunomodulation and the augmentation of tissue repair. These protection/repair therapies have already shown clinical benefit and also have direct implications for the treatment of age related disease. Since these approaches are well advanced in clinical trials and therefore most likely to find a clinical role in the current abdominal transplant field, this chapter, focuses principally on the potential of cell sources to protect or repair diseased organs.

The use of stem cells to grow functional, clinically useful tissue for the treatment of the diseases currently best managed by abdominal organ transplants remains entirely experimental. The progress and barriers to clinical use are also discussed.

Defined stem cell populations for clinical application

Despite this great promise, the use of regenerative medicine to effect repair of solid organs and tissues is still in its infancy. The type(s) of cell, or cell population, that is required to effect functional recovery remains to be defined, as does the mechanism, delivery system and indeed cell numbers to achieve this.

A range of cell types have been touted and tried as candidates for therapeutic use. These include embryo stem cells (ESCs) hematopoietic stem cells (HSCs), multipotent stromal cells (MSCs), endothelial progenitor cells (EPCs) and organ specific resident stem/progenitor cells, which are known to contribute to solid-organ tissue repair. The individual merits of these cells have been reviewed elsewhere (Stevenson et al 2009a). Currently, their use has been limited, but the field is developing rapidly and early clinical trials for solid organ repair are on going.

The main focus is on adult cell sources since the use of ESCs remains dogged by social and scientific uncertainty, due to moral or ethical issues or basic technical hurdles. The latter include controlling the directed differentiation of ESCs and the prevention of neoplasia or tissue dysfunction post transplant. Most current clinical potential resides with using adult cell types, such as MSCs. To date, only MSCs have been applied successfully in both experimental solid organ transplantation and clinical studies. These are discussed below, with reference to clinical applications in transplantation.

Multipotent stromal cells

MSCs were initially described, over thirty years ago by Freidenstein et al (1968) as a bone-marrow-derived mononuclear cell population which exhibited a fibroblast-like morphology when cultured *ex vivo* on an adherent substrate, such as plastic. MSCs are present in a wide range of adult tissues and exhibit the capacity to be differentiated into multiple specialized cell types from all three germ layers. They also demonstrate immuno-modulatory properties, though how this is achieved remains undefined (for a detailed review see Popp et al 2009). As such, they are of interest due to their capacity to make cells suitable for transplantation.

Recent clinical trials have tested the capacity of MSCs to treat cardiac, renal and liver damage, as noted below. What remains unclear, however, is the mode of action of such cells. It is uncertain whether these cells contribute to tissue building via direct differentiation into tissue specific cells, or modulate immune mediated damage at the

site of injury, or even provide trophic support for tissue regeneration (Crop et al 2009). Even the characterization of these cells is contentious.

A basic set of criteria has been proposed by The International Society for Cellular Therapy (ISCT) for MSCs (Dominici et al 2006). This appears to function well in practice.

(i) Adherence in vivo when grown on plastic.

(ii) Expression of a specific cell surface marker phenotype comprising (CD73+ CD90+ CD105+ CD34- CD45- CD11b- CD14- CD19- CD79a- HLA-DR-)

(iii) Differentiation potential to osteogenic, chondrogenic and adipogenic lineages.

One key question at this juncture, is whether the phenotype and properties exhibited by MSC in vitro, are maintained in vivo. MSCs in vitro, grow typically as an adherent monolayer, with a distinct immuno-phenotype. When grown under non-adherent conditions this phenotype changes and the cells grow in spherical clusters. This has been proposed to promote intercellular interactions, though this remains to be demonstrated formally (Frith et al 2010).

Some findings however, suggest that MSCs offer exciting therapeutic potential for organ transplantation. Secretory factors derived from MSCs have been demonstrated to have both pro-angiogenic and anti-inflammatory effects, which might be used to assist in solid organ and cellular transplantation. Furthermore, MSCs grown in the presence of pro-inflammatory cytokines also display enhanced immunosuppressive effects, which might be exploited to aid transplant success. (Di Nicola et al 2002; Imberti et al 2007; Van Poll et al 2008). The immuno-modulatory effect of MSCs appears to be dose-dependent and independent of the major histocompatibility complex (MHC) and mediation by antigen-presenting cells or regulatory T cells. (Le Blanc et al 2003; Krampera et al 2003)

MSC and solid organ transplantation

Following on the heels of a range of rodent studies demonstrating that transplanted MSCs can improve tissue damage (Yeagy et al 2011), clinical trials are underway. Currently, only three Phase III clinical trials have been concluded. These comprise trials for graft-versus-host disease (GVHD), Crohn's disease and perianal fistula. As such they are not yet directly relevant to abdominal organ transplantation, and the therapeutic approach is immunomodulatory, rather than building/repairing tissue architecture.

Early stage trials for use with solid organs are limited. Initial findings from a safety and clinical feasibility study (Perico et al ClinicalTrials.gov, NCT00752479) comprising autologous MSC administration in two subjects receiving living-related

donor kidneys showed that one year post transplant the patients had stable graft function and significantly, an enlargement of the regulatory T cell (Treg) pool in the peripheral blood, with a concomitant inhibition of memory T cells. This has demonstrated the feasibility of translating beneficial immunomodulatory findings from rodent models into a human clinical setting, though caution, based on the low power of the study is still advised.

Ongoing trials using MSC to aid outcome in liver renal transplantation continue at a number of centers with results awaited. Promising results on deriving liver and biliary cells in vitro using rodent progenitor cells have already been reported (see Stevenson et al 2009b), though these have yet to translate into clinical practice, as deriving human equivalents has proven problematic.

Recently, a significant technical breakthrough was reported with the identification of adult nephron progenitors capable of kidney regeneration in zebrafish (Diep et al 2010). These authors have provided proof of principle, that transplantation of single aggregates comprising 10-30 progenitor cells is sufficient to engraft adults and generate multiple nephrons. The identification of these cells opens up an avenue to isolating or engineering the equivalent cells in humans and developing novel renal regenerative therapies.

How MSCs might work

How MSCs work in clinical trials and animal models, is still debated. Any paracrine effect mediated by the secretion of growth factors remains problematic, as the speed of efficacy, duration of immuno-modulation and extent of tissue repair cannot readily be accounted for. This principally, is due to the transient existence of MSCs following in vivo administration and different syngeneic and allogeneic effects in transplantation models (Casiraghi et al 2008; Popp et al 2008).

Recent data from Stevenson et al (2011) sheds light some light on this, as even in a xenotransplant setting paracrine effects can invoke developmental recapitulation during organ regeneration. This is discussed more fully below with reference to Pathfinder cells.

Considerations for solid organ transplantation

Given the convincing in vivo demonstrations of the immuno-suppressive effects of MSCs, phase I clinical trials for the treatment of a range of diseases are already underway. However, potential pitfalls for their use in organ transplantation remain. Firstly, allogeneic MSCs, may induce memory responses, leading to accelerated graft rejection, which would not be observed with autologous MSCs. Secondly and conversely, autologous MSCs might induce donor-specific hypo-responsiveness

There is precedent for such a postulate based on previous donor-specific transfusions data [Waanders et al 2005].

Thirdly, the differentiation potential of MSCs, could lead to the loss of correct pattern of spatio-temporal development in a specific tissue or organ, with the formation of atypical cell types in it . Reports already exist of elevated levels of calcification in mice treated with MSCs to combat the effects of myocardial infarction(Breitbach et al 2007)

Fourthly, such differentiation and, or, paracrine support for damaged tissue could lead to neoplasia. This has yet to be observed in practice and use of such cells in bone marrow transplant without serious adverse consequences, over the past 40 years, is encouraging in this respect.

Fifthly, the wide spread dispersal of MSCs in vivo, following infusion, runs the risk of stimulating fibrosis through paracrine stimulation of tissue by MSC secreted factors. Precedent for such a scenario exists. Recent clinical data from experiments using adipose derived EPCs showed immediate fibrosis following lipoinjection into adipose-tissue (Yoshimura et al, 2008)

Finally, given that MSC have the capacity to modulate the immune system, the question of whether infusions of these cells will compromise overall immune surveillance arises. Initial primate studies have indicated that administration of high dose allogeneic MSCs affected allo-reactive immune responses. (Beggs et al 2006)

Pathfinder cells; an alternative to solid organ pancreas transplantation?

A further cell type with potential for usage in solid organ transplantation has been described. These are a novel cell population, termed Pathfinder cells (PCs) (Shiels 2004; Stevenson et al 2011), isolated from both adult rat and human tissues, so named on the basis that they appear to navigate a path towards sites of damage in vivo. PCs have proven efficacy in regenerating tissue in a number of solid organ damage models. Notably, these cell work across a species barrier, exert their influence on damage tissue in a paracrine fashion and have immuno-modulatory properties.

These cells share many properties with MSCs, in that they have an adherent phenotype when grown on plastic and can form spherical cell clusters. They display paracrine interactions with immune cells already well documented for MSCs. (Yagi et al 2010). Unlike MSCs, these cells can be CD90, CD105 and CD73 negative.

Direct intravenous injection of rat or human PCs into streptozotocin (STZ) induced diabetic mice resulted in a paracrine mediated normalization of blood glucose levels and restoration of mouse pancreatic architecture. Crucially, the insulin produced by these treated animals was principally mouse in origin and was of both type I (embryonic) and II (adult) (Stevenson et al 2011), indicative of stimulated

developmental recapitulation. Notably, the PCS do not persist indefinitely after infusion, analogous to MSCs and can only be detected at low levels (<0.1%) 100 days after administration. These observations are also in keeping with previous reports suggesting a means for novel therapeutic intervention without making differentiated cells for transplantation *ex vivo* (Shiels 2004, Dor et al 2004, Nir et al 2007). Significantly, PCs have demonstrated efficacy in both rodent models of renal and cardiac ischaemia which bodes well for their development as a clinical cellular therapeutic.

iPS cells

Derived as an alternative to working with stem cells, induced pluripotent stem (iPS) cells have been used to derive a number of specialized cell types and may eventually have a role in transplantation, though this would seem some way off at present. iPS derivation involves genetically manipulating adult cells to express a number of transcription factors normally required for maintaining stem cells in an undifferentiated state (Meissner et al 2007; Okita et al 2007). iPS cells show many similarities to ESCs in morphology, proliferation and the capacity for teratoma formation. Tumour formation in chimaeras, following iPS cell implantation, precludes their use in transplantation. Recently, iPS cells have shown success when used to provide a model system for studying complex human disease conditions (Zhang et al 2010). Such studies are an important correlate for the development of improved clinical strategies to treat disease. More recently, however, Pasi et al (2011) have reported that iPS cells are genetically unstable and possess a range of abnormalities more associated with neoplastic transformation, which suggests a serious impediment to their use as a therapeutic cell source.

Neo-organogenesis for transplantation

Most current approaches, with the exception of Pathfinder cell therapy, use stem or progenitor cells to build tissue directly, not by way of induction of natural developmental pathways. Extensive work has allowed the definition of many stem cell subtypes, many of which are pluripotent, as defined above, but persuading these cells to form the correct three dimensional tissue architecture of mature organs has proved far more problematic.

All abdominal organs develop from a stem cell population which aggregate, separate from surrounding structures (in the case of the kidney with the formation of a tough connective tissue capsule) and induce a complex network of blood vessels which allow growth to the large size of mature organs. Further ingrowth of additional cell types such as neuroendocrine pancreatic cells may also be necessary before the mature organ is properly formed (Figure 1).

These steps lie between implantation of a stem cell population and useful organ function unless – as in the case of a bone marrow or peripheral blood stem cell transplant – the desired function is one or more singly existing blood cell type. There is no better example of the difficulty of forming clinically useful tissue from stem cell sources than the inability of the entire scientific world to develop something as conceptually simple as quality-controlled erythrocyte populations for transfusion let alone a kidney.

Natural blueprints for stem cell to organ development: using foetal cells to grow an organ

Figure 1. shows that the foetal pre-organ may be considered the natural blueprint for stem cell assembly into the mature organ. Implantation of the foetal kidney rudiment has been described(Hammerman et al 2000) but cannot replicate the magnitude of glomerular filtration nor tubular function to sustain life(Marshall et al 2007; Clancy et al 2009). Transplantation of the less well defined pancreas rudiment has also shown promise but remains some way from clinical practice(Hammerman et al 2011).

Utilising these foetal preorgans as a template to allow stem cells, microinjected into the preorgan before implantation, to form functioning organ has been attempted. In the case of the kidney, functioning human glomeruli and tubules have been demonstrated in preinjected rat foetal kidney grafts but once again, this technology is some way short of being an alternative to kidney transplantation.(Yoko et al 2009)

Creating tolerant adult organs

The foetal organ may only represent a blueprint as far as a small, immature organ and may lack developmental cues relating to late pre-natal and post-natal growth and development. The adult organ contains a fully formed connective tissue architecture and vasculature and represents an alternative blueprint. Injection of autologous stem cells onto a decellularised human trachea has been successfully performed in a human patient(Baiguera et al 2010) however this only requires a single epithelial layer to form on the inside of the decellularised platform. This is no more complex than the cells' behavior in culture. Nevertheless this transplant is a landmark for stem-cell transplantation.

Repopulation of a heart with stem cells is also described experimentally(Taylor et al 2009) but the complexity of abdominal organs like kidney, liver and pancreas still remains a barrier to regrowing clinically useful and transplantable organs from stem cell sources.

The future

Despite many remaining obstacles, the use of cellular therapies to augment the transplant team's armamentarium and to treat previously intractable conditions is exciting. Translation of these strategies is rapidly advancing, though a legion of unanswered questions remain with respect to both the basic biology and long term success of treatments. Will these therapies replace damaged tissue without addressing any underlying pathology? Will stem cells be differentiated in vitro to form solid organs for transplant as they have with the relatively more simple trachea? What immune issues need to be dealt with? With the exception of bone marrow transplantation, obtaining enough of a given cell type, and ensuring the risk of cancer is minimized post transplant also remains an barrier.

Despite these hurdles, cell therapies offer significant potential for treating previously intractable conditions and understanding basic biological processes involved in development and in tissue homeostasis. Progress since the hyperbolic promise of the first embryonic stem cell lines seems slow however the next decade is likely to see cell based treatments cement their clinical role.

References

1. Thomson JA, Itskovitz-Eldor J, Shapiro SS, Waknitz MA, Swiergiel JJ, Marshall VS, Jones JM. Embryonic stem cell lines derived from human blastocysts. *Science*. 1998 Nov 6;282(5391):1145-7
2. Stevenson K, McGlynn L, Shiels PG. Stem cells: outstanding potential and outstanding questions. *Scott Med J*. 2009a 54(4):35-7.
3. Friedenstein AJ, Petrakova KV, Kurolesova AI, Frolova GP. Heterotopic of bone marrow. Analysis of precursor cells for osteogenic and hematopoietic tissues. *Transplantation* 1968;6:230-247. Felix C. Popp, Philipp Renner, Elke Eggenhofer, Przemyslaw Slowik, Edward K. Geissler, Pompiliu Piso, Hans J. Schlitt, Marc H. Dahlke
4. Felix C. Popp, Philipp Renner, Elke Eggenhofer, Przemyslaw Slowik, Edward K. Geissler, Pompiliu Piso, Hans J. Schlitt, Marc H. Dahlke
Mesenchymal stem cells as immunomodulators after liver transplantation
Liver Transplantation Volume 15, Issue 10, pages 1192–1198, October 2009

5. Crop M, Baan C, Weimar W, Hoogduijn M. Potential of mesenchymal stem cells as immune therapy in solid-organ transplantation. *Transpl Int*. 2009 Apr;22(4):365-76.
6. Dominici M, Le Blanc K, Mueller I, Slaper-Cortenbach I, Marini F, Krause D, Deans R, Keating A, Prockop Dj, Horwitz E. Minimal criteria for defining multipotent mesenchymal stromal cells. The International Society for Cellular Therapy position statement. *Cytotherapy*. 2006;8(4):315-7
7. Frith JE, Thomson B, Genever P. Dynamic three-dimensional culture methods enhance mesenchymal stem cell properties and increase therapeutic potential. *Tissue Eng Part C Methods*. 2010 Aug;16(4):735-49
8. van Poll D, Parekkadan B, Cho CH, et al. Mesenchymal stem cell derived molecules directly modulate hepatocellular death and regeneration in vitro and in vivo. *Hepatology* 2008; 47: 1634-8.
9. Imberti B, Morigi M, Tomasoni S, et al. Insulin-like growth factor-1 sustains stem cell mediated renal repair. *J Am Soc Nephrol* 2007; 18: 2921-9.
10. Di Nicola M, Carlo-Stella C, Magni M, et al. Human bone marrow stromal cells suppress T-lymphocyte proliferation induced by cellular or nonspecific mitogenic stimuli. *Blood* 2002; 99: 3838
11. Le Blanc K, Tammik L, Sundberg B, Haynesworth SE, Ringden O. Mesenchymal stem cells inhibit and stimulate mixed lymphocyte cultures and mitogenic responses independently of the major histocompatibility complex. *Scand J Immunol* 2003; 57: 11.
12. Krampera M, Glennie S, Dyson J, et al. Bone marrow mesenchymal stem cells inhibit the response of naive and memory antigen-specific T cells to their cognate peptide. *Blood* 2003; 101: 3722.
13. Yeagy BA, Harrison F, Gubler MC, Koziol JA, Salomon DR, Cherqui S. Kidney preservation by bone marrow cell transplantation in hereditary nephropathy. *Kidney Int*. 2011 Jan 19. [Epub ahead of print]
14. Perico N, Casiraghi F, Inrona M, Gotti E, Todeschini M, Cavinato RA, Capelli C, Rambaldi A, Cassis P, Rizzo P, Cortinovis M, Marasà M, Golay J, Noris M, Remuzzi G. Autologous Mesenchymal Stromal Cells and Kidney

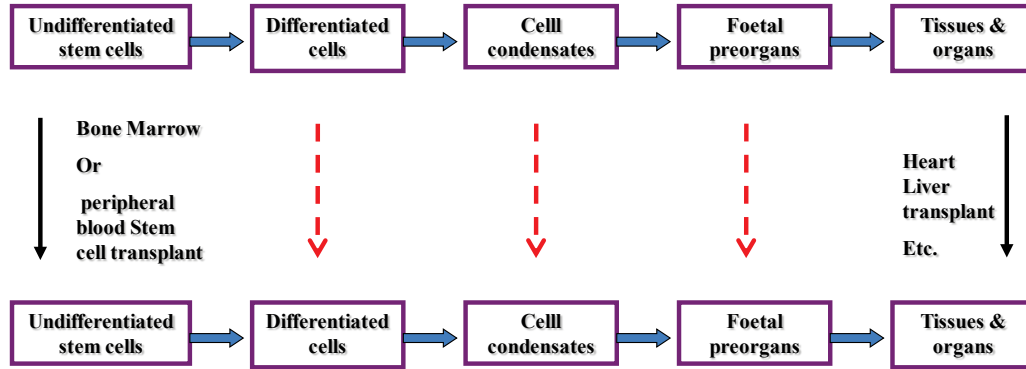
Transplantation: A Pilot Study of Safety and Clinical Feasibility. *Clin J Am Soc Nephrol*. 2010 Oct 7. [Epub ahead of print]

15. Diep CQ, Ma D, Deo RC, Holm TM, Naylor RW, Arora N, Wingert RA, Bollig F, Djordjevic G, Lichman B, Zhu H, Ikenaga T, Ono F, Englert C, Cowan CA, Hukriede NA, Handin RI, Davidson AJ. *Nature*. 2011 Feb 3;470(7332):95-100.
16. Stevenson KS, McGlynn L, Hodge M, McLinden H, George WD, Davies RW, Shiels PG. Isolation, characterization, and differentiation of thyl.1-sorted pancreatic adult progenitor cell populations. *Stem Cells Dev*. 2009b 18(10):1389-98.
17. Casiraghi F, Azzollini N, Cassis P, et al. Pre-transplant infusion of mesenchymal stem cells prolongs the survival of a semi-allogeneic heart transplant through the generation of regulatory T cells. *J Immunol* 2008; 181: 3933.
18. Popp FC, Eggenhofer E, Renner P, et al. Mesenchymal stem cells can induce long-term acceptance of solid organ allografts in synergy with low-dose mycophenolate. *Transpl Immunol* 2008; 20: 55.
19. Waanders MM, Roelen DL, Brand A, Claas FH. Theputative mechanism of the immuno-modulating effect of HLA-DR shared allogeneic blood transfusions on the allo-immuneresponse. *Transfus Med Rev* 2005; 19: 281
20. Breitbach M, Bostani T, Roell W, et al. Potential risks of bone marrow cell transplantation into infarcted hearts. *Blood* 2007; 110: 1362.
21. Yoshimura K, Aoi N, Suga H, et al. Ectopic fibrogenesis induced by transplantation of adipose-derived progenitor cell suspension immediately after lipoinjection. *Transplantation* 2008; 85: 1868.
22. Beggs KJ, Lyubimov A, Borneman JN, et al. Immunologic consequences of multiple, high-dose administration of allogeneic mesenchymal stem cells to baboons. *Cell Transplant* 2006; 15: 711.

23. Yagi H, Soto-Gutierrez A, Parekkadan B, Kitagawa Y, Tompkins RG, Kobayashi N, Yarmush ML. Mesenchymal stem cells: Mechanisms of immuno-modulation and homing. *Cell Transplant* 2010;19:667–679.
24. Shiels PG (2004) Adult stem cells mitigate the effects of STZ diabetes. *Horizons in Medicine* 17:241-249
25. Dor Y, Brown J, Martinez OI, Melton DA. Adult pancreatic beta-cells are formed by self-duplication rather than stem cell differentiation. *Nature* 2004;429:41–46.
26. Nir T, Melton DA, Dor Y. Recovery from diabetes in mice by beta cell regeneration. *J Clin Invest* 2007;117:2553–2561.
27. Karen Stevenson Daxin Chen Alan Mc Intyre Liane McGlynn David Russell Paul Montague Murali Subramaniam WD George R Wayne Davies and Anthony Dorling and Paul G Shiels
Complete reversal of streptozotocin induced diabetes by intravenous delivery of a novel adult rat cell type. *Rej. Res* – March 2011 Epub ahead of print
28. Meissner A, Wernig M, Jaenisch R. (2007)
Direct reprogramming of genetically unmodified fibroblasts into pluripotent stem cells. *Nat Biotechnol.* (10):1177-81.
29. Okita K, Ichisaka T, Yamanaka S. (2007)
Generation of germline-competent induced pluripotent stem cells. *Nature.* 448(7151):313-7
30. Zhang J, Lian Q, Zhu G, Zhou F, Sui L, Tan C, Mutalif RA, Navasankari R, Zhang Y, Tse HF, Stewart CL, Colman A. A human iPSC model of Hutchinson Gilford Progeria reveals vascular smooth muscle and mesenchymal stem cell defects. *Cell Stem Cell.* 2011 Jan 7;8(1):31-45. Epub 2010 Dec 23
31. C E Pasi, A Dereli-Öz, S Negrini, M Friedli, G Fragola, A Lombardo, G Van Houwe, L Naldini, S Casola, G Testa, D Trono, P G Pelicci, T D Halazonetis. Genomic instability in induced stem cells. *Cell Death and Differentiation*, 2011; DOI: 10.1038/cdd.2011.9
- (32) Aronovich A, Tchorsh D, Katchman H, Eventov-Friedman S, Shezen E, Martinowitz U et al. Correction of hemophilia as a proof of concept for treatment of monogenic diseases by fetal spleen transplantation. *Proc Natl Acad Sci U S A* 2006 December 12;103(50):19075-80.

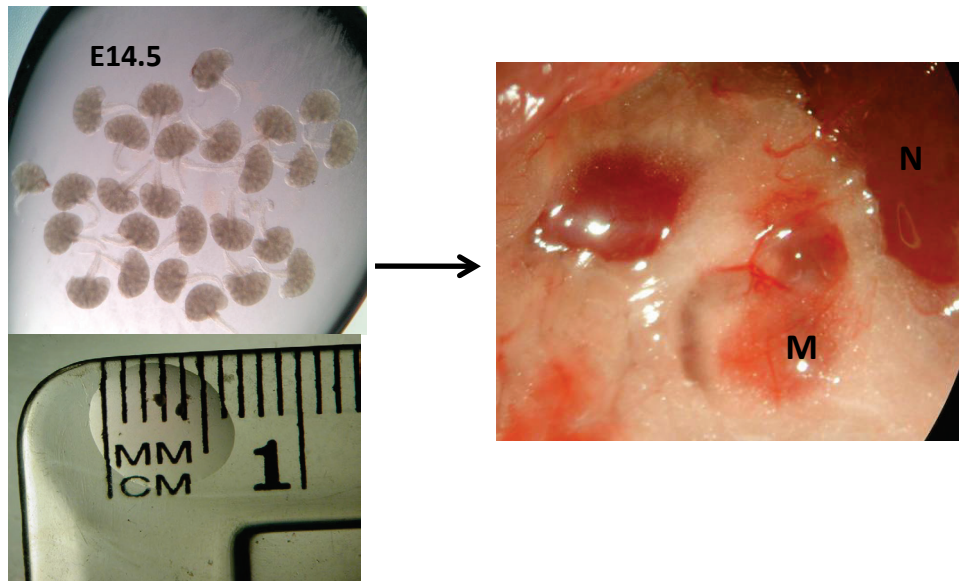
- (33) Froud T, Baidal DA, Faradji R, Cure P, Mineo D, Selvaggi G et al. Islet transplantation with alemtuzumab induction and calcineurin-free maintenance immunosuppression results in improved short- and long-term outcomes. *Transplantation* 2008 December 27;86(12):1695-701.
- (34) Hammerman MR. Transplantation of renal precursor cells: a new therapeutic approach. *Pediatr Nephrol* 2000 June;14(6):513-7.
- (35) Marshall D, Dilworth MR, Clancy M, Bravery CA, Ashton N. Increasing renal mass improves survival in anephric rats following metanephros transplantation. *Exp Physiol* 2007 January;92(1):263-71.
- (36) Clancy MJ, Marshall D, Dilworth M, Bottomley M, Ashton N, Brenchley P. Immunosuppression is essential for successful allogeneic transplantation of the metanephros. *Transplantation* 2009 July 27;88(2):151-9.
- (37) Hammerman MR. Xenotransplantation of embryonic pig kidney or pancreas to replace the function of mature organs. *J Transplant* 2011;2011:501749.
- (38) Yokoo T, Kawamura T. Xenobiotic kidney organogenesis: a new avenue for renal transplantation. *J Nephrol* 2009 May;22(3):312-7.
- (39) Baiguera S, Birchall MA, Macchiarini P. Tissue-engineered tracheal transplantation. *Transplantation* 2010 March 15;89(5):485-91.
- (40) Taylor DA. From stem cells and cadaveric matrix to engineered organs. *Curr Opin Biotechnol* 2009 October;20(5):598-605.

Fig.1 The developmental pathway from stem cells to mature organs



Schematic representation of the progress of organ development from undifferentiated stem cell populations to mature organs

Fig. 2 Experimental foetal organ rudiment transplant



Rat foetal kidney preorgan, the metanephros (shown to scale) transplanted to adult rat abdomen develop gross renal morphology (M) (next to native kidney (N) for scale after 17 days.